Molecular insights into Listeria monocytogenes persistence via label-free quantitative proteomics

Lydia Palaiodimou

université PARIS-SACLAY

Molecular insights into *Listeria monocytogenes* persistence via label-free quantitative proteomics

Approche moléculaire de la persistance de *Listeria monocytogenes* par la protéomique quantitative sans marquage (label-free)

Thèse de doctorat de l'université Paris-Saclay

Ecole doctorale : n°577, Structure et dynamique des systèmes vivants (SDSV)
Spécialité de doctorat : Microbiologie
Graduate School : Sciences de la vie et santé. Référent : Faculté des sciences d'Orsay

Thèse préparée dans l'unité de recherche **Micalis Institute** (Université Paris-Saclay INRAE, AgroParisTech), sous la direction d'**Alessandro PAGLIUSO**, Chargé de Recherche, et le co-encadrement de **Céline HENRY**, Ingénieure de Recherche

Thèse soutenue à Paris-Saclay, le 17 décembre 2024, par

Lydia PALAIODIMOU

Composition du Jury

Membres du jury avec voix délibérative

Florence DUBOIS-BRISSONNET Professeur des Universites, Université Paris-Saclay, AgroParisTech, MICALIS, Jouy-en-Josas	Présidente
Olivier DUSSURGET Professeur, Université Paris Cité, Institut Pasteur, Paris	Rapporteur & Examinateur
Natalie ROLHION Chargée de Recherche (HDR), INSERM, Paris	Rapporteur & Examinatrice
Luc CAMOIN Ingénieur de Recherche, CRCM, AMU, INSERM Marseille	Examinateur

THÈSE DE DOCTORAT
NNT : 2024UPASL115

Titre : Perspectives moléculaires sur la persistance de *Listeria monocytogenes* par label-free quantitative protéomique analyses.

Mots clés : Listeria monocytogenes, protéomique, trophoblastes, système immunitaire, VBNC, déficience de la paroi cellulaire

Résumé : *Listeria monocytogenes* (*Lm*) est un pathogène intracellulaire facultatif responsable de la listériose, une infection alimentaire particulièrement dangereuse pour les femmes enceintes et les personnes immunodéprimées. Connue pour son adaptabilité, *Lm* persiste dans divers environnements, rendant son contrôle difficile. Lors d'infections prolongées de cellules épithéliales, telles que les hépatocytes et les trophoblastes, *Lm* passe d'un état réplicatif à un état quiescent au sein de vacuoles de type lysosomal, appelées *Listeria*-containing vacuoles (LisCVs). Cette transition est associée à la perte de ActA, protéine permettant la nucléation de l'actine, et à l'arrêt de la polymérisation de l'actine à la surface bactérienne. Au sein des LisCVs, la majorité des bactéries restent intactes et entrent dans un état peu voire non réplicatif jusqu'à atteindre un état viable mais non cultivable (VBNC), une forme dormante permettant la survie dans des conditions défavorables. L'infection prolongée des hépatocytes par *Lm* perturbe l'immunité de l'hôte, notamment en diminuant la sécrétion des protéines de phase aiguë (APP), essentielles à la réponse immunitaire. Ce processus pourrait empêcher l'élimination complète de *Listeria* du foie et favoriser ainsi l'établissement d'infection persistante. *Lm* montre également une capacité d'adaptation remarquable dans des environnements en dehors de l'hôte, notamment dans les milieux aquatiques, où il peut entrer dans un état VBNC. Les pathogènes VBNC posent un risque sanitaire majeur, car ils échappent aux méthodes de détection basées sur la croissance tout en conservant la capacité à se réactiver vers des formes virulentes. Une étude récente montre que lorsqu'elle est exposée à des conditions pauvres en nutriments, *Lm* perd sa forme en bâtonnet pour devenir ronde en raison de la perte de sa paroi cellulaire. Ces formes sans paroi cellulaire (cell wall-deficient, CWD) peuvent s'adapter aux déséquilibres physico-chimiques en modifiant leur membrane et en produisant des protéines spécifiques.

La première partie de la thèse explore les interactions hôte-pathogène lors d'infections par *Lm*, en se focalisant sur les cellules trophoblastiques. À l'aide de la protéomique comparative par spectrométrie de masse (LC-MS/MS), cette étude compare les profils de sécrétome des cellules infectées et non infectées durant les phases réplicative (24h p.i.) et persistante (96h p.i) de l'infection.L'analyse des voies métaboliques mises en jeu dans le modèle trophoblastique indique que *Lm* module les réponses immunitaires par des processus intermédiaires tels que l'angiogenèse et les voies de signalisation, dont HIF-1α et MAPK, essentiels à la transduction du signal. Comme dans le foie, ces modulations pourraient être cruciales pour créer et maintenir une niche dans les cellules trophoblastiques ; cependant, les mécanismes restent à identifier.

La seconde partie de la thèse étudie la persistance environnementale de *Lm* via un modèle *in vitro* d'eau minérale et une analyse de protéomique comparative. Les données montrent une régulation à la baisse des protéines liées à la paroi cellulaire, en cohérence avec l'établissement de forme CWD. L'analyse fonctionnelle a révélé également des réponses aux stress, notamment une diminution de la transduction des signaux, de la virulence et de la production d'énergie, cohérentes avec l'état VBNC. Ces résultats éclairent les stratégies de survie environnementale de *Lm* et ses mécanismes de persistance.

Ce travail explore la persistance de *Lm* dans les trophoblastes et l'environnement, montrant son adaptation moléculaire à survivre dans des environnements variés. Dans les cellules hôtes, *Lm* réprime l'immunité, tandis que, dans des conditions pauvres en nutriments, elle privilégie l'acquisition de nutriments et la résistance aux stress. L'ensemble de ces données soulignent sa résilience et pourrait conduire à des applications potentielles pour détecter et traiter les infections persistantes.

Title: Molecular insights into *Listeria monocytogenes* persistence via label-free quantitative proteomics

Keywords: *Listeria monocytogenes*, Proteomics, Trophoblasts, Immune system, VBNC, Cell wall deficiency

Abstract: *Listeria monocytogenes* (*Lm*) is a facultative intracellular pathogen responsible for listeriosis, a severe foodborne illness in pregnant women and immunocompromised individuals. Known for its adaptability, *Lm* persists across varied environments, making it difficult to control. During long-term infection in epithelial cells, such as hepatocytes and trophoblasts, *Lm* shifts from a replicative to a quiescent state within lysosome-like vacuoles, termed *Listeria*-containing vacuoles (LisCVs). This transition is associated with the loss of the actin-nucleating protein ActA and the arrest of actin polymerisation at the bacterial surface. Within LisCVs, the majority of bacteria remain intact and enter a slow/non-replicative or a viable but non-culturable (VBNC) state, a dormant form enabling persistence under adverse conditions. Prolonged infection of hepatocytes by *Listeria* disrupts host immunity, particularly reducing the secretion of acute-phase proteins (APPs), key to the immune response. This process might prevent the complete elimination of *Listeria* from the liver, thereby favouring the establishment of persistent infection. *Lm* also displays notable adaptability outside host environments, particularly in water systems, where it can enter a VBNC dormant state. VBNC pathogens pose heightened health risks as they are undetectable by growth-based methods and can reactivate into a virulent form. A recent study shows that when exposed to these nutrient-poor conditions, the bacteria lose their rod shape and become round due to their cell wall loss. These cell wall-deficient (CWD) forms can adapt to physicochemical imbalances by modifying their membrane and producing specific proteins.

The first part of this thesis explores host-pathogen interactions during *Lm* infections, focusing on trophoblast cells. Using comparative proteomics via LC-MS/MS, this study analyses differences in secretome profiles between infected and uninfected cells across replicative (24h p.i.) and persistent (96h p.i.) infection phases. Pathway analysis in the trophoblast model indicates that *Lm* modulates immune responses through intermediary processes like angiogenesis and signalling pathways, including HIF-1α and MAPK, essential for signal transduction. Similar to the liver, these modulations may be crucial for creating and sustaining a niche in trophoblast cells; however, mechanisms remain to be identified.

The second part of this thesis investigates *Lm* environmental persistence using an *in vitro* mineral water model and comparative proteomics. Proteomic data identified the downregulation of cell wall-related proteins, consistent with the establishment of CWD form. Functional analysis showed additional stress responses, including decreased signal transduction, virulence, and energy production, all consistent with the VBNC state. These findings provide insight into *Lm* environmental survival strategies, aiding in the understanding of its persistence mechanisms.

This work examines *Lm* persistence in trophoblast cells and environmental conditions, demonstrating its molecular adaptation to survive in diverse environments. Within host cells, *Lm* emphasises immune repression, while in nutrient-poor conditions, it focuses on nutrient scavenging and stress resistance. These findings highlight its resilience and could lead to potential applications for detection and treatment of persistent infections.

Τίτλος: Μοριακές γνώσεις για την επιμονή του *Listeria monocytogenes* μέσω ποσοτικής πρωτεομικής χωρίς τη χρήση επισημάνσεων

Λέξεις-κλειδιά: *Listeria monocytogenes*, Πρωτεομική, Τροφοβλάστες, Ανοσοποιητικό σύστημα, VBNC, Έλλειψη κυτταρικού τοιχώματος

Περίληψη: Το *Listeria monocytogenes* (*Lm*) είναι ένας προαιρετικά ενδοκυτταρικός παθογόνος μικροοργανισμός, υπεύθυνος για τη λιστερίωση, μια σοβαρή τροφιμογενή λοίμωξη που επηρεάζει κυρίως έγκυες γυναίκες και ανοσοκατασταλμένα άτομα. Γνωστό για την προσαρμοστικότητά του, το Lm επιμένει σε ποικίλα περιβάλλοντα, καθιστώντας τον έλεγχό του δύσκολο. Κατά τη διάρκεια μακροχρόνιων λοιμώξεων σε επιθηλιακά κύτταρα, όπως ηπατοκύτταρα και τροφοβλάστες, το *Lm* μεταβαίνει από μια κατάσταση πολλαπλασιασμού σε μια λανθάνουσα κατάσταση μέσα σε κενοτόπια τύπου λυσοσώματος, γνωστά ως κενοτόπια που περιέχουν *Listeria* (*Listeria-containing vacuoles* ή LisCVs). Αυτή η μετάβαση συνδέεται με την απώλεια της πρωτεΐνης που πυρηνοποιεί την ακτίνη, ActA, και την αναστολή της πολυμερισμού της ακτίνης στην επιφάνεια του βακτηρίου. Στα LisCVs, η πλειονότητα των βακτηρίων παραμένει άθικτη και εισέρχεται σε μια αργή/μη πολλαπλασιαστική ή βιώσιμη αλλά μη καλλιεργήσιμη κατάσταση (VBNC), μια λανθάνουσα μορφή που επιτρέπει την επιμονή σε αντίξοες συνθήκες. Η παρατεταμένη λοίμωξη των ηπατοκυττάρων από τη *Listeria* διαταράσσει την ανοσία του ξενιστή, μειώνοντας ιδιαίτερα την έκκριση πρωτεϊνών οξείας φάσης (*acute-phase proteins* ή APPs), που είναι κρίσιμες για την ανοσοαπόκριση. Αυτή η διαδικασία μπορεί να εμποδίσει την πλήρη εξάλειψη της *Listeria* από το ήπαρ, ευνοώντας έτσι την εγκαθίδρυση χρόνιας λοίμωξης. Το *Lm* επιδεικνύει επίσης αξιοσημείωτη προσαρμοστικότητα εκτός ξενιστών, ιδιαίτερα σε υδάτινα συστήματα, όπου μπορεί να εισέλθει στη λανθάνουσα κατάσταση VBNC. Οι παθογόνοι οργανισμοί VBNC αποτελούν αυξημένο κίνδυνο για την υγεία, καθώς δεν ανιχνεύονται με μεθόδους που βασίζονται στην καλλιέργεια και μπορούν να επανενεργοποιηθούν σε μολυσματική μορφή. Πρόσφατη μελέτη δείχνει ότι όταν εκτίθενται σε συνθήκες πτωχών θρεπτικών στοιχείων, τα βακτήρια χάνουν το ραβδοειδές τους σχήμα και γίνονται στρογγυλά λόγω της απώλειας του κυτταρικού τοιχώματος. Αυτές οι μορφές χωρίς κυτταρικό τοίχωμα (*cell wall-deficient* ή CWD) μπορούν να προσαρμοστούν σε φυσικοχημικές ανισορροπίες τροποποιώντας την κυτταρική μεμβράνη τους και παράγοντας συγκεκριμένες πρωτεΐνες. Το πρώτο μέρος αυτής της διατριβής εξετάζει τις αλληλεπιδράσεις ξενιστή-παθογόνου κατά τη διάρκεια λοιμώξεων από Lm, εστιάζοντας στα κύτταρα τροφοβλάστης.

Με τη χρήση συγκριτικής πρωτεομικής μέσω LC-MS/MS, η παρούσα μελέτη αναλύει τις διαφορές στα προφίλ του εκκριτώματος μεταξύ μολυσμένων και μη μολυσμένων κυττάρων στις φάσεις πολλαπλασιασμού (24 ώρες μετά τη μόλυνση) και επιμονής (96 ώρες μετά τη μόλυνση). Η ανάλυση των μονοπατιών στο μοντέλο τροφοβλάστης υποδεικνύει ότι το *Lm* τροποποιεί τις ανοσολογικές αποκρίσεις μέσω ενδιάμεσων διαδικασιών, όπως η αγγειογένεση και μονοπάτια σηματοδότησης, συμπεριλαμβανομένων των HIF-1α και MAPK, που είναι κρίσιμα για τη μεταβίβαση σήματος. Όπως και στο ήπαρ, αυτές οι τροποποιήσεις μπορεί να είναι ζωτικής σημασίας για τη δημιουργία και τη διατήρηση μιας εστίας στα κύτταρα τροφοβλάστης, ωστόσο οι ακριβείς μηχανισμοί παραμένουν να ταυτοποιηθούν..

Το δεύτερο μέρος αυτής της διατριβής εξετάζει την περιβαλλοντική επιμονή του *Lm* χρησιμοποιώντας ένα *in vitro* μοντέλο μεταλλικού νερού και συγκριτική πρωτεομική. Τα δεδομένα πρωτεομικής ανέδειξαν τη μείωση των πρωτεϊνών που σχετίζονται με το κυτταρικό τοίχωμα, συμφωνώντας με την καθιέρωση της μορφής CWD. Η λειτουργική ανάλυση ανέδειξε επιπλέον αποκρίσεις στο στρες, όπως η μείωση της μεταβίβασης σήματος, της λοιμογόνου δράσης και της παραγωγής ενέργειας, όλα συμβατά με την κατάσταση VBNC. Αυτά τα ευρήματα προσφέρουν γνώσεις για τις στρατηγικές περιβαλλοντικής επιβίωσης του *Lm*, συμβάλλοντας στην κατανόηση των μηχανισμών επιμονής του.

Η παρούσα εργασία εξετάζει την επιμονή του *Lm* σε κύτταρα τροφοβλάστης και περιβαλλοντικές συνθήκες, καταδεικνύοντας την μοριακή του προσαρμογή για επιβίωση σε διάφορα περιβάλλοντα. Στα κύτταρα ξενιστή, το Lm δίνει έμφαση στην καταστολή του ανοσοποιητικού συστήματος, ενώ σε συνθήκες πτωχών θρεπτικών στοιχείων εστιάζει στη συλλογή θρεπτικών στοιχείων και στην αντοχή στο στρες. Αυτά τα ευρήματα αναδεικνύουν την ανθεκτικότητά του και θα μπορούσαν να οδηγήσουν σε πιθανές εφαρμογές για την ανίχνευση και τη θεραπεία επίμονων λοιμώξεων.

«Ἦθος ἀνθρώπῳ δαίμων»

-Ηράκλειτος

Στην οικογένεια μου

που υπερ-αγαπώ

Αδέρφια

Γιάννης Παλαιοδήμος

Φίλιππας Παλαιοδήμος 🎗

Ρία Παλαιοδήμου

Σοφία Παλαιοδήμου

Κώστας Μαντασάς

Δημήτρης Φλώρος

Ανίψια

Κωνσταντίνος Παλαιοδήμος

Αντρέας Παλαιοδήμος

Ελένη Φλώρου

Γιώργος Φλώρος

Γιαγιάκα

Φιλιππία Ανδρέου

Συνοδοιπόρος στην παράνοια

Μυρτώ Γκαντσίδου

Συνοδοιπόροι της ζωής

Δημήτρης Σάκκος

Μελί Καλό-Σκυλί

Μα κυρίως στους γονείς μου για την ανιδιοτελή αγάπη και υποστήριξη τους σε κάθε τομέα της ζωής μου

Κώστας Παλαιοδήμος και Ελένη Παλαιοδήμου

Acknowledgements

As this work comes to completion, I am deeply aware of the support and encouragement that made each step possible. This thesis is the achievement of not only my efforts but also the contributions, insights, and kindness of so many remarkable individuals. I am profoundly grateful to everyone who has guided, supported, and motivated me through this journey, and I would like to take this moment to express my heartfelt thanks to each of you. I am incredibly grateful to the academics I admire, my close friends, my partner Dimitris, our beloved dog Melie, and my family; my brothers, sisters, grandma, and, of course, my lovely parents. I'll do my best to thank everyone, and I apologise for expressing my family's acknowledgements in Greek.

First, I sincerely thank the Jury members: **Prof Olivier Dussurget, Dr Natalie Rolhion, Dr Luc Camoin, Prof Florence Dubois-Brissonnet,** and **Dr Hélène Barreteau.** I am deeply thankful for their willingness to accept our invitation to join the jury and share their expertise and insights. I also greatly appreciate their endless patience and understanding during the scheduling of this defence; navigating those arrangements proved to be equally challenging to the three years spent on the project.

Similarly, I would like to sincerely thank my thesis committee members: **Jost Enninga, Mariette Matondo,** and **Edward Fox.** Their contributions were vital to the successful completion of this thesis, and I am incredibly grateful for their support throughout these three years.

A special thank you to **Helene Bierne**, one of the most influential people I've had the privilege to meet. Her insights, advice, and guidance while she was still alive were invaluable, and I consider myself fortunate to have crossed paths with her and am grateful for the opportunity. Thanks to both of my supervisors; **Alessandro Pagliuso** and **Celine Henry**, for guiding this research. Despite the challenges faced along the way, I appreciate the valuable insights and moments of support they provided, which contributed to the development of this work.

I would like to extend my sincere gratitude to both the Epimic and PAPPSO teams. From Epimic, my warmest thanks to **Emma**, whose kindness helped me adapt to life in France and feel truly welcomed, and to **Filipe**, whose guidance on protocols was always appreciated. I also wish to thank **Goran** for his consistent willingness to help, which never went unnoticed. **Matthieu**, whom I admire for his patience and kindness and I consider a truly brilliant person. Many thanks also go to **Eliane**, for her insightful feedback and warm character, as well as to **Aurelie**, whose assistance with university administrative tasks was invaluable. **Delphine**, for her delicious treats that brought joy to many days. From PAPPSO, I am especially grateful to **Lydie** and **Carine** for their endless help with technical challenges during our proteomics analyses. A heartfelt thank you to **Olivier** and **Thierry** for their guidance, particularly during challenging bioinformatics moments.

Before finishing the Micalis thank you section, I want to express my heartfelt thanks to **Hadi, Yok,** and **Pierre C. Pierre C,** thank you for the delicious crepes, the rides to Versailles-Chantiers, and our 20K-step walks around Paris. You're one of the kindest people I've met, and I'm grateful for all our amazing talks. **Hadi**, words can't describe the support you've given me. From commuting-buddies to close friends, I cherish every moment; the commutes, coffee breaks, advice, and laughter. You'll always have a special place in my heart. And dear **Yok**, your warmth and energy have truly been a light in my life lately. You've helped me through tough times just by being your wonderful self, and you'll always hold a very special place in my heart, and I'm so grateful for your friendship.

Being part of the PEST-BIN consortium has been one of the most rewarding experiences of my life. I want to extend my deepest gratitude to **Prof Ivan Mijakovic** for creating this incredible project and for being such an influential and supportive figure. Thank you so much for offering your invaluable time to provide guidance and advice and I'm truly grateful to have met you! Special thanks to **Darko** for his continuous assistance and for always being available to answer questions. I'm grateful to all the PIs involved in the project and many special thanks to **Prof. Boris Macek** and

Prof. Roger Karlsson for hosting me during my secondments and for their invaluable guidance through feedback and discussions.

Throughout the PEST-BIN project, I have been fortunate to meet so many incredible people who have left a lasting impact: **Leonarda, Munis, Flavia, Ema, Sara R, Sara P, Mukil, Anja, Margaux, Thomas, Jose, Ghalib, Payal,** and **Hengzi**. I'm incredibly grateful to call many of you friends, and I treasure the time we've shared. Each one of you has his own inspiring personality and with your unique insights and sharp perspectives you have made our discussions deeply meaningful. All of these three years are filled with unforgettable memories and shared moments that I will always keep in my heart!! I'm truly lucky to have met each of you. Wishing you all the very best, and I look forward to the day we cross paths again!

Additionally, I am especially thankful to and deeply grateful to **Edward Fox** whose patience, encouragement and insights were invaluable to my work and personal growth not only during my PhD but since my MSc. Thank you for being an exceptional mentor, always finding time to offer feedback, advice, and guidance with such dedication. I could never thank you enough! Thank you so much!

Finally, my deepest thanks go to my friends. To **Vasilis V** and **Vassilis G**, for their invaluable feedback and encouragement to keep pushing forward; your motivation has truly been a highlight of this past year! And of course to **Vasilis Ntokas**, for his support and friendship, thank you for always being there to share a laugh and brighten each day. I cannot describe how happy I am that we are finally in the same country!

To the **Salva Serra family; Xisco, Guillem, Anielka,** and **Nouria**, for their motivational talks and support and all the unforgettable moments we shared over the past year! **Xisco**, thank you a million not only for your feedback but for your friendship that came out of nowhere and was a highlight of the PhD journey! And to my dear friend **Leonarda**, φίλη μου αγαπημένη, there aren't enough words to express my gratitude. You are one of the most brilliant and kind-hearted people I've ever had the pleasure of knowing. Having you in my life is a gift (more majestic than the cathedral in Palma de Mallorca), and no matter what happens or where we may find ourselves, you're always in my thoughts! ¡Muchísimas gracias de todo corazón por todo!

Το μόνο απολύτως βέβαιο γεγονός, ωστόσο, είναι ότι δε θα είχα καταφέρει ούτε τα μισά δίχως τη στήριξη δικών μου ανθρώπων.

Δανάη, σε ευχαριστώ τόσο πολύ για όλη σου τη βοήθεια με τις αιτήσεις, για όλη την προετοιμασία και τη στήριξη, και μακάρι να είχαν έρθει τούμπα τα πράγματα, αλλά μπουφ! Σε εκτιμώ βαθύτατα και σ' ευχαριστώ πάρα πολύ για όλα! **Νίκη**, σας ευχαριστώ τόσο πολύ για τη θετική σας ενέργεια που είναι πάντα αχτίδα φωτός μέσα σε δέκα στρώσεις συννεφιάς! Σας ευχαριστώ πολύ για τα πάντα, όλα, ιδίως για τα πεντανόστιμα μπιφτέκια σας, και σας αγαπώ πολύ! Πραγματικά, είστε άνθρωπος που ομορφαίνει τη ζωή! **Κρις μου**, είσαι ό,τι καλύτερο και σε ευχαριστώ για όλα τα απίστευτα relatable memes!

Μυρτώ μου, άλλο μου μισό! Νομίζω ειλικρινά ότι ό,τι κι αν πω δε μπορεί να περιγράψει ούτε στο ελάχιστο τη στήριξη που μου έχεις δώσει σε αυτήν την παράνοια, όχι μόνο της τριετίας, αλλά και της ζωής γενικότερα! Είσαι από τα σημαντικότερα κομμάτια της ζωούλας μου, χωρίς εσένα δε ξέρω τι θα είχα απογίνει. Σε ευχαριστώ για τα ΠΑΝΤΑ, και σ' αγαπώ, τρελή μου, τόσο πολύ!!!! Η ύπαρξή σου είναι ένα από τα ελάχιστα πράγματα για τα οποία ευχαριστώ το σύμπαν!!!

Ένα τεράστιο ευχαριστώ στη **γιαγιάκα μου**! Στην αγαπημένη μου γιαγιά και ίσως τη μεγαλύτερή μου αδυναμία! Γιαγιά μου, όπως σου έχω πει τόσες φορές, είσαι η καλύτερη γιαγιά του κόσμου. Σ' αγαπώ τόσο πολύ και σε ευχαριστώ για όλα! Έχω αμέτρητες υπέροχες αναμνήσεις μαζί σου, και πάντα θα έχεις τη δική σου ξεχωριστή θέση στην καρδιά μου. Σ' ευχαριστώ που πάντα πίστευες σε μένα!

Τι θα ήμουν χωρίς τα υπέροχα αδέρφια μου: τον **Γιάννη**, τον **Φίλιππα**, τη **Ρία**, τη **Σοφία**, και, φυσικά, τον **Καπετάνιο**, τον **Κώστα** και τη **Μαριάννα**. Είστε οι πιο καταπληκτικοί, οι πιο υποστηρικτικοί, και, ναι, οι πιο αυστηροί κριτές μου όταν χρειάζεται! Στηρίξατε το κάθε μου βήμα, ακόμα και τις στιγμές παραλογισμού μου, και για αυτό σας ευχαριστώ. **Γιάννη**, **αγαπημένε μου συγκάτοικε**, ξέρω πως τελευταία σε ψυχαγώγησα… λίγο και με τα παράπονά μου (χαχα)! Είναι κοινό οικογενειακό μυστικό ότι "άλλος έχει το όνομα και άλλος τη χάρη." Όσα χρόνια και πτυχία κι αν περάσουν, εσύ θα είσαι πάντα ο άνθρωπος που θα συμβουλεύομαι για καθετί ιατρικό και βιολογικό! Σ' ευχαριστώ για όλες τις κουβέντες που είχαμε και για όλη σου τη βοήθεια με το πρότζεκτ! Αγαπημένη **μικρή μαμά μου**, Ρία, σε ευχαριστώ για όλα! Για όλες τις συμβουλές (ακόμα κι αν δεν τις άκουγα πάντα), για τις ατελείωτες συζητήσεις μας και που με κάνεις να νιώθω πως δεν είμαι ποτέ μόνη. Το ότι υπάρχεις μου δίνει ασφάλεια! **Σοφ μου**, φίλη μου και αδερφούλα αγαπημένη, σ' ευχαριστώ που άντεξες αυτό το μαρτύριο δίπλα μου, για όλες τις συνταγές και τις γλυκές κουβέντες που γλύκαιναν τις μέρες και έδιναν λίγη υπομονή ακόμα. **Φίλιππα**, σε άφησα τελευταίο, μιας και μάλλον αυτά δεν θα τα διαβάσεις ποτέ… Πολλές φορές σε κατηγόρησα για την επιλογή μου, μα δεν έφταιγες εσύ· ήταν η δική μου διέξοδος-αδιέξοδος. Ελπίζω να είσαι κάπου κοντά μας, κι αν όχι, ξέρω πως θα έρθεις στα όνειρά μου, θα με αγκαλιάσεις και θα μου πεις «μπράβο, αδερφούλα». Λείπεις πολύ και πάντα θα λείπεις, μα θα είμαστε πάντα πέντε. Επιπλέον, πολλά ευχαριστώ στα ΠΙΟ ΥΠΕΡΟΧΑ ανίψια μου, **Κωνσταντίνος**, **Ανδρέας**, **μικρή Ελένη** και **Γιώργος…** Είστε το φως στη ζωή! Με το χιούμορ σας, τις ατάκες, τη ζωντάνια, τον χορό και τη χαρά σας, ο καθένας ξεχωριστά με το δικό του τρόπο με βοήθησε να φτάσω μέχρι εδώ. Είστε η μεγάλη μου αδυναμία, ο καθένας για τους δικούς του μοναδικούς λόγους!

Μάου μου, σε ευχαριστώ ΓΙΑ ΟΛΑ! Που όχι μόνο ήσουν ο δικηγόρος μου και ο άνθρωπός μου, αλλά και που με υπέμεινες αυτά τα παράλογα χρόνια! Σου υπόσχομαι να γίνω ο άνθρωπος που ήμουν πριν μπλέξω σε όλο αυτό. Σε ευχαριστώ που ήρθες μαζί μου στο Παρίσι, δε θα ήταν το ίδιο χωρίς εσένα! Μα πιο πολύ από όλα, σε ευχαριστώ που με βοήθησες και με βοηθάς να ξεπερνώ τα πάντα, κάθε λογής δυσκολία! Μου μαθαίνεις πού να δίνω βαρύτητα, με βοηθάς να σκέφτομαι, να εξελίσσομαι, να ωριμάζω… Με εμπνέεις!! Το να σε έχω στη ζωή μου με κάνει καλύτερο άνθρωπο! Σε ευχαριστώ που με αγάπησες και που με αγαπάς! Είσαι μοναδικός για μένα, μάου μου! Εσύ και η **Μελί** είστε μοναδικοί και σας αγαπώ πολύ! (Επίσης, δε θα μπορούσα ποτέ να σε ευχαριστήσω αρκετά για το python script που μου έγραψες και μου έσωσε τη ζωή… Αν δεν ήταν αυτό, ακόμα θα έψαχνα τις πρωτεΐνες μία-μία!)

Μανούλα και Μπαμπάκα μου!!! Είμαι το πιο ευτυχισμένο παιδί στον κόσμο που έχω εσάς για γονείς!!! ΣΑΣ ΕΥΧΑΡΙΣΤΩ ΓΙΑ ΤΑ ΠΑΝΤΑ: για το χθες, το σήμερα, και το για πάντα!! Είμαι ευγνώμων για όλες σας τις θυσίες, αλλά κυρίως για την υπομονή σας, την αγάπη σας, την υποστήριξή σας, και τη δύναμη που μου δίνετε. Δεν είστε μόνο σπουδαίοι γονείς – είστε σπουδαίοι άνθρωποι! Σας θαυμάζω και σας εκτιμώ με τρόπους που τα λόγια δεν μπορούν να περιγράψουν. Σας ευχαριστώ που με μεγαλώσατε με την αντοχή να ξεπερνώ τις δυσκολίες και να «κολυμπώ» μόνη μου. Και σας ευχαριστώ που ακόμα μου μαθαίνετε να «πετάω». Ξέρω ότι πολλές φορές στενοχωρηθήκατε για τα όσα πέρασα, αλλά με διδάξατε πώς να αντέχω. Μέσα από αυτό το ταξίδι, κατάλαβα τι έχει πραγματική σημασία!!

Κι όπως είπε και ο Καβάφης…

«Σα βγεις στον πηγαιμό για την Ιθάκη,
να εύχεσαι να 'ναι μακρύς ο δρόμος,
γεμάτος περιπέτειες, γεμάτος γνώσεις.
Τους Λαιστρυγόνας και τους Κύκλωπας,
τον θυμωμένο Ποσειδώνα μη φοβάσαι…»

Μέσα σε αυτά τα δέκα χρόνια ξενιτιάς, η φωνή και η ύπαρξή σας ήταν η μεγαλύτερη παρηγοριά μου. Δεν υπάρχουν λόγια να σας πω πόσο σας αγαπώ και πόσο σας ευχαριστώ!

Στους πιο όμορφους ανθρώπους, στους γονείς μου

Table of contents

Abbreviations

Δ	Deficient
µl	microlitre
24h p.i.	24 hours post infection
96h p.i.	96 hours post infection
ActA	Actin assembly inducing protein
AGE/RAGE	Advanced Glycation End Product/Receptor of Advanced Glycation End Product
APP	Acute Phase Proteins
BC	Benzalconium Chloride
BHI	Brain Heart Infusion
BHIA	Brain Heart Infusion Agar
CC	Clonal Complex
CFU	Colony Forming Unit
cgMLST	Core Genome Multilocus Sequence Typing
CMV	*Cytomegalovirus*
Csps	Cold Shock Proteins
CT	cgMLST types
CTBs	Cytotrophoblasts
CW	Cell Wall
CWD	Cell Wall Deficient
D14/D0	Ratio D14 to D0
D28/D0	Ratio D28 to D0
D7/D0	Ratio D7 to D0
DavID NCBI	Database for Annotation Visualisation and Integrated Discovery NCBI
DDA	Data Dependent Acquisition
DIA	Data Independent Acquisition
DIA-NN	Data Independent Acquisition based on Neural Networks model
DNA	Deoxyribonucleic Acid
dpf	Days post fertilisation
DTT	Dithiothreitol
E-cad	E-cadherin
ECM	Extracellular Matrix
eEVTs	Endovascular Extravillous Trophoblasts
EFSA	European Food Safety Agency
EGFR	Epidermal Growth Factor Receptor
ERBB3	Erb-B2 Receptor Tyrosine Kinase 3
ESI	Electrospray Ionisation
eSLAPs	epithelial Spacious *Listeria* containing Phagosomes
EVTs	Extravillous Trophoblasts
FBS	Foetal Bovine Serum
FGF	Fibroblast Growth Factor
FPEs	Food Processing Environments
FSS	Fluid Shear Stress
GW-domain	(Gly-Tryp) dipeptide domain
HGF	Hepatocytes Growth Factor
HGT	Horizontal Gene Transfer
HIF-1α	Hypoxia Induced Factor-1 alpha
Hsps	Heat Shock Proteins
HSV	Herpes Simplex Virus
I	Infected Samples
I 96h/24h	Ratio Infected 96 hours to 24 hours
I/NI 24h	Ratio Infected to Uninfected 24h

I/NI 96h	Ratio Infected to Uninfected 96h
IAA	Iodoacetamide
ICM	Inner Cell Mass
iEVTs	Interstitial Extravillous Trophoblasts
IF	Immunofluorescence
IL1RAcP	Interleukin-1 Receptor Accessory Protein
inlAB	Internalins A and B locus
IPTL	Isobaric Peptide Terminal Labelling
iTRAQ	Isobaric Tags for Relative and Absolute Quantitation
JEG3	Epithelial human choriocarcinoma cell line from placenta
KEGG	Kyoto Encyclopedia of Genes and Genomes
LAMP1	Lysosomal Associated Membrane Protein 1
LAP	*Listeria* Adhesion Protein
LBQ	Label Based Quantification
LC-MS/MS	Liquid Chromatography Tandem Mass Spectrometry
LC3	Microtubule associated protein 1A/1B light chain 3
LFQ	Label Free Quantification
LGI2	*Listeria* Genomic Island 2
LIPI-1	*Listeria* Pathogenicity Island 1
LisCVs	*Listeria* Containing Vacuoles
LLO	Listeriolysin O
m/z	Mass to Charge ratio
min	Minute
MAPK	Mitogen-Activated Protein Kinase
MLST	Multi Locus Sequence Typing
MOI	Multiplicity Of Infection
Mpl	Metalloproteinase
MS	Mass Spectrometer
MVLST	Multi Virulence Sequence Typing
MVs	Membrane Vesicles
ng	Nanogram
NK cells	Natural Killer cells
NLRP3	Nucleotide-binding and leucine-rich repeat receptors family pyrin domain containing-3
NPC	Nuclear Pore Complex
Pbps	Penicillin Binding Proteins
PBS	Phosphate Buffer Saline
PCA	Principal Component Analysis
PE	Pre-eclampsia
PFA	Paraformaldehyde
PFGE	Pulsed Field Gel Electrophoresis
PI3K/Akt	Phosphatidylinositol 3-kinase/Protein Kinase B
PLCs	Phospholipases
PrfA	Positive Regulatory Factor A
PSMs	Peptide Spectrum Matches
PTMs	Post-Translational Modifications
PTS	Phosphotransferase System of bacteria
PtsI	Enzyme I of the PTS
QACs	Quaternary Ammonium Compounds
RNA	Ribonucleic Acid
ROS	Reactive Oxygen Species

rSLAPs	Replication-permissive Spacious *Listeria* containing Phagosomes
RTE	Ready to Eat
SC	Spectral Counts
SCID	Severe Combined Immunodeficient
sec	Second
SigB	Sigma factor B
SigH	Sigma factor H
SigL	Sigma factor L
SILAC	Stable Isotope Labelling by Amino Acids
SL	Sublineage
SLAPs	Spacious *Listeria* containing Phagosomes
SrtA	Sortase A
SSIs	Stress Survival Islets
STBs	Syncytiotrophoblasts
Stp	Serine/Threonine Phosphatase (Lmo1821)
TA system	Toxin/Antitoxin System
TE	Trophectoderm
TEM	Transmission Electron Microscopy
TKIs	Tyrosine Kinase Inhibitors
TMT	Tandem Mass Tag
TORCH	Acronym of *Toxoplasma, Others, Rubella, Cytomegalovirus, HSV*
TrxA	Thioredoxin A
TTP	TimsTOF Pro
NI	Uninfected Samples
NI 96h/24h	Ratio Uninfected 96h to 24h
v/v	Volume per volume
VBNC	Viable But Non Culturable
VEGF	Vascular Endothelial Growth Factor
WHO	World Health Organisation
WT	Wild Type
WTA	Wall Teichoic Acids
XIC	Extracted Ion Chromatogram

List of Tables

Introduction

Results and Discussion

Table 17: Statistically significant variable proteins identified with MaxQuant and Perseus D28/D0

Table 18: Variable proteins maintaining their up- or down-regulation pattern throughout the complete time course

Table 19: Protein markers selected for generation of deletion mutants to assess any potential effect on the transition of *L. monocytogenes* into VBNC.

List of Figures

Introduction

Part A

Part B

Part C

Objectives

Results and Discussion

Chapter 1

Chapter 2

Introduction

A. *Listeria monocytogenes*

Listeria monocytogenes is a Gram-positive and facultative intracellular bacterium that belongs to the Firmicutes phylum, recently renamed to Bacillota, together with other notable members such as *Bacillus, Clostridium, Enterococcus, Streptococcus* and *Staphylococcus* genera. More specifically, upon the ingestion of contaminated food, *L. monocytogenes* causes a foodborne disease, listeriosis, which is a rare disease but with a high mortality rate around 26% especially to those who are more susceptible to it (Huang et al., 2023), including the elderly, young children, immunocompromised and pregnant women including their foetuses who can be contaminated via transplacental infection.

I. Discovery/History

Following an epidemic in rabbits at the Pathology Department of the University of Cambridge in 1924, Murray, Webb and Schwann isolated a Gram-positive bacillus which was found to be the causative agent of the weight loss and eventually the sudden death of the rabbits (Murray et al., 1926). This Gram-positive pathogen was named *Bacterium monocytogenes* due to its characteristic symptomatology, that is, both liver necrosis and monocytosis (Murray et al., 1926). In 1927, a second epidemic causing sudden death in gerbils was observed in South Africa and J. Harvey Pirie isolated a bacterium responsible for it, naming it *Listerella hepatolytica* (Pirie et al., 1927). As both isolates were of the same species, the pathogen was renamed to *Listerella monocytogenes*. However, the name *Listerella* was already assigned to a species of *Mycetozoa* and thus, in 1940 Pirie suggested an alternative name that was *Listeria monocytogenes* (Pirie, 1940). Since 1929, listeriosis cases in humans were rare and thus *L. monocytogenes* was considered mainly as an animal pathogen. In the early 80s, a food-poisoning outbreak in Canada related to the consumption of cabbage was the first evidence that *L. monocytogenes* can be transmitted via the ingestion of contaminated food (Schlech et al., 1983). That initiated an increased interest in the *Listeria* research area followed by increased surveillance.

II. Taxonomy, Phylogeny, Classification

The genus *Listeria* belongs to the phylum Firmicutes (Bacillota), class Bacilli, order Bacillales, family *Listeriaceae*. Currently, 28 species of *Listeria* have been identified (Figure 1) and classified into two distinct groups; the *sensu stricto* and the *sensu lato*. The *sensu stricto* clade is considered as a monophyletic (clade I) and is comprised of 10 species; *L. monocytogenes, L. seeligeri, L. welshimeri, L. innocua, L. ivanovii, L. marthii, L. farberi, L. immobilis, L. cossartiae* and *L. swaminathanii*. The *sensu stricto* species are considered the most closely related between them and they also include the first *L. monocytogenes* species that was identified back in 1924. Despite the increased number of *Listeria* species classification in *sensu stricto*, *L. monocytogenes* and *L. ivanovii* remain the only pathogenic for humans and animals. Before 2020, all members of clade I were found in the faeces or gastrointestinal tract of animals, as well as in foods of animal origin, suggesting a specific interaction of these species with mammalian hosts. However, the *L. farberi, L. immobilis, L. cossartiae* and *L. swaminathanii* described in 2021 have only been found in natural environments. On the other hand, the *sensu lato* clade (clade II) is considered paraphyletic and consists of 18 species that are less phylogenetically related to *L. monocytogenes* and have been isolated from surfaces associated with food or the environment. It has been recommended by Orsi and colleagues (Orsi et al., 2016) the re-classification of *sensu lato* into three genera; first the *Murraya* genus which contains only one *Listeria* species, *L. grayi*; secondly, the *Mesolisteria* genus composed of 8 species: *L. floridensis, L. fleischmanii, L. aquatica, L. costaricensis, L. ilorinensis, L. goaensis, L. thailandensis* and *L. valentina*, species that suggest the mesophilic nature of *Listeria* and share the characteristic of their inability to grow at 4 ℃; and finally, the *Paenilisteria* composed of 9 species: *L. booriae, L. riparia, L. weihenstephanensis, L. portnoyi, L. rocourtiae, L. newyorkensis, L. grandensis, L. cornellensis* and *L. rustica*, and they reveal some key characteristics that separate them from the *sensu stricto* clade, that is, their non-motility (except *L. immobilis* that is the only non-motile *sensu stricto* species) and both their negative Voges-Proskauer test and their ability to reduce nitrate to nitrite.

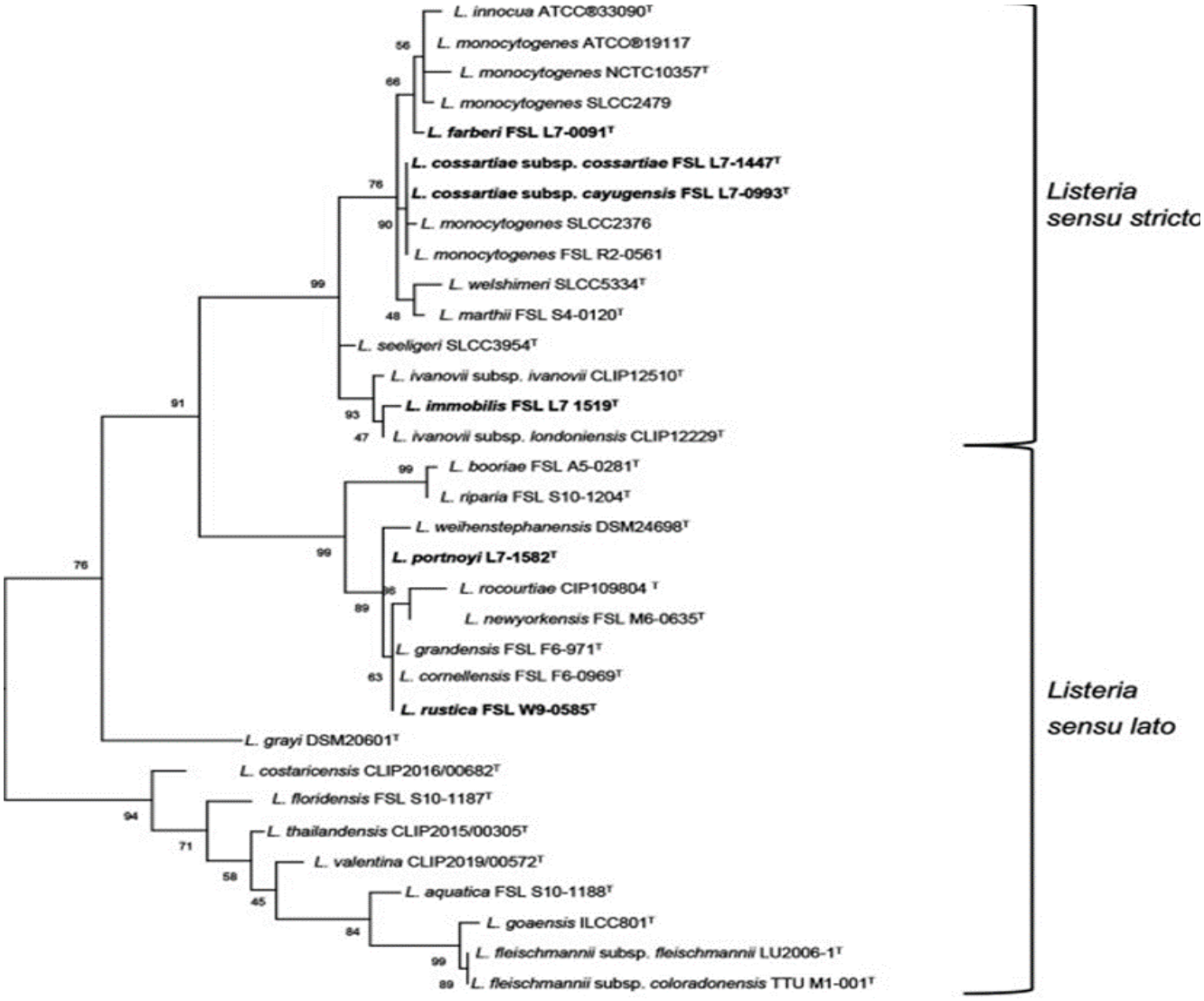

Figure 1: Maximum-likelihood via 16S rRNA phylogenetic tree of the genus *Listeria*. The tree has been constructed with 1000 bootstrap replicates and the Kimura two-parameter model by using the MEGA X software (Adapted from Carlin et al., 2021).

III. *Listeria monocytogenes* biodiversity

3.1 Serotypes

Due to the epidemiological problem posed by listeriosis, it has been crucial to create methods assisting the characterisation and discrimination of *Listeria* species and *L. monocytogenes* strains. The conventional/phenotypic subtyping approaches used to be the most commonly used. More specifically, the serotyping that was first introduced in 1940 by Peterson and that was later optimised by Seeliger and Hohne in 1979 (Paterson, 1940; Seeliger and Hohne, 1979) contributed in the categorisation of *L. monocytogenes* via distinct serotypes. The serotyping takes into account the principle that different strains express different antigens on their surface and therefore they can be differentiated based on this. More specifically, it works by exploiting the antigenic reaction between 14 somatic (O) and 4 flagellar (H) antigens that has led to the generation of 13 unique serotypes (Table 1), (Seeliger and Jones, 1986). However, the conventional/phenotypic subtyping methods show poor accuracy when it comes to foodborne pathogens and the genotypic/molecular subtyping approaches (Pulsed-Field-Gel-Electrophoresis (PFGE), Ribotyping and Multi-Locus-Sequence-Typing (MLST) have started being more widely used since the early 2000s.

Table 1: Serotypes of *L. monocytogenes* (Seeliger and Hohne, 1986 ; Kortebi, 2018)

Species	Serotypes	Somatic Antigen (O)	Flagellar Antigen (H)
L.monocytogenes	1/2a 1/2b 1/2c	I II III	AB ABC BD
	3a 3b 3c	II III IV II III IV XII XIII	AB ABC BD
	4a	III V VII IX	ABC
	4ab	III V VI IX X	
	4b	III V VI	
	4c	III V VII	
	4d	III V VI VIII	
	4e	III V VI VIII IX	
	7	III XII XIII	

3.2 Lineages

Conventional and molecular subtyping analyses including Multilocus Enzyme Electrophoresis (MLEE), PFGE, Ribotyping and MLST have contributed in clustering the different *L. monocytogenes* serotypes into 4 distinct lineages (I, II, III, IV) as shown in Table 2. Initially it was shown that lineage III isolates were further allocated into three subgroups (IIIA, IIIB, IIIC) but sub-lineage IIIB has been suggested as a distinct lineage by many scientists (Liu et al., 2006, Orsi et al., 2006 and Ward et al., 2008) and therefore it has been re-assigned as the lineage IV. Over a 13-year study (1999-2011), among clinical cases of listeriosis, approximately 70% of strains belonged to Lineage I with around 50% being strains of 4b serotype; the remaining around 30% were Lineage II (Goulet et al., 2012). *L. monocytogenes* strains isolated from animal listeriosis belong to these two lineages, as well (Dreyer et al., 2016; Steckler et al., 2018). As for the strains isolated from foods, food processing and natural environments are mostly found in lineage II. Regarding the last two lineages (III and IV), they are more rarely reported, and are usually identified in ruminants (Orsi et al., 2011).

Table 2: Summary and characteristics of *L. monocytogenes* lineages.

Lineage	Initial Identification	Serotypes	Genetic Characterisation	Distribution
I	MLEE, 1989	1/2b ; 3b ; 4b ; 4d ; 4e ; 7	Least diverse	Many sources; overrepresented in human
II	MLEE, 1989	1/2a ; 1/2c ; 3a ; 3c	Most diverse	Many sources; overrepresented in foods and FPEs
III	Partial sequence data analysis, 1995	4a ; 4b ; 4c	Very diverse	Ruminants
IV	Partial sequence data analysis 2006-2008	4a ; 4b ; 4c	Quite diverse	Ruminants

3.3 Clonal Complexes

To better tackle the listeriosis epidemic, many phylogenetic subtyping techniques have been employed to understand the link not only between outbreaks and sources but also with lineages and clonal complexes as well. The MultiLocus Sequence Typing (MLST) method was employed in order to classify the *L. monocytogenes* strains into Sequence Types (STs). This was achieved based on sequence comparisons of housekeeping genes (Salcedo et al., 2003). More specifically, a first MLST analysis that was carried out in 2003 resulted in the identification of 29 Sequence Types with ST2 and ST6 accounting for the majority of the *L. monocytogenes* isolates (Salcedo et al., 2003). Additionally, in 2008, a second optimised analysis resulted in the identification of 126 STs (Ragon et al., 2008). Approximately 58 of all the identified STs were grouped into seven Clonal Complexes (CC1, CC2, CC3, CC4, CC5, CC7 and CC9), (Figure 2), based on common STs common ancestry. The strains belonging in each CC had a single or dominant serotype (4b for CCs 1, 2 and 4; 1/2b for CCs 3 and 5; 1/2a for CC7 and 1/2c for CC9) (Ragon et al., 2008). In 2016, Maury and colleagues conducted a 9-year study in which 63 Clonal Complexes were identified, with 12 CCs of them being responsible for around 80% of all the strains in the study (Mauray et al., 2016). The predominant CCs containing isolates from clinical samples belong to lineage I (CC1, CC6, CC2, CC4), while those overrepresented in food samples are lineage II (CC121, CC9).

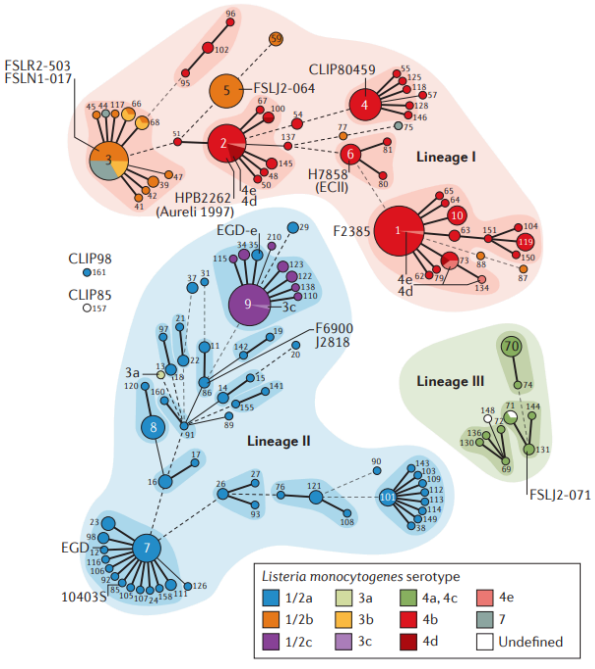

Figure 2: Prevalence and distribution of MLST categories of *L. monocytogenes*; lineages, serotypes and clonal complexes for *L. monocytogenes* differentiation (Adapted from Radoshevich and Cossart, 2018).

3.4 Molecular Subtyping Techniques

The characterization of *Listeria* is based on molecular subtyping techniques, tools used for epidemiological analyses and contributing to the identification of the causative agent, the source, and the route of contamination (Fox et al., 2015; Cherifi et al., 2018; Wang et al., 2017). There are many methods used for the classification of *Listeria* but the most common tools are the Pulsed-Field Gel Electrophoresis (PFGE), Multi-Locus Sequence Typing (MLST) or Multi-Virulence Sequence Typing (MVLST) and the Whole Genome Sequencing (WGS).

3.4.1 Pulsed Field Gel Electrophoresis (PFGE)

For many years, PFGE was considered as the gold-standard due to its very high discriminatory power (Fox et al., 2011). It works by comparing DNA fragments which have been generated by micro-digestion with the restriction enzymes *Asc*I and *Apa*I and have been separated by gel electrophoresis under a pulsed field (Filipello et al., 2017; Wang et al., 2017;Hein et al., 2011). PFGE typically classifies *Listeria* species into genetic lineages, with strains of the same ST generally clustered together (Fox et al., 2015). Despite its advantages, there are a few disadvantages, including the need for expertise, and that it is a labour-intensive technique (Sperry et al., 2008).

3.4.2 Multi-Locus Sequence Typing (MLST) & Multi-Virulence Sequence Typing (MVLST)

MLST is a useful tool since it provides information about both the phylogeny and the evolution of the species (Smith et al., 2019; Fox et al., 2016). It is used for comparison of genomes of closely related species, and is based on sequence analysis of 7 housekeeping genes: *abcZ, bglA, cat, dapE, dat, ldh and lhkA* (Wang et al., 2017). MLST classifies *Listeria* in Sequence Types (STs) and Epidemic Clones (ECs) which are then clustered in Clonal Complexes (CCs). Strains of the same CC share identical sequences for 6 out of the 7 housekeeping genes. MVLST is a similar technique to MLST, however it sequences the internal fragments of 6 *Listeria* virulence genes: *clpP, dal, inlB, inlC, lisR* and *prfA,* and clusters the strains in Virulent Types (VTs) (Zhang et al., 2004). Both techniques have both lower resolution and discriminatory power compared to PFGE, but they provide unambiguous data providing excellent reproducibility.

3.4.3 Whole Genome Sequencing (WGS)

WGS is now considered the leading epidemiological tool for analysis of both national and international outbreak data (Hurley et al., 2019). WGS focuses on genomic characterization of *Listeria* isolates to provide information related to aspects such as stress tolerance and pathogenicity (Fox et al., 2016).

With the reduction in sequencing costs, whole-genome comparative analysis has emerged as the preferred approach for molecular examination of bacterial species. This methodology, known as core genome MLST (cgMLST), relies on gene-by-gene allelic profiling of the core genome and is recognized as the foremost diagnostic tool for strain typing (Ruppitsch et al., 2015). Originally designed for *L. monocytogenes*, the cgMLST encompasses a core genome of 1748 genes (Moura et al., 2017). Its utilisation in analysing 1,696 strains sourced from diverse origins has enhanced the precision of defining the population structure of *L. monocytogenes* compared to traditional PFGE techniques. "CgMLST types" (CTs) are established as categories of cgMLST profiles exhibiting more than seven allelic mismatches. The classification of strains into lineages and sub-lineages (SLs) based on cgMLST aligns well with the MLST sequence-based phylogenetic tree. Lineages III and IV exhibit dispersion into several rare SLs, whereas lineages I and II demonstrate a highly structured organisation into extensive SLs, each encompassing multiple closely related strains. Comparative analysis between SLs identified by cgMLST and CCs defined by MLST highlights a direct correspondence between the two techniques. Consequently, the nomenclature for *Listeria* strains established by cgMLST (SL and CT) can be seamlessly correlated with the widely adopted MLST-defined nomenclature (CC and ST). Furthermore, cgMLST has proven effective in identifying environmentally persistent strains and revealing the international transmission patterns of major SLs (Moura et al., 2017).

IV. General Microbiology

L. monocytogenes is a rod-shaped bacillus of 0.5 to 2 µm long and 0.4 to 0.5 µm in diameter. It is a non-capsulated and non-spore-forming bacterium (Ryser and Marth, 2007) which is motile via flagella movement (Figure 3) at temperatures of 30 °C or below. At temperatures of 37 °C or higher, there is no flagellar biosynthesis and therefore the majority of *L. monocytogenes* are immotile (Nilsson et al., 2011). *L. monocytogenes* is considered as a facultative anaerobic bacterium and during its chemotaxonomy process it has been shown to be positive for catalase and Voges-Proskauer test, while it was negative for oxidase and it is also capable of fermenting many carbohydrates (Anses, 2011).

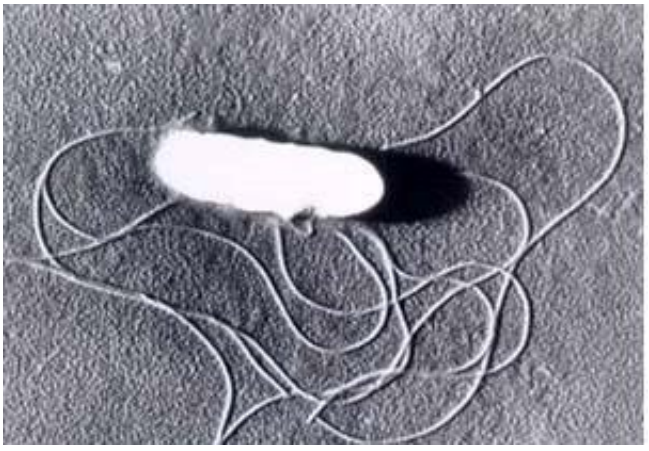

Figure 3: Scanning-Electron-Microscopy (SEM) of *L. monocytogenes* with flagella motility.

L. monocytogenes has a large temperature window which is between 4 °C to 41 °C but with optimal growth between 30 °C to 37 °C (Gandhi and Chikindas, 2007). The ability of *L. monocytogenes* to survive in such a temperature range, allows it to colonise not only in foods but in numerous ecological niches, as well. Additionally, *L. monocytogenes* is highly tolerant in both high salt concentrations and a wide range of pH, but with optimal growth at neutral pH. *L. monocytogenes* is able to survive at acidic pH of 4 for long periods, but it is generally inactivated quickly under more acidic (pH < 3) environments over a 30-minute exposure (Smith et al., 2012).

The high resistance and adaptability of *L. monocytogenes* pose a serious risk to both agricultural and food processing environments (FPEs), increasing the need for monitoring the evolution of this pathogen. Samples deriving from a variety of environments such as sewage plant sludge, manure or

soil are isolated in Fraser broth or in a medium of similar composition and incubated at 30°C or 37°C for 24 to 48 hours. The species identification is based on selective media that allows grow at 37°C for 24h to 48h, including: a) PALCAM Agar and Oxford Agar; which is a combination of lithium chloride and antibiotics aiming to the contaminating microflora inhibition and therefore to the selective growth and isolation of *Listeria* species, b) ALOA-Agar; that is *L. monocytogenes*-specific, and, c) Rapid *Lmono* Agar; which is also a selective medium in order to prevent contaminating microflora from growing. Pathogenic *Listeria*, namely *L. monocytogenes* and *L. ivanovii*, are forming blue colonies while any other *Listeria* species forms white colonies. To differentiate between the two pathogenic species, an extra test that requires xylose fermentation is applied, (*L. ivanovii*, xylose + :Yellow halo; *L. monocytogenes*, xylose - : No halo) (Kortebi, 2018).

V. *L. monocytogenes* cellular envelope

The cell envelope of bacteria is a physicochemical barrier that provides bacteria with the ability to not only perform nutrient and signalling exchanges but to also allow communication between the inside and outside part of the bacterial cell (Bierne and Cossart, 2007).

Bacteria are categorised into Gram positive or negative based on their cell envelope composition. More specifically, the Gram-negative bacteria or diderms are composed by two membranes that are distinguished by a periplasmic intermediate space. On the other hand, Gram positive bacteria or monoderms are characterised by the presence of a cell wall and a single cytoplasmic membrane. As discussed earlier, *L. monocytogenes* is a Gram-positive bacterium and many studies have revealed the importance of its cellular envelope in its pathogenicity and virulence process.

The cell wall of *L. monocytogenes* is formed by the N-acetylglucosamine and N-acetylmuramic acid peptidoglycan, Teichoic Acids (TAs) and Lipoteichoic Acids (LTAs) that are of great importance due to their contribution in anchoring or transporting molecules, carbohydrates and many covalent or noncovalent proteins via a C-terminal LPXTG or other motifs, respectively (Bierne and Cossart, 2007). The cytoplasm is surrounded by a phospholipid bilayer membrane of which the protein content is around 60% (Ghosh and Carroll, 1968). Many of them can be integral membrane proteins, meaning that they are cytosolic proteins but attached to the membrane via transmembrane domains and/or lipoproteins namely covalently attached proteins to the acyl group of two fatty acids (Bierne and Cossart, 2007).

The genome of *L. monocytogenes* EGDe 1/2a strain is composed of 2,944,528 base pairs (bp) and its protein surfaceome is of around 133 proteins (Figure 4) (Cabannes et al., 2002). The proteosurfaceome of *Listeria* has been shown to support the proliferation and adaptability of the bacterium via many processes including: adhesion, invasion and virulence (Cabannes et al., 2002; Bierne and Cossart, 2007). The study of the proteosurfaceome is quite tricky due to not only the low solubility and abundance but also the challenges of extracting surface proteins with low cell lysis contamination. However, many successful studies in the area of *Listeria* proteosurfaceome have been performed throughout the years and they have offered vital insights in terms of its virulence potential (Trost et al., 2005; Dumas et al., 2008; Donaldson et al., 2009).

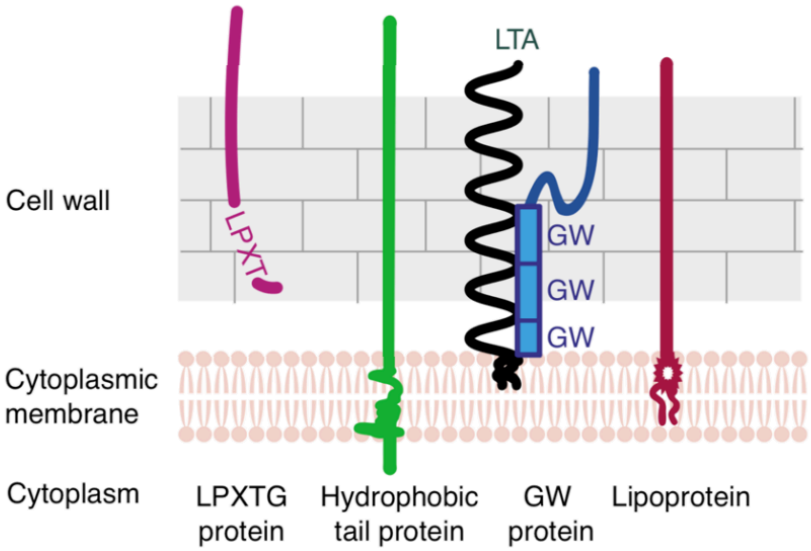

Figure 4 : Cellular envelope proteins of *L. monocytogenes;* The most essential types of surface proteins found in *L. monocytogenes*; 41 LPXTG cell wall anchored proteins, 11 hydrophobic tail proteins, 9 GW with signal peptide proteins and 68 Lipoproteins (Cabanes et al., 2002).

In the early 2000s, Trost and colleagues (Trost et al., 2005) performed a comparative proteomic analysis between pathogenic *L. monocytogenes* and non-pathogenic *L. innocua* strain. What they observed is that there were specific proteins to *L. monocytogenes* of which 16 of them showed no orthologues in the *L. innocua* strain. More specifically, 9 out of these 16 proteins were known virulent markers suggesting one of the first examples in understanding the importance of proteomics in *Listeria* virulence (Trost et al., 2005). Similarly, another proteomic study has suggested the possibility of a virulence pattern for example between the overall protein expression and serotypes but no significant effect was observed between the protein abundance and virulence when comparing different strains (Dumas et al., 2008). On the contrary, Donaldson et al., 2009 performed another comparative proteomic analysis and suggested a significant difference between the abundance of 413 proteins with various roles in cell wall maintenance, stress response, DNA repair and more, when he compared different strains (Donaldson et al., 2009).

Overall, the cellular envelope of *L. monocytogenes* provides a rich environment for deciphering the pathogenicity and virulence potential of *L. monocytogenes.*

VI. Asymptomatic Carriage

Listeriosis is a relatively uncommon disease, however, there has been growing interest in exploring the possibility of a *L. monocytogenes* carriage without causing any noticeable disease. This state has been characterised as asymptomatic carriage.

Around 20 years ago, two distinct studies, one in the USA (Sauders et al., 2005) and one in Austria (Grif et al., 2001) revealed that *L. monocytogenes* was found with a low frequency and more specifically, within 0.12% to 4.7%. Another recent study also showed that *L. monocytogenes* was in less than 5% of the faecal shedding of healthy individuals (Schoder et al., 2022). In 2003 Grif et al., conducted a 3-year-study in which faecal samples from healthy individuals were analysed. The study revealed that 1.2% of the samples were positive for *L. monocytogenes* carriage with all the isolates belonging to the serogroups 1/2a and 1/2b (Grif et al., 2003; Schoder et al.,2022). Another study performed stool analysis of healthy individuals compared to diarrhetic individuals and *L. monocytogenes* was found at 10% and 20.8%, respectively (Hafner et al., 2021). However, several studies have been performed previously with the rate of *L. monocytogenes* carriage to vary from study to study. This could be partially be explained by the differences in: a) the sample group, b) cultivation techniques, as the same stool samples processed with standard microbiological culture and molecular-based techniques have resulted to 2 different carriage rates (Grif et al., 2001), c) replicates and d) samples manipulation.

Studies have shown that the low frequency of *L. monocytogenes* carriage in the stools could be an outcome of the protective effect of gastric acid against pathogens. More specifically, it has been shown that patients that had undergone gastric-suppressant therapy revealed an increase in the *L. monocytogenes* carriage, that was around 20%, with none of these patients developing listeriosis (Cobb et al., 1996). The carriage of *L. monocytogenes* has also been studied among pregnant women to check for a link between *L. monocytogenes* carriage and pregnancy. More specifically, a 2% faecal carriage rate was reported in 51 pregnant women (10-16 weeks), compared to a 3.4% rate observed in 59 non-pregnant women in the same clinic (Lamont and Postlethwaite, 1986; Schoder et al., 2022). These findings would suggest that pregnancy does not affect the *L. monocytogenes* carriage.

Furthemore, Hafner and colleagues (Hafner et al., 2021) also showed that there is an association between faecal carriage and virulence of pathogenic *Listeria* species; *L. monocytogenes* and *L. ivanovii*. Interestingly, it was shown that cows could act as reservoirs of *L. monocytogenes*. More

specifically, among all the *Listeria* species identified in cattle stool samples (6.3%), it was *L. monocytogenes* that was found to be the most abundant. In the healthy human faecal analysis, *Listeria* species were also identified (around 5.2%) but the abundance of *L. monocytogenes* was 40 times less than in the cattle (Hafner et al., 2021).

Additionally, similarities between the gut microbiota associated with *L. monocytogenes* infection and the known microbiome upon infection with other foodborne pathogens have been observed. These observations could suggest that *L. monocytogenes* could be carried asymptomatically (Hafner et al., 2021; Schoder et al., 2022).

Overall, asymptomatic carriage of *L. monocytogenes* especially in healthy carriers and animals as described in Figure 5, could act as reservoirs of *Listeria* meaning that once the conditions are favourable, *Listeria* can be reactivated, replicated and lead to its release in the environment increasing the chance/threat of recurrent listeriosis (Bierne et al., 2018).

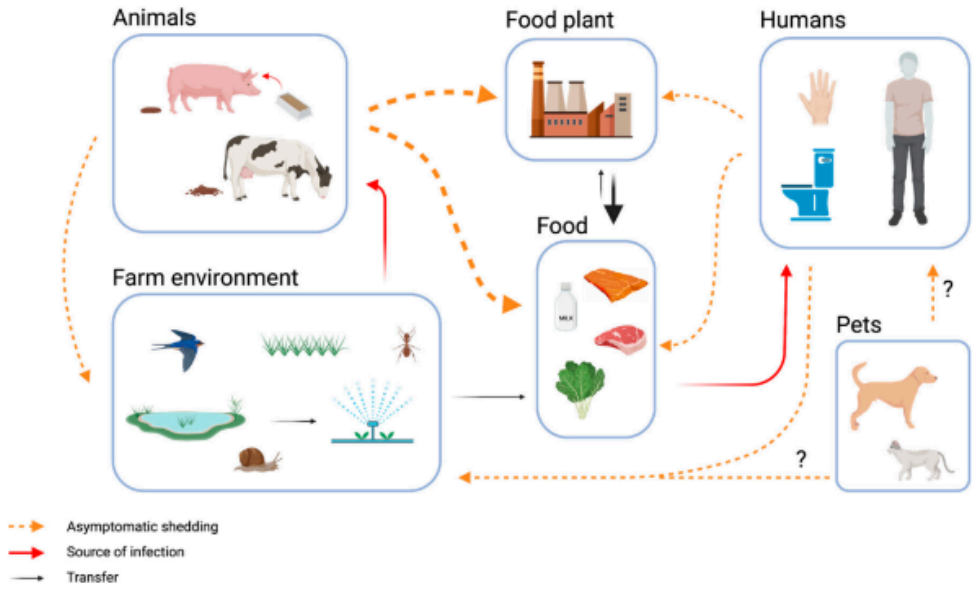

Figure 5: Illustration of the role of asymptomatic faecal carriage of *L. monocytogenes* by humans and animals in various environments (food plants, farms) with a focus on food safety (Schoder et al., 2022).

VII. Infection Process of *L. monocytogenes*

7.1 Host invasion - *in vivo* infection and dissemination

L. monocytogenes is a foodborne pathogen entering the host during the consumption of contaminated food and via the digestion tract. The *in vivo* infection process has been predominantly studied in two different animal models; transgenic mice and guinea pigs. It has been shown that InlA is a central factor in the infection of *L. monocytogenes* at the intestinal level. More specifically, through cell wall-associated InlA, *L. monocytogenes* interacts with the E-cadherin (E-cad) receptor found on epithelial cells and situated beneath tight junctions. Instead of directly disrupting tight junctions, *L. monocytogenes* finds E-cad available at irregular areas of the epithelium, such as cell extrusion sites at the tops of villi, junctions between mucus-secreting goblet cells and adjacent enterocytes, or within the folds of villi, which allows it to enter the cells (Pentecost et al., 2006, 2010; Nikitas et al., 2011). Within goblet cells, *L. monocytogenes* is found in a vacuole, which is then transported to the basal side of the cell via a transcytosis-like process and released into the lamina propria.

The crossing of the intestinal barrier by *Listeria as* described in the transgenic mouse model suggested that human E-cad is exposed in enterocytes suggesting *L. monocytogenes'* internalisation and transcytosis in the intestinal lumen leading, eventually, to its release into the lamina propria by exocytosis and, thus, dissemination via the bloodstream (Nikitas et al., 2011). The second study performed in the guinea pig showed that the intestinal villi could be an ideal niche for bacterial replication as *L. monocytogenes* is undergoing replication, multiplication, and dissemination to neighbouring cells through cell-to-cell spread. *L. monocytogenes* is then passed onto lamina propria from where it manages to disseminate into the intestinal lumen infecting Peyer's patches, leukocytes and other enterocytes (Melton-Witt et al., 2012). *L. monocytogenes* is then disseminated to the liver and the spleen via the bloodstream and/or the lymphatic system (Figure 6).

More specifically, dissemination to the liver can occur through two pathways: directly via the hepatic portal vein from the intestine or indirectly from the spleen or mesenteric lymph nodes but the vast majority of the *Listeria* carriage in the liver is based on dissemination via the direct route. (Melton-Witt et al., 2012). The bacteria reach the bone marrow, liver, and spleen, where most are phagocytosed by macrophages. In the liver, *L. monocytogenes* rapidly replicates within resident

macrophages and invades hepatocytes. At this stage, the disease is often controlled in immunocompetent individuals, resulting in a minimal, often asymptomatic infection. However, when the host's immune defence system fails to control the infection, *L. monocytogenes* replicates and spreads in other vital organs including the brain and the placenta by crossing the host's epithelial barriers, particularly in immunocompromised individuals and pregnant women.

Dissemination of *L. monocytogenes* to the central nervous system results in meningoencephalitis, a disease affecting both the meninges and the brain. Internalin B (InlB) has been characterised as the key mediator for the neuroinvasion. More specifically, it prevents infected monocytes from apoptosis resulting in spreading and replication of *L. monocytogenes* in the brain (Maudet et al., 2022).

As for the transplacental contamination, many studies have been conducted over the years but the molecular mechanisms responsible for it are yet to be described. Overall, it has been shown that host invasion and infection internalisation virulence markers are essential for placenta infection as well. Nevertheless, the placenta phase of listeriosis is described in more detail in the following section B.

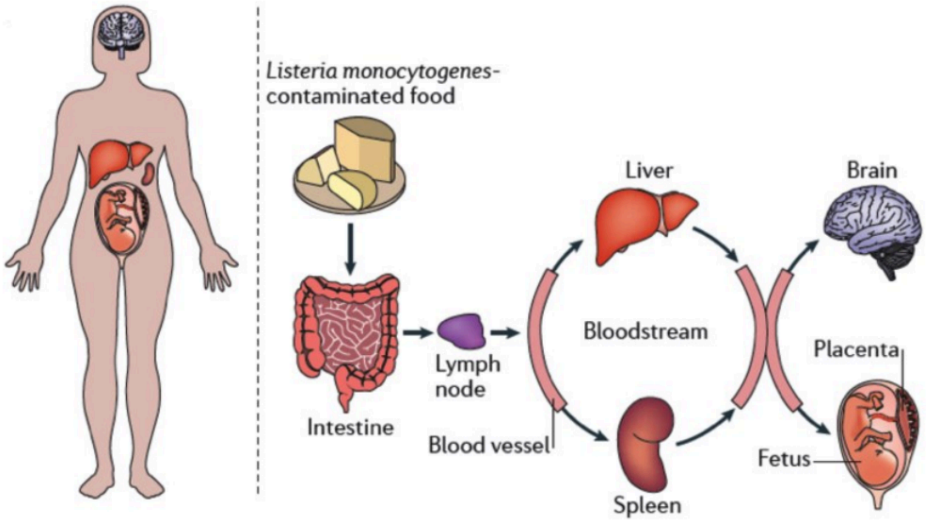

Figure 6: Upon ingestion of the contaminated food, *L. monocytogenes* passes into the intestines and the lymph nodes from where it disseminates to other vital organs via bloodstream circulation (crossing of blood brain barrier, blood placenta barrier, etc) leading to potential severe diseases (Adapted from Radoshevich and Cossart, 2018).

7.2 Cellular infection

L. monocytogenes is a facultative anaerobic and intracellular bacterium. It can both survive phagocytosis in macrophages and dendritic cells and it can invade and multiply in non-phagocytic cells, namely in epithelial and endothelial cells. *L. monocytogenes* is entering into the host cell and it is trapped into a primary or entry vacuole from which it escapes rapidly with the help of inlA and inlB, PlcA and PlcB virulent factors that are discussed in more detail in section 7.3. *L. monocytogenes* is then free in the cytoplasm to replicate and at this point there is an upregulation of the ActA protein and bacteria take control of the host's actin cytoskeleton resulting in them moving in neighbouring cells into some protrusion forms, resulting into the secondary vacuole (Figure 7). These vacuoles are also lysed, and *L. monocytogenes* are free in the cytoplasm again. This process allows *L. monocytogenes* to efficiently spread in a cellular monolayer (Camejo et al., 2011).

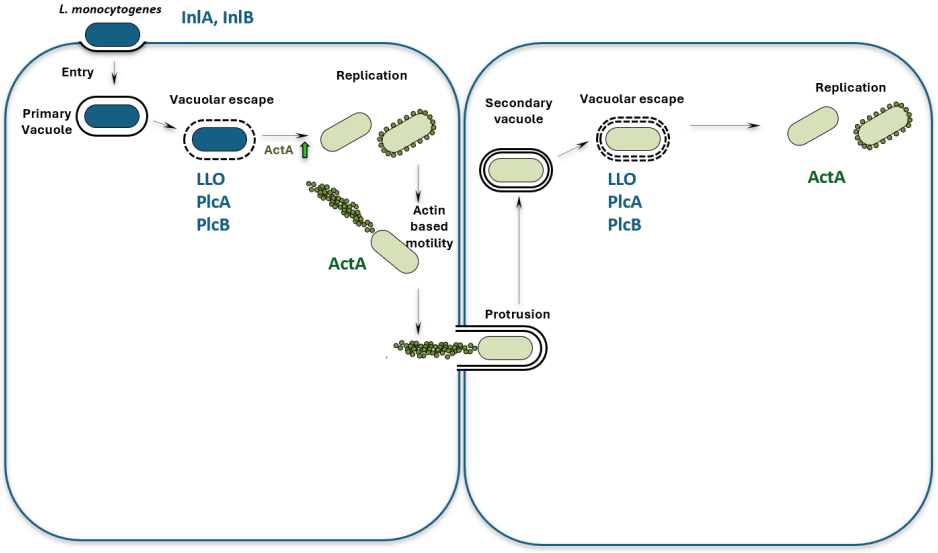

Figure 7: *L. monocytogenes* internalization into epithelial cells is mediated by the internalins A and B (InlA, InlB). Once internalized, the bacteria are captured into a vacuole, from which they escape by secreting two phospholipases (PlcA, PlcB) and a pore-forming toxin, listeriolysin O (LLO). *L. monocytogenes* is then free in the cytoplasm to replicate. In addition, *L. monocytogenes* facilitates actin polymerization via its surface protein ActA enabling its entry into neighbouring cells into membrane protrusion forms. *L. monocytogenes* is then trapped into a secondary vacuole and the infection cycle repeats as the bacterium escapes the double-membrane vacuole in neighboring cells (Kortebi et al., 2017).

7.3 Virulence Factors

The 1980-1990 window can be characterised as the gold decade for molecular biology advancements. It is thanks to the flourishing of this study that our understanding for the pathogenicity and virulence of *L. monocytogenes* was established. In this section the most important virulent players that allow the *L. monocytogenes* proliferation during different stages of intracellular infection are briefly explained. These genes are regulated by PrfA which is the master transcriptional regulator of the *L. monocytogenes virulence* cohort. The PrfA regulon is splitted into two main chromosomal regions, the *inlAB* locus; encoding the *inlA* and *inlB* and the LIPI-1, standing for *Listeria* Pathogenicity Island 1, that is composed by *prfA, hly, actA, plcA, plcB* and *mpl* (Figure 8). Overall, the intracellular lifestyle of *L. monocytogenes can* be separated into 3 stages : i) internalisation supported by the *inlAB* locus, ii) vacuolar and cytosolic phases and iii) cell-to-cell spread, accompanied by different virulent genes part of the LIPI-1.

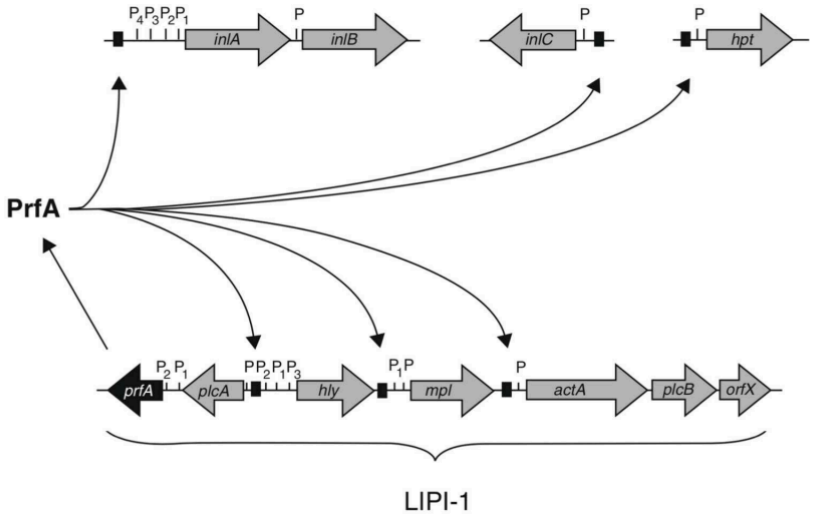

Figure 8 : The core *L. monocytogenes* PrfA regulon (PrfA in black box); LIPI-1 encoding *prfA, hly, actA, plcA, plcB, mpl* and *orfX*, plus another major chromosomal locus; the *inlAB* operon and two more chromosomal loci; the *inlC* and *hpt* monocistronic (adapted from las Heras et al., 2011).

7.3.1 Internalisation via InlAB locus

L. monocytogenes manages to infect the host via zipper mechanisms that are described by its internalisation into non-phagocytic cells, like epithelial cells, assisted by the *inlAB* locus. The *inlAB* locus contains the *inlA* and *inlB* that are part of a wider family called internalins. Internalins can have various functions but all of them have an N-terminal signal peptide and Leucine-Rich-Repeats suggesting a structural resemblance within the complete family cohort. In *L. monocytogenes the*

inlAB was first characterised in 1991 by Gaillard and colleagues (Gaillard et al., 1991) where it was observed that knock-out *inlAB* mutants were unable to invade Caco-2 epithelial cells confirming that the InlAB interactions with host surface receptors allowed the internalisation of *L. monocytogenes*. More specifically, InlA binds the human E-cadherin while the InlB binds to Met, the receptor of the hepatocyte growth factor (HGF), and through interactions with InlA the entry into mammalian cells is established.

7.3.2 Vacuolar and Cytosolic lifestyles

Once *L. monocytogenes* engulfment has been established the bacterium is captured in a membrane bound vacuole. During the first 20-30 minutes, *L. monocytogenes* manages to escape the vacuole via the activations of both a) the LLO, a cholesterol dependent pore forming toxin, encoded by the *hly* gene inducing haemolysis and b) that of the secreted phospholipases C (PLC), PlcA that is in active form and PlcB that is activated by the zinc metalloproteinase (Mpl). Apart from activating the PlcB under ideal pH conditions, the Mpl is also essential for the formation and retaining of protrusions into secondary vacuoles. The LLO has distinct features compared to other cholesterol dependent cytolysins resulting in its key intracellular characteristics that prevent the host plasma membrane from permeabilization and consequently cell death. The PLCs act together with LLO to promote *L. monocytogenes* escape from both primary and secondary vacuoles (Pizarro-Cerda and Cossart, 2018).

7.3.3 Cell-to-cell spread

Upon its escape from the early vacuoles and while in the cytosol, *L. monocytogenes* takes control of the host's epithelial machinery and there is an upregulation of the actin assembly inducing protein (ActA). ActA is responsible for the formation of comet tails and promotes the motility of *L. monocytogenes* within the cytosolic environment. This adaptation trait of *L. monocytogenes* is of utmost importance as it contributes in evading autophagy and allows dissemination within the tissues. More specifically, *L. monocytogenes* is spreading into neighbouring cells via protrusion forms, namely double-membrane-vacuoles of which it manages to escape again and keep replicating in the newly infected cells. Several studies have suggested that deletion mutants are impaired in terms of virulence. Additionally, another set of studies have highlighted other functions of ActA. Some of them are ActA supporting not only extracellular aggregation but biofilm formation and autophagy evasion, as well. These properties highlight once more the importance of this virulence factor.

VIII. Mechanisms of *Listeria monocytogenes* persistence

There are many different ways to define persistence, but, in principle, persistence is affected by a variety of genetic and/or phenotypic variations. Most usually persistence is defined as the long-term survival of a pathogen in the host which is described as persistent infection (Lotoux et al., 2022). Additionally, the long-term survival of a food-pathogen, in e.g. a food processing environment, is described also as persistence (Ferreira et al., 2014). Similarly, certain subpopulations of persistent bacteria that are antibiotic-resistant are called persisters. In addition, another form of persistence is characterised by the Viable-But-Non-Culturable (VBNC) bacteria, (Ayrapetyan et al., 2018; Lotoux et al., 2022). VBNC bacteria are viable but unable to grow on routine media and are characterised by a low metabolic state. As VBNC do not grow, they are also resistant to a plethora of antibiotics that normally target vegetative cells (VBNC in section 8.3).

8.1 Persistence in Food Processing Environments (FPEs)

Given its tolerance to a wide range of environmental conditions for growth or survival, *L. monocytogenes* demonstrates an ability to adapt in a variety of environments, including FPEs. *L. monocytogenes* generally manages to establish and persist in FPEs due to insufficient sanitisation methods, however a number of molecular mechanisms have been implicated in persistence. The persistence of strains in niches within the FPE are considered of vital importance for the dissemination and post-processing contamination of foods. As mentioned, although persistence of *L. monocytogenes* can be a problem linked to poor hygiene, a number of studies have shown the involvement of genetic markers related to *L. monocytogenes* adaptation in low and high temperatures, in acidic and alkaline environments, the benefit of biofilms, and resistance to disinfectants and heavy metals, as well (Osek et al., 2022).

8.1.1 Adaptation to wide range of temperature

Resistance of *L. monocytogenes* to low temperature results in tolerance and persistence of *L. monocytogenes* in refrigeration conditions (Osek et al., 2022; Tasara and Stephan, 2006). In order to prevent the cell membrane from alterations that could impact bacteria's structural and functional integrity, *L. monocytogenes* implements the use of cold-shock proteins (Csps) and cytoprotective compounds (Gandhi and Chikindas, 2007; Bukur et al., 2008). More specifically, at around 4-10 °C *L. monocytogenes* produces Csps, small proteins with roles in modulation of stress and virulence

(Bayles et al., 1996; Eshwar et al.,2017). More specifically, the *cspA* gene has been recently found to offer resistance to low temperatures (Muchaamba et al., 2021). Similarly, *L. monocytogenes* produces Heat-Shock proteins (Hsps) which are classified into three distinct categories: I) stabilisation and repair of denatured proteins (Bukur et al., 2018), II) transcriptionally SigB-dependent stress proteins and III) proteases (ClpP) and molecular chaperones (ClpE, ClpC) (Karatzas et al., 2003). Thermal treatment is a method of removing *L. monocytogenes* from products when the temperature is higher than 45 °C, and ideally when bacteria are treated at 55 °C for 10 min and then at 65 °C for 25 sec (Osek et al., 2022; Bucur et al., 2018); however, *L. monocytogenes* can demonstrate resistance to high temperatures. Strain serotype also appears to impact heat inactivation efficacy; for example, serotype 1/2a is typically less resistant to high temperatures compared with the more heat-resistant 1/2b and 4b serotypes (Doyle et al., 2001; Osek et al., 2022).

8.1.2 Stress Resistance

L. monocytogenes has not only acquired methods to resist a wide range of temperatures, but it has acquired mechanisms to resist several other stressors. *L. monocytogenes* contains mobile genetic elements such as the Stress Survival Islets (SSIs), part of the accessory genome that allow bacteria to surpass a range of stresses and thus persist under adverse environmental conditions despite the long-term cleaning procedures (Harter et al., 2017). SSI-1, an 8.7 kbp region that consists of five genes, is regulated by the SigB factor and can be activated both under stress and non-stress conditions but mostly under acidic stresses (Ryan et al., 2010; Hein et al., 2011; Harter et al., 2017). *L. monocytogenes* may survive acidification- or sanitization-associated conditions and persist in such environments, in a similar manner to that of host infection (Ryan et al., 2008; Osek et al.,2022). SSI-2 consists of two genes and it is activated under alkaline and oxidative conditions; this genetic element is linked primarily to food system-associated ST121 isolates. It has been suggested that SSI-2 has been transferred from *L. innocua* to *L. monocytogenes* via Horizontal Gene Transfer (HGT), as the GC content of SSI-2 is closer to that of *L. innocua* than of *L. monocytogenes*, and this marker has been identified in both species. Additionally, SSI-2 is believed to be either self-regulated or by other regulators such as SigH, which participates in the adaptation of bacteria under both nutrient limitation and alkaline stresses or SigL which benefits the survival of the cells in low temperature and in the presence of organic acids, antibiotic compounds and toxins (Ryan et al., 2010; Hein et al., 2011; Harter et al., 2017). Alkaline components are used in many disinfectants targeting the elimination of *L. monocytogenes*. However, their concentration is sometimes sublethal to *L.*

monocytogenes and that results in a resistance, and therefore persistence, of *L. monocytogenes* in FPEs. In order to survive in the alkaline environments of around pH 8-8.5, Giotis and colleagues (Giotis et al., 2007) has shown that *L. monocytogenes* not only change their length and radius but they also modify their lipid composition in the cell membrane. More specifically, an increase of the ratio of anteiso-branched chain fatty acids (BCFAs) was shown, that could result in the survival of *L. monocytogenes* in alkaline environments (Giotis et al., 2007; Giotis et al., 2009).

8.1.3 Disinfectants resistance

Disinfectants are widely used in FPEs hygiene regimes to eradicate or eliminate *L. monocytogenes* from the environment and equipment, and prevent cross-contamination of products (Bridier et al., 2011). Among the most commonly used sanitizers, Quaternary Ammonium Compounds (QACs), especially Benzalkonium Chloride (BC), are utilised, since they are considered to have low toxicity and non-corrosive properties (Kode et al., 2021). Disinfectants consist of active agents that interact with the cytoplasmic membrane, or they bind to the bacterial DNA (Zinchenko et al., 2004). More specifically, these active agents are absorbed in the bacterial cell wall proceeding to a disruption of cytoplasmic membrane and the release of the intracellular content following by protein and DNA degradation and ending up in the lysis of the bacterial cell wall by autolytic enzymes (McDonnel, 2017). The widespread use of disinfectants can pose a threat for development of resistance to disinfectants through selective pressure mechanisms, driving genetic mutation or acquisition of genetic markers through horizontal gene transfer events within the FPEs (McDonnell and Russell, 1999; Ferreira et al., 2014; Fox et al.,2011; Palaiodimou et al.,2021). It has been proposed by several studies that disinfectant resistance could be a characteristic of persistence in FPEs. This suggestion was supported by the prevalence of specific *L. monocytogenes* STs, e.g. ST121 and ST204, that are highly associated with food and FPE contamination, but the correlation between the persistence of specific strains in FPEs fluctuates (Kastbjerg and Gram 2009; Fox et al. 2011; Schmitz-Esser et al., 2015; Fox et al., 2016; Rodrıguez-Campos et al. 2019; Palaiodimou et al.,2021). Several comparative analyses between persistent and presumed non-persistent strains have been conducted aiming to the identification of genetic markers that could have an implication to the disinfectant resistance and therefore persistence of *L. monocytogenes* in the FPEs. However, no clear link between persistence and disinfectants' tolerance has been shown (Holah et al., 2002; Kastbjerg and Gram, 2009; Wang et al., 2015; Costa et al., 2016; Palaiodimou et al.,2021).

8.1.4 Heavy Metals Resistance

Heavy metal resistance has been associated with *L. monocytogenes* persistence in the FPEs. Heavy metals can be found in soils and fertilisers, and do not readily degrade over time; as such, their presence may influence the adaptation of heavy metal resistant strains of *Listeria*. Cadmium and arsenic resistance cassettes are two of the most interesting stress related resistance markers linked to *L. monocytogenes* endurance in the food industries, and they have also been linked with major food listeriosis outbreaks worldwide. Studies assessing the prevalence of cadmium resistance have indicated a range within 50-66% and that a pattern of cadmium resistance has been observed in repeatedly isolated strains compared to sporadically ones, especially in the case of dairy products. Cadmium is usually isolated from 1/2a serotypes while arsenic is mostly associated with 4b serotypes (Parsons et al., 2018; Parsons et al., 2020). In addition, studies have revealed that cadmium is more prevalent across food related samples compared to arsenic that is mostly found in clinical samples (Parsons et al., 2018; Parsons et al., 2020). Several studies have also shown that ArsR members, that are metal associated transcription regulators, act as a regulator of the PhoPR two component regulatory system that is responsible for genes related to virulence and persistence in *Mycobacterium* species (Parsons et al., 2018). It has been indicated that in *L. monocytogenes*, the cadmium resistance regulator CadC is part of the ArsR family and it has been shown to affect the virulence of *L. monocytogenes* when tested *in vivo*. Other studies have also shown that when it comes to serotype 4b, the cadmium and arsenic can co-exist in a 35 kb chromosomal region, LGI2, and it has additionally been observed that arsenic resistant isolates are also cadmium resistant, while the reverse is not always the case (Parsons et al., 2018; Parsons et al., 2020). The arsenic cassette has been described in mobile genetic elements too, like in the case of the transposon Tn*554*, which has been linked with the prevalence of other to 4b serotypes (Parsons et al., 2018; Parsons et al., 2020).

8.1.5 Biofilms

Biofilms are defined as communities of microorganisms that can be attached to both biotic or abiotic environments (Santos 2022). They form this matrix by producing a water-rich-gel-like extracellular polymeric substance allowing bacteria to be bound together. In *L. monocytogenes*, biofilm formation not only protects bacteria from adverse conditions in FPEs like the application of antibacterials, disinfectants and/or heavy metals, but it also increases their resistance to such compounds. It has been shown that *L. monocytogenes* can produce biofilms in a variety of temperatures, but at 37 °C it

is significantly thicker, thus, more resistant (Santos 2022). However, the high resistance of *L. monocytogenes* to a diverse temperature window, increases the possibility of cross-contamination within the FPEs. Additionally, it has been shown that *L. monocytogenes* once in a biofilm can survive for up to 49 days against desiccation conditions (Santos 2022). Therefore, it has been suggested that the hydrophilic nature of biofilms can enable the resistance to desiccation and thus increase *L. monocytogenes* persistence in the FPE settings.

8.2 Persistence in Hosts

8.2.1 Spacious *Listeria* containing phagosomes (SLAPs)

In 1998, a study focusing on chronic listeriosis and performed in Severe Combined ImmunoDeficiency (SCID) mice revealed a new intracellular niche for *L. monocytogenes* (Bhardwaj et al., 1998). More specifically, after a 3-week-infection, samples from hepatic macrophages were analysed and the vast majority of *L. monocytogenes* were captured into large single-membranous vacuoles (Bhardwaj et al., 1998). A decade later, a similar experiment performed again in SCID mice, identified that 86% of *L. monocytogenes* were captured into large vacuoles of around 7 μm diameter and positive for the endosomal/lysosomal marker LAMP1 (Birmingham et al., 2008) (Figure 9). It was further shown that these vacuoles are derived from non-lysed phagosomes as they never made it into mature phagolysosomes. It was also shown that these vacuoles were non-acidic and marked by the autophagy marker LC3. and thus, they were named as Spacious-*Listeria*-Containing-Phagosomes (SLAPs). The intra-SLAPs *L. monocytogenes* revealed a low abundance of LLO which resulted in decreased ability of *L. monocytogenes* to exit the phagosome. However, the production of LLO was at sufficient levels in order to prevent the phagosome from maturation and therefore assist to the SLAPs formation (Birmingham et al., 2008). Another set of studies performed in 2013 provided deeper insights regarding the formation of SLAPs. More specifically, it has been shown that the SLAPs biogenesis is indeed LC3-associated which occurs via LAP which is a non-canonical autophagy pathway (Lam et al., 2013). More essentially, LC3 protein is recruited to the phagosomal membrane and it is later undergoing a lipidation process through the production and employment of Reactive Oxygen Species (ROS) (Schille et al., 2018). Ultimately, it has been suggested that *L. monocytogenes* takes control over the LAP pathway for their benefit, avoiding self-degradation via a mechanism assisted by LLO production, as suggested by Birmingham et al., 2008, leading to the first characterised form of intravacuolar persistence (Lam et al., 2013).

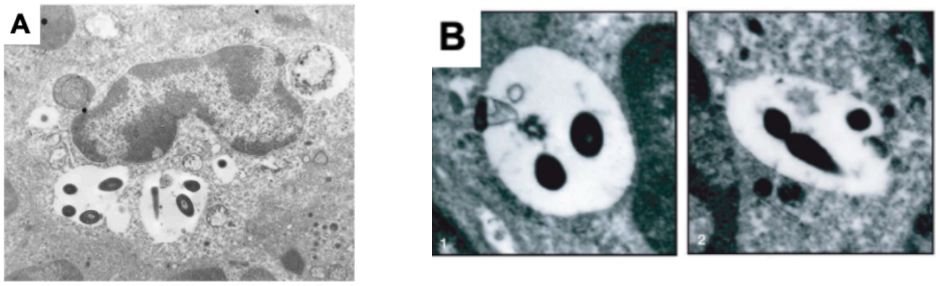

Figure 9: Transmission Electron Microscopy of SLAPs; (A) Transmission electron microscopy of liver macrophages from SCID mice infected for 21 days. Intact *L. monocytogenes* are identified in phagolysosomes in mononuclear cells (Bhardwaj et al., 1998), (B) Transmission electron microscopy SLAP in hepatic granulomas after 21 days of infection of SCID mice (Birmingham et al., 2008). (Figure adapted from Lotoux et al., 2022)

8.2.2 Epithelial SLAP-like (eSLAPS)

Recently, such an intracellular vacuole was described in intestinal epithelial cells (LoVo cell lines) and more specifically with characteristics quite similar to the SLAPs (Table 3) (Peron-Cane et al., 2020). These newly identified vacuoles were named as eSLAPS standing for epithelial SLAPs. In contrast to the SLAPs that are slow-growing forms and potentially serving as persistent intravacuolar niches for *L. monocytogenes* (Birmingham et al., 2008; Bierne et al., 2018), eSLAPS are transient for several hours and they allow efficient replication of *L. monocytogenes* (Penon-Cane et al., 2020).

8.2.3 *Listeria* containing vacuoles (LisCVs)

As was described earlier, during its infection process and until the acute phase of infection, *L. monocytogenes* is captured within a primary and a secondary vacuole that contribute to *L. monocytogenes* attachment and entry to the host cell and dissemination to neighbouring cells, respectively (Figure 10). In 2017, it was identified by our laboratory that during the chronic phase of infection which was described at around 72h post-infection (p.i.), there is a downregulation of the actin-nucleating protein (ActA) and *L. monocytogenes* is captured into a tertiary vacuole which occurs by a xenophagy-like process together with some lysosomal fusion (Figure 10). This tertiary vacuole has been called as LisCVs which stands for *Listeria*-Containing-Vacuoles.

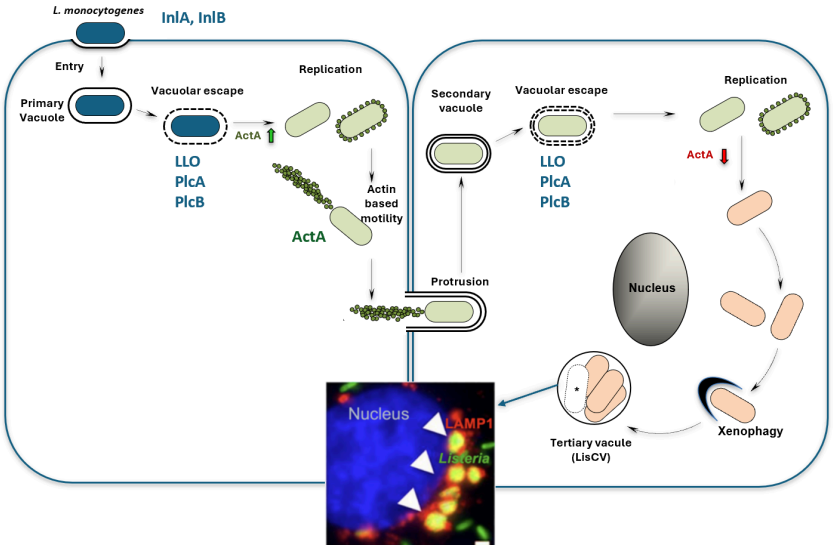

Figure 10: Following its escape from the secondary vacuole, during the later stages of infection (72h p.i), *L. monocytogenes* ceases ActA production. While the bacteria continue to replicate in the cytosol, by 72h p.i., they are captured through an uncharacterized xenophagy-like mechanism that involves fusion with lysosomes, forming a tertiary vacuole known as the LisCV. These LisCVs contain a heterogeneous bacterial population, including degraded bacteria (marked with *) and intact bacteria with reduced metabolic activity (adapted from Kortebi et al., 2017).

LisCVs have been studied in epithelial cells and more specifically in hepatocytes and trophoblasts (Figure 11). More specifically, LisCVs are single-membranous and LAMP1-positive vacuoles and are quite different from SLAPs and eSLAPs intracellular compartments (Table 3). Fundamentally, LisCVs are positive for the lysosomal marker cathepsin-D, they are acidic, and do not derive from primary vacuoles. Instead, they are formed by a still-uncharacterized mechanism, independent from classical autophagy, which engulf cytosolic bacteria. Importantly, despite their acidic environment, the majority of *L. monocytogenes* remains intact inside LisCVs. Inside LisCVs bacteria are mostly non-dividing and a subpopulation enters into the VBNC state inside LisCVs (Kortebi et al., 2017).

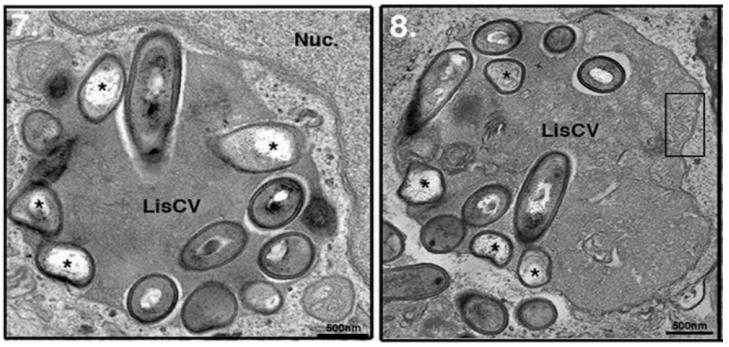

Figure 11: Illustration of intracellular lifestyle of *L. monocytogenes* in LisCVs via TEM. (Adapted from Kortebi et al., 2017)

On top of that, it has been found that 60-80% of *Listeria* were already intravacuolar at 72h post-infection (p.i.) which suggests that *L. monocytogenes* was entering into a non-motile state. Additionally, LisCVs have been shown to remain intact during mitosis and segregate randomly in daughter cells, suggesting that non-replicating *L. monocytogenes* could spread during tissue regeneration after acute infection (Bierne et al., 2018). It has been suggested that *L. monocytogenes* uses the intravacuolar lifestyle in order to successfully evade the cytosolic surveillance pathways, for example autophagy, during the long-term infection to create a persistence life-form within the host (Bierne et al., 2018). The intravacuolar lifestyle could therefore have a role in the asymptomatic carriage and transmission of *L. monocytogenes* (Bierne et al., 2018).

8.2.4 Replication-permissive SLAPs (rSLAPs)

In 2022, a new intracellular lifestyle that allows the slow intravacuolar replication of *L. monocytogenes* was studied in macrophages. This new vacuole is single-membranous and with close proximity to mitochondria and has been named as rSLAPs standing for replication-permissive SLAPs (Figure 12). Their biogenesis requires the presence of the PrfA regulator and more specifically it has been shown that once the activity of PrfA is inhibited, *L. monocytogenes* cannot escape from the phagosomes. rSLAPs are formed with the involvement of LLO protein which also provides the necessary conditions for intravacuolar replication (Birmingham et al., 2008; Peron-Cane et al., 2020). The rSLAPs show many cross-similarities with all the aforementioned intravacuolar lifestyles (SLAPs, eSLAPs and LisCVs), (Table 3). It has been proposed that rSLAPs formation is a result of both bacterial and host associated features and that rSLAPs mature into degradable lysosomal compartments fast (Tran et al., 2022). Therefore, due to the *L. monocytogenes* elimination it has been assumed that rSLAPs intravacuolar lifestyle does not necessarily implies intracellular persistence (Tran et al., 2022) which comes in contrast with Bierne and colleagues suggestion that slow replication of intravacuolar *L. monocytogenes* could promote asymptomatic carriage leading to latent listeriosis (Bierne et al., 2018).

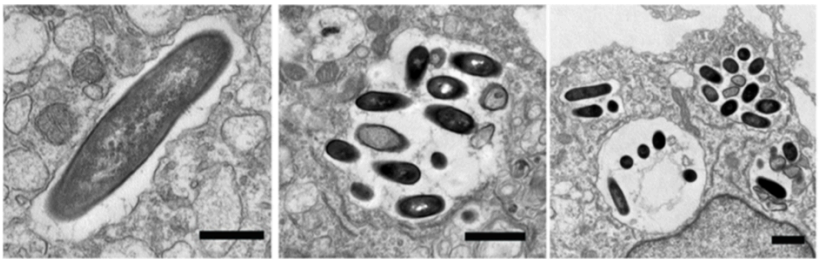

Figure 12: Formation of rSLAPs observed by TEM at 4h (left), 10h (middle) and 24h (right) in murine bone marrow-derived macrophages (Adapted from Tran et al., 2022).

Overall, the formation of intracellular niches such as SLAPs (Spacious *Listeria*-containing Phagosomes) and LisCVs (*Listeria*-containing Vacuoles) can enhance the persistence of *L. monocytogenes*. Within SLAPs, located in macrophages, *L. monocytogenes* bacteria are protected from degradation and can survive long-term because SLAPs do not fuse with lysosomes (Birmingham et al., 2008; Lam et al., 2013). In LisCVs, *L. monocytogenes* mutants lacking the ActA protein (EGDe-ΔactA) are more effectively contained within vacuoles compared to the wild-type strain after 3 days of infection. Over a 10-day period, these bacteria are visible within vacuoles with an intact membrane but do not form colonies on plates, indicating they might persist in epithelial cells for days or weeks in a viable but non-culturable (VBNC) state.

Table 3 : Characteristics of the different intravacuolar lifestyles of *L. monocytogenes.*

Category	Spacious *Listeria*-containing Phagosomes (SLAPs)	Epithelial SLAP-like Vacuoles (eSLAPs)	Replication-permissive SLAPs (rSLAPs)	*Listeria*-containing Vacuoles (LisCVs)
Cell Types	Murine macrophages: - Cell lines (RAW264.7, J774) - Bone marrow-derived macrophages	Epithelial cells: - Colon cancer cell lines (LoVo, Caco-2)	Murine macrophages: - Cell lines (RAW264.7)	Human epithelial cells: - Hepatocyte cell lines (HepG2, Huh7), trophoblast cell lines (JEG-3, BeWo) - Primary human hepatocytes
Vacuole Characteristics	Large single-membrane vacuole	Large single-membrane vacuole	Large single-membrane vacuole	Single-membrane vacuole
Markers	LAMP1-positive	LAMP1-positive	LAMP1-positive	LAMP1-positive
pH	Neutral	Neutral	Acidic	Acidic
Infection Time	Early infection (1-4h)	Short infection (up to 24h)	Early infection (4-24h)	Late infection (2-3 days)
Proportion of Internalised Lm	Low proportion	Low proportion (12% for EGD-e)	High proportion	High proportion (70-80% after 3 days)
Replication	Slow or non-existent	Rapid	Rapid	Slow or non-existent
Process	May be associated with phagocytosis LC3	Process similar to LAP	Derives from entry vacuole (phagosome)	Passage to cytosol before LisCVs formation
Evidence in Tissues	Presence in SCID mouse tissues for 21 days with strain 10403S	No evidence in tissues	No evidence in tissues	No evidence in tissues
References	Bhardwaj et al., 1998; Birmingham et al., 2008	Peron-Cane et al., 2020	Tran et al., 2022	Kortebi et al., 2017

8.3 Viable But Non Culturable Bacteria (VBNC)

Persistence is usually a term used to describe a specific state referring to a subset of bacteria that can withstand lethal stress and be repeatedly isolated from samples. This concept encompasses the long-term survival of pathogens in different environments such as the host, on surfaces, in food matrices, or within biofilms. Survival mechanisms associated with persistence include low metabolism, dormancy and/or eventually a state known as viable but not culturable (VBNC) (Figure 13). The shift to VBNC state is a survival tactic used by many bacteria, including *L. monocytogenes*, to withstand various environmental challenges. The VBNC state involves a reversible form of dormancy

where bacterial cells slow down their activity and can survive for extended periods without dividing. VBNC bacteria temporarily lose their ability to proliferate on standard culture media, where they typically form colonies. However, they can regain their growth potential under specific conditions through a process known as resuscitation (Oliver, 2010; Zhao et al., 2017). The VBNC state of *L. monocytogenes* has been described both environmentally; in aquatic environments (Besnard et al., 2000; Carvalho et al., 2024) and in human cells, as well (Kortebi et al., 2017). Additionally, VBNC bacteria could not only evade detection methods in FPEs leading to product cross-contamination but are also thought to be involved in asymptomatic infections and play a role in bacterial persistence within the host, too (Lotoux et al., 2022).

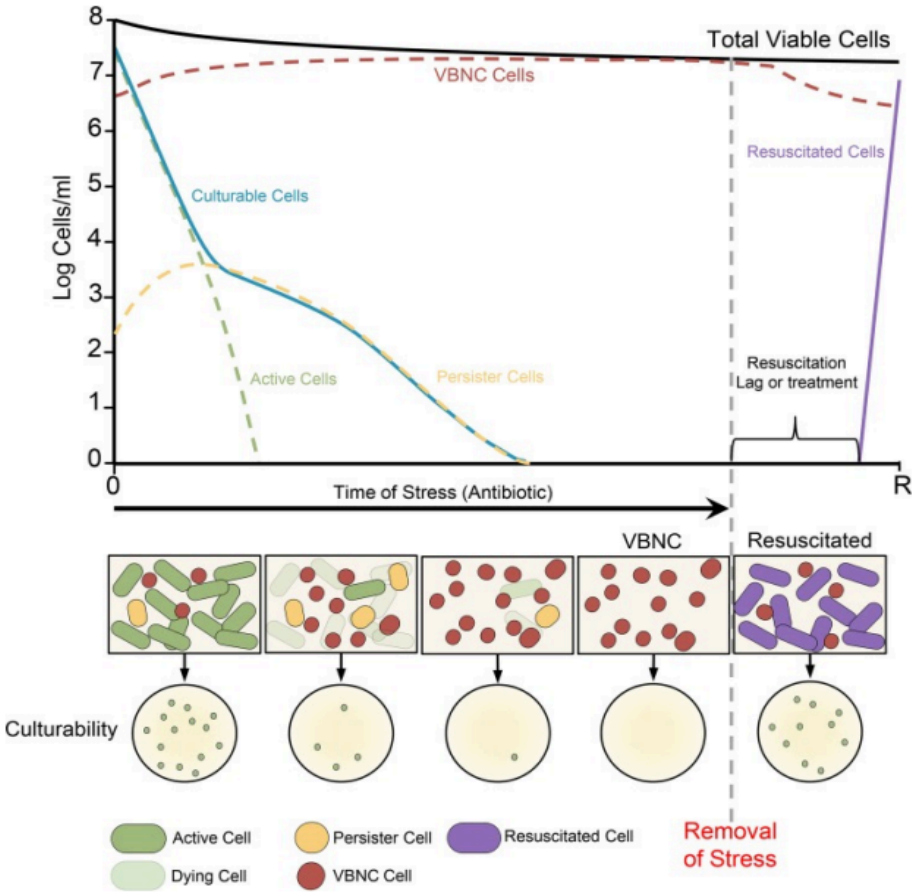

Figure 13 : Identification of dormant *L. monocytogenes* cells, persisters and VBNC cells upon antibiotic exposure, (Adapted from Ayrapetyan et al., 2018).

B. Placenta and placental phase of listeriosis

Having explained the pathogenesis of the intracellular human pathogen *L. monocytogenes*, how the disease is being internalised, how infection progresses both *in vitro* and *in vivo* and most importantly how *L. monocytogenes* manages to persist and enter into the VBNC state, we will focus on an organ that *L. monocytogenes* has a known tropism: the placenta.

I. The human placenta

During the early stages of pregnancy, the placenta is the first foetal organ to be developed. The placenta is a circular and discoidal-like organ (Turco and Moffet, 2019). A normal delivered placenta varies in diameter, thickness and weight that are usually around 22cm, 2.5cm and 470g, respectively (Turco and Moffet, 2019; Cindrora-Davies and Sferruzzi-Perri, 2022). There are four stages of placenta development: a) pre-implantation, b) pre-lacunar, c) lacunar and d) villus (Figure 14). The key to a successful pregnancy is the right function of the trinity: placentation, decidualization and implantation (Khorami-Sarvestani et al., 2024). All three support different functions of a healthy placenta and all are equally essential for its maintenance and thus for a normal pregnancy (Turco and Moffet, 2019; Cindrora-Davies and Sferruzzi-Perri, 2022).

In the first phase, which occurs at around the 5 day post-fertilization (dpf), the trophectoderm (TE) that is the outer layer of the blastocyst starts to be formed (Turco and Moffet, 2019). The blastocyst consists of two lineages, the TE and the inner cell mass (ICM), where their shared surface is adjacent to the endometrium. Upon attachment to the endometrium and at around the 6-7 dpf, the TE is being fused to generate the primary syncytium. This phase is called the pre-lacunar stage (Turco and Moffet, 2019; Cindrora-Davies and Sferruzzi-Perri, 2022).

By day 14, the blastocyst has been implanted into the decidua, a specialised tissue deriving by the invasion of the primary syncytium into the surface epithelium, thus, into the underlying endometrium (Turco and Moffet, 2019). At this point, fluid-filled spaces termed as lacunae are formed within the syncytium and later transformed into trabeculae, completing the lacunar phase of the placental development. In the final phase of the development, the villous stage, the cytotrophoblasts, namely the trophoblasts located under the syncytium start multiplying and eventually leading to the formation of the primary villi (Turco and Moffet, 2019; Cindrora-Davies and Sferruzzi-Perri, 2022). The latter will later lead to the formation of a syncytiotrophoblast layer

resulting from fusion with differentiated villous cytotrophoblasts. This syncytiotrophoblast layer forms a protective barrier and provides an interface for foetal-maternal interactions (Turco and Moffet, 2019; Cindrora-Davies and Sferruzzi-Perri, 2022).

By day 18, the cytotrophoblasts keep multiplying and rupturing through the syncytiotrophoblast network leading to the generation of secondary and tertiary villus trees consisting of a cytotrophoblast core with an outer layer of syncytiotrophoblasts (Turco and Moffet, 2019; Cindrora-Davies and Sferruzzi-Perri, 2022). At the same time, a protective cytotrophoblast-shell that surrounds the embryo between the villi and the maternal decidua is being generated by the continuous proliferation of the cytotrophoblasts. At the maternal-foetal interface, there are certain regions where the cytotrophoblast shell comes in contact with the maternal decidua (Turco and Moffet, 2019). This results in the biogenesis of the extravillous trophoblasts, that are individual cytotrophoblast cells deriving from their migration and invasion into the maternal decidua in order to finalise the blueprint of the placenta (Turco and Moffet, 2019; Cindrora-Davies and Sferruzzi-Perri, 2022).

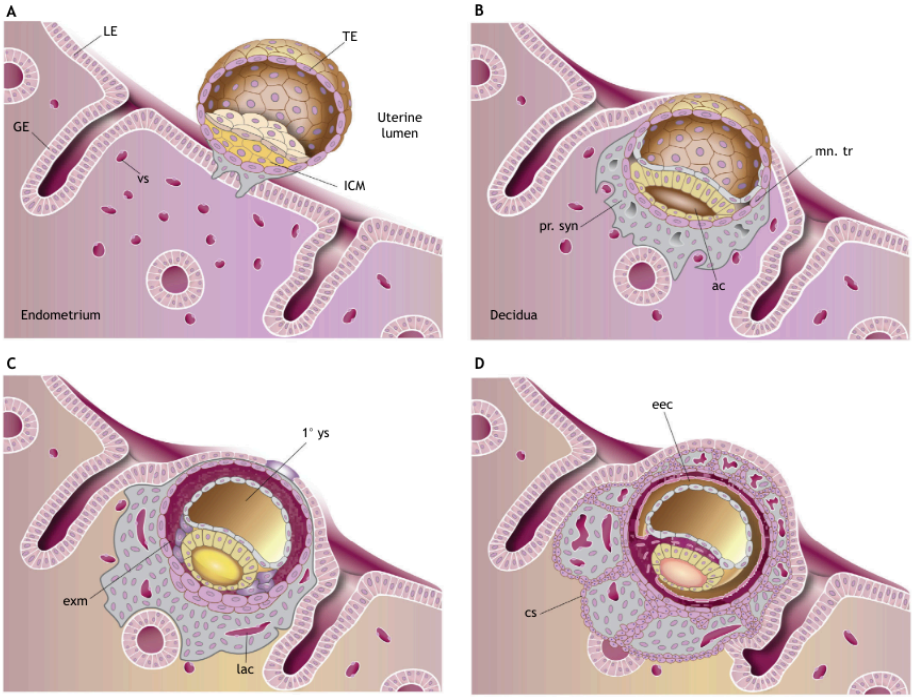

Figure 14: Illustration of the initial stages of placenta formation following blastocyst implantation. (A, B) Pre-lacunar stages. (C) Lacunar stage. (D) Primary villous stage. Abbreviations: 1° ys, primary yolk sac; ac, amniotic cavity; cs, cytotrophoblastic shell; eec, extra-embryonic coelom; exm, extra-embryonic mesoderm; GE, glandular epithelium; ICM, inner cell mass; lac, lacunae; LE, luminal epithelium; mn. tr, mononuclear trophoblast; pr. syn, primary syncytium; TE, trophectoderm; vs, blood vessels (Picture and legend adapted from Turco and Moffet, 2019).

II. Structure and Composition : Specialised Placental Cells - Trophoblasts

The trophoblasts are the major cell player for the placenta development and they are considered an evolutionary advance of placental mammals. Trophoblasts were first characterised in 1889 by the embryologist Ambrosius Arnauld Willem Hubercht who described them as essential for both the transport of nutrients and mainly the biogenesis of the protective barrier between the maternal-foetal interface. The trophoblasts are separated into three subcategories where each one is responsible for a different functional regulation in favour of the successful placenta development; Cytotrophoblasts (CTBs), Syncytiotrophoblasts (STBs) and the Extravillous trophoblasts (EVTs) (Turco and Moffet, 2019; Cindrora-Davies and Sferruzzi-Perri, 2022).

2.1 Cytotrophoblasts (CBTs)

Upon blastocyst's implantation, the CBTs are the first cells to arise and they are considered as the impregnation cells of the trophoblast due to their ability to replicate and multiply (Figure 15). CBTs are cuboidal-like cells with a quite high nucleus:cytoplasm ratio. During the establishment of the placenta through villous tree generation, the CBTs are becoming discontinuous and consist only of 25% of the villous surface. However, they maintain their key role as one of the three protective layers of the blastocyst as they are responsible for the generation of the shell coming in direct contact to the maternal decidua (Turco and Moffet, 2019; Cindrora-Davies and Sferruzzi-Perri, 2022).

2.2 Syncytiotrophoblasts (SCTs)

The outer line of the placenta villi is composed of SCTs and they provide the main site of the maternal-foetal exchange of gases and nutrients responsible for the growth of the feto-placental unit (Figure 15). More specifically, SCTs are multinucleated cells without borders and therefore allowing the diffusion of nutrients and, at the same time, preventing the conceptus from pathogens. Among many vital contributions, SCTs are rich in receptors for growth factors, hormones, in both amino acid and glucose transporters and in efflux pumps. Additionally, the SCTs are considered as an endocrine system due to their roles in the physiological and metabolic state of pregnancy through the secretion of hormones. Apart from that, SCTs not only express the neonatal Fc receptor that allows the transportation of maternal IgG to the foetal circulation and activating the foetal Natural Killer cells that protect the embryo before the birth, but they define an immunological barrier that does not express any Human Leukocyte Antigen (HLA) protein and therefore protects the SCT layer by being

attacked by the maternal immune system, as well (Turco and Moffet, 2019; Cindrora-Davies and Sferruzzi-Perri, 2022).

2.3 Extravillous Trophoblasts (EVTs)

The EVTs derive from the protective shell and the anchoring villi and are considered as the last category of the trophoblasts that play a role in the establishment of the placenta (Figure 15). Their function is split into the interstitial EVTs (iEVTs) and the endovascular EVTs (eEVTs). The iEVTs are responsible for the fibrinoid-like shape of the arteries that provide resistance to high conductance at low pressure which is essential for the right regulation of pregnancy. The eEVTs start to emerge after the arterial transformation by creating a plug in the arteries that prevent the blood from entering the intervillous space. This occurs until the end of the first trimester where the hemochorial placentation that supports the growth of the foetus via gas and nutrients exchanges, has been established (Turco and Moffet, 2019; Cindrora-Davies and Sferruzzi-Perri, 2022).

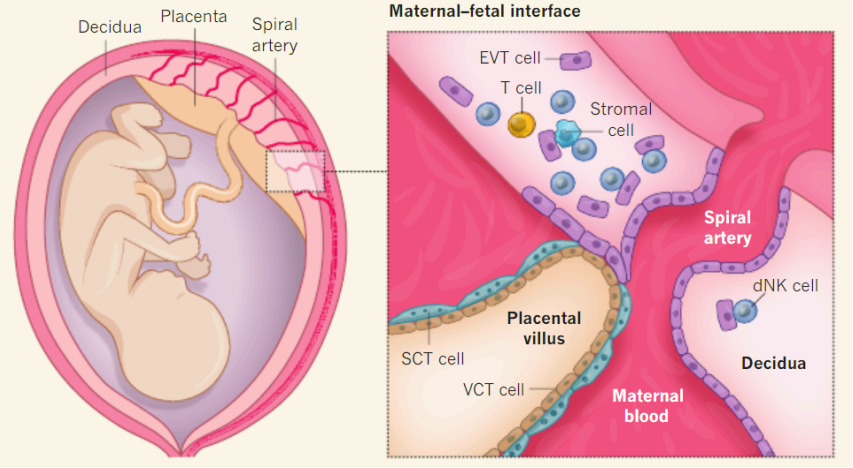

Figure 15: Cells at the maternal-foetal interphase; Villous cytotrophoblast (VCT or CBTs) cells, syncytiotrophoblast (SCT) cells and extravillous trophoblast (EVT) cells, several types of maternal immune cell (T Cells and three subsets of decidual natural killer (dNK) cell, and three types of stromal cell, which provide structural support for the decidua) (adapted from Rajagopalan and Long, 2018).

III. Functions of Placenta

Foetal Development and Protection

The placenta provides many nutritional and endocrine regulations during the pregnancy to assist the pregnancy and ascertain the right growth and development of the foetus. Some of its regulations are the O_2 regulations which not only has an effect in the formation of the placenta but also assists the embryo, towards the end of the 1st trimester that the nutrition changes from histotrophic to hemotrophic and the levels of O_2 are thrice higher inside the placenta. More specifically, during the end of the 1st trimester the hemotrophic nutrition of the foetus is being established. Usually, this enlargement of the placenta is followed by an increase in maternal blood flow essential to optimise the capacity for nutritional exchange. Additionally, a protective niche is being set through the formation of aggregates in the spiral arteries that protect the overflow of the maternal erythrocytes and therefore leading to low O_2 levels and simultaneously maintaining a non-hypoxic environment (Megli and Coyne, 2022; Khorami-Sarvestani et al., 2024).

Transport of nutrients is another essential function performed at the foetal-maternal interface. The placental villi together with the exocoelomic cavity and the yolk sac function as one to assist the transport of nutrients including amino acids, vitamins, metal, (in)organic ions, hormones etc for the growth of the embryo. Transcriptomic analysis has shown that genes associated with Endoplasmic reticulum activation, O_2 and lipids transport, but also genes associated with glycolytic pathway, like the production of purines that is essential for rapid cell proliferation are highly enriched (Megli and Coyne, 2022; Khorami-Sarvestani et al., 2024).

Placenta can be characterised as an endocrine organ as well. It has been shown that placenta is responsible for secreting many essential factors like glycoproteins, steroids, peptide hormones and more, where, many of them participate not only in the prevention of foetal rejection and in the maternal metabolism but also to the establishment of the lactational system, as well. Transcriptomic analysis has also suggested that growth hormones of the prolactin family can regulate the maternal insulin levels decreasing the diabetes incidence during pregnancy. Due to their direct link to placenta, endocrine factors have been considered as good diagnostic biomarkers for predicting pregnancy complications (Megli and Coyne, 2022; Khorami-Sarvestani et al., 2024).

Overall, placenta offers a wide range of benefits to assist the development of the embryo. From nutrient transport, as discussed, gas exchange and waste export via pumps in SCTs layer, to protective mechanisms including the transfer of maternal immunoglobulin leading to passive immunity, the foetal development via hormone secretion and regulation and finally the physical and immunological protection against vertical transmission of infectious agents which will be discussed more on the following section (Megli and Coyne, 2022; Khorami-Sarvestani et al., 2024).

IV. Placental pathogens (TORCH) and route of infection

The placenta is by default the primary barrier to prevent haematogenous transmission of infectious agents. The defence properties of the placenta could be split into: (a) physical and (b) immunological defences. The physical defences can be characterised by, firstly, the lack of cell-to-cell junctions within the SCTs layer that prevent its compromise by inflammation mediated damage and, secondly, by the presence of a dense actin network preventing the chorionic villi from microbial attachment and invasion. Regarding the immunological defences, firstly, the villous trophoblasts release immunomodulators including exosomes containing anti-viral microRNAs which could explain why most viruses cannot proliferate in the SCTs, and, secondly, release of cytokines (e.g. interferons-type-III and interleukins) through the activation of innate immunity (Robbins et al., 2012; Arora et al., 2017; Megli and Coyne, 2022; Khorami-Sarvestani et al., 2024).

Despite the fact that placenta provides physical and immunological defences against pathogens, there are certain pathogenic microbes that manage to overcome the defences and lead to disease. These pathogens are defined as TORCH and are known not only for having adverse effects to the foetus but for posing the mother at risk, as well. The acronym was initially standing for TO= *Toxoplasma gondii*, R= *Rubella*, C= *Cytomegalovirus* and H= *Herpes Simplex Virus*. However, throughout the years many more pathogenic microbes with implications in the pregnancy have been characterised and therefore the O now stands for Others, of which many important infectious agents like T*reponema pallidum*, *Zika Virus* and *L. monocytogenes* are part (Robbins et al., 2012; Arora et al., 2017; Megli and Coyne, 2022; Khorami-Sarvestani et al., 2024).

There are different routes through which TORCH pathogens manage to make their way into the placenta. More specifically, they can either reach the intra-amniotic environment through vertical transmission which can be split into sub-categories including the direct transplacental transmission, or passage via malfunctioning and misdeveloped placenta and/ or through the hematogenous pathway. There are two sites where infection could take place in the hematogenous route: a) Blood - SCTs and b) Uterus - Trophoblasts interfaces (Figure 16), (Robbins et al., 2012; Arora et al., 2017; Megli and Coyne, 2022; Khorami-Sarvestani et al., 2024).

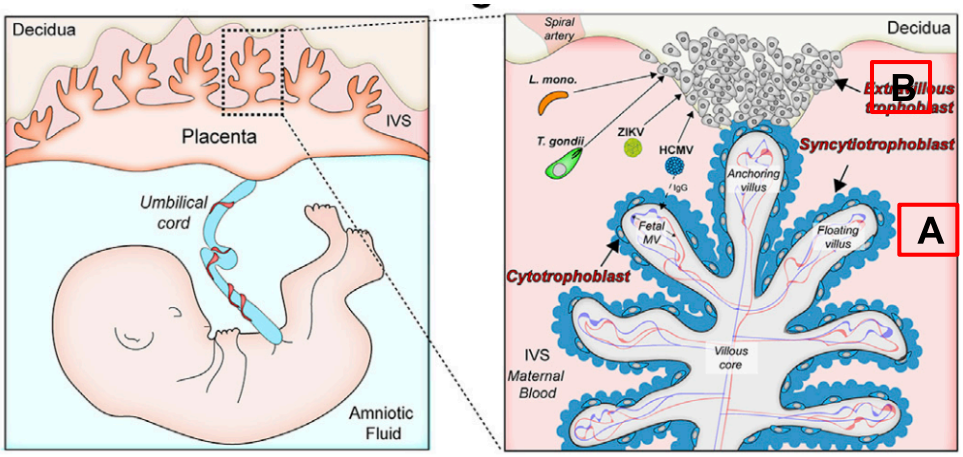

Figure 16 : Vertical Transmission of TORCH pathogens during human pregnancy; (A) Maternal Blood - SCTs and (B) Decidua - EVTs interphases. (Adapted from Arora et al., 2017)

The Maternal Blood - SCTs route is considered as the largest maternal-foetal interphase. It is mainly characterised by the molecular exchange essential for the foetal growth and by the absence of intercellular junctions that are used as a preventative method against cell-to-cell spread that certain TORCH pathogens use to proliferate. For example, the *Cytomegalovirus* (*CMV*) only infects the CTBs and the *Herpes Simplex Virus* (*HSV)* cannot infect the SCTs layer unless there is an enzymatic-like damage to the syncytium barrier. Additionally there is no significant expression of receptors found in the surface of SCTs that could be used for the internalisation of *CMV* or *HSV*. As for bacteria and parasites like *L. monocytogenes* and *T. gondii*, respectively, it has been shown that SCTs are resistant against them both. As for *L. monocytogenes*, it has been suggested that its extracellular internalisation is being allowed via interactions of E-cadherin with inlA probably on the surface of the SCTs. On top of that, *L. monocytogenes* is able to spread via protrusion forms, which is not effective in the case of SCTs due to its lack of the cellular borders (Robbins et al., 2012; Arora et al., 2017; Megli and Coyne, 2022; Khorami-Sarvestani et al., 2024).

On the other hand, the Decidua - EVTs is the smaller interphase that comes in direct contact to the EVTs and it is considered as the weak spot of the construction. Morphologically-wise, the EVTs are set side to side with innate immune players (NK cells, lymphocytes and macrophages) and studies have shown the EVTs acting as innate immune cells too and more specifically not only highlighting their bactericidal activity against intracellular pathogens, like in *L. monocytogenes*, but also impairing the

growth of parasites like *T. gondii,* as well (Robbins et al., 2012; Arora et al., 2017; Megli and Coyne, 2022; Khorami-Sarvestani et al., 2024).

However studies have revealed that crossing the maternal-foetal barrier is not required for adverse effects on and during the pregnancy. For example, it has been shown in guinea pigs that placental inflammation or pregnancy loss occur even if *L. monocytogenes* has not traversed the epithelial barrier. Apart from foetal-related consequences, the mother might also suffer complications. In fact it has been shown that placenta enables the proliferation of *L. monocytogenes* and it has been considered as a reservoir of maternal re-infection. Finally, maternal-foetal infections might lead to placental insufficiency that might result in other types of diseases like pre-eclampsia (PE) or preterm labour (Khorami-Sarvestani et al., 2024). This is also the case with other pathogens that do not necessarily cross the maternal-foetal epithelial barrier like in the case of TORCH (Robbins et al., 2012; Arora et al., 2017; Megli and Coyne, 2022; Khorami-Sarvestani et al., 2024).

V. Placental phase of listeriosis

L. monocytogenes placenta infection has been characterised by two hallmarks; firstly its potential to initiate placenta infection with only 1 bacterium and secondly its ability to establish a reservoir for reinfection from the placenta to the maternal organs and back (Bakardiev et al., 2005). The potential of *L. monocytogenes* to surpass protective barriers have imposed it as a formidable pathogen (Bakardiev et al., 2005).

Overall, placenta infections are followed by inflammation. Infections in the placental-foetal unit cause harm not only by the presence of pathogens but also through the resulting inflammation (Megli et al., 2020; Johnson et al., 2021). This inflammation can lead to preterm birth and disrupt foetal immunological tolerance, potentially causing foetal rejection and abortion (Maltepe and Fisher, 2015; Johnson et al., 2021). Transcriptomic analyses of healthy preterm human placentas have shown that *L. monocytogenes* alters the inflammatory signature of the placenta (Johnson et al., 2021). More specifically, the initial inflammatory response of trophoblasts recruit maternal neutrophils and monocytes leading to the NLRP3 inflammasome activation, which contributes in fighting the infection (Johnson et al., 2021). However, when the infection persists, the trophoblasts keep producing proinflammatory mediators resulting in deleterious effects, including negative impacts to pregnancy like miscarriage or preterm birth (Johnson et al., 2021).

It is especially evident in the case of pregnancy that the placenta is forced to maintain a balance between protecting the mother and the foetus and simultaneously preventing the foetus from being rejected. However, the molecular mechanisms enabling the transplacental transmission are yet to be elucidated. There are several studies suggesting that the virulence mediators for host invasion (LLO, ActA, E-cad, Met and InlAB) are essential for placenta infection (Vasquez-Boland et al., 2017 ; Charlier et al, 2020). It has also been suggested that another secreted protein, InlP, member of the internalins might have a potential role in the crossing of the basement membrane of the chorionic villi, ultimately and cooperatively enabling *L. monocytogenes* transmission and placenta infection (Vasquez-Boland et al., 2017 ; Charlier et al, 2020; Johnson et al., 2021)

Therefore, understanding how trophoblasts respond to infections and contribute to placental immunity and inflammation is crucial.

C. Proteomics and Mass Spectrometry

Proteomics have contributed greatly in understanding complex bacterial proteomes and providing insights about virulence and pathogenicity of pathogens. The use of Mass Spectrometry has really broadened new horizons for this area of research. Therefore, in this section proteomic techniques and their input in microbiology are assessed.

I. Introducing Proteomics

The molecular biology or central dogma was first introduced in the late 50s by Francis Crick who suggested the mechanisms through which the genetic information circulates within a biological system (Crick, 1958). Apart from the criticism that the dogma encountered, it was finally accepted as a solid hypothesis and many studies and technological advancements have both assessed and contributed to its optimisation. The nucleic acid DNA can self-replicate and also transcribed into another nucleic acid, the RNA. RNA can self-replicate as well and at the same time not only it can get transcribed back to DNA via reverse transcription but it is also translated into proteins via a one-way relation. The proteome is an unpredictable set of information as it changes based on not only environmental settings but also due to random events like splicing, degradation of proteins and Post-Translational-Modifications (PTMs) (Gilmore and Washburn, 2010; Santos 2020). However, the proteome remains of vital importance as proteins play key roles in the gene functions and expressions through a series of pathways including molecular signalling and catalysis (Wilkins et al., 1996). Proteomics is the -omics area used to analyse proteins and it was first introduced in late 1990s in an effort to assess the relation between genome and proteome (Wilkins et al., 1996). The 20th century can be considered a milestone for proteomics thanks in particular to advances in genome sequencing and Mass Spectrometry (MS) advancements as well (Marchetti-Deschmann and Allmaier, 2011). Proteomics not only acts as a method of protein identification but as a quantification of the proteome as well as information regarding the protein abundance, namely the level of protein abundance, is essential for actionable studies (Santos 2020). In Liquid Chromatography Tandem Mass Spectrometry (LC-MS/MS) which is the sector of MS that we will focus on in this section, there are two methods of quantitative proteomics; label-based and label-free quantification. However, in this section we are mainly discussing label-free quantification and MS acquisition via Data-Dependent and Data-Independent acquisition.

II. Proteomic Approaches

To meet the standards of resolving complex analytical data-sets, two approaches are normally used; top-down and bottom-up approach.

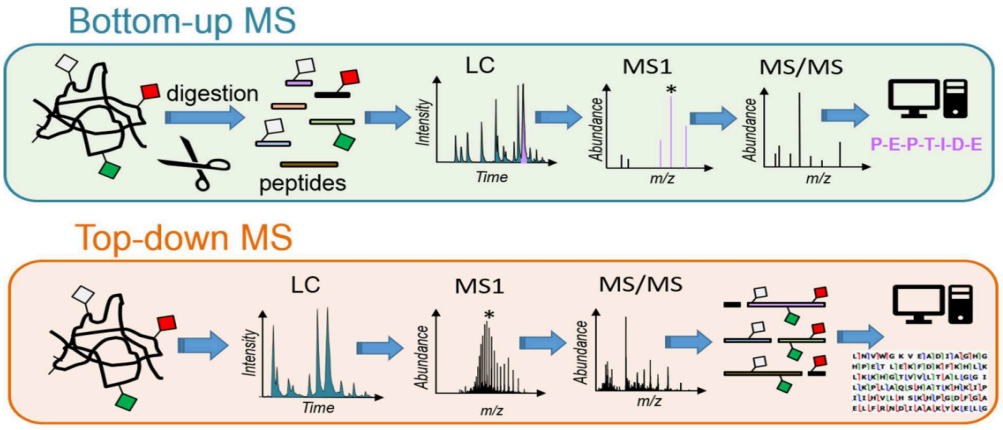

Figure 17: Workflow of Bottom-up MS proteomics approach, where proteins are subjected to proteolytic digestion, generating a mixture of peptides. These peptides are subsequently separated and analyzed by LC-MS/MS, with MS1 and MS/MS spectra acquired for the eluting peptides. Protein identification is achieved through database search-based analysis of the resulting spectra. Top-down MS approaches involve analyzing intact proteins, where a mixture of proteins is separated and studied using LC-MS/MS. In this method, both MS1 and MS/MS spectra are obtained directly from the intact proteins as they elute, preserving the full context of modifications for each proteoform. (Picture and legend adapted from Brodbelt, 2022)

2.1 Top-Down Approach

The top down approach is focusing on the analysis of intact proteins through injections into a gas phase by Electrospray Ionisation (ESI) and consequently by fragmentation with MS (Chait, 2006; Rabilloud and Lelong, 2011). The most described technique of top down, is the two dimensional gel electrophoresis (2DE), via which the abundance and any covalent modifications are assessed based on the staining intensity in the gel and on the electrophoretic motility, accordingly (Santos, 2020). The top down approach is focusing on the primary structure of the protein, preventing the loss of information due to PTMs as they can affect the structure and thus the function of the protein (Figure 17), (Santos 2020). However, there are certain cons that come with this technique. More specifically, due to the complexity of the sample, only a limited number of highly abundant proteins can be detected, and usually these proteins were not informational in a deep-wise way (Santos 2020). Therefore, the top down approach offers the possibility to analyse fully the primary structure of a protein but at the same time this is not always possible due to difficulties in fragmenting protein ions especially when deriving from large, complex proteins (Rabilloud and Lelong, 2011). However, in our

work and because of the complexity of proteome in placenta cells, we have ultimately focused on the Bottom-up approach and therefore I will not get into more detail about the top-down proteomics in the rest of the review.

2.2 Bottom-Up Approach

Bottom-up proteomics is the most widely used technique in the area of mass spectrometry proteomics (Figure 17), (Santos 2020). Instead of injecting intact proteins like in the case of top-down approach, the bottom-up approach is focusing on the injections of digested proteins, namely peptides, that are digested usually via the use of the enzyme trypsin leading to a high level of identification since tryptic peptides are easily solubilised and separated (Chait 2006; McArdle and Menikou 2020). At the same time, poor or insufficient protein digestion could lead to a limited number of peptide identification. On a similar scope, peptides might not get caught by the column or pre-column and/or even not ionised into the source could lead to poor peptide identification, thus, bottom-up approach is usually characterised as an insufficient method for the analysis of Post-Translational Modifications (PTMs) (Chait 2006). Nevertheless, 100% coverage is almost impossible to achieve and thus a bottom-up approach is sufficient for protein identification as only two peptides are required for protein validation.

2.2.1 Workflow

The bottom-up approach workflow starts with the recovery of the sample which is then undergoing a sample preparation based on four key steps; protein denaturation, reduction of disulphide bonds, alkylation of reduced cysteines and digestion of proteins to peptides with trypsin (Santos 2020). Tryptic peptides are injected into the liquid chromatography for peptide separation and then injected into the MS, proceeding into data analysis for identification, quantification and statistical analysis. The protocol above can be modified as optimization varies based on the needs of every lab (Resing and Ahn, 2005). All of the aforementioned steps are mandatory to get a reproducible and robust experiment (Resing and Ahn, 2005, Santos 2020). On top of that, the sample preparation of the original sample or protein extraction is of paramount significance and always depends on the nature of the sample, for example secretome that will be discussed in more detail in the Material and Methods section.

2.2.2 LC-MS/MS

Liquid Chromatography (LC) is a widely used technique for separating and analysing compounds in a mixture. In the context of nano LC, smaller sample volumes are analysed with both higher resolution and sensitivity (Sanders and Edwards 2020). Nano LC employs a stationary phase that is non-polar, while the mobile phase is polar, a configuration known as reverse phase chromatography. This setup enables separation through the hydrophobic interactions between the analytes and the stationary phase (Sanders and Edwards 2020). Therefore, nano LC is considered very efficient for analysing low-abundance proteins and peptides in complex samples. The mass spectrometer used for this study is a timsTOF Pro (Bruker). The timsTOF Pro is a state-of-the-art mass spectrometer developed by Bruker that embeds a Trapped Ion Mobility Spectrometry (tims) which adds an additional dimension of separation by distinguishing ions based on their shape and size, complementing the traditional mass-to-charge ratio separation in tims, ions are separated in an electric field based on their mobility before entering the mass analyzer. This technique enhances the resolution and identification of complex mixtures by reducing ion interference and improving the accuracy of peptide and protein quantification. The timsTOF Pro integrates these capabilities with high-resolution mass spectrometry, offering significant improvements in sensitivity and analytical performance.

2.2.3 Data Analysis & Quality Assessment

Upon the peptide separation with LC the next step is screening the samples for MS/MS spectra. Frankly, the more MS/MS spectra detected, the higher the coverage of the proteome and thus the more accurate the abundance for variable proteins (Hackett 2008). The obtained spectra are then compared to theoretical spectra based on a database of interest digested *in silico* with trypsin (Granholm and Kall, 2011). The bottom-up approach simplifies the MS/MS sequencing but discontinues the connectivity between peptides and proteins leading to both a complicated analysis and interpretation (Santos 2020). The MS/MS spectra provide information about the Peptide Spectrum Matches (PSMs) but most search engines have been optimised in a user-friendly way providing the user with an output of protein lists (Santos 2020). However, there are some disadvantages to this method like the protein inference, namely when proteins share a peptide. Therefore, many search engines cluster the proteins sharing peptides in protein groups. It is essential to take into account the unique peptides in order to have more robust identifications. Nevertheless, sometimes the protein identifications might be impacted due to restrictions occurring from this method like the low quality or/and both incorrect or presence of non-unique peptides. Many

softwares have been developed to solve such issues and combining different search engines in order to provide a more accurate match (Santos 2020).

III. Quantitative Proteomics

Quantitative information is of utmost importance especially when it comes to actionable questions like targeting and designing of biomarkers and drugs, respectively (Zhou et al., 2009; McArdle and Edwards 2020). As has already been stated, accuracy is the key to figure out the mechanisms of biological systems. There are two methods to quantitatively assess proteomic samples. The Isotopic Quantification which takes into account labelling of the isotope, namely the Label-Based Quantification (LBQ) and the Label-Free Quantification (LFQ) which is the approach used in our work and is explained in detail in the following section. LFQ relies on techniques such as Spectral Counts (SC) and Extracted Ion Chromatogram (XIC) to quantify protein abundance without the need for labelling, making it well-suited for large-scale proteomic analyses (Figure 18).

3.1 Label-Based Quantification (LBQ)

The LBQ was first introduced in the early 2000s with the ICAT and 15N labelling methods. In the next 20 years followed, there were even more label-based techniques appearing including SILAC, iTRAQ, TMT and IPTC (Santos, 2020). Intact or digested proteins can be used but mainly most of these methods are focusing on the proteolytic peptides as most of these peptides contain at least one labelling site and more specifically a primary amine group allowing the labelling of all the peptides in the mixture via the same mechanism (Santos 2020; Tian et al., 2021). Label-based proteomics offer the ability for analysing multiple samples at the same time due to the proteolytic peptides MS handling in the first place; namely the differentially expressed peptides and the merging of labelled samples before LC-MS (Santos 2020; Tian et al., 2021). There are various isotopes used including the 13C, 15N, 17O and 2H with the majority of labelling techniques focusing on 13C and 15N (Santos 2020; Tian et al., 2021). Apart from the pros of the label based methods like the better precision and less time consuming there are a few cons as well including the extra steps of labelling, the complexity that comes with these protocols, the high cost of reagents especially for large-scale studies and the need of specific softwares (Santos 2020. However, we will not get into more detail about the LBQ methods as this study was based on LFQ (section 3.2).

3.2 Label-Free Quantification (LFQ)

To manage to avoid and overcome the issues facing LBQ, the interest for LFQ has been increased. LFQ has been linked to a quantification offering faster, cheaper, cleaner and simpler quantification results as all the detected peptides can be used for quantification. Additionally, technological

advancements in the MS sector have contributed immensely via creations of commercial softwares that increase the robustness of LC-MS/MS and decrease the risk of errors due to run-to-run variations deriving from, for example, retention time alignment and/or match between runs (Zhou et al., 2009; Blein-Nicolas and Zivy, 2016). Therefore, the LFQ is considered indeed as a fast and low cost method towards protein abundance analysis. The LFQ could be performed with two quantification methods; the relative and the absolute (Zhou et al., 2009; Blein-Nicolas and Zivy, 2016). We will not get into much detail about the absolute quantification (dedicated to quantification of few proteins) as we have mainly focused on the relative quantification in our work. Two of the most well-known and used methods in relative quantification via LC-MS/MS are the peak intensity or area based on the extracted ion chromatogram (XIC) and the Spectral Counts (SC) methods (Blein-Nicolas and Zivy, 2016).

3.2.1 Extracted Ion Chromatogram (XIC)

In 2002 Chelius and Bondarenko first introduced the peak area, XIC, as a way to measure the abundance of proteins and peptides based on the MS1 signal (Chelius and Bondarenko 2002). They have shown that the concentration of protein digests was correlating linearly with the chromatographic peak area (Chelius and Bondarenko 2002). In principle, XIC is based on the MS1 spectra and works by measuring all the peptide ions assigned to a protein and for every peptide ion in LC-MS/MS there is a m/z value corresponding to it, which is then translated into a specific intensity under a specific time frame (Chelius and Bondarenko 2002; Zhou et al., 2009; Blein-Nicolas and Zivy 2016). The XIC method offers a wide range of advantages. For example, this method not only enables the detection of very low-abundance proteins by matching peptide signals across multiple experimental runs, or else known as match between runs, but it also relies on a robust quantitative statistical model. This helps address the challenges often associated with bottom-up proteomics approaches, such as inconsistent peptide detection and quantification across different samples, therefore, XIC is considered as a very sensitive and precise method (Blein-Nicolas and Zivy, 2016). Apart from the advantages of the XIC method there are a few disadvantages, too, mainly when it comes to complex biological samples (Zhou et al., 2009). The most notable one, was the variation levels for the same peptides as sample preparation and even the injection process can vary from test-to-test, run-to-run and even within replicates (Zhou et al., 2009). Therefore the importance of normalisation has been highlighted during troubleshooting. Additionally, when multiple samples are injected through the same reverse phase liquid chromatography column, shifts in the retention times

(RT) have been observed leading to errors in analysing and comparing the data (Zhou et al., 2009). Therefore, a different technique in which ions (charged particles) were matched based on their mass-to-charge ratio (m/z) and retention time (RT) across different runs, even in the absence of a deeper analysis (MS2), which provides more detailed identification, was employed in this study. This method allowed the detection and identification of peptides that were present in very low amounts, which might not have been detected otherwise. Additionally, it is essential to proceed to the preparation of control samples that could be used as mediators for retaining a similar RT along all the sample sets (Zhou et al., 2009; Blein-Nicolas and Zivy 2016). Finally, the LC-MS/MS analysis generates a great load of output data which is impossible to handle without automation. The scientific community was quite aware about these potential issues and therefore many measures have been taken to control any adverse outcome and maintain only the advantages coming with XIC, mainly referring to the high sensitivity of the model due to the how-to XIC process the peptide information.

3.2.2 Spectral Counts (SC)

In contrast to XIC, in SC the relative protein abundance is measured based on comparative analysis of the MS/MS spectra deriving from the same protein of multiple LC-MS/MS data (Zhou et al., 2009; Blein-Nicolas and Zivy 2016). An increase in the number of protein digests leads to a higher total count of MS/MS spectra, which consequently results in an increased abundance of the specified/targeted protein (Zhou et al., 2009). In 2004, there was a study conducted by Liu and colleagues (Liu et al., 2004) aiming to check correlations between the level of protein abundance with sequence coverage, number of unique identified peptides and spectral counts, and eventually showing a strong correlation between the protein abundance and the spectral counts (Liu et al., 2004). Therefore, spectral counts were used as the primary quantification method due to not only its extreme simplicity but its accuracy as well and detection of presence/absence of proteins (Liu et al., 2004; Zhou et al., 2009; Blein-Nicolas and Zivy 2016). However, similarly to XIC, it has been noted that normalisation is really essential to avoid variation from run-to-run again due to sample preparation (Zhou et al., 2009). However, in 2007, a normalisation factor called NSAF, namely normalisation spectral abundance factor was generated allowing the comparison of the abundance of one protein across a set of independent samples leading to quick and accurate quantifications (Paoletti et al., 2006; Zhou et al., 2009). As for the statistical analyses, there are many options based on the nature and number of conditions in the experiment. Some of the most used statistical tests

are the Fisher's exact test, the G-test and the Student's-t test with the latter being the favourite choice when it comes to more than three replicates (Zhou et al., 2009).

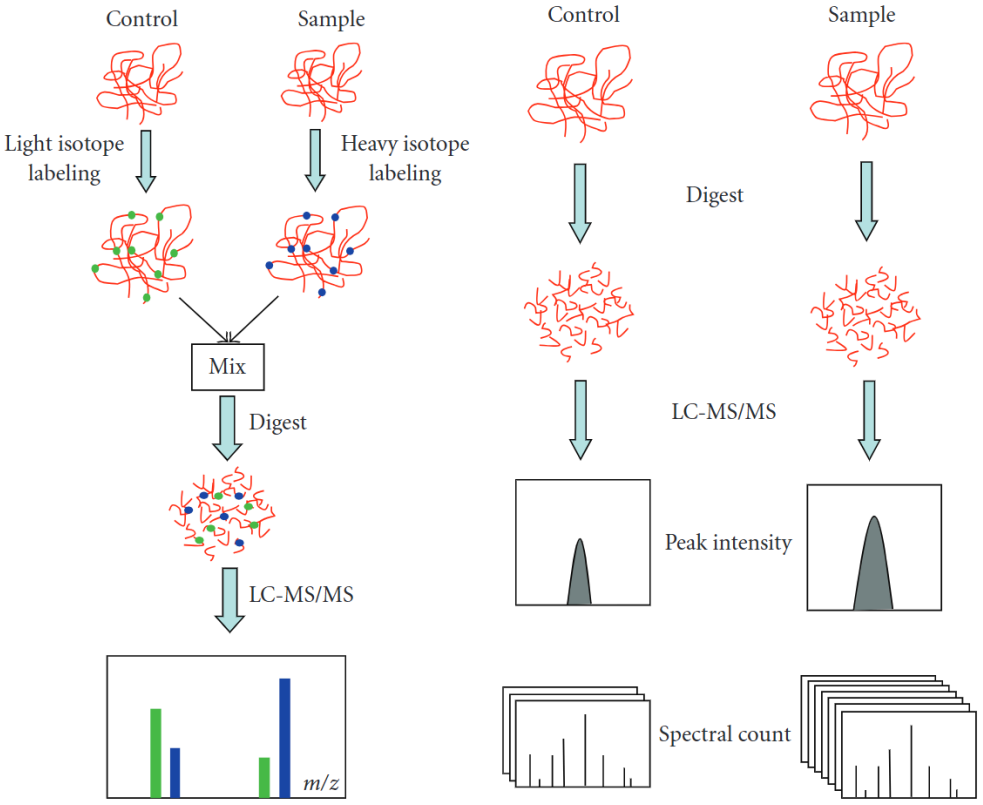

Figure 18: Quantitative proteomic approaches (LBQ, left) and (LFQ, right). LBQ; Following labeling with light and heavy stable isotopes, the control and sample are mixed and subjected to analysis using LC-MS/MS. Quantification is then determined by measuring the intensity ratios of the isotope-labeled peptide pairs. LFQ; control and sample undergo individual LC-MS/MS analysis. Quantification is based on the comparison of peak intensity (Extracted Ion Chromatogram, XIC) of the same peptide or the spectral count (SC) of the same protein (Adapted from Zhou et al., 2009).

3.3 Data-Dependent (DDA) vs Data- Independent (DIA) Acquisitions

Quantitative proteomics seem to be the key for figuring out vital biological questions. However, technical issues are usually prohibiting complete and successful outcomes with the most important parameter being the reproducibility. Reproducibility is essential for not only the biological experiment but for the output data (e.g protein identification and quantification), as well. Nevertheless, multiple efforts and studies in order to troubleshoot such technical issues are always on site. One of the key challenges in mass spectrometry (MS) is variability in data collection, which can lead to inconsistencies in identifying and quantifying proteins. To overcome this, automated

methods such as DDA and DIA have been developed. These techniques help standardise data acquisition by reducing manual intervention, improving reproducibility, and minimising errors in protein identification and quantification (Fernandez-Costa et al., 2020; Li et al., 2021).

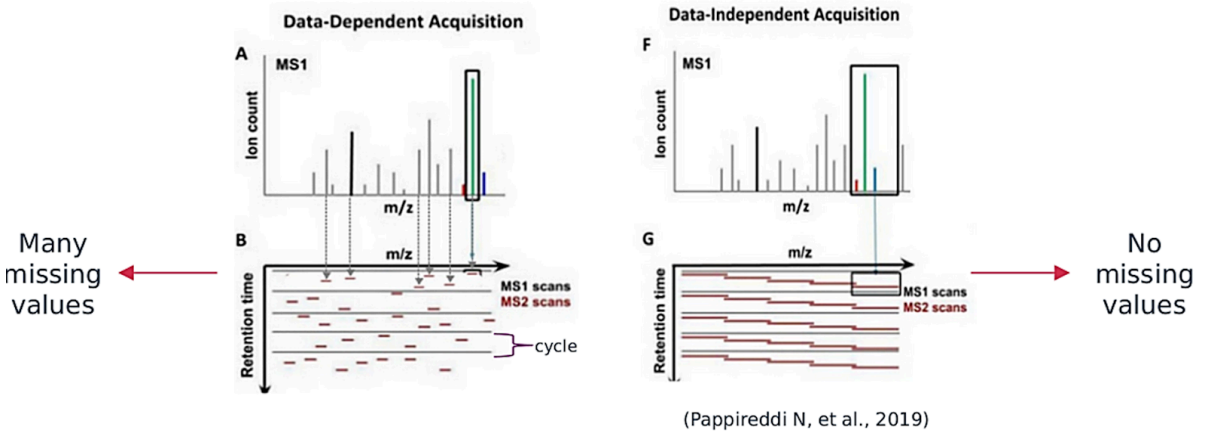

Figure 19: Comparison of MS acquisition methods; Data Dependent Acquisition (DDA) *vs* Data Independent Acquisition (DIA) (Adapted from Pappireddi et al., 2019)

For over 20 years, LC-MS/MS-based proteomics has used data-dependent acquisition (DDA) mode, where only the most intense peptides detected in MS1 are fragmented and analysed in MS2 (Figure 19). With the development of high-resolution mass spectrometers, a new method called Data-Independent Acquisition (DIA) has emerged. Unlike DDA, DIA fragments all peptides within a defined mass-to-charge ratio (m/z) range simultaneously and measures the resulting fragments together in MS2 (Figure 19). DIA offers advantages such as a broader dynamic range, higher peptide identification rates, and improved reproducibility and accuracy in quantification. However, it requires more complex data processing due to peptide co-fragmentation (a deconvolution algorithm must be used). Traditional approaches use pre-generated spectral libraries, which are time-consuming, but recent "library-free" methods include creating in-silico libraries from full proteome digests or generating libraries directly from DIA data (Bruderer et al., 2015; Tsou et al., 2015).

Many comparative analyses between DDA and DIA have been performed over the years and in all of these works, DIA was always outperforming DDA (Fernandez-Costa et al., 2020; Li et al., 2021). Despite the many advantages of DIA especially in terms of reproducibility, the need of such a library was complexing the procedure (Fernandez-Costa et al., 2020; Li et al., 2021). Due to the complexity of the DIA output itself, the library was needed to reconnect the fragmented peptides to the

precursor ones and this was resulting to not only a time consuming analysis but also to poor quantification in the cases that a peptide was absent from the spectral lists, as well (Fernandez-Costa et al., 2020; Li et al., 2021). Recently there has been a library free DIA but the complexity of its output remained the same (Fernandez-Costa et al., 2020; Li et al., 2021). The advancements of science and most specifically the deep learning field, offered a solution to this problem. In 2020 Demichev and colleagues (Demichev et al., 2020) created an automation software, DIA-NN which works with neural networks training resulting in a much higher proteomic coverage just from a single injection and making DIA a key player for highly complex data (Demichev et al., 2020). In spite of how promising DIA might be, there are still many studies that show a preference towards the DDA method not only because it is more straightforward but also because quantification with DIA might be a little bit tricky. In the first chapter of our work, we have prepared and injected our samples both with DDA and DIA but most of the results we present are based on the DDA method, while DIA is still underway.

3.4 Identification *vs* Quantification with PAPPSO softwares

In proteomics studies, the processes of protein identification and quantification are handled by different software tools, each with distinct methodologies that explain why we observe quantification ratios for proteins identified in only one condition, such as in the case of infection. i2MassChroQ is used for the identification step, where it analyses MS/MS spectra to match detected peptide fragments to known protein sequences stored in a database (mass machting). This process is based on the presence or absence of specific peptides in each condition. If a protein is identified only in the infected condition, it suggests that its corresponding peptides were detected exclusively under infection, leading to the initial assumption that it may be condition-specific.

However, when moving to the quantification step, which is performed by MCQR, the approach differs. MassChroQ estimates the relative abundance of proteins based on the intensity of detected peptide fragments (XIC). More specifically, MassChroQ provides a matrix based on XIC intensity which is then used by MCQR to calculate; protein abundance, fold change and statistical significance. Even if a protein is identified only in the infected condition, MCQR still attempts to calculate a quantification ratio between conditions. This is done by assigning a small imputed intensity value to the protein in the non-infected condition to avoid infinite or undefined ratios. This imputation

reflects the idea that just because a protein was not identified in one condition does not mean it is entirely absent as it may be present at levels below the detection threshold. MCQR's quantification step then produces a very high but finite ratio, indicating a significant upregulation of the protein in the infected condition compared to the non-infected condition (http://pappso.inra.fr/bioinfo/masschroq/).

Therefore, the distinct methods used by i2MassChroQ for identification and MCQR for quantification may lead to discrepancies, particularly when a protein is detected in only one condition but is quantified across both. MCQR addresses missing data by imputing values, allowing proteins detected solely in one condition, such as infection, to be still quantified and compared across conditions. This approach facilitates meaningful biological interpretations, enabling the identification of proteins potentially involved in infection-specific processes. To ensure the reliability of our findings, we prioritise statistically significant variable proteins identified using ANOVA tests. By focusing on these secreted proteins, we aim to capture the critical factors involved in infection dynamics, while effectively managing the limitations posed by missing data in the quantification process.

IV. Proteomics in microbiology

The higher the organism, the more complex the investigations of the proteome (Santos 2020). Having said that, it can be assumed that microbiology is a more simplistic approach due to the smaller scale of organisms. Several studies have been performed in analysing the proteome of different microorganisms and even try to map genome, transcriptome to the proteome and *vice versa*. As it has been discussed at the beginning of the proteomics section, proteins are the building blocks of genetic information. Understanding how microbial proteomes are, could be of vital importance in answering key biological questions (Chao and Hansmeier, 2012). Microbial proteomics grants the opportunity to dig into the functions of, for example, pathogenic bacteria and try to figure out virulence and pathogenicity potential based on the level of protein abundance (Van Oudenhove and Devreese, 2013).

In addition, many studies have focused on figuring out pathways and functional changes based on the different environmental settings that bacteria are part of. One of the most interesting research areas in the field of microbial proteomics, could be the proteosurfaceome (Olaya-Abril et al., 2014). Bacterial surface proteins have been linked to not only virulence and pathogenicity like in the case of *L. monocytogenes* but in understanding mechanisms of host invasion like in the *L. monocytogenes*, *Mycobacterium tuberculosis, Salmonella enterica* and more, as well (Malen et al., 2007; Santos 2020). Similarly, on the host side, the human secretome can be considered as a research area in proteomics that could be used for biomarkers detections. Overall, diagnostics is a very promising and significant area of research as it could contribute in detecting a latent microorganism minimising the mortality rates in the context of pathogenic bacteria diseases (McArdle and Menikou 2020).

Proteomics, particularly through the use of LC-MS/MS, serves as a powerful tool for elucidating the molecular mechanisms underlying *L. monocytogenes* infection. By analyzing the protein profiles of both the bacterium and/or the host, proteomics can provide valuable insights into not only the bacterium itself but also host-pathogen interactions. For example, proteomic studies of *L. monocytogenes* have led to the identification of novel proteins, such as the miniprotein Prli42, which plays a crucial role in bacterial stress responses and virulence (Impens et al., 2018). These findings underscore the critical role of LC-MS/MS in mapping complex proteomes, highlighting how high-throughput techniques enable comprehensive global insights into bacterial systems. Specifically, proteomics could offer a deeper understanding of virulence mechanisms and stress adaptation

pathways of *L. monocytogenes*, presenting potential advancements in therapeutic and diagnostic approaches. As our ability to map proteomes on a larger scale grows, these technologies offer critical insights not only into bacterial biology but also into tackling challenges related to infectious diseases and antimicrobial resistance. In this context, high-throughput methods are pivotal in advancing our understanding of microbial systems, potential diagnostic tools and therapeutic targets.

While quantitative microbial proteomics may appear challenging, scientific advancements continue to bridge these gaps, ensuring accurate, robust, and reproducible results.

Thesis Objectives

Overall scope of the thesis

L. monocytogenes is a facultative intracellular pathogen ubiquitously found in the environment. The widespread distribution of *Listeria* is mostly due to its capability to adapt to different stressful conditions, which includes utilising mechanisms such as biofilms, or entering in a quiescent non-replicative state. The Epigenetics and cellular Microbiology team, my host laboratory, is interested in elucidating the molecular events underlying microbial persistence of *L. monocytogenes* in different contexts; both in cellular infection and in the environment. This thesis aims to unravel the events leading to *L. monocytogenes* persistence, not only during cellular infection in a trophoblast model but in the environment, as well. Therefore, the thesis is split into two main objectives.

The first part focuses on understanding how persistent infection impacts the physiology of host cells, and in particular their secretory response. In 2021 our team published their work assessing the potential of chronic infections with *L. monocytogenes* in a hepatocytes model via transcriptomic and proteomic analyses (Figure 20), (Descoeudres et al., 2021). Upon comparisons of the acute and chronic phases of the hepatocyte's infection model, it has been suggested that during the acute phase *L. monocytogenes* invades hepatocytes, spreads to neighbouring cells and triggers immune responses including the release of cytokines and interferons. This results in the activation of acute phase proteins (APPs), which are proteins with antimicrobial properties, contributing to the clearance of *L. monocytogenes* from the host. On the other hand, during the chronic phase *L. monocytogenes* inhibits the activity of these antimicrobial-like proteins via undescribed mechanisms, possibly involving interactions with transcription regulators and/or epigenetic regulators. The downregulation of ActA at the chronic phase (Kortebi et al., 2017), results in the engulfment of *L. monocytogenes* in the LisCVs. These two observations have led to the hypotheses that *L. monocytogenes* might disrupt hepatocytic innate immune responses hindering the eradication of *L. monocytogenes* in the liver niche, thus, promoting the formation of a favourable microenvironment for intracellular persistence. Furthermore, this may influence adaptive immunity, fostering tolerance toward cells that harbour dormant pathogens (Descoeudres et al., 2021). Our project was inspired by Descoeudres and colleagues (Descoeudres et al., 2021) and since LisCVs have been described in trophoblasts in a similar manner as in hepatocytes by Kortebi and colleagues (Kortebi et al., 2017), we were interested to investigate how cells behave upon infection with *L. monocytogenes* in the two different infection phases; 24h p.i. for acute and 96h p.i. for chronic infection. To assess this, we

focused our analysis on the secretome of the trophoblast cells, which we extracted at these two different timepoints for comparative analysis using shotgun proteomics; uninfected cells served as our control.

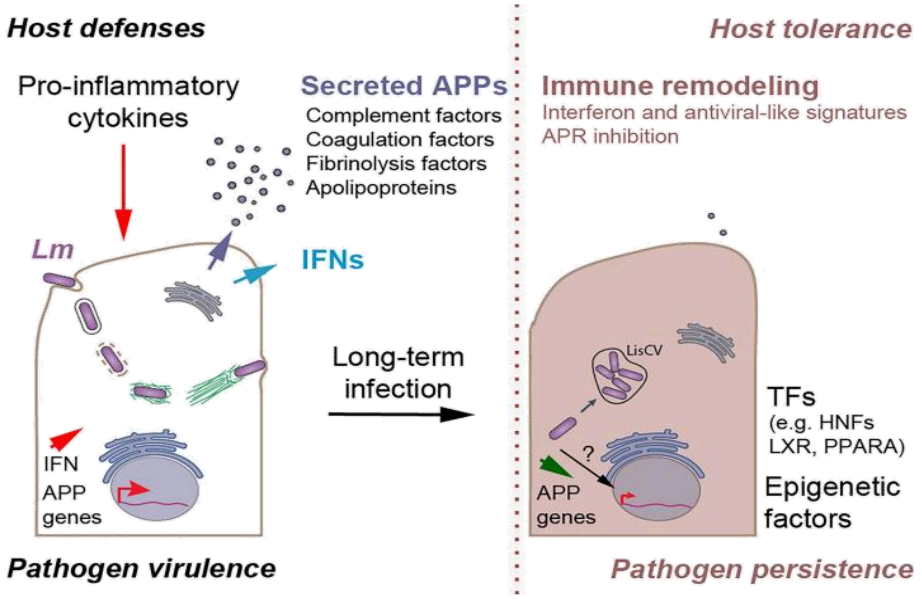

Figure 20: Favourable environment for persistent infection in a hepatocytes model and characterisation of the mechanism promoting the persistence phenotype in the specified model (Adapted from Descoeudres et al., 2021).

The second objective focuses on the VBNC state, a dormancy state that *L. monocytogenes* can enter under stressful environmental conditions. Our lab recently proposed that nutrient deprivation drives *L. monocytogenes* into a VBNC state via a process of cell wall (CW) shedding that generates osmotically stable CW-deficient (CWD) coccoid forms (Figure 21). This phenomenon occurs in multiple *L. monocytogenes* strains as well as in other *Listeria* species, suggesting it may be a stress-adapting process transversal to the *Listeria* genus. Transcriptome analyses and gene-target approaches identified the SigB global regulator and the autolysin NamA, as the main regulators responsible for not only the CWD phenotype but also *L. monocytogenes'* transition into VBNC state. Our team has also found that the VBNC state is temporary as *L. monocytogenes* is able to revert into a fully virulent and walled *L. monocytogenes* once inoculated into chicken embryonated eggs (Carvalho et al., 2024). Our work focuses on the proteomic characterisation of the VBNC part. More specifically, the aim was to investigate the VBNC state of *L. monocytogenes* and to also assess the

CWD phenotype of *L. monocytogenes* on a weekly basis over a one-month time course via LC-MS/MS proteomic analyses.

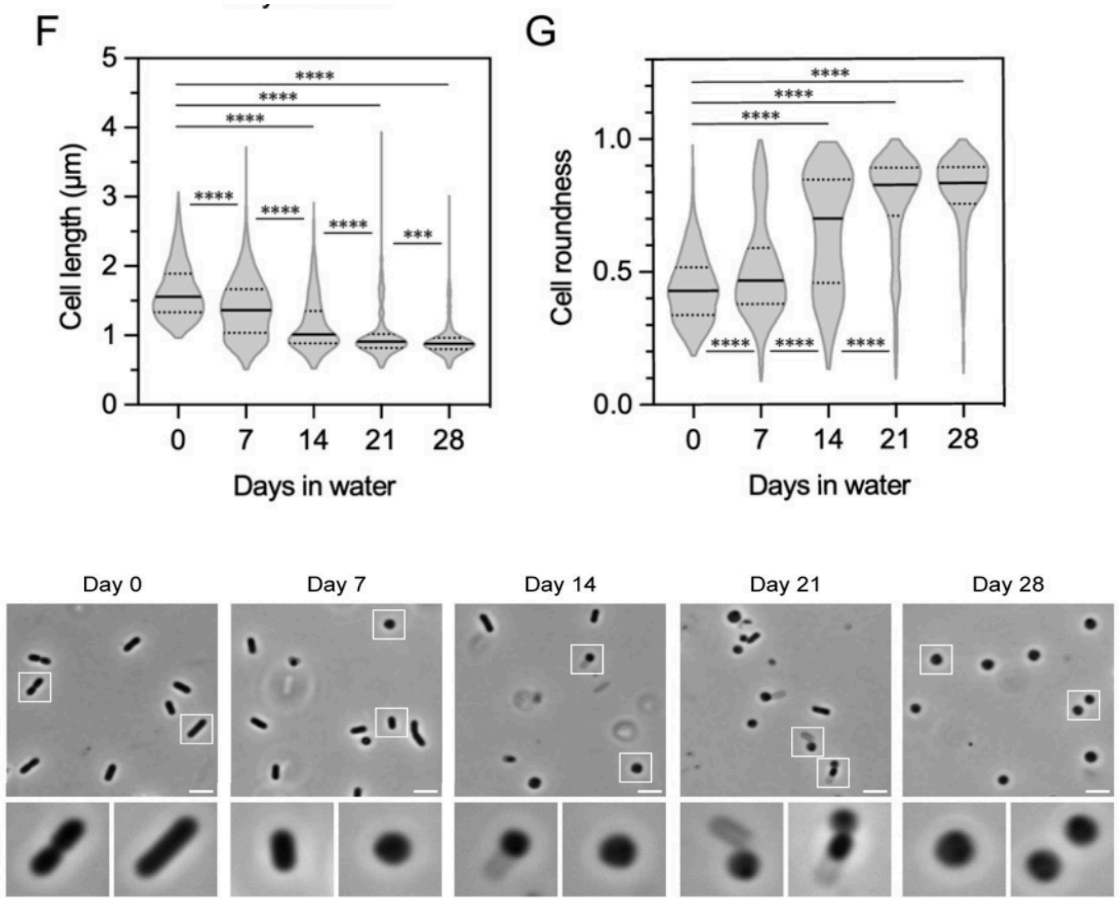

Figure 21: Morphological transition of *L. monocytogenes* into the VBNC state through CWD phenotype (Adapted from Carvalho et al., 2024). F: alterations in cell length over a 28-day time course; G: alterations in average cell roundness over a 28-day time course (roundness value of 1 indicates a perfectly round shape, while values closer to **0 i**ndicate an elongated or irregular shape); Right: microscopy of cells over the 28-day time course, showing typical rod-shaped cell morphology transitioning to morphologies of coccoid cells having shed their cell wall.

Results & Discussion

Chapter 1 - Secretome analysis of infected trophoblast cells with *L. monocytogenes*

I. Overview

One of the main focuses of the EpiMic team is understanding how persistent *L. monocytogenes* infection affects host cell physiology. In 2018, our team characterised the intravacuolar lifestyle of *L. monocytogenes* within LisCVs in both hepatocytes and trophoblast cells (Kortebi et al., 2018). In 2021, the team conducted a comparative study of the replicative and persistent infection phases in hepatocytes, using mainly transcriptomic analyses and proteomics as validation. It was found that during the persistent phase, *L. monocytogenes* suppresses the expression of Acute Phase Proteins (APPs) through unknown mechanisms. This suppression indicates a likely manipulation of the host's adaptive immune responses by downregulating canonical pathways, which enables the pathogen to evade elimination and establish a persistence phenotype in the hepatocyte niche (Descoeudres et al., 2021) (Figure 22).

More specifically, cellular models of persistent infection were established using HepG2 and Huh7 human hepatocyte cell lines, along with primary mouse hepatocytes. After three days of infection, *L. monocytogenes* consistently transitioned into the persistence phase. RNA-sequencing analysis revealed a deeply altered transcriptional landscape, where a common signature of long-term *L. monocytogenes* infection was identified across these hepatocyte models. Key findings included (i) the upregulation of genes involved in antiviral immunity, particularly interferon responses (type I in primary mouse hepatocytes and type III in HepG2 cells), and (ii) the downregulation of numerous APP-encoding genes, particularly those involved in the complement and coagulation systems. Interestingly, Huh7 cells remained largely unresponsive to the infection, suggesting a differential response based on cell type. These transcriptional blocks on APP expression were maintained even under pro-inflammatory cytokine stimulation, further reinforcing the pathogen's ability to manipulate the host's immune response. Moreover, quantitative proteomics analyses of the hepatocyte secretome demonstrated that the reduced protein abundance correlated with the observed transcriptomic downregulation.

Building upon these findings, our current project focuses on investigating *L. monocytogenes* infection in trophoblast cells at 24h p.i., representing the replicative/acute phase and the 96h p.i., namely the

persistent/chronic phase. The goal of this study is to identify specific proteomic signatures, with a focus on the secretome, and compare that of the active phase to the persistent phase of infection. By doing so, we aim to uncover differences that could provide critical insights into the mechanisms that *L. monocytogenes* uses to establish persistent infection. The use of comparative shotgun proteomics, enabled by liquid chromatography-tandem mass spectrometry (LC-MS/MS), offers a powerful analytical platform for a global inventory of complex proteomes. This method allows us to track protein expression changes and identify potential biomarkers or pathways that contribute to the persistence phenotype in trophoblast cells, similar to the hepatocytes model described previously. Our findings could pave the way for a deeper understanding of *L. monocytogenes* persistence across different cellular environments.

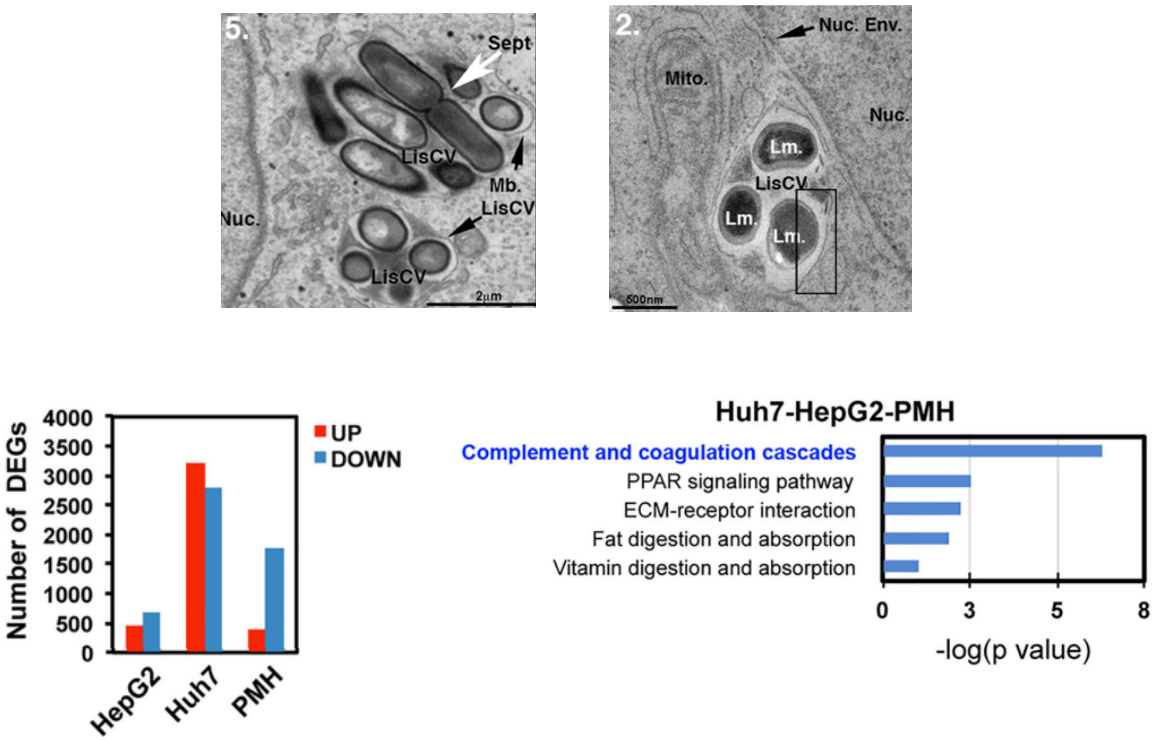

Figure 22: TEM pictures of LisCVs in hepatocytes (top left) and trophoblasts (top right). Number of differentially expressed genes (DEGs) for the three different hepatocyte lines tested (bottom left) and top 5 downregulated pathways (bottom right) of the hepatocytes model. The top pictures adapted from Kortebi et al., 2018 and the bottom pictures from Descoeudres et al., 2021.

II. Experimental Set-Up

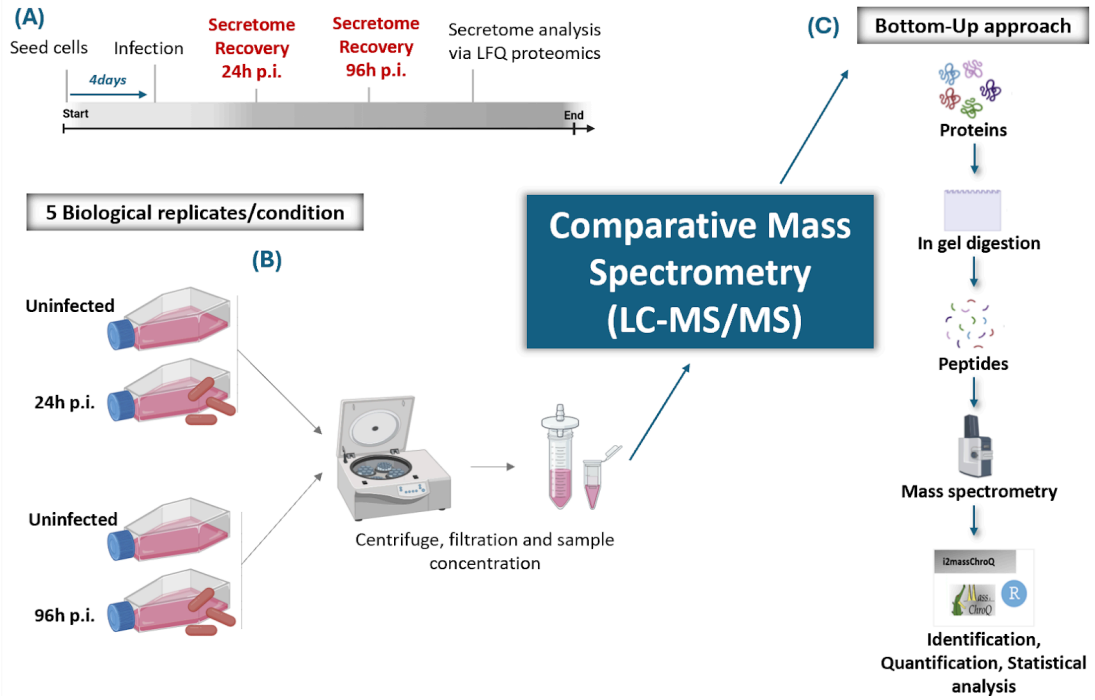

Figure 23: Graphical representation of thesis objective 1. (A) Timeline of infection; seeding cells, infection with *L. monocytogenes* 10403S WT, secretome recovery at 24h p.i. and 96h p.i. of infection and secretome analysis via LFQ proteomics. (B) Illustration of secretome recovery methodology both for the uninfected and infected samples (five biological replicates per condition) and (C) comparative mass spectrometry via LC-MS/MS following a classical bottom up approach.

For our experiment, we used the JEG3 choriocarcinoma trophoblast cell line, which we infected with *L. monocytogenes* 10403S WT. Two different timepoints were studied: 24h p.i. (the acute infection stage, I-24) and 96h p.i. (the chronic infection phase, I-96); in addition, uninfected cells served as controls for each of the 24h p.i. and 96h p.i. timepoints (controls NI-24 and NI-96, respectively). Targeting secreted proteins specific to 96h p.i. was selected, as that is the timepoint that LisCVs biogenesis has been described. This study compared the differential expression of proteins at both the chronic and persistent infection phases. This provided insights into specific deregulated proteins or pathways at the chronic phase of infection to understand how the secretion potential of the infected trophoblast is being altered upon long-term exposure to *L. monocytogenes*. For our experiment, we set up five biological replicates, starting with five different cell passages and five independent overnight bacterial cultures. The supernatant of infected (I) and non-infected (NI) samples was collected and manipulated further for comparative LC-MS/MS (Figure 23; see Material and Methods section).

III. Results

3.1 Experiment Assessment

Infection assessment via immunofluorescence characterisation of cultures was performed to confirm the appropriate cell state was achieved (i.e. acute or chronic, data not shown). Samples were then prepared for proteomic analysis via LC-MS/MS in DDA, as described in the Materials and Methods section. We conducted a quality assessment based on statistical analysis using Spectral Counts (SC) with Principal Component Analysis (PCA) and heatmap visualisations to assess sample quality and biological replicates clustering (Figure 24, Figure 25). The results demonstrated strong similarity among biological replicates and notable differences across the following conditions: Non-Infected 24h (NI-24), Infected 24h (I-24), Non-Infected 96h (NI-96), and Infected 96h (I-96). This was further supported by heatmap analysis, which consistently grouped replicates within each condition and visualised protein abundance of all the identified proteins (n=2657) based on the i2massChroQ software (Figure 25). The heatmap clearly displayed how the abundance of the identified proteins fluctuated across conditions.

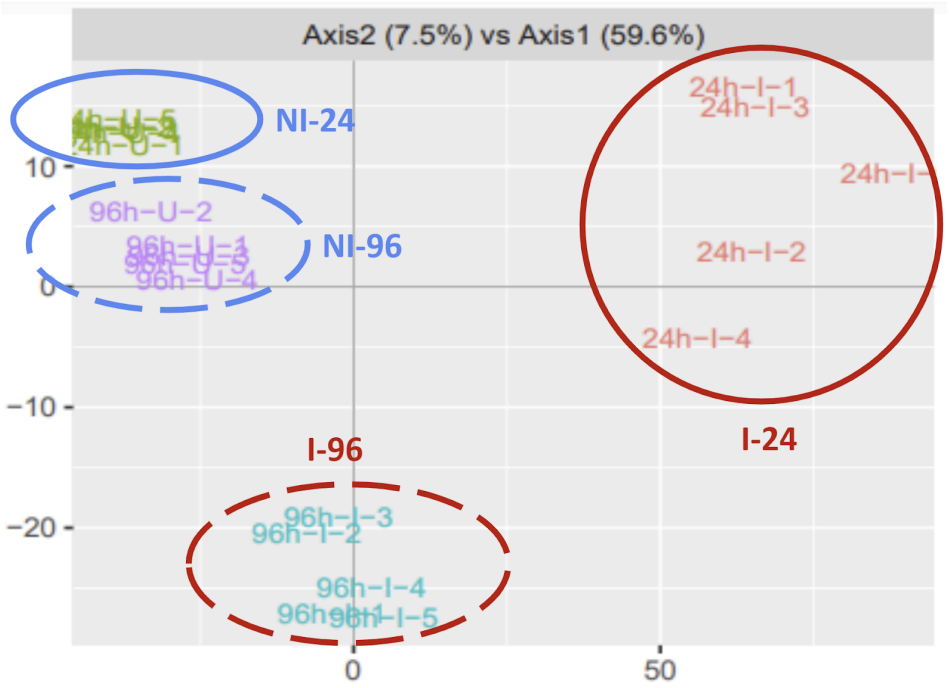

Figure 24: Principal Component Analysis (PCA) showing all the replicates per conditions forming clusters; the first two components accounted for 59.6% and 7.5% of the variances, respectively. The X-axis represents the principal component (PC1)while the Y-axis corresponds to (PC 2).

Significant changes were observed after 24h p.i., with signs of adaptation becoming evident by 96h p.i. Six distinct protein clusters (A, B, C, D, E, and F) with differential abundance were identified (Figure 25):

- Cluster A comprised proteins at predominantly reduced abundance in infected cell secretomes at both 24h and 96h p.i., relative to uninfected cells.
- Clusters B, D and F comprised proteins predominant at higher abundance in infected cell secretomes at both 24h and 96h p.i., relative to uninfected cells.
- Clusters C and E comprised proteins predominantly at higher abundance 24h p.i. in infected cell secretomes, which then observed a trend of low-abundance 96h p.i.

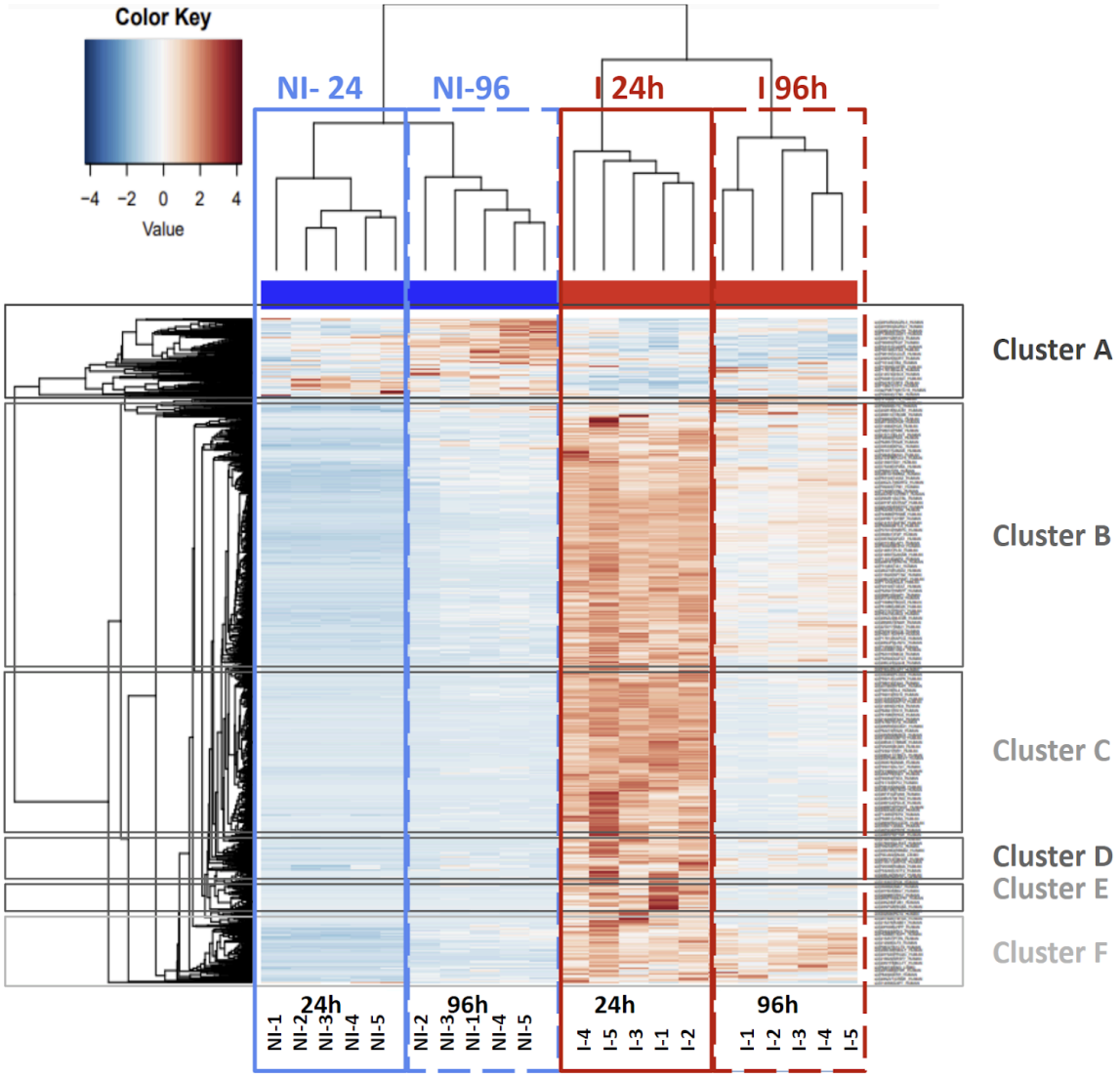

Figure 25: Heatmap depicting the abundance of proteins identified by LC-MS/MS analysis in our in vitro infection trophoblasts - *L. monocytogenes* model across different conditions. Protein abundance is represented

on a log2-transformed scale, with blue indicating low abundance and red indicating high abundance. Rows represent individual proteins, and columns represent each experimental condition. A heatmap was generated with all identified proteins (2657 proteins) based on i2massChroQ software, and clustering was performed using hierarchical clustering with the default ward.D method to highlight the change in the abundance of proteins in different conditions. X axis: experimental conditions and biological replicate, Y axis: Clustering of identified proteins. The colour key illustration of the median centred log2 protein abundance values; Blue- relatively lower level of protein abundance, White- no difference in protein abundance, and Red- High level of protein abundance.

3.2 Identification and Quantification (SC and XIC) of secreted proteins in DDA

A total of 2657 protein subgroups were identified (using a criterion of at least 2 peptides per protein and a protein E-value of 10^{-4} and peptide E-value of $4*10^{-3}$). While the number of proteins varied considerably across the four experimental conditions (Table 4a), the reproducibility of the five biological replicates for each condition was high, with over 60-70% consistency in DDA analysis and only minor deviations from the mean (Table 4c). Although the total number of identified proteins was higher in the infected samples (1672 proteins were detected in I-24 compared to 319 in NI-24, and 1008 proteins in I-96 compared to 621 in NI-96, Table 4b), the percentage of secreted proteins, which are typically released under controlled physiological processes, was lower. This reduction could be attributed to cell lysis, as the breakdown of cellular membranes releases intracellular proteins, diluting the pool of proteins that would normally be secreted under standard conditions.

Table 4 : Number of (a) Average and (b) shared identified proteins, (c) percentage of reproducibility within each condition, (d) Average and (e) shared number of secreted proteins and (f) percentage of secreted proteins in the overall population.

Condition	(a) Average number of identified protein subgroups (incl. range of protein subgroups across replicates)	(b) Number of shared identified proteins subgroups within the replicates	(c) Reproducibility of replicates	(d) Average number of secreted protein subgroups (incl. range of protein subgroups across replicates)	(e) Number of shared secreted protein groups within the replicates	(f) (%) Secreted Proteins
NI-24	432 (401-473)	319	60.20%	160 (149-168)	116	36 %
NI-96	902 (713-988)	621	61.20%	193 (175-207)	150	24 %
I-24	2129 (2037-2317)	1672	69.70%	180 (159-197)	133	7.9 %
I-96	1379 (1289-1453)	1008	66.50%	186 (181-190)	142	14 %

A significant overlap in proteins was found between infected samples (I-24 and I-96), with 440 proteins (24.6%) unique to infection, regardless of time point. The largest proportion, 38.7% (693 proteins), was unique to I-24, likely reflecting the dynamics of early infection. Nineteen proteins were specific to I-96, some of which may serve as markers of persistence. In the uninfected samples, we identified a subset of 21 proteins consistently present at all time points, along with 12 proteins unique to NI-24 and 27 unique to NI-96 (Figure 26).

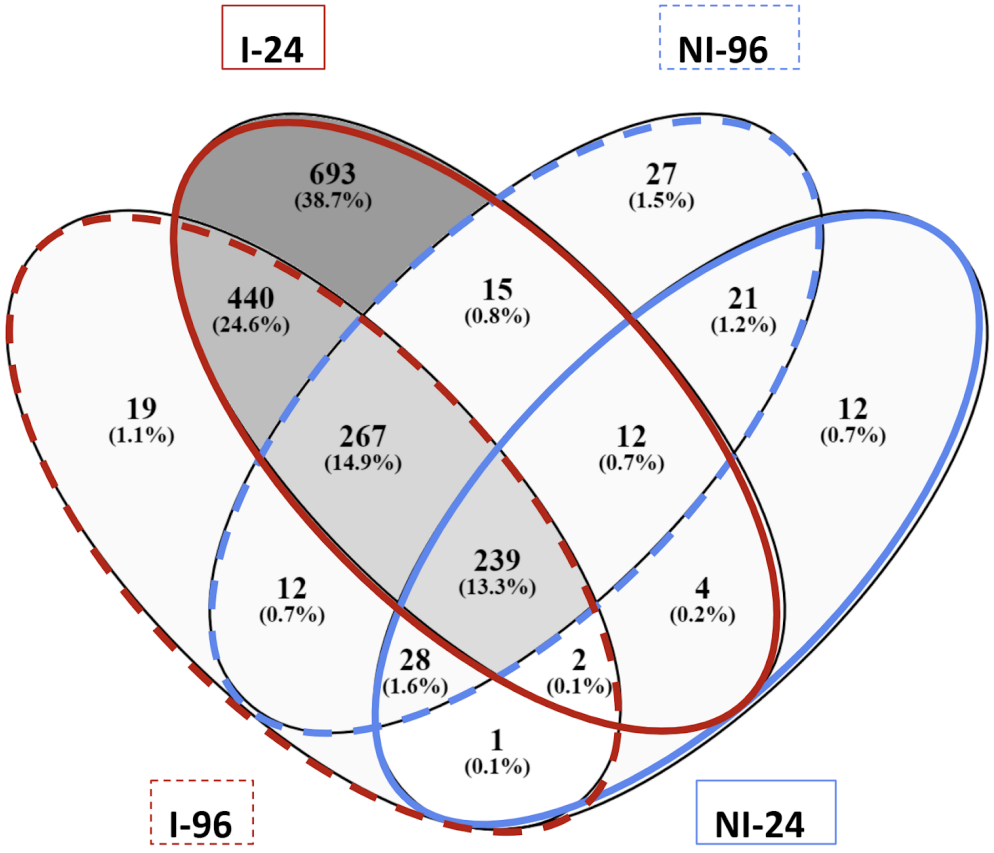

Figure 26 : Venn diagram depicting the number of proteins identified reproducibly for each condition. Red; I-24, Dotted-red; I-96, Blue; I-24 and Dotted-blue; NI-96.

In the context of secreted proteins, the reproducibility of the five biological replicates per condition was high (Table 4d). In terms of infection-specific proteins, 9 were identified as being consistently present during infection at both time points, while 10 proteins were unique to I-24 and 6 proteins were specific to I-96, highlighting potential time-dependent protein expression during the course of infection (Table 5). More specifically, we identified 9 proteins consistently present in the NI samples,

regardless of the time point. Additionally, we observed 7 proteins specific to NI-96 and 5 proteins specific to NI-24, likely secreted proteins sensitive to cell confluency (Table 6). Furthermore, 78 proteins were found to be constitutively secreted, unaffected by either infection phase (acute or persistent) or cell confluency.

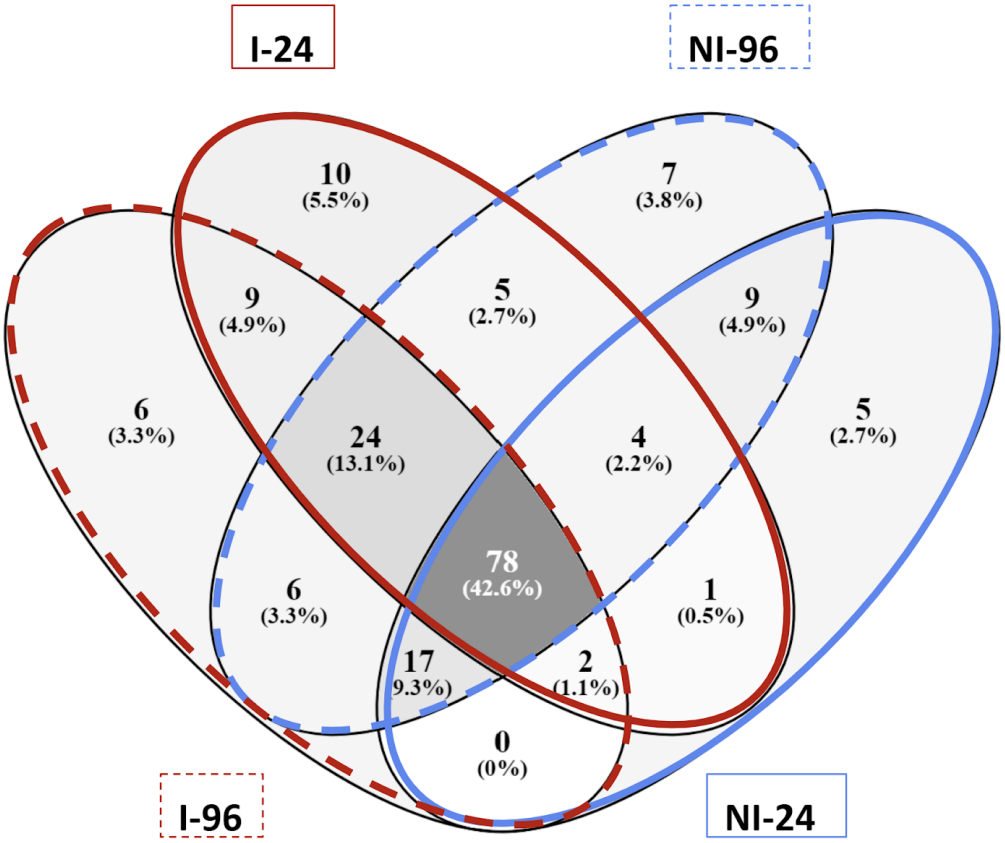

Figure 27 : Venn diagram representing the number of reproducibly identified secreted proteins cohort for each condition. Red; NI-24, Dotted-red; NI-96, Blue; I-24 and Dotted-blue; NI-96.

3.3 Identification of secreted protein abundance across the conditions

3.3.1 Infected Samples associated proteins

In the following section and based on the Venn analysis (Figure 27), preliminary insights into the differential abundance of proteins, which could have potential implications for understanding host responses to *L. monocytogenes* infection and/or identifying possible biomarkers are discussed (Tables 5 and 6).

Table 5: Secreted proteins specifically identified with i2MassChroQ to Infected samples (I-24 and I-96). Fold change of normalised abundance for each grouped quantification via MCQR (both SC and XIC) is shown. INF; proteins with infinite ratio for the corresponding group, (-) indicates the absence of a numerical ratio based on MCQR analysis.

Identification (i2MassChroQ)	Quantification (MCQR)					
	Uniprot Accession	Protein Name	Fold Change of normalised protein abundance			
			I/NI 24h	I/NI 96h	I 96h/24h	NI 96h/24h
I-24 only	P14735	Insulin-degrading enzyme	2.88	-	0.55	-
	Q08J23	RNA cytosine C(5)-methyltransferase NSUN2	INF	-	0.18	-
	P14174	Macrophage migration inhibitory factor (MIF)	2.38	-	-	-
	Q13361	Microfibrillar-associated protein 5 (MFAP-5)	0.5	-	3.7	2.25
	P02771	Alpha-fetoprotein	0.25	0.37	5.24	0.36
	Q8N474	Secreted frizzled-related protein 1 (FRP-1)	INF	5	-	-
	Q8NCW5	NAD(P)H-hydrate epimerase	INF	2.02	-	-
	Q9BXX0	EMILIN-2	INF	18.75	-	-
	Q07021	Complement component 1 Q subcomponent-binding protein	2.36	3.04	1.7	-
	Q5JS37	NHL repeat-containing protein 3	0.43	0.52	1.6	-
Common	P31947	14-3-3 protein sigma (Stratifin)	4	2.21	1.88	3.4
	P26583	High mobility group protein B2 (HMG-2)	346	0.37	0.56	-
	O00515	Ladinin-1 (Lad-1)	INF	6.92	2.72	-
	Q66K79	Carboxypeptidase Z (CPZ)	INF	3.48	3.44	2
	P17693	HLA class I histocompatibility antigen, alpha chain G (HLA G antigen)	5.67	-	1.98	4.67
	Q12904	Aminoacyl tRNA synthase complex-interacting multifunctional protein 1	4.89	45	0.51	-
	Q9NZV1	Cysteine-rich motor neuron 1 protein (CRIM-1)	4.43	1.94	3.95	-
	Q9BWS9	Chitinase domain-containing protein 1	0.13	-	-	-
	Q00796	Sorbitol dehydrogenase (SDH)	27	-	1.58	-
I-96 only	P12259	Coagulation factor V	0.3	-	-	0.37
	P21246	Pleiotrophin (PTN)	-	15	2.29	-
	P05161	Ubiquitin-like protein ISG15	-	23.71	23.42	-
	P04004	Vitronectin (VN)	0.07	-	5.76	0.32
	P08123	Collagen alpha-2(I) chain	0.08	-	3.96	0.32
	P28799	Progranulin (PGRN)	-	-	3.11	-

Table 5 examines proteins identified via i2MassChroQ in infected samples, revealing distinct regulatory patterns over time. Several proteins exhibit significant upregulation during both the acute and chronic phases of infection. For instance, insulin-degrading enzyme (IDE, P14735) and macrophage migration inhibitory factor (MIF, P14174) show fold changes of 2.88 and 2.38, respectively, when compared to NI samples at 24h p.i.. This suggests their roles in enhancing immune responses or regulating metabolism during infection. Some examples are:

Insulin Degrading Enzyme (IDE)

Notably, IDE plays a central role in cellular insulin breakdown, disrupting intercellular peptide signaling. Its involvement in infections has also been documented, particularly in varicella-zoster virus (VZV) infection, where IDE serves as a receptor that facilitates viral activation and cell-to-cell spread (Li et al., 2006). Additionally, it has been shown that IDE is implicated in the antigen processing pathway of CD8+ cytotoxic T lymphocytes (Chavez-Arroyo and Portnoy, 2020). In a murine model of intravenous *L. monocytogenes* infection, immunization with a sublethal bacterial dose initiates rapid intracellular bacterial replication, followed by bacterial clearance and the development of cell-mediated immunity (CMI), primarily mediated by antigen-specific CD8+ T cells (Chavez-Arroyo and Portnoy, 2020). This effective immune response relies on replicating bacteria and may be linked to bacterial secreted proteins that engage with the MHC class I antigen processing pathway. The upregulation of IDE during the acute infection phase (I/NI 24h) likely reflects an active immune response. Conversely, its downregulation in the I 96/24 might indicate immune modulation or disruptions as the infection progresses.

Macrophage Migration Inhibitory Factor (MIF)

Similarly, MIF, a proinflammatory cytokine of the innate immune response, has been shown to play a dual role in pathogenic infections; detrimental or beneficial (Oddo et al., 2005). For instance, in Mtb infections it has been shown to impact its growth while in the context of *L. monocytogenes* infection, MIF has been found to have a detrimental effect during lethal infections (Oddo et al., 2005). The study shows that MIF levels increase significantly early in infection with lethal *L. monocytogenes* infection, but not in sublethal infections (Sashimani et al., 2006). While blocking MIF with antibodies does not affect bacterial clearance in sublethal infections, it significantly improves survival in lethal infections (Sashimani et al., 2006). Overall the study has shown that MIF worsens the outcome of lethal *Listeria* infections, likely by modulating IL-10 and cortisol levels, contributing to a harmful inflammatory response (Sashimani et al., 2006). In our case, the upregulation of MIF at I/NI 24 comes in line with the increased activity of MIF in the cited study.

Alpha-fetoprotein (AFP)

Alpha-fetoprotein (AFP), produced during fetal development, has immunoregulatory properties that influence immune responses. Disruptions in AFP levels can lead to alpha-fetoprotein deficiency

(AFPD), which, while not affecting development, has been linked to conditions like Down syndrome and hereditary persistence of AFP (HPAFP) in adults, as well as spina bifida (McVey et al., 1993; Petit et al., 2009). AFP dampens cytokine activity, including IFN-γ and TNF, in natural killer (NK) cells and macrophages, helping to maintain immune tolerance during pregnancy. However, this immunosuppressive effect can hinder immune responses to infections, such as *L. monocytogenes*, as demonstrated in an in vivo study where AFP's suppression of key cytokines impaired the mice's ability to eliminate the bacteria (Yamashita et al., 1994). In our study, AFP is downregulated in both I/NI 24 and I/NI 96 samples, while highly upregulated in the I 96/24 comparison. This suggests that AFP downregulation may enhance immune responses against infection, while its upregulation could indicate a host mechanism to support pregnancy under stress.

3.3.2 Proteins with Infection-Specific Abundance

Several proteins display infection-specific abundance, suggesting roles in gene regulation, signalling, and immune modulation. NSUN2, linked to RNA stability and the innate immune response in viral infections, shows high abundance at I/NI 24h, reflecting a role in *L. monocytogenes* infection responses. Its reduced abundance from acute to chronic phases (I 96/24) suggests a diminished need as infection progresses. SFRP-1, an inhibitor of Wnt signalling, regulates cell proliferation and tissue repair. Its upregulation during both acute (infinite fold change) and chronic (I 96/24) phases may help manage early infection-induced damage but could lead to impaired tissue repair over time (Foronjy et al., 2010). Ladinin-1 (LAD-1), essential for ECM stability and cell adhesion, shows upregulation in the acute phase, suggesting ECM stabilisation in response to infection, transitioning to moderate levels in the chronic phase as part of adaptive tissue remodelling (Moon et al., 2020). Pleiotrophin (PTN), upregulated at 96h p.i., promotes tissue repair and angiogenesis, potentially supporting healing in chronic infection (Herradon et al., 2019). Its roles in cell migration and immune cell recruitment indicate involvement in sustaining tissue function under prolonged stress.

The observed upregulation of these proteins reflects host adaptive responses to combat infection and modulate immune defences, while the variations between acute and chronic phases highlight shifting mechanisms in immune and inflammatory responses over time. Understanding these changes offers insights into infection dynamics and therapeutic targeting for recovery.

3.3.3 Non-Infected Samples associated proteins

Similarly, Table 6 focuses on proteins present in NI samples, with an emphasis on identifying negative markers for potential biomarker studies. Quantitative analysis reveals that several proteins are present at very low levels when comparing I to NI samples, suggesting their potential as negative biomarkers, meaning that the absence of such a protein could indicate the presence of infection.

Table 6: Secreted proteins specifically identified with i2MassChroQ to Non-Infected samples (NI-24 and NI-96). Fold change of normalised abundance for each grouped quantification via MCQR (both with SC and XIC) is shown. INF; proteins with infinite ratio for the corresponding group, (-) indicates the absence of a numerical ratio based on MCQR analysis.

Identification (i2MassChroQ)	Quantification (MCQR)					
	Uniprot Accession	Protein Name	Fold Change of normalised protein abundance			
			I/NI 24h	I/NI 96h	I 96h/24h	NI 96h/24h
NI-24 only	P55268	Laminin subunit beta-2	0.27	-	-	0.25
	Q6PCB0	von Willebrand factor A domain-containing protein 1	0.23	0.51	1.92	0.28
	P29400	Collagen alpha-5(IV) chain	-	-	8.64	-
	P51884	Lumican (KSPG lumican)	0.03	-	4.9	0.24
	P00740	Coagulation factor IX	-	-	-	0.28
Common	Q9BTY2	Plasma alpha-L-fucosidase	0.07	0.17	-	0.44
	P10915	Hyaluronan and proteoglycan link protein 1	0.05	0.14	2.69	2.14
	Q92673	Sortilin-related receptor (SorLA)	0.26	0.03	0.05	-
	Q6EMK4	Vasorin	0.09	0.29	-	1.81
	O60462	Neuropilin-2	0.11	0.45	3.59	0.3
	Q8WVQ1	Soluble calcium-activated nucleotidase 1 (SCAN-1)	0.17	0.28	-	0.53
	P19827	Inter-alpha-trypsin inhibitor heavy chain H1	0.1	0.39	2.98	0.35
	P02753	Retinol-binding protein 4	0.09	-	7.51	0.49
	P09958	Furin	-	0.28		0.55
NI-96 only	P08174	Complement decay-accelerating factor	0.15	0.29	2.5	0.64
	Q86Y38	Xylosyltransferase 1	-	4.76	-	2.75
	Q9UBQ6	Exostosin-like 2	0.09	0.19	1.71	0.55
	O00584	Ribonuclease T2	0.1	0.24	-	0.53
	P08253	72 kDa type IV collagenase	-	0.09	-	10
	Q9H1B5	Xylosyltransferase 2	-	0.2	-	4.29
	Q92484	Cyclic GMP-AMP phosphodiesterase	0.18	0.29	-	-

In the context of our study, protein abundance patterns of specific proteins suggest their potential utility as negative markers for chronic disease detection. Analysis of NI samples over time, informed by UniProt data, reveals intriguing trends. For instance, hyaluronan and proteoglycan link protein 1 (HAPLN-1, P10915) exhibits a fold change of 2.69 in NI 96h/24h. This increase may indicate a role in

maintaining cellular integrity, particularly during pregnancy establishment. Retinol-binding protein 4 (RBP4, P02753), with a low fold change of 0.09, underscores its significance in cellular homeostasis. Furthermore, xylosyltransferase 1 and 2 (XYLT1, XYLT2) show significant upregulation (fold change of 2.75 and 4.29, respectively) in NI 96h/24h, suggesting involvement in natural healing through proteoglycan synthesis and extracellular matrix (ECM) maintenance.

3.3.4 Summary

In conclusion, the findings from both datasets highlight the dynamic modulation of specific secreted proteins in response to *L. monocytogenes* infection, suggesting critical cellular processes involved in infection outcomes. For instance, the deregulation of proteins such as IDE, MIF, AFP, SFRP-1, LAD-1 and both XYLTL2 and HLPL-1 might indicate the host's adaptive response mechanisms, including immune evasion and inflammation regulation. These patterns observed across acute and chronic phases not only reflect the host's responses but also differentiate between infected and non-infected states, providing valuable insights into the underlying physiological profiles. Identifying these proteins as potential biomarkers underscores the necessity for further validation studies and exploration of their regulatory mechanisms, which could significantly inform therapeutic strategies and enhance diagnostic tools for detecting persistent *L. monocytogenes* infections. By elucidating these specific responses, this research could contribute with new insights into the field of infection biology.

3.4 Quantification of secreted protein abundance across the conditions

A comparative proteomic quantification analysis was performed across four experimental conditions: Infected/Non-Infected at 24h (I/NI 24h), Infected/Non-Infected at 96h (I/NI 96h), Infected 96h/24h (I 96h/24h), and Non-Infected 96h/24h (NI 96h/24h), to examine the temporal dynamics of secreted protein expression (Supplementary Tables 1A to 4C, pages 199-220). This analysis initially included all variable proteins identified through SC and XIC, which were subsequently filtered to retain only statistically significant secreted proteins. Protein abundance and fold changes were calculated for each condition, revealing how infection with *L. monocytogenes* influences host cell responses, particularly in terms of protein secretion (Table 7, Figure 28). By comparing these conditions, we aimed to uncover differential protein expression during infection and over time, offering valuable insights into host-pathogen interactions.

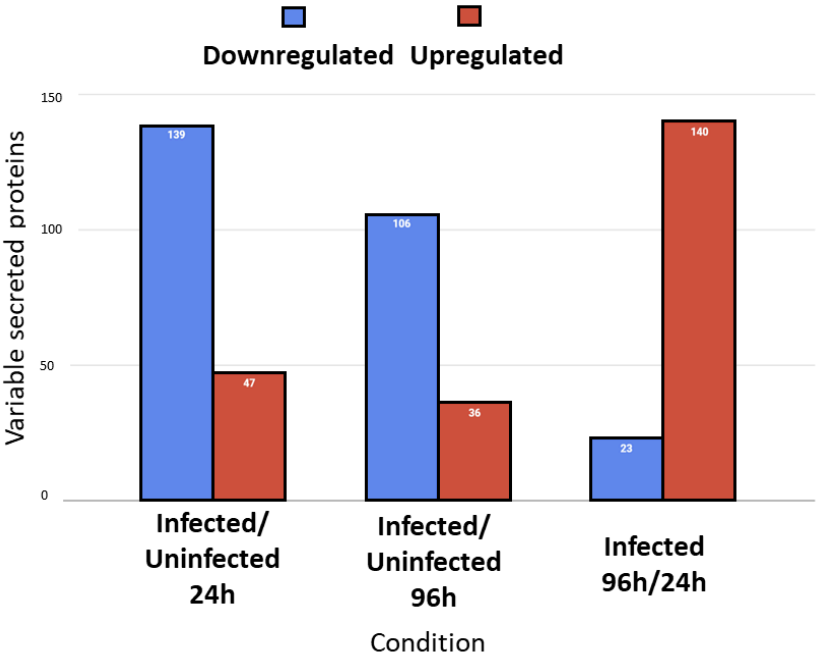

Figure 28 : Total number of statistically significant variable proteins, both upregulated and downregulated for the three conditions; I/NI 24h, I/NI 96h, I 96h/24h.

The merged quantification between SC and XIC methods revealed 186 significant proteins for I/NI 24h, 142 proteins for I/NI 96h, 163 proteins for I 96h/24h, and 186 proteins for NI 96h/24h (Table 7). Our data suggest a strong downregulation of protein secretion during *L. monocytogenes* infection, particularly during the acute phase (I/NI 24h), (Figure 28). Additionally, we examined statistically significant variable proteins for I 96h/24h to identify potential markers specific to chronic infection (Figure 28). A stronger upregulation was observed in the 96h Infected samples (I 96h/24h), while in the control group (NI 96h/24h), most secreted proteins were downregulated (Figure 28).

Table 7 : Number of deregulated secreted proteins with two complementary quantification methods.

Number of Statistically Significant proteins	**ONLY** Spectral Counts (SC)	**FOUND IN BOTH**	**ONLY** Extracted Ion Chromatogram (XIC)	Total number of deregulated proteins
I/NI 24H Downregulated	4	49	86	139
I/NI 24H Upregulated	32	13	2	47
I/NI 96H Downregulated	9	39	58	106
I/NI 96H Upregulated	18	12	6	36
I 96H/24H Downregulated	21	2	-	23
I 96H/24H Upregulated	2	22	116	140
NI 96H/24H Downregulated	-	13	107	120
NI 96H/24H Upregulated	44	19	3	66

Table 8 : Secreted proteins identified as statistically significant by SC and/or XIC quantification methods (n=168). Classification has been performed in accordance with the level of significance (padj < 0.05) as used for the heatmap below. Proteins highlighted in pink; only with XIC, in blue; only with SC and green; both with SC and XIC.

Uniprot Accession	Protein Name	padj (< 0.05)	Uniprot Accession	Protein Name	padj (< 0.05)
P08238	Heat shock protein HSP 90-beta (HSP 90)	1.00E-120	P01008	Antithrombin-III (ATIII) (Serpin C1)	5.30E-07
P26583	High mobility group protein B2 (HMG-2)	3.52E-119	P20742	Pregnancy zone protein	5.59E-07
P09429	High mobility group protein B1 (HMG-1)	2.19E-112	P00734	Prothrombin	5.91E-07
P06744	Glucose-6-phosphate isomerase (GPI)	5.90E-91	P22455	Fibroblast growth factor receptor 4 (FGFR-4)	6.65E-07
P07355	Annexin A2 (Annexin II)	2.31E-84	P02458	Collagen alpha-1(II) chain (Alpha-1 type II collagen)	7.06E-07
P62937	Peptidyl-prolyl cis-trans isomerase A (PPIase A)	3.96E-72	Q8IUL8	Cartilage intermediate layer protein 2 (CILP-2)	8.25E-07
P67809	Y-box-binding protein 1 (YB-1)	1.56E-62	P05121	Plasminogen activator inhibitor 1 (PAI)	8.29E-07
P07237	Protein disulfide-isomerase (PDI)	3.52E-59	P11047	Laminin subunit gamma-1	9.31E-07
Q15046	Lysine--tRNA ligase (LysRS)	2.46E-46	Q16651	Prostasin	1.10E-06
P53621	Coatomer subunit alpha (Alpha-coat protein)	1.32E-44	Q86Y38	Xylosyltransferase 1	1.14E-06
O75882	Attractin (DPPT-L)	8.86E-40	Q8NCC3	Lysosomal phospholipase A and acyltransferase	1.15E-06
Q12904	Aminoacyl tRNA synthetase complex-interacting multifunctional protein 1 (EMAP-II)	1.74E-39	P0DMV8	Heat shock 70 kDa protein 1A	1.28E-06

O00391	Sulfhydryl oxidase 1 (hQSOX)	4.10E-39	P05543	Thyroxine-binding globulin (Serpin A7)	1.42E-06
Q96HE7	ERO1-like protein alpha (ERO1-L)	2.61E-36	P02461	Collagen alpha-1(III) chain	1.70E-06
O00515	Ladinin-1 (Lad-1)	5.45E-33	Q6EMK4	Vasorin (Protein slit-like 2)	1.76E-06
Q9H4A4	Aminopeptidase B (AP-B)	1.96E-27	Q9NZV1	Cysteine-rich motor neuron 1 protein (CRIM-1)	1.99E-06
Q8WUM4	Programmed cell death 6-interacting protein (PDCD6-interacting protein)	1.16E-26	M5A8F1	Suppressyn	2.19E-06
Q9BTY2	Plasma alpha-L-fucosidase (Alpha-L-fucosidase 2)	8.19E-24	P20908	Collagen alpha-1(V) chain	2.22E-06
P14735	Insulin-degrading enzyme (Insulysin)	2.51E-23	P04114	Apolipoprotein B-100 (Apo B-100)	2.34E-06
P51858	Hepatoma-derived growth factor (HDGF)	7.98E-23	Q08380	Galectin-3-binding protein	2.78E-06
P98160	Basement membrane-specific heparan sulfate proteoglycan core protein (HSPG)	1.57E-18	P02771	Alpha-fetoprotein	3.13E-06
P43490	Nicotinamide phosphoribosyltransferase (NAmPRTase)	2.65E-18	P09486	SPARC	3.14E-06
P04083	Annexin A1 (Annexin I)	1.47E-17	P15291	Beta-1,4-galactosyltransferase 1 (Beta-1,4-GalTase 1)	3.72E-06
O00468	Agrin	1.78E-16	O60462	Neuropilin-2 (Vascular endothelial cell growth factor 165 receptor 2)	3.73E-06
P10599	Thioredoxin (Trx)	1.15E-14	P02749	Beta-2-glycoprotein 1 (APC inhibitor)	4.41E-06
Q66K79	Carboxypeptidase Z (CPZ)	1.92E-13	P07996	Thrombospondin-1 (Glycoprotein G)	4.82E-06
Q07021	Complement component 1 Q subcomponent-binding protein (C1qBP)	1.93E-13	P02753	Retinol-binding protein 4	5.34E-06

P21246	Pleiotrophin (PTN)	1.56E-12	P07711	Procathepsin L	5.73E-06
A6NKQ9	Choriogonadotropin subunit beta variant 1	1.60E-12	Q12884	Prolyl endopeptidase FAP	5.94E-06
P36955	Pigment epithelium-derived factor (PEDF)	4.58E-11	P12111	Collagen alpha-3(VI) chain	7.44E-06
Q9BXX0	EMILIN-2 (Elastin microfibril interface-located protein 2)	7.48E-11	Q13822	Autotaxin	8.30E-06
Q8N474	Secreted frizzled-related protein 1 (FRP-1)	9.94E-11	O43278	Kunitz-type protease inhibitor 1 (HAI-1)	8.61E-06
Q04756	Hepatocyte growth factor activator (HGF activator)	1.10E-10	P16035	Metalloproteinase inhibitor 2	1.04E-05
P08697	Alpha-2-antiplasmin (Alpha-2-AP)	1.49E-10	P02452	Collagen alpha-1(I) chain (Alpha-1 type I collagen)	1.08E-05
P01024	Complement C3 (C3 and PZP-like alpha-2-macroglobulin domain-containing protein 1)	1.49E-10	P02750	Leucine-rich alpha-2-glycoprotein (LRG)	1.13E-05
P22626	Heterogeneous nuclear ribonucleoproteins A2/B1 (hnRNP A2/B1)	1.49E-10	P00740	Coagulation factor IX	1.14E-05
P14543	Nidogen-1 (NID-1)	1.49E-10	O15230	Laminin subunit alpha-5	1.19E-05
Q8WVQ1	Soluble calcium-activated nucleotidase 1 (SCAN-1)	1.66E-10	P08123	Collagen alpha-2(I) chain (Alpha-2 type I collagen)	1.41E-05
Q08J23	RNA cytosine C(5)-methyltransferase NSUN2	3.67E-10	Q14624	Inter-alpha-trypsin inhibitor heavy chain H4	1.66E-05
Q99988	Growth/differentiation factor 15 (GDF-15)	4.18E-10	P08253	72 kDa type IV collagenase	2.13E-05
Q9H1B5	Xylosyltransferase 2	7.02E-10	P26927	Hepatocyte growth factor-like protein	2.26E-05

Q9NPH3	Interleukin-1 receptor accessory protein (IL-1R3)	7.28E-10	P00747	Plasminogen	2.50E-05
P19883	Follistatin (FS)	7.34E-10	P61769	Beta-2-microglobulin	3.74E-05
P35052	Glypican-1	8.64E-10	P31431	Syndecan-4 (SYND4)	1.02E-04
P02760	Protein AMBP (Protein HC)	3.24E-09	P06396	Gelsolin (AGEL)	1.03E-04
P30740	Leukocyte elastase inhibitor (LEI)	3.49E-09	Q969H8	Myeloid-derived growth factor (MYDGF)	1.83E-04
P05155	Plasma protease C1 inhibitor (C1 Inh)	3.73E-09	P27797	Calreticulin (CRP55)	2.75E-04
P02786	Transferrin receptor protein 1 (TR)	3.73E-09	P31947	14-3-3 protein sigma (Epithelial cell marker protein 1) (Stratifin)	4.47E-04
Q03167	Transforming growth factor beta receptor type 3 (TGFR-3)	3.90E-09	P10909	Clusterin (Apolipoprotein J)	5.20E-04
P05161	Ubiquitin-like protein ISG15 (hUCRP)	5.08E-09	P55268	Laminin subunit beta-2	5.42E-04
P02774	Vitamin D-binding protein (DBP)	1.54E-08	P12109	Collagen alpha-1(VI) chain	8.15E-04
O60568	Multifunctional procollagen lysine hydroxylase and glycosyltransferase LH3	1.68E-08	P04004	Vitronectin (VN)	1.15E-03
Q6H9L7	Isthmin-2	1.77E-08	P17693	HLA class I histocompatibility antigen, alpha chain G (HLA G antigen)	1.37E-03
P23142	Fibulin-1 (FIBL-1)	1.98E-08	P07602	Prosaposin (Proactivator polypeptide)	1.40E-03
P19823	Inter-alpha-trypsin inhibitor heavy chain H2 (ITI heavy chain H2)	2.03E-08	Q9UBQ6	Exostosin-like 2	1.54E-03
P51884	Lumican (Keratan sulfate proteoglycan lumican)	3.40E-08	P24043	Laminin subunit alpha-2	1.85E-03

Q92820	Gamma-glutamyl hydrolase (GH)	3.69E-08	O76061	Stanniocalcin-2 (STC-2)	2.31E-03
P10915	Hyaluronan and proteoglycan link protein 1 (Cartilage-linking protein 1)	3.82E-08	P43251	Biotinidase (Biotinase)	3.44E-03
P19021	Peptidyl-glycine alpha-amidating monooxygenase (PAM)	4.57E-08	P14174	Macrophage migration inhibitory factor (MIF)	3.80E-03
P98095	Fibulin-2 (FIBL-2)	5.01E-08	Q02818	Nucleobindin-1 (CALNUC)	4.01E-03
P00533	Epidermal growth factor receptor	5.56E-08	P61916	NPC intracellular cholesterol transporter 2	4.09E-03
Q92673	Sortilin-related receptor	5.60E-08	P00746	Complement factor D	4.31E-03
P0C0L4	Complement C4-A	5.81E-08	P00450	Ceruloplasmin	5.31E-03
P02788	Lactotransferrin (Lactoferrin)	6.35E-08	O75487	Glypican-4	6.37E-03
P35443	Thrombospondin-4	7.64E-08	P02675	Fibrinogen beta chain	8.30E-03
P01033	Metalloproteinase inhibitor 1	8.70E-08	P21128	Uridylate-specific endoribonuclease	9.13E-03
Q6ZRP7	Sulfhydryl oxidase 2	9.12E-08	P09958	Furin	1.08E-02
P04746	Pancreatic alpha-amylase (PA)	1.10E-07	P05067	Amyloid-beta precursor protein (APP)	1.08E-02
P01031	Complement C5	1.11E-07	P41250	Glycine--tRNA ligase	1.25E-02
Q9BXJ4	Complement C1q tumor necrosis factor-related protein 3	1.21E-07	P12259	Coagulation factor V	1.30E-02
Q92876	Kallikrein-6	1.54E-07	O00560	Syntenin-1	1.32E-02
P43652	Afamin	1.57E-07	Q6UY14	ADAMTS-like protein 4 (ADAMTSL-4)	1.61E-02

Q00796	Sorbitol dehydrogenase (SDH)	1.83E-07	Q16610	Extracellular matrix protein 1 (Secretory component p85)	1.77E-02
P01034	Cystatin-C	2.42E-07	Q9Y240	C-type lectin domain family 11 member A	2.04E-02
Q8NCW5	NAD(P)H-hydrate epimerase	2.60E-07	P55145	Mesencephalic astrocyte-derived neurotrophic factor	2.17E-02
P07942	Laminin subunit beta-1	2.71E-07	P03952	Plasma kallikrein	2.21E-02
O00584	Ribonuclease T2	2.71E-07	Q14118	Dystroglycan 1	2.27E-02
O43852	Calumenin	2.94E-07	Q13361	Microfibrillar-associated protein 5 (MFAP-5)	2.47E-02
Q9BWS9	Chitinase domain-containing protein 1	3.15E-07	P49747	Cartilage oligomeric matrix protein (COMP) (Thrombospondin-5)	2.76E-02
P02787	Serotransferrin (Transferrin)	3.21E-07	Q99542	Matrix metalloproteinase-19 (MMP-19)	3.04E-02
P05452	Tetranectin (TN)	3.50E-07	P02751	Fibronectin (FN)	3.78E-02
P13591	Neural cell adhesion molecule 1 (N-CAM-1)	3.50E-07	P02649	Apolipoprotein E (Apo-E)	4.42E-02
P03973	Antileukoproteinase (ALP)	4.99E-07	Q12805	EGF-containing fibulin-like extracellular matrix protein 1	4.80E-02
P01023	Alpha-2-macroglobulin (Alpha-2-M)	5.18E-07	Q15582	Transforming growth factor-beta-induced protein ig-h3 (Beta ig-h3)	5.91E-02

Proteins highlighted in pink; only with XIC, in blue; only with SC and green; both with SC and XIC.

The secreted proteins were clustered into a heatmap, as shown in Figure 29, to visualize their abundance patterns. These proteins were identified as statistically significant based on ANOVA tests with a p-value threshold of <0.05, using both XIC and SC. The heatmap reveals a pattern consistent

with the trends observed in Figure 28, specifically a pronounced downregulation at 24h p.i., which persists, albeit to a lesser extent, at 96h p.i. Consequently, to gain deeper insights all downregulated secreted proteins were merged into one cohort and all upregulated secreted proteins into another. This approach is discussed in greater detail in Section 3.7, page 107.

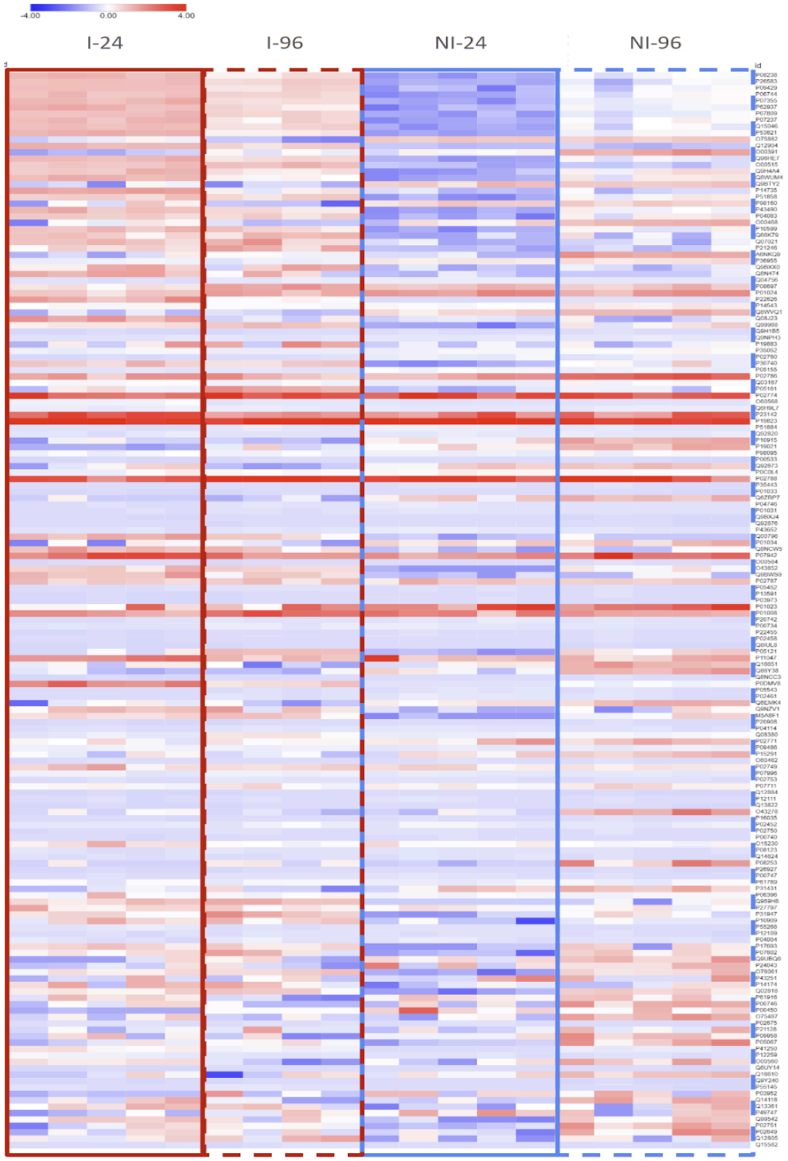

Figure 29: Heatmap illustrating the 168 significantly variable secreted proteins identified through the quantification methods of XIC and SC. Among these, 85 proteins were detected using SC, 44 with XIC, and 39 proteins were common to both methods. The heatmap is organised according to the p-values (adjusted p-value < 0.05) obtained from an ANOVA test, displaying the proteins in order of significance from most to least. The data were normalised using Z-scores and visualised with Morpheus. The sample I3 96h has been excluded from the overall analysis as it appeared as an outlier while analysing with XIC. The heatmap is annotated with distinct colour-coded boxes to differentiate between conditions and time points better to

illustrate temporal and condition-specific differences in protein abundance: I-24 is highlighted by a red solid box, I-96 by a red dotted box, NI-24 by a blue solid box, and NI-96 by a blue dotted box.

3.5 Putative biomarkers identification for chronic disease detection

One of the primary objectives of this study was to identify specific secreted proteins at 96 p.i. that could serve as biomarkers of persistent infection. The focus was not only on proteins with differential abundance between infected (I) and uninfected (NI) conditions but also on those exclusively present in either I-96 or NI-96. Proteins uniquely present in I-96 could potentially act as positive biomarkers for disease detection, while those exclusive to NI-96 could serve as negative biomarkers.

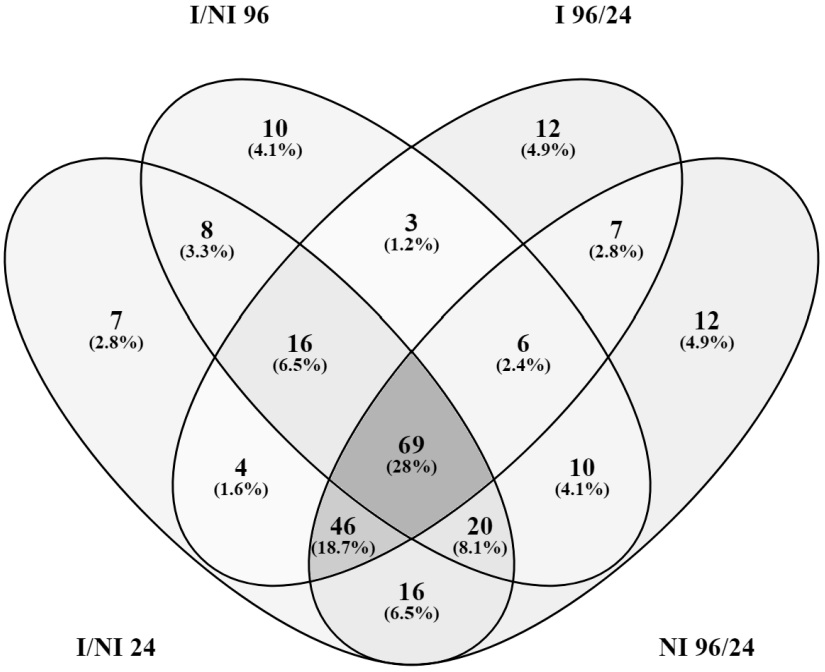

Figure 30: Venn diagram comparing the four conditions to identify significant secreted variable proteins, based on SC and XIC data quantification. The diagram emphasises on proteins specific to I/NI 96h conditions.

By integrating SC and XIC quantification methods, we identified 186 significant proteins for I/NI 24h, 142 for I/NI 96h, 163 for I 96h/24h, and 186 for NI 96h/24h (Table 7). These findings highlight a marked downregulation of protein secretion during the acute phase of infection, which persisted to a lesser degree during the chronic phase.

To further refine our analysis, we examined all statistically significant proteins across the four tested conditions (I/NI 24h, I/NI 96h, I 96h/24h, and NI 96h/24h), with a specific focus on proteins unique to I/NI 96h and absent from other conditions (Figure 30). This analysis identified 10 proteins exclusive to I/NI 96h, all of which were downregulated and absent in the other conditions (Table 9). Notably, a subset of these proteins include receptor proteins, suggesting the presence of membrane vesicle (MV)-associated proteins in our samples, potentially containing transmembrane (TM) receptors (Figure 31).

Table 9 : Significant secreted proteins specific to I/NI 96h condition. Table shows uniprot accession number, protein names, fold change from I/NI 96h and significance based on padj<0.05.

Uniprot Accession	Protein names	Fold Change (I/NI 96h)	padj < 0.05
P29508	Serpin B3 (Protein T4-A) (SCCA-1)	0	1.86E-02
Q14393	Growth arrest-specific protein 6 (GAS-6)	0.16	2.25E-03
P43251	Biotinidase (Biotinase)	0.24	7.17E-03
Q6ISS4	Leukocyte-associated immunoglobulin-like receptor 2 (LAIR-2)	0.26	1.80E-02
P21860	Receptor tyrosine-protein kinase erbB-3	0.3	1.10E-02
Q9UHI8	A disintegrin and metalloproteinase with thrombospondin motifs 1 (ADAM-TS 1)	0.31	1.91E-02
O75503	Bis(monoacylglycerol)phosphate synthase CLN5	0.35	1.49E-02
O75629	Protein CREG1 (Cellular repressor of E1A-stimulated genes 1)	0.37	5.41E-03
P04085	Platelet-derived growth factor subunit A (PDGF subunit A)	0.46	1.97E-02
P22455	Fibroblast growth factor receptor 4 (FGFR-4)	0.52	3.71E-02

The overall downregulation of proteins in the infected (I) condition compared to the non-infected (NI) condition at 96h p.i. is illustrated by fold change values, all below 1, indicating significant suppression of several proteins involved in biological processes during infection. Adjusted p-values (padj) confirm the statistical significance of these differences. Based on UniProt database, we explored the functions of specific proteins:

- Serine protease inhibitor B3 (Serpin B3, P29508): Exhibits a fold change of 0, meaning it is entirely absent in the I-96 condition compared to the NI-96, suggesting it is unique to NI-96 and could serve as a negative biomarker for the disease. This protein is involved in inhibiting proteases and plays a role in cell survival and proliferation.

- Growth arrest-specific protein 6 (GAS-6, Q14393): A regulator of apoptosis and immune modulation, shows a significant reduction in abundance, hinting at a potential strategy by *L. monocytogenes* to limit anti-inflammatory signalling.
- Biotinidase (P43251) and Leukocyte-associated immunoglobulin-like receptor 2 (LAIR-2, Q6ISS4): Both downregulated, suggesting that infection might disrupt metabolic pathways and impair immune regulation.
- Receptor tyrosine-protein kinase erbB-3 (ERBB3, P21860) and Fibroblast growth factor receptor 4 (FGFR-4, P22455): Proteins involved in cell signalling and tissue repair, exhibit reduced abundance, implying manipulation of growth and repair pathways that might limit host tissue regeneration, facilitating infection progression.
- A disintegrin and metalloproteinase with thrombospondin motifs 1 (ADAM-TS-1, Q9UHI8) and Protein CREG1 (CREG1, O75503): Involved in tissue remodelling and cellular proliferation, are downregulated, potentially contributing to inhibition of host tissue repair processes.
- Fibroblast growth factor receptor 4 (FGFR-4, P22455) and Platelet-derived growth factor subunit A (PDGF-A, P04085): Both promote cell growth and wound healing, indicating the possibility that *L. monocytogenes* fine-tunes the suppression of growth signals rather than completely inhibiting them.

Overall, the data highlights widespread downregulation of proteins involved in immune defence, metabolic regulation, and tissue repair during infection. This pattern suggests a pathogen-driven strategy to suppress key host pathways, allowing infection persistence by potentially evading immune detection. However, deeper analysis and validation are required to determine the candidacy of these proteins as biomarkers for persistent *L. monocytogenes* infection. Functional and pathway analyses have been performed for further insights.

3.6 Transmembrane proteins within the dataset

Knowing the presence of proteins with TM domains in our dataset, we further characterised the secreted proteins via two computational tools: TOPCONS (https://topcons.cbr.su.se/) and SignalP v5 (https://services.healthtech.dtu.dk/services/SignalP-5.0/)(Supplementary table 5, pages 221-224). The rationale for using these tools was to gain a deeper understanding of the structural properties of the identified proteins, specifically to determine whether they contained signal peptides that direct secretion and to check for the presence of TM domains that could suggest membrane association rather than classical secretion, probably meaning that our sample preparations might contain membrane vesicle (MV) proteins, which may contain transmembrane (TM) receptors. Therefore, TOPCONS was used to predict the proteins' topology and presence of transmembrane helices. This step was crucial because transmembrane proteins, although sometimes secreted via non-classical pathways, are typically membrane-bound, which may influence their role in cellular processes, especially in host-pathogen interactions. SignalP v5 was applied to identify signal peptides at the N-terminus of the proteins, characteristic of proteins destined for the secretory pathway. The presence of these peptides could support the hypothesis that the proteins are secreted and play a role in the extracellular environment or in communication between the bacterium and host cells.

The analysis, represented in the bar chart (Figure 31), shows a distinct distribution of secreted proteins and proteins with transmembrane domains across different conditions. Overall, this analysis highlights that while many of the proteins exhibit classical secretory signals, a subset also contains transmembrane domains, as predicted by TOPCONS. This finding is particularly interesting because it suggests that some of these proteins may have dual roles being both membrane-associated and secreted or probably meaning that our sample preparations might contain membrane vesicle (MV) proteins, which may contain transmembrane (TM) receptors

Membrane vesicles (MVs) are small, lipid-bound structures that cells release into their extracellular environment, playing key roles in cell communication, immune response, and the transport of proteins, lipids, and nucleic acids (Thery et al., 2009). In the context of trophoblast cells infected with *L. monocytogenes,* the release of membrane vesicles can be part of the host cell's response to infection. These vesicles often contain a variety of host-derived proteins, including those involved in immune signalling and stress responses (Thery et al., 2009). When analysing the secreted proteins from trophoblasts, it is not surprising to find proteins associated with membrane vesicles because

infection can trigger vesicle release as part of the host defence mechanism. The vesicles may carry proteins involved in modulating the immune system or in maintaining cell integrity under infection conditions (Thery et al., 2009; Sangiorgio et al., 2024)). Thus, identifying human proteins related to membrane vesicles during an infection may provide insights into how trophoblasts respond to *L. monocytogenes* and how vesicles contribute to the immune response and intercellular signalling. Therefore, since MVs are known to play a role in intercellular communication, particularly in the activation of innate immunity, the TM receptor proteins in our study could act as intermediates in cell-to-cell signalling (Thery et al., 2009; Sangiorgio et al., 2024).

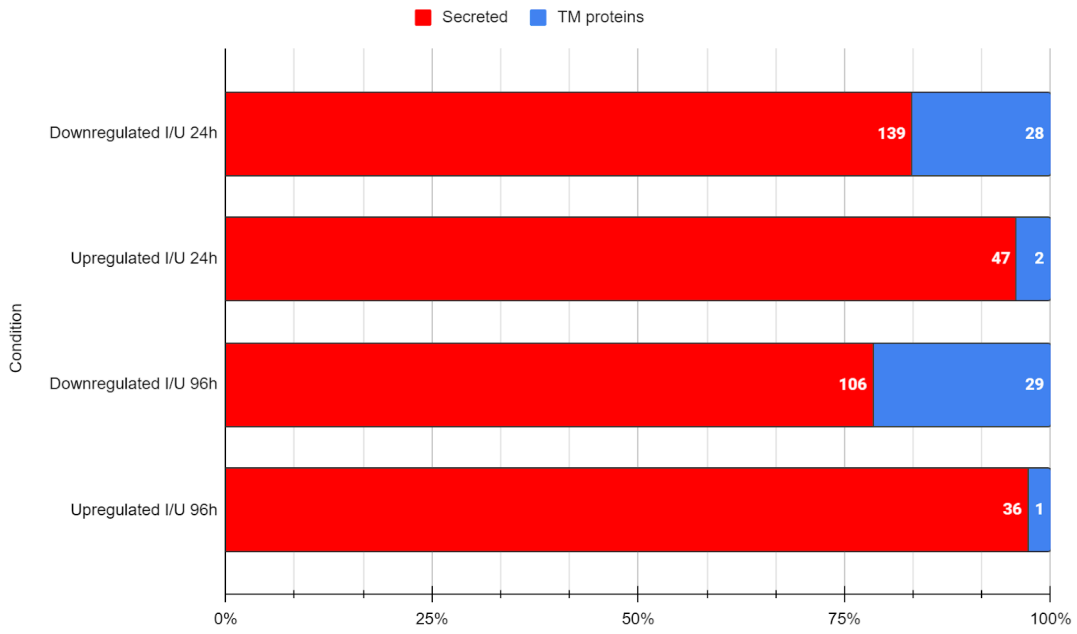

Figure 31 : Bar chart depicting the number of secreted and transmembrane proteins per condition suggesting the presence of membrane vesicles.

3.7 Functional and Pathway Analysis of *L. monocytogenes* infection in Trophoblast cells

As outlined in Section 3.4, individual cluster analyses and their graphical representations did not yield substantial insights. To address this, all downregulated secreted proteins were consolidated into a single cohort, and similarly, all upregulated proteins were grouped into another. A comprehensive functional and pathway analysis was then conducted using the DAVID database from NCBI to better understand the biological processes involved in *L. monocytogenes* infection. Specifically, protein lists consistently identified as upregulated or downregulated across two quantification methods, XIC and SC, were compiled and analyzed independently for each infection time point (24h p.i. and 96h p.i.). These datasets were subjected to DAVID analysis to identify enriched biological processes and KEGG pathways. The results were visualized through Biological Functional Analysis (Figure 32) and KEGG Pathway Analysis (Figure 33), generated using RStudio. These analyses highlighted the key pathways and biological functions associated with the differentially regulated proteins at each stage of infection, providing a deeper understanding of the host-pathogen interaction.

3.7.1 Functional Analysis

Our analysis revealed distinct patterns of biological process regulation across the course of *L. monocytogenes* infection, showing clear differences between the replicative phase at 24h p.i. and the persistent phase at 96h p.i.. At 24h p.i., 13 biological processes were significantly enriched, while only 8 remained enriched at 96h p.i. (Figure 32, Supplementary Tables 6-7, pages 225-227). Importantly, the processes seen at 96h p.i. were a subset of those identified earlier at 24h p.i., suggesting that persistent infection does not trigger the deregulation of additional host pathways. Instead, the host's biological responses become more refined or targeted over time.

Of the processes that persisted across both time points, seven showed greater enrichment at 24h p.i., implying more robust activation in the early phase of infection. For example, angiogenesis, which showed a two-fold increase in enrichment at 96h p.i., appears to be a key process manipulated by *L. monocytogenes* within the host. This might suggest that while certain processes are downregulated early on, some may later be co-opted by the pathogen to aid its long-term persistence.

In contrast, the upregulated processes presented a more stable profile between the two phases, with four biological functions enriched at both 24h p.i. and 96h p.i. (Figure 32, Supplementary Tables 6 and 7, page 225-227). While most of these functions became more prominent at 96h p.i., innate

immunity was an exception, showing significantly higher enrichment and significance at 24h p.i.. This could suggest an early, strong immune activation that may lose effectiveness as the infection progresses into its chronic phase, where *L. monocytogenes* might evade or suppress the immune response (Diakovich and Gorvel, 2010). By 96h p.i., stress response pathways became more enriched, hinting at a potential state of immune dysregulation induced by prolonged infection.

During the acute phase (24h p.i.), there is a strong upregulation of innate immune responses and inflammatory pathways, reflecting the host's immediate defence mechanisms against the invading pathogen (Thakur et al., 2019). As the infection shifts to the chronic phase (96h p.i.), the biological processes expand to include a broader range of immune and tissue remodelling pathways. The chronic infection is characterised by prolonged inflammation, immune modulation, and tissue repair mechanisms, such as angiogenesis and extracellular matrix organisation. These processes not only reflect the host's efforts to control the infection but might also suggest an attempt to repair tissue damage caused by the persistent immune response.

This transition from acute to chronic infection highlights the complexity of host-pathogen interactions over time. The early focus on rapid immune activation evolves into a more complex response that includes tissue remodelling and damage control as the infection becomes chronic. This shift suggests that *L. monocytogenes* may exploit the host's immune system, manipulating it to support its own survival, while the host tries to maintain homeostasis in the face of ongoing infection.

3.7.2 KEGG Pathway Analysis

To gain deeper insights into the effects of *L. monocytogenes* infection on the host secretome, we performed a KEGG pathway analysis using the DAVID NCBI database. This analysis identified 21 enriched pathways at both 24h p.i. and 96h p.i., reflecting the evolving biological response to infection. Of these, 14 pathways were enriched at both time points, with 12 showing greater significance at 24h p.i., underscoring the intense biological activity during the acute phase (Figure 32, Supplementary tables 8-9, pages 225-227).

At 24h p.i., seven pathways were uniquely enriched, including those related to infectious diseases such as *Staphylococcus aureus* infection, toxoplasmosis, and pertussis. This could indicate the host's immediate defensive response to bacterial invasion, with immune-related pathways predominating. By contrast, a different set of seven pathways was uniquely enriched at 96h p.i., predominantly involving signalling pathways like the MAPK and Ras signalling pathways (Figure 33, Supplementary

tables 8 and 9, page 225-227). This shift from disease-related to signaling pathways indicates a transition from an acute immune response to a more regulated cellular state as the infection advances into its chronic phase. This change may reflect the host's adaptation to the persistent bacterial presence or emphasise on the potential distinct mechanisms that pathogens exploit in acute versus chronic infection (Brodsky and Medzhitov, 2009).

The survival of *L. monocytogenes* during infection relies on its ability to evade the host immune system through various mechanisms. For example, the pathogen can overcome bactericidal defences by escaping the phagosome and avoiding autophagy using virulence factors like LLO, ActA, and InlK. It further modifies its peptidoglycan through PgdA and OatA, disrupting the release of microbe-associated molecular patterns (MAMPs) and inhibiting pathogen recognition receptors (PRRs), leading to impaired pro-inflammatory cytokine production (Zhong and Kyriakis, 2007; Dussurget et al., 2014). Moreover, *L. monocytogenes* manipulates host immune responses at the chromatin level by secreting LLO, which alters histone modifications, thus downregulating immune-related gene transcription, while simultaneously activating pathways like p38 and ERK MAPK to boost the transcription of genes that promote bacterial survival (Dussurget et al., 2014).

The differential pathway enrichment observed during chronic infection suggests that *L. monocytogenes* may impair signal transduction and cellular migration to support its persistence within host cells. This manipulation of host signalling, particularly in the later stages of infection, indicates that the bacterium actively modulates these pathways to create a more conducive environment for its survival (Brodsky and Medzhitov, 2009). For instance, the MAPK cascade, a critical pathway that induces cytokine production and stimulates the innate immune response to clear bacterial pathogens, is a target of manipulation by several enteric pathogens (Nandi and Aroeti, 2023). These pathogens deploy effector proteins to block different steps in the MAPK cascade, thereby suppressing the host’s immune defence mechanisms and facilitating pathogen survival (Nandi and Aroeti, 2023). In a similar manner, *L. monocytogenes* may utilise analogous mechanisms to interfere with key signalling pathways like MAPK, hindering the host immune response and promoting chronic infection (Tang et al., 1994; Nandi and Aroeti, 2023). The observed downregulation of processes such as angiogenesis, coupled with shifts in immune responses, might further support this notion. Extensive analysis of key signalling pathways at 96h p.i. is provided later on this section and it highlights potential disruptions in signal transduction, underscoring *L. monocytogenes’* ability to manipulate host biology and evade immune clearance during chronic infection.

In summary, the KEGG pathway analysis highlights the dynamic interaction between *L. monocytogenes* and host cellular processes across the infection timeline. The pathogen could utilise a complex array of strategies to manipulate the host immune system, from evading early immune defences to reshaping signalling pathways during chronic infection as shown with other intracellular pathogens (Brodsky and Medzhitov, 2009). These findings not only deepen our understanding of the infection's progression but also offer potential therapeutic targets for addressing persistent *L. monocytogenes* infections.

Overall, our functional and pathway analyses revealed a general trend of downregulation in biological processes and pathways when comparing the acute phase to the chronic phase of *L. monocytogenes* infection in trophoblast cells. This downregulation was most pronounced during the acute phase, with a partial recovery of this phenotype at 96h p.i., indicating that the cellular response may adapt as the infection transitions into its chronic stage. What stands out in our results is the significant downregulation of angiogenesis and various signalling pathways at 96h p.i.. These findings suggest that *L. monocytogenes* may manipulate key host processes during the chronic phase of infection. The downregulation of angiogenesis, in particular, may reflect the pathogen’s strategy to alter host immune responses and cellular functions, creating a more favourable environment for persistence within trophoblast cells.

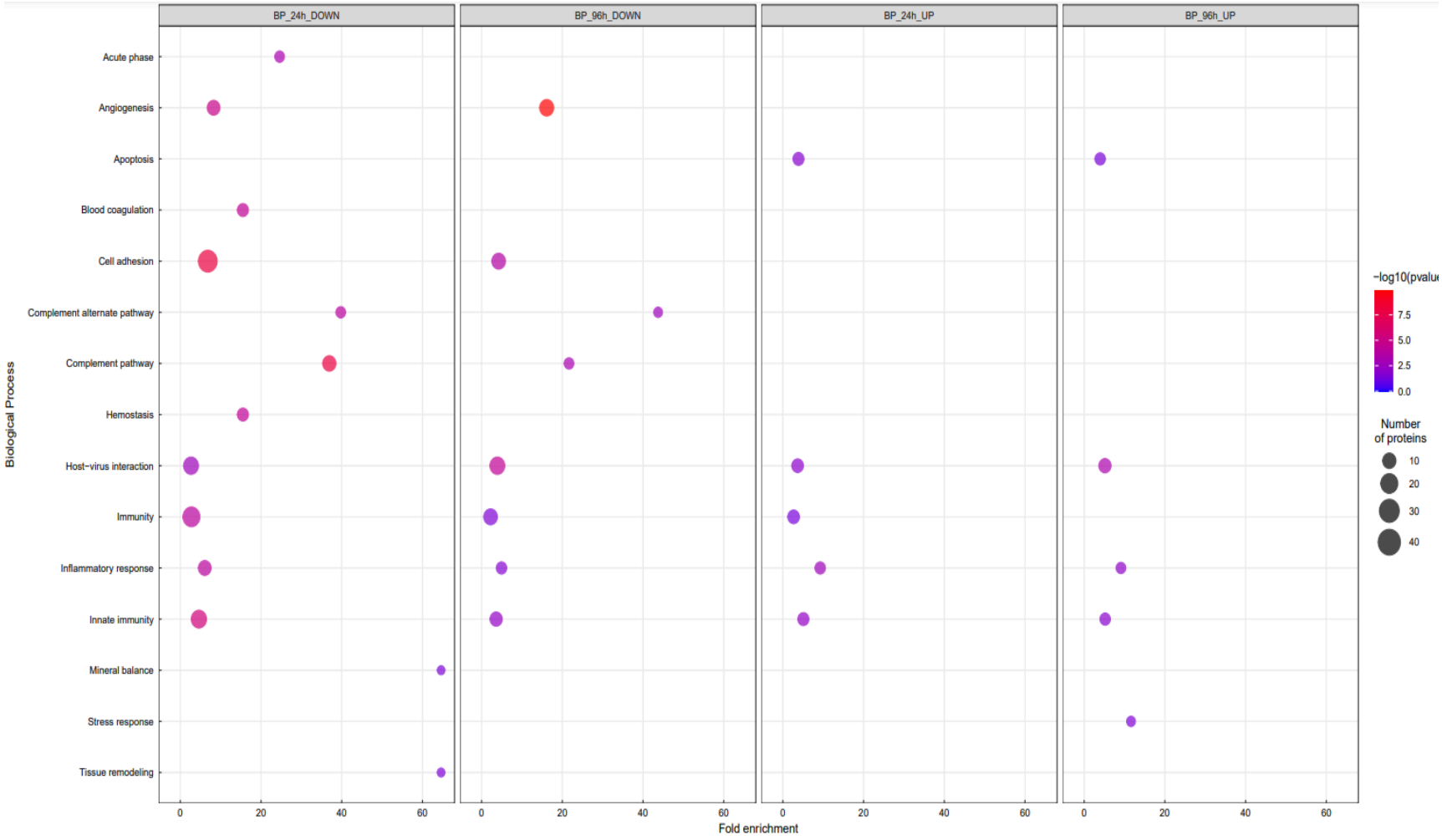

Figure 32 : Significantly enriched biological processes via David database that were transformed into graphical illustrations based on RStudio including number of proteins, fold enrichment and significance based on a -log10(p-value).

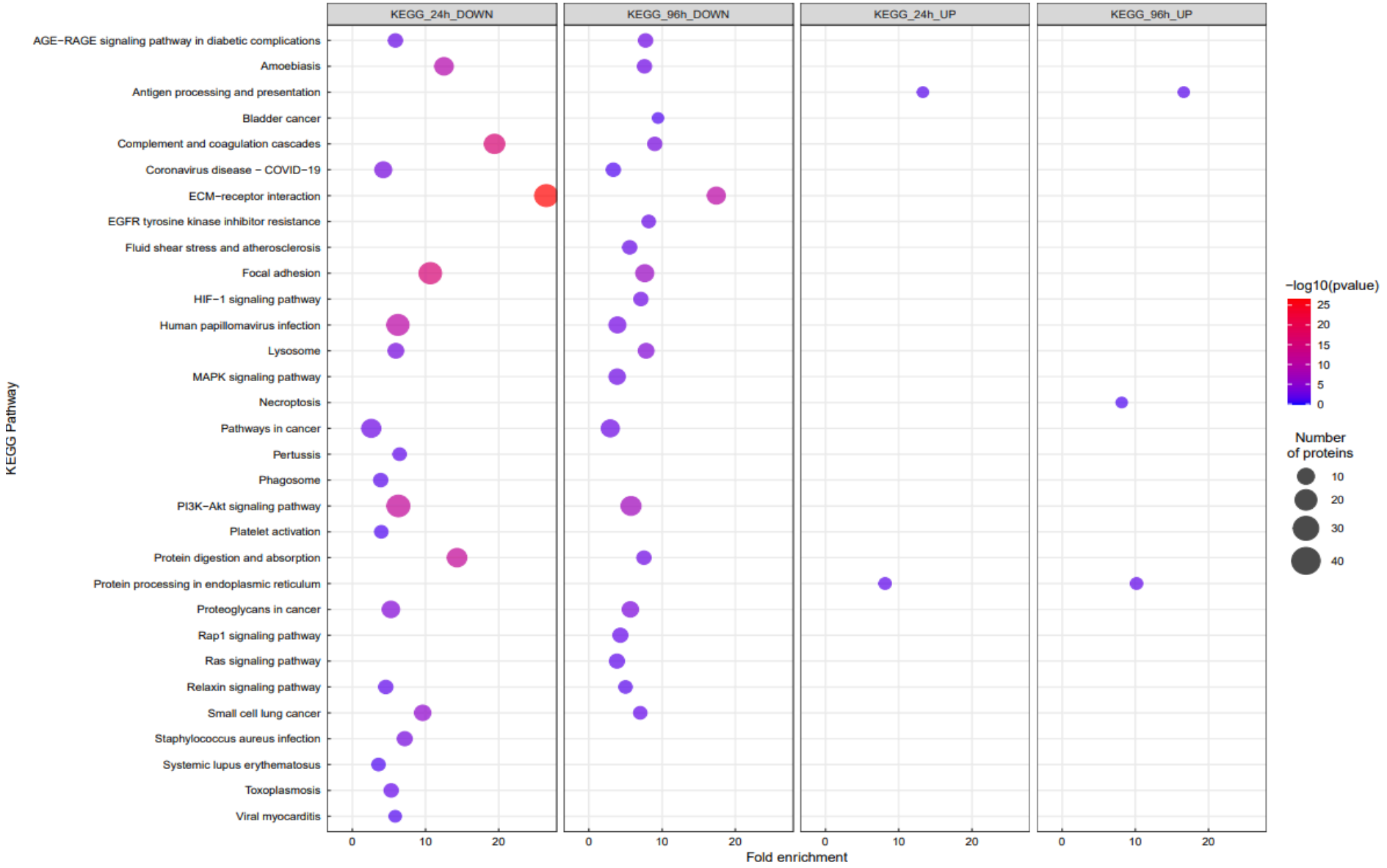

Figure 33 : Significantly enriched KEGG pathways via David database that were transformed into graphical illustrations based on RStudio including number of proteins, fold enrichment and significance based on a -log10(p-value).

3.7.3 Angiogenesis and HIF-1a Signalling Pathway

To begin with, angiogenesis is defined as the formation of new blood vessels from pre-existing ones, a process crucial for developing and maintaining the vascular system. This complex process is initiated and regulated by various chemical signals, primarily involving key proteins such as hypoxia-inducible factor 1-alpha (HIF-1α), vascular endothelial growth factor (VEGF), fibroblast growth factor (FGF), angiopoietin-2, and a range of chemokines (Osherov and Ben-Ami, 2016; Ortega et al., 2022). Angiogenesis in the placenta is particularly critical, as it establishes the fetomaternal circulation, ensuring an adequate blood exchange between the mother and the foetus (Ortega et al., 2022). This exchange is vital for supporting foetal development by delivering essential oxygen and nutrients (Ortega et al., 2022).

In a healthy placenta, angiogenesis is finely tuned, resulting in the formation of well-structured and functional blood vessels that are essential for the growth of the foetus and the overall health of the pregnancy (Reynolds and Redmer, 2001; Chen and Zheng, 2013; Bardin et al., 2015; Ortega et al., 2022). Proper regulation of this process is crucial, as it directly impacts the efficiency of nutrient and oxygen delivery to the foetus (Reynolds and Redmer, 2001; Chen and Zheng, 2013; Bardin et al., 2015; Ortega et al., 2022). However, when angiogenesis is disrupted, as can occur during infections or other pathological conditions, the resulting blood vessels may be insufficient in number, poorly formed, or dysfunctional (Reynolds and Redmer, 2001; Chen and Zheng, 2013; Bardin et al., 2015; Ortega et al., 2022). Such disruptions are closely linked to complications like preeclampsia (PE) and intrauterine growth restriction (IUGR), where impaired blood vessel formation leads to inadequate oxygen and nutrient supply to the foetus, potentially compromising foetal development and pregnancy outcomes (Ortega et al., 2022).

In our experiment, we observed several of these angiogenesis-related proteins exhibited significant variability at 96h p.i., with a notable enrichment during the chronic phase of *L. monocytogenes* infection (Table 10). This suggests that the infection may profoundly impact angiogenic pathways, potentially contributing to the pathological changes observed in infected tissues. Indeed, it is well-established that many pathogenic microorganisms including fungi, bacteria, parasites, protozoa, and viruses can manipulate host angiogenic responses to facilitate their own proliferation and persistence (Osherov and Ben-Ami, 2016). Depending on their needs, these pathogens may either enhance or suppress angiogenesis to create a more favourable environment for their survival (Osherov and Ben-Ami, 2016).

For instance, certain TORCH pathogens, such as *CMV* and *HPV*, have been shown to upregulate angiogenesis through various mechanisms, ultimately promoting their persistence within the host (Osherov and Ben-Ami, 2016). Similarly, Gram-positive and Gram-negative bacteria can modulate angiogenic responses differently (Osherov and Ben-Ami, 2016). For example, *Mycobacterium tuberculosis* has been documented to enhance angiogenesis, which may aid in its survival and spread. In contrast, pathogens like *Bacillus anthracis* and *Pseudomonas aeruginosa* are known to suppress angiogenesis, potentially to evade immune detection and clearance (Osherov and Ben-Ami, 2016).

Table 10: Abundance of significantly variable proteins in the Angiogenesis process between the acute and chronic phase with *L. monocytogenes* infection.

Angiogenesis		24h	96h
Q12884	Prolyl endopeptidase FAP	0.06	0.56
P02462	Collagen alpha-1(IV) chain	0.20	0.42
P49763	Placenta growth factor	0.25	0.63
P20827	Ephrin-A1	0.03	0.35
P08572	Collagen alpha-2(IV) chain	0.52	0.53
Q16610	Extracellular matrix protein 1	0.33	0.39
P98160	Basement membrane-specific heparan sulphate proteoglycan core protein	0.12	0.37
P07996	Thrombospondin-1	0.23	*
P02751	Fibronectin	0.27	0.26
P15692	Vascular endothelial growth factor A	0.47	0.47
P08253	72 kDa type IV collagenase	*	0.09
O14786	Neuropilin-1	*	0.35
Q9Y264	Angiopoietin-4	*	0.40

The (*) stands for proteins absent to the specific time point.

Additionally, angiogenesis is interdependent to HIF-1a signalling responses, namely linked to hypoxia (Ortega et al., 2022). It has been shown that placenta hypoxia can lead to both (a) abnormal trophoblasts behaviour like upregulated apoptosis and necrosis, angiogenesis, oxidative stress, tissue ageing, endocrine dysfunction all leading to endothelial altered responses and (b) immune dysregulation including oxidative stress and altered cytokines responses that are associated to endothelial dysfunction, as well (Ortega et al., 2022).

Hypoxia-inducible factor-1α (HIF-1α) is a transcription factor initially recognized as a key regulator of cellular responses to low oxygen, namely hypoxia (Knight and Stanley, 2019). Recent research has revealed its significant role in macrophage-based immune responses, particularly in defending against

intracellular pathogens (Knight and Stanley, 2019). HIF-1α generally enhances classical inflammatory responses against such pathogens, though some studies suggest it can also suppress immune responses and hinder infection (Knight and Stanley, 2019). HIF-1α influences the expression of inflammatory cytokines, chemokines, and antimicrobial peptides, promoting pro-inflammatory activity while also downregulating excessive inflammation, such as in the case of sepsis (Cramer et al., 2003; Knight and Stanley, 2019). HIF-1α is crucial for antibacterial immunity, particularly in macrophages and neutrophils (Cramer et al., 2003; Knight and Stanley, 2019. Its role was first highlighted in *Streptococcus* infections, where HIF-1α-deficient macrophages failed to effectively kill the bacteria, leading to increased susceptibility in mice (Knight and Stanley, 2019). Similarly, HIF-1α is essential for controlling intracellular bacterial pathogens like *Francisella tularensis*, which actively avoids HIF-1α activation to enhance its survival, and *Mycobacterium* species, where HIF-1α manages infections by regulating immune responses such as IL-1β and nitric oxide production (Knight and Stanley, 2019). HIF-1α also aids in the defence against bacteria in epithelial cells, including *Escherichia coli* and *Yersinia enterocolitica* (Knight and Stanley, 2019). The importance of HIF-1α in controlling *L. monocytogenes* infections has also been noted, as its absence in macrophages leads to diminished immune responses and poor infection control, particularly in the liver due to reduced TNF-α production and glycolytic activity (Knight and Stanley, 2019). Overall, HIF-1α plays a critical role in managing intracellular bacterial pathogens and promoting effective immune responses (Knight and Stanley, 2019).

More specifically, HIF-1a signalling pathway is among the many signalling pathways found downregulated at the chronic state of 96h p.i. (Figure 33, Table 11). This downregulation together with downregulation of angiogenesis could suggest that chronic infection with *L. monocytogenes* might affect the growth and behaviour of trophoblast cells (Ortega et al., 2022). Additionally, many studies in the literature have suggested the importance of signalling pathways as a host response (Koul et al., 2004; Bhavsar et al., 2007; Brodsky and Medzhitov, 2009). Signalling pathways are used as an intermediate for innate immune responses activation under a potential threat or infection (Koul et al., 2004; Bhavsar et al., 2007; Brodsky and Medzhitov, 2009). A few studies conducted in *Mycobacteria* species have indicated that these bacteria indeed manipulate the host signalling pathways for their benefit to prevent their phagocytosis (Koul et al., 2004). Overall, *L. monocytogenes* could potentially block both angiogenesis and signalling pathways resulting in immune dysregulations and therefore persistence of *L. monocytogenes* within the trophoblast niche.

Table 11: Abundance of specifically enriched HIF-1a pathway at 96h p.i. during *L. monocytogenes* infection.

HIF-1 Signalling Pathway		Ratio I/NI 96h
P01033	Metalloproteinase inhibitor 1	0.41
P15692	Vascular endothelial growth factor A	0.47
Q9Y264	Angiopoietin-4	0.4
P00533	Epidermal growth factor receptor	0.38
P02787	Serotransferrin	0.27
P02786	Transferrin receptor protein 1	0.31

3.7.3.1 Angiogenesis and the angiogenic cytokine VEGF-A

Vascular endothelial growth factor A (VEGFA) is a critical angiogenic cytokine that plays a significant role in mediating inflammation. It is primarily induced by hypoxia, as well as by pro-inflammatory cytokines such as interleukins IL-6 and IL-1, and growth factors like insulin-like growth factor (IGF). VEGFA is known for its ability to stimulate the formation of new blood vessels, a process vital for both normal physiological functions and pathological conditions. Research has demonstrated that VEGFA binds to receptors such as neuropilin-1 (O14786) and heparan sulfate (P98160), leading to the activation of motor neuron development during embryogenesis.

In the context of our study, neuropilin-1 is specifically identified at the chronic phase of infection while the heparan sulfate maintains its downregulation in both the acute and chronic phases of *L. monocytogenes* infection. This persistent downregulation of VEGFA and its associated signalling molecules may suggest a continuous inflammatory impairment. Such sustained changes in protein level could inhibit critical cellular processes, including cell migration, which is essential for tissue repair and regeneration. This finding underscores the potential for a chronic inflammatory environment to negatively impact not only angiogenesis but also overall tissue homeostasis leading to *L. monocytogenes* persistence in the trophoblasts.

3.7.3.2 HIF-1a Signalling pathway associated proteins

Metalloproteinases inhibitor 1 (TIMP1, P01033) serves dual functions as both an inhibitor and a growth factor, playing a crucial role in regulating various cellular processes, including cell differentiation, migration, and apoptosis (programmed cell death). TIMP1 also activates cellular signalling cascades through interactions with CD63 and integrin beta-1 (ITGB1). These interactions are

essential for mediating the biological effects associated with TIMP1, highlighting its significance in modulating cell behaviour and maintaining tissue homeostasis.

Serotransferrin (TRFE, P02787) and transferrin receptor protein 1 (TFRC, P02786) are involved in iron transport within the body. Serotransferrin facilitates the movement of iron from absorption sites and heme degradation to areas designated for storage and utilisation. Beyond its critical role in iron transport, serum transferrin may also stimulate cell proliferation. In the context of microbial infections, transferrins act as vital iron sources for various pathogens. For example, *Neisseria* species capture transferrin to extract its iron for metabolic needs (Noinaj et al., 2012). Similarly, the parasite *Trypanosoma brucei* binds to transferrin via its own transferrin receptor, enabling it to acquire iron necessary for growth and survival (Trevor et al., 2019).

3.7.4 Mitogen-Activated Protein Kinase (MAPK) Signalling pathway, Ras and Rap1 Signalling pathways

The MAPK (Mitogen-Activated Protein Kinase) pathway is a crucial signal transduction mechanism central to the host immune response (Hashino et al., 2015) that regulates various cellular processes, including proliferation, differentiation, and stress responses including modulations of cytokines and inflammatory mediators production (Weiglein et al., 1997; Tang et al., 1998). MAPKs are divided into four primary subfamilies: extracellular signal-regulated kinases (ERKs), c-Jun NH2-terminal kinases (JNKs), p38 isoforms (p38s), and ERK5 (Hashino et al., 2015).

Many bacterial pathogens have evolved ways to manipulate these pathways to establish infections. More specifically, *Mycobacterium tuberculosis*, *Yersinia spp.*, *Salmonella enterica*, and *Vibrio parahaemolyticus*, use effector protein to interfere with the phosphorylation of MAPK kinases, either inhibiting or activating them. This manipulation helps bacteria control their replication and survival within host cells. For example, *S. typhimurium* attachment to the cell surface has been linked to EGF activation, stimulation of signalling cascades, phosphorylation, and activation of MAPK pathway (Velge et al., 1994). In the *L. monocytogenes* case, it often uses effector proteins to activate or inhibit MAPK pathways resulting in triggering Nuclear Factor kappa-light-chain-enhancer of activated B cells (NF-kB), Interferon Regulatory Factor 3 (IRF3), Interferon Regulatory Factor 7 (IRF7), and Activator Protein 1 (AP-1) pathways associated with transcriptional activation of IFN genes and immune responses (Dussurget et al., 2014). A previous study using a model of the blood-cerebrospinal fluid barrier demonstrated that *L. monocytogenes* infection activates ERK1/2 and p38 MAPK pathways, which are necessary for infection. LLO, a toxin produced by *L. monocytogenes*, can both activate and inhibit MAPK signalling. For example, in epithelial cells, LLO promotes MAPK activation, aiding bacterial invasion (Tang et al., 1998), and few years later it has also been established in trophoblast giant (TG) cells that LLO inhibits MAPK activation contributing to infection-related abortion (Hashino et al., 2015). In addition, Cheng et al., 2020 have shown that during *L. monocytogenes* infection in intestinal epithelial cells, the pair of Thr515-Leu516 that allows permeabilisation of host cell membranes leads to activation of the MAPK signalling pathway via the ERK1/2 phosphorylation and thus manipulation of the host immune responses, including pro-inflammatory responses for host defence.

Overall, modulation of the MAPK pathway is mediated by growth factors (GFs) and tyrosine protein receptors (RTKs), that we can also see in our dataset (Katz et al., 2007) (Table 12). Activation of these signal transduction pathways via GFs and RTKs eventually leads to cellular alterations (Katz et al.,

2007). The MAPK signalling pathway has been associated with cell proliferation and migration (Katz et al., 2007). Cell migration essentially involves the use of many GFs like HGF, EGFR, PDGF and IGF-1 and inhibition of MAPK/ERK1/2 pathway has been linked to impaired cell migration (Katz et al., 2007).

Many of these associated proteins we have also identified as significantly downregulated in our dataset when comparing the infected with the non-infected cells at the chronic level of infection. Overall, the MAPK signalling pathway was found as specifically and significantly downregulated at the 96h p.i. could suggest that *L. monocytogenes* might manipulate this pathway to disrupt cell migration, leading to impaired signal transduction, thus, overcoming cellular immune responses and establishing its intracellular survival and persistence (Nandi and Aroeti, 2023).

Table 12: Abundance of significantly secreted proteins associated with the MAPK signalling pathway, Ras pathway and Rap1 pathway that are specifically enriched during the chronic *L. monocytogenes* infection. Proteins with (▪) are only identified in the MAPK Signalling Pathway.

MAPK Signalling Pathway, Ras Pathway, Rap1 Pathway		96h
Uniprot Accession	Protein Name	Ratio1/NI
P49763	Placenta growth factor	0.63
P15692	Vascular endothelial growth factor A	0.47
▪Q9NPH3	Interleukin-1 receptor accessory protein	0.49
P20827	Ephrin-A1	0.35
▪P21860	Receptor tyrosine-protein kinase erbB-3	0.3
P04085	Platelet-derived growth factor subunit A	0.46
Q9Y264	Angiopoietin-4	0.4
P00533	Epidermal growth factor receptor	0.38
P22455	Fibroblast growth factor receptor 4	0.52

Ras and Rap1 are small GTPases that act as molecular switches, playing pivotal roles in various cellular processes (Molina and Adjei, 2006; Hilbi and Kortholt, 2017). They function by cycling between inactive GDP-bound and active GTP-bound states, a transition that is regulated by specific guanine nucleotide exchange factors (GEFs) and GTPase-activating proteins (GAPs) (Hilbi and Kortholt). This regulatory mechanism allows both proteins to trigger cellular signalling pathways, ensuring appropriate responses to external stimuli (Copp et al., 2003; Hilbi and Kortholt, 2017).

Ras proteins regulate critical cellular processes such as proliferation, survival, growth, migration, and differentiation. Upon activation, Ras interacts with various effectors, including Raf, PI3K, and RALGDS,

thereby initiating crucial signalling cascades like the MAPK pathway (Copp et al., 2003). In response to extracellular signals such as growth factors, receptor tyrosine kinases, and integrins, Ras-mediated signalling plays a vital role in shaping immune responses. In parallel, Rap1 significantly influences cell adhesion, migration, and proliferation, regulating integrins and other adhesion molecules essential for maintaining cell-cell and cell-matrix interactions (Hilbi and Kortholt, 2017).

Studies have shown that activation of the Ras-MAPK pathway facilitates the uptake of *Listeria monocytogenes* by host cells (Copp et al., 2003). Consequently, downregulation of this pathway during the chronic phase of infection may indicate alterations in the host's immune response. Specifically, *L. monocytogenes* may exploit these signaling pathways to limit further activation of downstream signaling and, in doing so, suppress inflammatory and immune responses. This strategic manipulation likely aids the bacterium in creating a more favorable environment for persistence in our trophoblast model.

3.7.4.1 Proteins shared among MAPK, Ras and Rap1 pathways

Functional analysis using UniProt reveals the critical roles of several proteins in angiogenesis and cellular signaling. Placental growth factor (PGF, P49763) is central to angiogenesis by promoting endothelial cell proliferation and migration. PGF interacts with Fms-like tyrosine kinase 1 (VEGFR-1), mediating its pro-angiogenic effects. Additionally, the isoform placental growth factor-2 uniquely binds to neuropilin-1 (NRP1) and neuropilin-2 (NRP2) in a heparin-dependent manner, enhancing its bioavailability and modulating signaling pathways involved in vascular development. This dynamic interplay underscores PGF's importance in regulating endothelial cell behavior and promoting angiogenesis. Another key protein is Ephrin-A1 (EFNA1, P20827), which is involved in cell communication and adhesion, particularly during developmental processes such as neuronal, vascular, and epithelial growth. Fibroblast growth factor receptor 4 (FGFR4, P22455), a tyrosine kinase receptor, mediates cellular differentiation, migration, and metabolism. When activated by FGF ligands, FGFR4 influences metabolic processes, including bile acid synthesis, glucose and lipid metabolism, and muscle energy utilization, all of which contribute to maintaining energy balance and metabolic health. Similarly, Angiopoietin-4 (Q9Y264) is associated with Angiopoietin-1 signaling, playing a significant role in cell survival, migration, and enhanced angiogenesis. These proteins collectively highlight a coordinated network of signaling pathways essential for vascular development and metabolic regulation.

3.7.4.2 Proteins specific to MAPK signalling pathway; ERBB3 and IL1RAcP

Most of the proteins identified in our datasets were shared between the MAPK, Ras, and Rap1 signalling pathways (Table 12). However, Interleukin-1 receptor accessory protein (IL1RAcP, Q9NPH3) and Receptor tyrosine-protein kinase erbB-3 (ERBB3, P21860) were specific to the MAPK pathway (Table 12). ERBB3, a member of the EGFR family, functions as a cell surface receptor and plays key roles in cell differentiation. IL1RAcP, part of the cytokine family, regulates not only inflammatory cascades but also cellular differentiation and proliferation (Mehrabadi et al., 2021).

IL1RAcP, in conjunction with IL-1 and IL-1R1, activates several signal transduction pathways, including NF-kB (Irikura et al., 1999; Kayal et al., 2002; Mehrabadi et al., 2021). Beyond its anti-inflammatory role, IL1RAcP has been linked to preeclampsia (PE), a condition associated with heightened maternal inflammatory responses (Mehrabadi et al., 2021). Specifically, its overexpression in hypoxic trophoblast cells has been shown to alter cellular invasion and proliferation (Mehrabadi et al., 2021). Therefore, the observed downregulation of IL1RAcP in our study may imply disruptions in cell migration (Mehrabadi et al., 2021).

In conclusion, all the proteins identified in these pathways were downregulated. Given their involvement in inflammatory and immune responses, cell adhesion, migration, and proliferation, this suggests that *L. monocytogenes* may manipulate signal transduction to establish a prolonged infection in the trophoblast niche, characterised by blocking the host innate immune system, and eliciting a chronic infection.

3.7.5 Fluid shear stress and atherosclerosis pathway

Atherosclerosis, a multifactorial chronic inflammatory disease, can be caused by infectious agents either via direct infections of vascular cells or indirectly through cytokine release or APPs (Evani et al., 2013). Shear stress, a mechanical force caused by blood flow, has been shown to impair the atherosclerotic process by altering the inflammatory microenvironment. In addition to its effects on vascular cells, shear stress impacts various cell types including epithelial cells (Espina et al., 2023). It is possible that shear stress and atherosclerosis pathways might modify signalling pathways, such as the MAPK pathway, which is involved in activating immune responses to mitigate stress (Espina et al., 2023).

Evani et al., 2013 have shown that *Chlamydia pneumoniae* infection triggers an inflammatory response in monocytes, while this response is impaired by shear stress, resulting in the migration of leukocytes to the plaque site an essential factor in atheroprogression (Evani et al., 2013). Consequently, mechanical forces like shear stress may be critical in accelerating disease progression by modulating vascular inflammation during systemic infections (Evani et al., 2013).

However, in the context of *L. monocytogenes* infection in trophoblast epithelial cells, the downregulation of shear stress and atherosclerosis may represent either a host defence mechanism to prevent further bacterial adhesion and regulate bacterial load, or another bacterial strategy to evade immune responses and proliferate within the trophoblast niche.

Table 13: Abundance of specifically enriched Fluid shear stress and atherosclerosis pathway at 96h p.i. during *L. monocytogenes* infection.

Fluid shear stress (FSS) and atherosclerosis		96h
Uniprot Accession	Protein Name	Ratio I/NI
P35052	Glypican-1	0.22
P07711	Procathepsin L	0.47
P15692	Vascular endothelial growth factor A	0.47
P04085	Platelet-derived growth factor subunit A	0.46
P08253	72 kDa type IV collagenase	0.09
P31431	Syndecan-4	0.34

3.7.5.1 Proteins specifically characterised in FSS and atherosclerosis

In contrast to the previously discussed signalling pathways, the FSS and atherosclerosis pathway involves a distinct set of downregulated proteins (Table 13). Notably, two proteoglycans are involved: Glypican-1 (GPC1, P35052) and Syndecan-4 (P31431). According to Uniprot functional annotations, GPC1 plays a dual role, as it binds to heparan sulfate, facilitating the myelination of Schwann cells, which in turn supports nerve signal transmission. Additionally, GPC1 inhibits fibroblast growth factor 2 (FGF2), thus contributing to muscle differentiation. Similarly, Syndecan-4 is involved in signal transduction and cytoskeletal rearrangements. Its roles have also been examined in the context of *Neisseria gonorrhoeae* infection, where it is identified as a key factor in bacterial internalisation (Banerjee et al., 2004).

Additionally, Platelet derived growth factor subunit A (PDGFA, P04085), is a growth factor essential for embryonic development, particularly in promoting cell proliferation and migration. Procathepsin L (P07711), a versatile protease, plays significant roles in various physiological processes. In its secreted form, it cleaves collagen XVIII alpha-1 chain (COL18A1), generating endostatin, a fragment known for its anti-angiogenic properties, which inhibit the formation of new blood vessels. Moreover, Procathepsin L is critical for maintaining cardiac structure and function, underlining its importance in heart development and morphology.

Finally, the 72 kDa type IV collagenase or matrix metalloproteinase-2 (MMP2, P08253) is a ubiquitously expressed enzyme involved in numerous physiological processes, including vascular remodelling, angiogenesis, tissue repair and inflammation. It also plays a critical role in the rupture of atherosclerotic plaques. This enzyme is also linked to oxidative stress within cardiac cells, further emphasising its role in cardiovascular pathologies.

3.7.6 Epidermal Growth Factor Receptor (EGFR) tyrosine kinase inhibitors (TKIs) pathaway

Epidermal Growth Factor Receptors (EGFR), part of the human epidermal receptor tyrosine kinase family, are approximately 180 kDa in size and play critical roles in cellular homeostasis. This family includes receptors such as EGFR (also known as ERBB1/HER1), ERBB2 (neu/HER2), ERBB3 (HER3), and ERBB4 (HER4) (Garrett et al., 2002; Adnan et al., 2022). These receptors can form homodimers or heterodimers, enabling diverse signalling pathways essential for various cellular functions (Adnan et al., 2022). EGFR is involved in regulating trophoblast cell migration, nerve and pancreatic cell motility and wound re-epithelialization (Katz et al., 2007). Mutations in the EGFR or protein overexpression activate downstream pathways linked to various cancers. Tyrosine kinase inhibitors (TKIs) targeting EGFR are commonly used in treatment, especially for patients with EGFR mutations. However, resistance to TKI therapy often develops, leading to tumour recurrence. Several mechanisms contribute to this resistance, including secondary EGFR mutations (e.g., T790M), activation of alternative pathways (such as c-Met, HGF, and AXL), and mutations in downstream molecules like K-RAS. Impairments in EGFR-mediated apoptosis pathways, histological transformations, and alterations in post-translational modifications (PTMs) are also involved (Adnan et al., 2022).

Interestingly, pathogens like *L. monocytogenes* interact with EGFR and other receptors like E-cadherin to induce endocytosis, potentially utilising a common bacterial invasion strategy (Adnan et al., 2022). Similarly, *Neisseria meningitidis* binds to endothelial cells, causing ERBB2 receptor clustering and subsequent activation of downstream signalling molecules that facilitate bacterial internalisation (Hoffmann et al., 2001). Likewise, *CMV* binds to EGFR, triggering tyrosine phosphorylation via heterodimerization with ERBB3, promoting viral entry and protein synthesis (Adnan et al., 2022). Additionally, pathogens manipulate host PTMs to interfere with cellular functions, hijacking the caveolin-endocytic machinery for entry and internalisation. In the case of *L. monocytogenes*, proteins like caveolin-1, cavin-2, and EHD2 mediate this process, supporting bacterial invasion and persistence within host cells (Adnan et al., 2022).

In our infection model, the EGFR and TKIs signalling pathway has been found notably downregulated at 96h p.i., suggesting that *L. monocytogenes* might exploit this pathway to enhance its proliferation and persistence in the placental niche during the chronic state of infection. Many of the proteins involved are the ones described before for MAPK, Ras, Rap1 and Shear stress pathways including VEGFA, ERB3, PDGFA and EGFR itself (Table 14). In addition, the Growth arrest specific protein 6

(GAS6, Q14393), has also been identified (Table 14). The GAS6 protein binds to the tyrosine-protein kinase receptors AXL, TYRO3, and MER, namely receptors belonging to the TAM receptor family, which is involved in immune regulation, tissue homeostasis, and cellular responses to stress and damage influencing cell growth, survival, adhesion, and migration.

Table 14: Abundance of specifically enriched EGFR tyrosine kinase inhibitor resistance pathway at 96h p.i. during *L. monocytogenes* infection.

EGFR tyrosine kinase inhibitor resistance		96h
Uniprot Accession	Protein Name	Ratio I/NI
P15692	Vascular endothelial growth factor A	0.47
P21860	Receptor tyrosine-protein kinase erbB-3	0.3
P04085	Platelet-derived growth factor subunit A	0.46
Q14393	Growth arrest-specific protein 6	0.16
P00533	Epidermal growth factor receptor	0.38

3.7.7 Comparison of Hepatocytes and Trophoblasts in *L. monocytogenes* infection model

In a study conducted by Descoeudres and collegues, the chronic infection of *L. monocytogenes* in a hepatocyte model was explored, revealing mechanisms by which the bacterium evades host immune responses (Descoeudres et al., 2021). The liver's immunotolerant nature allows it to harbour persistent *L. monocytogenes* infections, coinciding with the depletion of complement and coagulation pathways. This occurs particularly through the downregulation of a specific group of cytokines known as acute-phase proteins (APPs). The placenta, functioning as both a physical and immunological barrier, shares similar protective roles and is characterised by the secretion of various cytokines, chemokines, and immune-modulatory molecules (Megli et al., 2020).

Recognizing that *L. monocytogenes* exhibits a persistent phase and an intravacuolar lifestyle within LisCVs in both hepatocytes and trophoblasts, we aimed to compare these two infection models to uncover potential similarities or differences in how *L. monocytogenes* manipulates host immune responses. Our analysis revealed a similar depletion of key canonical pathways across both models, particularly in pathways related to complement and coagulation cascades and ECM interactions.

As reported by Descoeudres et al., 2021, chronic *L. monocytogenes* infection in hepatocytes led to the downregulation of genes associated with complement and coagulation pathways, a finding confirmed by proteomics analysis. Given the placenta's immunogenic properties and the enrichment of these pathways, we were particularly interested in exploring whether similar effects could be observed at the protein level in trophoblasts.

Our findings indicate that, although fewer variable proteins associated with these pathways were identified in trophoblasts compared to hepatocytes, the most intriguing observation was that *L. monocytogenes* appears to affect the complement and coagulation pathways as early as the acute phase of infection in the trophoblast model suggesting that *L. monocytogenes* could behave differently depending on the tissue. Many of the proteins involved in these pathways were present at 24h p.i. but began to diminish as the infection progressed to the chronic phase. This could suggest that *L. monocytogenes* may manipulate host immune responses already early in the infection process potentially contributing to persistence.

This early interference with critical immune pathways highlights the pathogen's ability to alter the host's defence mechanisms, facilitating its survival and establishing a niche within immunotolerant

organs such as the liver and placenta. These findings underscore the importance of understanding the dynamics of *L. monocytogenes* infection, particularly in identifying key stages where therapeutic interventions could be most effective in preventing the establishment of chronic infection.

IV. Summary

Similar to the liver, the placenta serves as an immunotolerant organ that activates protective mechanisms through the secretion of various proteins, including cytokines and immune modulators (Megli et al., 2020; Megli & Coyne, 2022). This immunotolerance is crucial for balancing foetal and maternal protection while preventing excessive immune responses that could risk pregnancy (Megli et al., 2020; Megli & Coyne, 2022). However, pathogens like *L. monocytogenes* have developed sophisticated strategies to exploit these host defences, potentially enabling them to establish chronic infections in such immunoprivileged sites, though the specific dynamics within the placental environment remain to be fully elucidated (Arora et al., 2017; Johnson et al., 2021).

For example, in studies of liver and more specifically in *in vitro* hepatocytes model, *L. monocytogenes* has been shown to affect the host's immune responses by altering the secretion of APPs, assisting the bacteria in evading immune detection and establishing potential persistent infections (Descoeudres et al., 2021). Long-term infection with *L. monocytogenes* in hepatocyte models leads to modifications in APP secretion, suggesting an environment favourable for bacterial proliferation and dormancy (Descourdes et al., 2021).

Our study investigated the host cell response to *L. monocytogenes* in the placental context. Therefore, investigations of the acute (24h p.i.) and chronic (96h p.i.) *L. monocytogenes* infection in a trophoblast model were performed and analyses were based on LC-MS/MS proteomics. Our findings revealed notable similarities between hepatocytes and trophoblasts, particularly in the modulation of complement and coagulation pathways, which were significantly downregulated in both models. These pathways are critical to the host innate immune responses, facilitating pathogen recognition and clearance (Descoeudres et al., 2021). The observed downregulation may indicate that *L. monocytogenes* could potentially downregulate these pathways to evade immune responses, creating a more permissive environment for its persistence.

Furthermore, our data indicated significant downregulation of angiogenesis pathways during the chronic phase of infection. Angiogenesis, the formation of new blood vessels from pre-existing ones, is essential for establishing fetomaternal circulation, ensuring adequate blood exchange between mother and foetus to support foetal development (Osherov and Ben-Ami, 2016; Ortega et al., 2022) . Key proteins regulating angiogenesis include hypoxia-inducible factor 1-alpha (HIF-1α), vascular endothelial growth factor A (VEGFA), and fibroblast growth factor (FGF). Disruptions in this process,

especially due to infections, can lead to complications such as preeclampsia (PE) and intrauterine growth restriction (IUGR), compromising foetal and maternal health (Osherov and Ben-Ami, 2016; Ortega et al., 2022).

In the chronic phase of *L. monocytogenes* infection, we observed downregulation of both angiogenesis and HIF-1α pathways, suggesting adverse effects on trophoblast cell growth and behaviour (Ortega et al., 2022). The role of HIF-1α is particularly significant, as it regulates cellular responses to hypoxia and influences immune responses against intracellular pathogens. Its absence could probably increase susceptibility to various bacterial infections. Additionally, in the context of chronic inflammation, VEGFA plays a critical role in stimulating new blood vessel formation. In our findings, the presence of neuropilin-1 and the persistent downregulation of heparan sulfate during the chronic phase indicate ongoing inflammatory impairment, affecting essential processes like cell migration and tissue repair, thereby facilitating *L. monocytogenes* persistence in trophoblasts (uniprot). More specifically, notable variability in angiogenesis-related proteins was observed during chronic *L. monocytogenes* infection. Pathogens can manipulate host angiogenic responses to promote their proliferation, either enhancing or suppressing angiogenesis based on their needs (Osherov and Ben-Ami, 2016). For instance, certain pathogens, like *M. tuberculosis (Mtb)*, promote angiogenesis, while others, like *Bacillus anthracis*, suppress it to evade immune detection (Osherov and Ben-Ami, 2016).

Interestingly, the enrichment of downregulated pathways was evident during both the acute and the chronic phase of infection. However, many signalling pathways only appeared as the infection progressed to the chronic phase. The manipulation of MAPK, Ras, and Rap1 signalling pathways by *L. monocytogenes* may further disrupt host immune responses, inhibiting inflammation and creating an environment essential to pathogen survival (Hashino et al., 2015; Nandi and Aroeti, 2023). The MAPK signalling pathway is essential for host immune responses, regulating cellular processes such as proliferation, differentiation, and stress responses, including the production of cytokines and inflammatory mediators (Weiglein et al., 1997; Hashino et al,m 2015). Many bacterial pathogens exploit the MAPK for their benefit (Nandi and Aroeti, 2023). The downregulation of MAPK signalling at chronic infection stages may suggest that *L. monocytogenes* might disrupt cellular signalling similarly to other pathogens, impairing immune responses and promoting persistence (Nandi and Aroeti, 2023).

An interesting observation was that many of the secreted proteins retained their downregulation between the two timepoints but, despite that, at 96h the abundance was higher showing a gradual upregulation. This trend may reflect a shift in host responses, with increased secretion or production of acute-phase proteins by 96h p.i., indicating a recovery in secretion activity rather than merely an immune evasion strategy by the pathogen.

In summary, our findings suggest that chronic infection with *L. monocytogenes* could allow the pathogen to establish a potential favourable niche within trophoblasts by selectively modulating host immune responses via signalling pathways as has also described in other pathogens through the manipulation of MAPK signalling pathway e.g *Mtb*, and in enteropathogens; *Enteropathogenic (EPEC)* and *enterohaemorrhagic (EHEC) E. coli, Shigella* species*, Salmonella enterica and Vibrio* species, as well (Nandi and Aroeti, 2023). The probability that *L. monocytogenes* might create a stable, immune-tolerant environment, particularly through the downregulation of specific signalling pathways at 96h p.i., poses significant challenges for maternal and foetal health. In addition, the fact that certain proteins both in angiogenesis and HIF-1a pathway show an upregulation trend, could suggest that the host is trying to fight the infection while *L. monocytogenes* tries to establish a persistent infection. Understanding the interplay between angiogenesis and in particular, the 96h p.i. signalling pathways and host-pathogen interactions, may yield valuable insights into potential therapeutic targets for preventing or treating *L. monocytogenes* infections.

V. Material and Methods

5.1 Bacterial Strains and Human Cell Line

Listeria monocytogenes strain 10403S WT was used as the infection agent in our model. Bacteria were grown overnight on Brain-Heart Infusion (BHI) medium at 37℃ with agitation. The human choriocarcinoma cell line JEG3 was grown under standard cell culture conditions in Dulbecco's Modified Eagle Medium (DMEM, Gibco) supplemented with 10% Foetal Bovine Serum (FBS, Sigma) at 37℃ and in a humidified 5% CO_2 incubator. During the infection assays, both infected and non-infected cells were transferred in a 10% CO_2 incubator.

5.2 Culture of Human Cell Line JEG3

Cells were seeded with MEM w/ GlutaMax+NEAA+Sodium Pyruvate+10% FBS in T75 cell culture flasks and were placed at 37 ℃ in 5% CO_2 incubator for four days prior infection until reaching confluency. Each plate corresponded to an independent biological replicate (different cell line passage and different bacteria inoculum for infection). Overall, there were five biological replicates for each condition, Infected (I) and Uninfected (NI); I-24h, NI-24h, I-96h and NI-96h.

5.3 Bacterial Infection

Before infection and in order to determine the multiplicity of infection (MOI), cells were counted using a hemocytometer (Neubauer-improved, Hausser Scientific). Bacterial inocula were prepared in serum-free culture medium using bacteria grown overnight to stationary-phase and washed three times in PBS. Cells were infected as per the standard infection protocol described by Bierne et al., 2021, and subsequently incubated for the indicated times with culture media containing 25 µg/ml gentamicin to prevent the growth of extracellular bacteria. Cells were washed in serum-free culture medium and lysed in cold 0.5% TXT in PBS (1X) to determine the number of intracellular bacteria at the 0h, 24h and 96h post infection (p.i). Serial dilutions of cell lysates were performed and plated on BHI agar plates. The infection process was assessed by counting colony-forming units (CFU) at the specified timepoints.

5.4 Antibodies and Immunofluorescence

The primary antibodies employed in our investigation comprised a polyclonal rabbit antibody against *Listeria monocytogenes* (BD Difco, 223001) and a monoclonal mouse antibody targeting human

LAMP1 (BD Bioscience, 555801). The secondary antibodies Alexa Fluor 488-conjugated goat anti-rabbit (Life Technologies) and Alexa Fluor Cy3-conjugated goat anti-mouse (Jackson ImmunoResearch Laboratories) were used for fluorescent visualisation. Additionally, Alexa Fluor 647-conjugated phalloidin (Life Technologies) was used for labelling F-actin and Hoechst (Thermo Fisher Scientific) was utilised for the specific labelling of nuclei. The process of the infection was also assessed via Immunofluorescence. More specifically, intracellular *L. monocytogenes* was observed by fluorescent microscopy as described by Bierne et al., 2021. Cells were grown in squared and sterile coverslips and upon fixation with 4% PFA in PBS, cells were permeabilized with 0.5% TXT in PBS and followed by 3 washes in PBS and finally a 20-minute incubation in blocking solution 2% BSA in PBS. Cells were then incubated with the primary antibodies for 1h and eventually with the secondary antibody including phalloidin and Hoeachst in 2% BSA for a 30-minute-incubation. Finally, the coverslips were mounted on glass slides using Fluoromount-G mounting medium (Interchim, Montlucon) and were analysed with a Carl Zeiss AxioObserver.Z1 microscope. The images were further processed with the Zeiss software.

5.5 Secretome Analysis

JEG3 cells were either left uninfected or were infected with *L. monocytogenes* 10403S (MOI~0.1). After 8h post infection, cells were washed twice with serum-free medium and left for 16h in serum-free medium with 25 μg/ml gentamicin. The same procedure was followed for the chronic state of infection, at 72h of infection, cells remained in serum-free medium for another 16h. Conditioned media was then collected, centrifuged twice (300 × g, 5 min) and the supernatant was filtered by 0.22 μm filters. Cells were lysed in 500 ul of RIPA buffer (20 mM Tris HCl pH 7.5, 150 mM NaCl, 1% TXT-100, 0.1% SDS, supplemented with protease inhibitors) and incubated on ice for 15 min. The cell lysate was cleared by centrifugation (13000 × g, 15 min, 4°C) with the supernatant assayed for protein concentration using the Bradford assay.

5.5.1 Sample Preparation

For the secretome analysis, 1ml of sample (~500μg/ml) was concentrated using an Amicon centrifugal filter unit (3KDa cut-off, Millipore) and loaded in a short migration 1D gel electrophoresis (NuPAGE® 4-12 % Bis-Tris 1.5mm Gel, Novex). Proteins were stained using Coomassie G-250 (SimplyBlue™ SafeStain, Invitrogen) and the protein lane (7mm*8mm) was cut into 1 mm pieces. They were subsequently washed using Solvent A (10 % v/v acetic acid, 40 % v/v ethanol) and Solvent B (50 % v/v 50 mM ammonium bicarbonate, 50 % v/v acetonitrile). The protein samples were then

reduced with 10 mM dithiothreitol (DTT) (Sigma) to break the bonds and alkylated by 55 mM iodoacetamide (IAA) (Sigma) to prevent the recreation of the bonds. The proteins were then digested with 50 ng of trypsin (Promega) and peptides were extracted using an extraction buffer of 0.5 % v/v trifluoroacetic acid and 50 % v/v acetonitrile. The peptides were dried completely using a SpeedVac concentrator (Savant™ SPD121D, Thermo Fisher Scientific) and then resuspended in 20µl loading buffer (0.5 % Formic Acid , 2 % v/v Acetonitrile) for LC-MS/MS proteome analysis.

5.5.2 Liquid Chromatography Tandem Mass Spectrometry (LC-MS/MS)

The proteomic analysis was conducted in the PAPPSO platform using the Mass spectrometer timsTOF Pro coupled with an ion mobility module (Tims) by Bruker. Specifically, a volume of 1µl was loaded on a Acclaim PepMap C18 (100um x 2cm) trap column and peptides separation was enabled through an Aurora ultimate C18 (25cm x 75um x 1.7um) separation column with a 70 min gradient Mass spectrometry acquisition was set to DDA-PASEF with mass range from 100 to 1700 m/z, active exclusion of MS/MS and release after 0.4min. The source capillary voltage (CaptiveSpray) was set to 1.6 kV with a total cycle time of 1.3 sec and 6 PASEF MS/MS scans per run.

5.5.3 Data Analysis

H. sapiens database (Uniprot, version 2023, taxonomy id 9606, number of entries 20472) was used as a reference for identification of proteins by using i2MassChroQ v.2. All settings were to default with tryptic digestion as one cleavage. Proteins identification was filtered with the following parameters (peptide Evalue <0.001, minimum 2 peptides/protein and protein Evalue $<10^{-4}$). Quantification was performed based on two complementary methods (SC and XIC). MassChroQ and R packages (MCQR, (https://forgemia.inra.fr/pappso/mcqr) developed by PAPPSO were used for quality assessment and statistical analysis. The abundance in the number of spectra was modelled using the GCM and Poisson distribution. Filtering of proteins showing low number of spectra per replicate for each condition to cutoff=5 meaning that any protein showing less than 5 spectra are removed. The selection criteria was set to cutoff= 1.5 for the ratio of min/max abundances. Statistical analysis was conducted with multiple ANOVA tests and p-value was adjusted to the Benjamin-Hochberg approach with p-value < 0.05.

5.5.4 Bioinformatic Analysis

All the proteomic data were analysed with R studio based on the MCQR script developed by PAPPSO. Functional and pathway analysis were performed with DaviD NCBI online database (https://david.ncifcrf.gov/) considering the significance threshold at p-value < 0.05. For visualisation of the output data, R studio using ggplot2 based on the R script provided by an online protocol (Bonnot et al., 2019) was used. Graphs and figures were either generated with Biorender or normally via google sheets graph generation.

Chapter 2 - Proteomic investigations of the Viable but non culturable (VBNC) state of *L. monocytogenes* over a 28-day-time course

I. Overview

Recent studies conducted by our team, EpiMic, have monitored the development of the VBNC state in *L. monocytogenes* following extended nutrient deprivation in mineral water. In particular, Carvalho et al., 2024, described that various *Listeria* species, including *L. monocytogenes*, enter a dormant state after 28 days of nutrient starvation. Samples were collected on a weekly basis and more specifically at the specified timepoints; Day (D) D0, D7, D14 and D28, and both culturability and viability assays were performed to determine the extent of VBNC induction in *L. monocytogenes*. It has been suggested that nutrient depletion induces *L. monocytogenes* into the VBNC state through a process of cell wall (CW) shedding, leading to the formation of osmotically stable, cell wall-deficient (CWD) coccoid forms (as illustrated in Figure 21). The observation of this phenotype across the *Listeria* genus suggests it may represent an adaptive response to osmotic stress.

Transcriptomic analyses and gene-targeted approaches have identified SigB and the autolysin NamA as key regulators involved in the transition to the CWD phenotype and the VBNC state (Figure 34). Specifically, genes regulated by SigB were found to be upregulated, prompting studies with ΔSigB mutants. Most Δ*sigB* cells had already adopted the CWD phenotype, suggesting that SigB plays a critical role in *L. monocytogenes* adaptation to nutrient-deprived conditions and in CWD formation, though it is not essential for bacterial viability. Overall, these experiments demonstrated that *L. monocytogenes* lacking SigB entered the VBNC state more rapidly (2-log culturability reduction) than wild-type cells, with significant transitions occurring by D7 (Figure 34C, D).

Similarly, NamA has been shown to promote cell wall loss upon entry into the VBNC state. Deletion studies comparing Δ*namA* to wild-type *L. monocytogenes* revealed delayed VBNC dynamics in the mutant, contrasting the rapid entry observed in Δ*sigB* cells (Figure 34A, B). By D7, most Δ*namA* cells retained their culturability and cell wall integrity, indicating a delayed transition to the CWD phenotype. The involvement of NamA was further confirmed through studies of SecA2, a protein essential for NamA export to the bacterial surface. Furthermore, our team has demonstrated that

the VBNC state in *L. monocytogenes* is reversible. Upon inoculation into embryonated chicken eggs, the bacteria can revert to a fully virulent and walled state (Carvalho et al., 2024).

Therefore, this thesis's second objective aims to further characterise the proteomic landscape of the VBNC state using LC-MS/MS. Specifically, we were interested to investigate the weekly progression of *L. monocytogenes* into the VBNC and CWD phenotypes over a 28-day period, identifying key proteomic factors involved both during the transition of *L. monocytogenes* in the VBNC state and also proteomic players in *L. monocytogenes* CW loss.

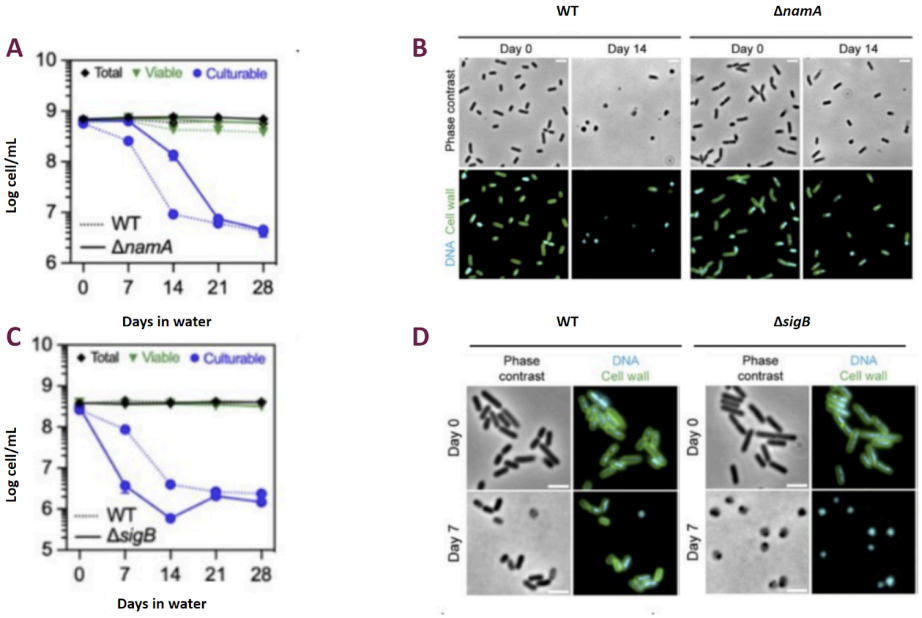

Figure 34 : Monitoring of the VBNC entry via culturability over a 28-day time course and immunofluorescence assessments of both Δ*namA* (D0 to D14) and Δ*sigB* (Do to D7) compared to the EGDe *L. monocytogenes* WT. (A, C) Cell number of total (black), viable (green), culturable (blue) of WT *L. monocytogenes* compared to Δ*namA* (top) and Δ*sigB* (bottom). (B, D) Phase contrast and immunofluorescence (scale bar 2µm, DNA; blue, Cell wall green;) of the cell populations quantified by CFU enumeration and flow cytometry by CFDA in (A,C). (Figures adapted by Carvalho et al., 2024).

II. Experimental Set-Up

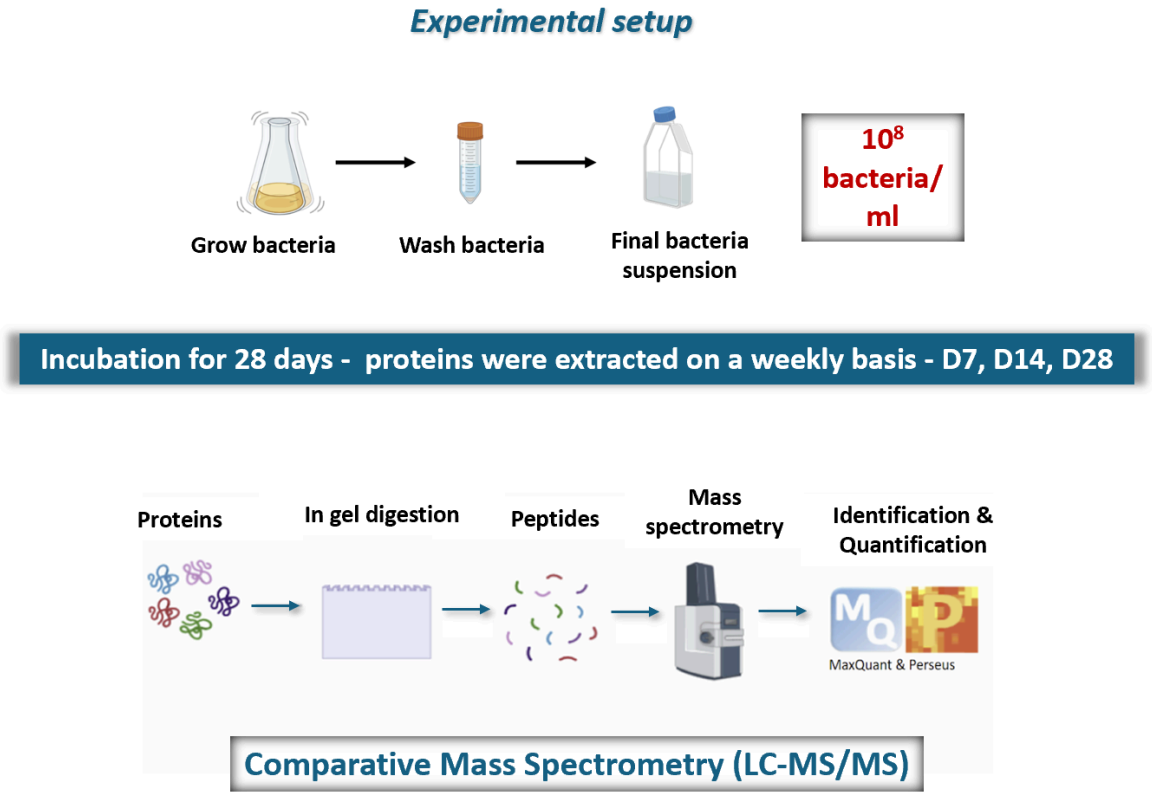

Figure 35 : Workflow of the second experimental objective focusing on the VBNC phenotype of *L. monocytogenes* via LC-MS/MS proteomics. Five biological replicates corresponding to five independent time courses were generated. Samples from D0, D7, D14 and D28 were extracted and prepared for proteomic analysis via bottom-up in-gel digestion approach, (see Material and Methods, page 173).

III. Results

3.1 Global proteome characterisation of VBNC *L. monocytogenes* shows an increase in upregulated and downregulated proteins.

The proteomic analysis of *L. monocytogenes* in the VBNC state under nutrient starvation in mineral water reveals significant protein abundance changes over a 28-day time course. By utilising MaxQuant and Perseus for protein identification, quantification and statistical analysis, the study highlights the dynamic shifts in both upregulated and downregulated proteins at different time points (D0, D7, D14, and D28). A first interesting observation is the increase in the total number of deregulated proteins both upregulated and downregulated as the VBNC state progresses (Figure 36). This could suggest that as *L. monocytogenes* adapts to prolonged nutrient starvation, there is a growing need to modulate its protein machinery, likely to conserve energy and maintain minimal metabolic functions essential for survival.

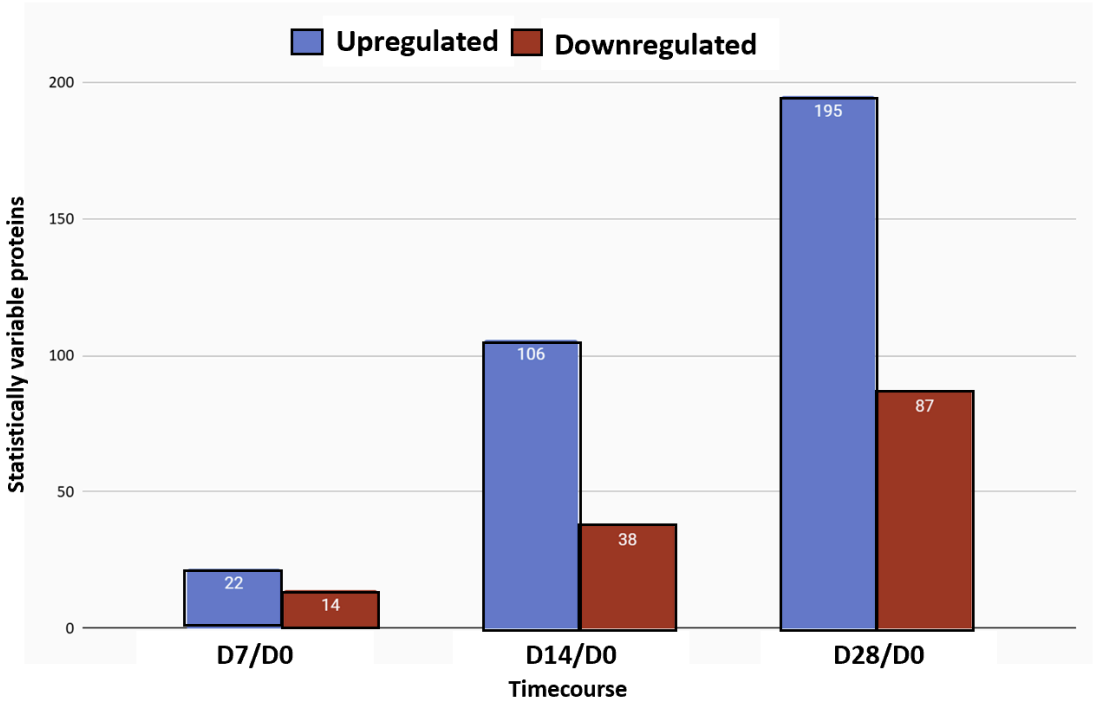

Figure 36: Graph illustrating the number of differential identified proteins in *L. monocytogenes* VBNC cultures over the 28-day time course. The number of proteins upregulated (blue) and downregulated (red) at each time point (D7/D0, D14/D0, and D28/D0) is shown relative to D0. The analysis was performed with MaxQuant and Perseus softwares, (Tables 15-17).

Table 15: Statistically significant variable proteins identified at D7 compared to D0 (D7/D0). The table presents −log(p-value) values obtained from a t-test performed using Perseus software; with higher values indicating greater statistical significance, along with log2 fold changes for each protein. Subcellular localization was determined using SignalP v5 and TOPCONS software.

	Accession Number	Locustag	Name	Product	Functional Category/COG	-Log(p-value)	Log2(D7/D0)	Localisation
UP	Q8Y9K2	lmo0525	NA	hypothetical protein	Function unknown	2.36	3.24	Cytoplasmic
	P66221	lmo0244	rpmG	50S ribosomal protein L33 type II	Translation	4.45	1.38	Cytoplasmic
	Q929L4	lmo2158	NA	hypothetical protein	Function unknown	2.01	1.26	Cytoplasmic
	Q8Y702	lmo1528	NA	hypothetical protein	Function unknown	1.30	1.15	Cytoplasmic
	P66207	lmo2047	rpmF	50S ribosomal protein L32	Translation	2.85	1.14	Cytoplasmic
	P66290	lmo2609	rpmJ	50S ribosomal protein L36	Translation	4.25	1.09	Cytoplasmic
	Q8Y3W6	lmo2713	NA	GW domain-containing glycosaminoglycan-binding protein	Cell wall protein; Function unknown	4.39	1.05	Cytoplasmic Membrane
	Q927H3	lmo2666	NA	PTS galacticol transporter subunit IIB	Carbohydrate transport and metabolism	2.06	0.98	Cytoplasmic
	Q8Y5K1	lmo2059	NA	potassium channel protein	Inorganic ion transport and metabolism	1.32	0.88	Cytoplasmic Membrane
	Q8Y9E9	lmo0580	NA	hypothetical protein	Lipid transport and metabolism; General function prediction only	1.73	0.86	Cytoplasmic
	Q8Y9N9	lmo0486	rpmF	50S ribosomal protein L32	Translation	2.93	0.82	Cytoplasmic
	Q8Y8Q9	lmo0836	psiE	phosphate-starvation-inducible protein PsiE	Signal transduction mechanisms	1.72	0.78	Cytoplasmic Membrane
	P64032	lmo1355	efp	elongation factor P	Translation	1.42	0.77	Cytoplasmic
	Q927M5	lmo2614	rpmD	50S ribosomal protein L30	Translation	2.38	0.77	Cytoplasmic
	Q8Y7E5	lmo1338	NA	hypothetical protein	Function unknown	2.45	0.74	Cytoplasmic
	Q8Y9U3	lmo0427	NA	PTS fructose transporter subunit IIB	Carbohydrate transport and metabolism	1.48	0.72	Cytoplasmic
	Q8YAQ0	lmo0067	NA	dinitrogenase reductase ADP-ribosylation protein	Posttranslational modification, protein turnover, chaperones	1.33	0.69	Cytoplasmic
	Q8Y5F6	lmo2108	nagA-like	N-acetylglucosamine-6-phosphate deacetylase	Cell wall metabolism	1.44	0.69	Cytoplasmic
	Q8Y7N5	lmo1239	NA	nucleoside-triphosphatase	Nucleotide transport and metabolism	2.27	0.67	Cytoplasmic
	Q8Y4K1	lmo2437	NA	hypothetical protein	Function unknown	1.63	0.66	Cytoplasmic
	Q8Y4G3	lmo2481	NA	pyrophosphatase PpaX	Posttranslational modification, protein turnover, chaperones	1.54	0.62	Cytoplasmic
	P66503	lmo1480	rpsT	30S ribosomal protein S20	Translation	2.84	0.60	Cytoplasmic
DOWN	Q8Y7H8	lmo1301	NA	hypothetical protein	Posttranslational modification, protein turnover, chaperones; General function prediction only	1.63	-0.62	Cytoplasmic
	Q8Y872	lmo1045	NA	molybdopterin converting factor subunit 1	Coenzyme transport and metabolism	1.39	-0.63	Cytoplasmic
	Q8Y5L8	lmo0441	pbpB3	penicillin-binding protein B3	Cell wall metabolism	1.61	-0.64	Cytoplasmic Membrane
	Q8Y994	lmo0639	NA	transcripitonal regulator	Transcription	1.72	-0.65	Cytoplasmic Membrane
	Q8Y5F8	lmo2106	NA	hypothetical protein	Function unknown	2.17	-0.69	Unknown
	Q8Y8Y7	lmo0755	NA	hypothetical protein	Lipid transport and metabolism; General function prediction only	1.70	-0.73	Unknown
	P13128	lmo0202	hly	listeriolysin O precursor	Secreted protein; Virulence mechanisms	3.87	-0.76	Extracellular
	Q8Y5E3	lmo2121	NA	maltose phosphorylase	Carbohydrate transport and metabolism	2.78	-0.89	Cytoplasmic
	Q8Y7P9	lmo1224	NA	hypothetical protein	Transport and Metabolism (ABC transporter)	2.56	-0.91	Cytoplasmic Membrane
	Q8Y8E0	lmo0964	yjbH	Protease adaptor	Secondary metabolites biosynthesis, transport and catabolism	1.31	-1.11	Cytoplasmic
	Q8Y5J8	lmo2062	NA	copper transporter	Inorganic ion transport and metabolism	1.46	-1.19	Cytoplasmic Membrane
	Q8Y5W4	lmo1941	NA	hypothetical protein	Function unknown	3.62	-1.62	Cytoplasmic Membrane
	Q8Y8F4	lmo0950	NA	hypothetical protein	Cell wall metabolism; General function prediction only	2.64	-2.69	Unknown
	Q8Y4D2	lmo2518	TagTUV	Wall teichoic acid ligase	Cell wall metabolism	3.45	-2.73	Cytoplasmic Membrane

Table 16: Statistically significant variable proteins identified at D14 compared to D0 (D14/D0). The table presents –log(p-value) values obtained from a t-test performed using Perseus software; with higher values indicating greater statistical significance, along with log2 fold changes for each protein. Subcellular localization was determined using SignalP v5 and TOPCONS software.

	Accession Number	Locustag	Name	Product	Functional Category/COG	-Log(P-value)	Log2(D7/D0)	Localisation
UP	Q8Y9K2	lmo0525	NA	hypothetical protein	Function unknown	2.89	3.72	Cytoplasmic
	Q8Y882	lmo1035	NA	PTS beta-glucoside transporter subunit IIABC	Carbohydrate transport and metabolism	2.71	2.07	Cytoplasmic Membrane
	Q8Y702	lmo1528	NA	hypothetical protein	Function unknown	1.89	1.68	Cytoplasmic
	Q8Y5S6	lmo1979	NA	hypothetical protein	Function unknown	1.52	1.62	Cytoplasmic
	Q8Y6E4	lmo1743	NA	hypothetical protein	Function unknown	1.84	1.61	Cytoplasmic
	Q8Y9N1	lmo0494	NA	hypothetical protein	Lipid transport and metabolism; General function prediction only	2.11	1.56	Cytoplasmic
	Q8Y3R8	lmo2765	NA	PTS cellbiose transporter subunit IIA	Carbohydrate transport and metabolism	2.65	1.51	Cytoplasmic
	Q92D14	lmo1008	NA	hypothetical protein	Function unknown	2.83	1.48	Cytoplasmic
	Q8Y5A6	lmo2162	NA	hypothetical protein	Carbohydrate transport and metabolism; General function prediction only	1.31	1.44	Cytoplasmic
	Q8Y824	lmo1094	NA	hypothetical protein	Function unknown	3.39	1.36	Cytoplasmic
	Q8Y9X6	lmo0391	NA	hypothetical protein	Function unknown	2.94	1.33	Cytoplasmic
	Q8Y411	lmo2667	NA	PTS galacticol transporter subunit IIA	Carbohydrate transport and metabolism	3.97	1.33	Cytoplasmic
	Q8Y4K1	lmo2437	NA	hypothetical protein	Function unknown	3.32	1.31	Cytoplasmic
	Q8Y9Z0	lmo0377	NA	hypothetical protein	Function unknown	2.86	1.30	Cytoplasmic
	Q8Y892	lmo1022	liaR	two-component response regulator	Transcription; Signal transduction mechanisms; Posttranslational modification, protein turnover, chaperones; Antibiotic/Drug transport and metabolism	1.72	1.26	Cytoplasmic
	Q8Y9U3	lmo0427	NA	PTS fructose transporter subunit IIB	Carbohydrate transport and metabolism	3.03	1.26	Cytoplasmic
	Q8Y8U3	lmo0800	NA	hypothetical protein	Function unknown	1.74	1.23	Cytoplasmic
	Q927H3	lmo2666	NA	PTS galacticol transporter subunit IIB	Carbohydrate transport and metabolism	3.07	1.22	Cytoplasmic
	Q9AGE7	lmo2069	groES	co-chaperonin GroES	Posttranslational modification, protein turnover, chaperones	2.30	1.17	Cytoplasmic
	Q8Y6S4	lmo1609	NA	thioredoxin	Energy production and conversion	3.21	1.16	Cytoplasmic
	P28764	lmo1439	sod	superoxide dismutase	Inorganic ion transport and metabolism; Virulence mechanisms	4.25	1.15	Cytoplasmic
	Q8Y424	lmo2651	NA	PTS mannitol transporter subunit IIA	Carbohydrate transport and metabolism	2.78	1.15	Cytoplasmic
	Q8Y987	lmo0646	NA	hypothetical protein	Function unknown	1.96	1.13	Cytoplasmic
	Q8YA59	lmo0302	NA	hypothetical protein	Function unknown	1.81	1.08	Cytoplasmic
	Q8Y9L5	lmo0512	NA	hypothetical protein	Function unknown	2.29	1.08	Cytoplasmic
	Q8Y9X0	lmo0398	NA	PTS sugar transporter subunit IIA	Carbohydrate transport and metabolism	3.00	1.08	Cytoplasmic
	Q8Y6Q5	lmo1629	trpF	N-(5'-phosphoribosyl)anthranilate isomerase	Amino acid transport and metabolism	1.93	1.06	Cytoplasmic
	Q8Y859	lmo1059	NA	hypothetical protein	Function unknown	3.98	1.04	Cytoplasmic
	Q8Y9V0	lmo0420	NA	hypothetical protein	Function unknown	2.12	1.01	Cytoplasmic
	Q8Y4F3	lmo2491	pdeE	phosphodiesterase	Nucleotide transport and metabolism	3.19	1.01	Cytoplasmic
	P64032	lmo1355	efp	elongation factor P	Translation	1.87	1.00	Cytoplasmic
	Q8Y6D7	lmo1750	NA	hypothetical protein	Function unknown	1.46	1.00	Cytoplasmic
	Q8Y866	lmo1051	def	peptide deformylase	Translation	2.21	0.99	Cytoplasmic
	Q8Y8T3	lmo0811	NA	carbonic anhydrase	Inorganic ion transport and metabolism	2.72	0.99	Cytoplasmic
	Q8Y6Y6	lmo1545	minC	septum formation inhibitor MinC	Cell division/elongation	1.61	0.98	Cytoplasmic
	Q8Y484	lmo2571	NA	nicotinamidase	Coenzyme transport and metabolism	3.02	0.98	Cytoplasmic
	Q8Y8K6	lmo0894	rsbW	serine-protein kinase RsbW	Signal transduction mechanisms; Posttranslational modification, protein turnover, chaperones	2.87	0.97	Cytoplasmic
	Q8Y7X9	lmo1140	NA	hypothetical protein	Function unknown	1.86	0.96	Cytoplasmic
	Q8Y5R1	lmo1995	dra	deoxyribose-phosphate aldolase	Nucleotide transport and metabolism	3.18	0.96	Cytoplasmic

	Q8Y8U6	lmo0796	NA	hypothetical protein	Function unknown	2.37	0.96	Cytoplasmic
	Q8Y553	lmo2223	NA	hypothetical protein	Transcription; General function prediction only	2.22	0.95	Cytoplasmic
	Q8Y3Y2	lmo2697	NA	PTS mannose transporter subunit IIA	Carbohydrate transport and metabolism	2.84	0.95	Cytoplasmic
	Q8Y6R3	lmo1621	NA	hypothetical protein	Replication, recombination and repair; General function prediction only;	2.29	0.94	Cytoplasmic
	P0A438	lmo1002	ptsH	phosphocarrier protein HPr	Carbohydrate transport and metabolism	3.07	0.94	Cytoplasmic
	Q8Y419	lmo2658	NA	acyltransferase	Transcription; General function prediction only;	1.58	0.94	Cytoplasmic
	Q8Y3W6	lmo2713	NA	GW domain-containing glycosaminoglycan-bindin g protein	Cell wall protein; Function unknown	3.96	0.92	Cytoplasmic Membrane
	Q8Y425	lmo2650	NA	MFS transporter	Carbohydrate transport and metabolism; Amino acid transport and metabolism; Inorganic ion transport and metabolism; General function prediction only;	1.88	0.92	Cytoplasmic
	Q8Y7J2	lmo1285	NA	hypothetical protein	Function unknown	3.14	0.91	Cytoplasmic
	Q8Y8H4	lmo0930	yhfI	hypothetical protein	Function unknown	4.18	0.90	Cytoplasmic
	Q8Y7V9	lmo1160	pduL	PduL protein	Secondary metabolites biosynthesis, transport and catabolism	1.92	0.90	Cytoplasmic
	Q8Y8Y2	lmo0760	NA	hypothetical protein	Function unknown	3.07	0.88	Cytoplasmic
	Q8Y8D9	lmo0965	NA	hypothetical protein	Function unknown	4.49	0.88	Cytoplasmic
	Q8Y6P1	lmo1643	NA	hypothetical protein	Function unknown	1.96	0.87	Cytoplasmic
	Q8Y757	lmo1448	NA	manganese-dependent inorganic pyrophosphatase	Energy production and conversion	3.55	0.86	Cytoplasmic
	Q8Y5V1	lmo1954	drm /deoB	phosphopentomutase	Nucleotide transport and metabolism	2.46	0.85	Cytoplasmic
	Q8Y5F6	lmo2108	nagA-li ke	N-acetylglucosamine-6-ph osphate deacetylase	Cell wall metabolism	1.42	0.84	Cytoplasmic
	Q8Y678	lmo1821	stp / prpC	phosphoprotein phosphatase	Signal transduction mechanisms; Posttranslational modification, protein turnover, chaperones; Virulence mechanisms	1.97	0.83	Cytoplasmic
	Q8Y8J8	lmo0903	NA	hypothetical protein	Function unknown	1.93	0.83	Cytoplasmic
	Q8Y7N5	lmo1239	NA	nucleoside-triphosphatas e	Nucleotide transport and metabolism	2.47	0.83	Cytoplasmic
	Q8Y3K4	lmo2831	NA	phosphoglucomutase	Carbohydrate transport and metabolism	2.22	0.81	Cytoplasmic
	P0A4L3	lmo1233	trxA	thioredoxin A	Energy production and conversion	2.12	0.81	Cytoplasmic
	Q8Y4E5	lmo2501	phoP	two-component response phosphate regulator	Transcription; Signal transduction mechanisms;	3.62	0.80	Cytoplasmic
	Q8Y7L8	lmo1256	NA	hypothetical protein	Function unknown	2.42	0.79	Cytoplasmic
	Q8Y640	lmo1860	msrA	methionine sulfoxide reductase A	Posttranslational modification, protein turnover, chaperones	2.85	0.77	Cytoplasmic
	Q8Y9E9	lmo0580	NA	hypothetical protein	Lipid transport and metabolism; General function prediction only	2.18	0.77	Cytoplasmic
	Q8Y8A5	lmo1005	NA	3-hydroxyisobutyrate dehydrogenase	Lipid transport and metabolism	2.02	0.77	Cytoplasmic
	Q8Y5V2	lmo1953	pnp	purine nucleoside phosphorylase	Nucleotide transport and metabolism	3.68	0.76	Cytoplasmic
	Q8YAB7	lmo0230	NA	hypothetical protein	Function unknown	2.63	0.76	Cytoplasmic
	Q8YAQ0	lmo0067	NA	dinitrogenase reductase ADP-ribosylation protein	Posttranslational modification, protein turnover, chaperones	1.45	0.74	Cytoplasmic
	Q8Y6E2	lmo1745	virR	two-component response regulator	Transcription; Signal transduction mechanisms;	2.16	0.74	Cytoplasmic
	Q8Y701	lmo1529	NA	hypothetical protein	Function unknown	1.92	0.74	Cytoplasmic Membrane
	Q8Y684	lmo1813	NA	phosphoglycerate dehydrogenase	Amino acid transport and metabolism	2.12	0.73	Cytoplasmic
	Q8Y4L2	lmo2425	NA	glycine cleavage system protein H	Amino acid transport and metabolism	1.89	0.72	Cytoplasmic
	Q8Y716	lmo1510	NA	hypothetical protein	Function unknown	1.64	0.71	Cytoplasmic
	Q8YAC8	lmo0218	NA	hypothetical protein	Translation; General function prediction only	1.35	0.71	Cytoplasmic
	Q8Y4F1	lmo2493	NA	ArsR family transcriptional regulator	Transcription	2.99	0.69	Cytoplasmic

	Q8Y449	lmo2611	adk	adenylate kinase	Nucleotide transport and metabolism	1.91	0.69	Cytoplasmic
	P66221	lmo0244	rpmG	50S ribosomal protein L33 type II	Translation	1.45	0.68	Cytoplasmic
	Q8YAE0	lmo0191	NA	phospho-beta-glucosidase	Carbohydrate transport and metabolism	1.38	0.67	Cytoplasmic
	Q8Y8Y3	lmo0759	NA	hypothetical protein	Amino acid transport and metabolism; General function prediction only	3.70	0.67	Cytoplasmic
	Q8Y6M7	lmo1657	tsf	elongation factor Ts	Translation	3.61	0.67	Cytoplasmic
	Q8Y9B9	lmo0613	NA	oxidoreductase	Energy production and conversion; General function prediction only;	2.80	0.66	Cytoplasmic
	Q8Y4M2	lmo2415	NA	ABC transporter ATP-binding protein	Transport and Metabolism (ABC transporter); Inorganic ion transport and metabolism	4.03	0.66	Cytoplasmic
	P0DJL9	lmo1619	daaA	D-amino acid aminotransferase	Amino acid transport and metabolism; Coenzyme transport and metabolism;	2.76	0.65	Cytoplasmic
	Q8Y8L0	lmo0888	mazF	endoribonuclease that cleaves mRNA at specific sites	Transcription; RNA metabolism;	1.54	0.65	Cytoplasmic
	Q8Y5F4	lmo2110	NA	mannnose-6 phospate isomerase	Carbohydrate transport and metabolism	3.12	0.65	Cytoplasmic
	Q8YA66	lmo0293	NA	rRNA large subunit methyltransferase	Translation	2.08	0.65	Cytoplasmic
	Q8Y4S4	lmo2358	gamA	N-acetylglucosamine-6-phosphate isomerase	Cell wall metabolism	4.82	0.65	Cytoplasmic
	Q8Y6B9	lmo1772	purC	phosphoribosylaminoimidazole-succinocarboxamide synthase	Nucleotide transport and metabolism	1.33	0.65	Cytoplasmic
	Q8Y5Q4	lmo2002	NA	PTS mannose transporter subunit IIB	Carbohydrate transport and metabolism	1.99	0.64	Cytoplasmic
	Q8Y9D0	lmo0602	NA	transcripitonal regulator	Transcription; General function prediction only;	1.64	0.64	Cytoplasmic
	Q8Y7J4	lmo1283	NA	LacX protein	Carbohydrate transport and metabolism	3.95	0.64	Cytoplasmic
	Q8Y7N4	lmo1240	NA	hypothetical protein	Function unknown	2.20	0.63	Cytoplasmic
	Q8Y627	lmo1873	dfrA	dihydrofolate reductase	Coenzyme transport and metabolism	1.42	0.63	Cytoplasmic
	Q8Y4R5	lmo2369	NA	general stress protein 13	Signal transduction mechanisms	1.86	0.61	Cytoplasmic
	Q8Y3Y6	lmo2693	tmk	thymidylate kinase	Nucleotide transport and metabolism	1.46	0.61	Cytoplasmic
	Q8Y3Y3	lmo2696	NA	dihydroxyacetone kinase	Carbohydrate transport and metabolism	3.45	0.61	Cytoplasmic
	Q8Y4V1	lmo2329	NA	hypothetical protein	Transcription; Phage	1.57	0.61	Cytoplasmic
	Q8Y560	lmo2216	NA	histidine triad (HIT) protein	Signal transduction mechanisms	1.58	0.61	Cytoplasmic
	Q8YAG5	lmo0161	NA	hypothetical protein	Signal transduction mechanisms; General function prediction only	3.22	0.61	Cytoplasmic
	Q8Y7N8	lmo1236	NA	hypothetical protein	Function unknown	2.00	0.61	Cytoplasmic
	Q8Y4I9	lmo2450	NA	carboxylesterase	Lipid transport and metabolism	2.24	0.61	Cytoplasmic
	Q8Y6U7	lmo1584	NA	hypothetical protein	Function unknown	2.27	0.61	Cytoplasmic Membrane
	Q8Y414	lmo2663	NA	polyol dehydrogenase	Carbohydrate transport and metabolism	1.80	0.60	Cytoplasmic
	Q8Y4G6	lmo2477	galE	UDP-glucose 4-epimerase	Cell wall metabolism	2.75	0.59	Cytoplasmic
	Q8Y8U5	lmo0797	NA	hypothetical protein	Function unknown	1.77	0.59	Cytoplasmic
DOWN	Q8Y3Y8	lmo2691	murA / NamA	autolysin; N-acetylglucosaminidase	Cell wall metabolism	2.78	-0.59	Extracellular
	Q8Y657	lmo1843	NA	RluA famoiy 23S pseudouridylate synthase	Translation; General function prediction only	1.32	-0.59	Cytoplasmic
	Q8Y3S4	lmo2757	NA	ATP-dependent DNA helicase	Replication, recombination and repair	1.94	-0.59	Cytoplasmic
	Q8Y649	lmo1851	NA	carboxy-terminal processing proteinase	Amino acid transport and metabolism	2.65	-0.59	Cytoplasmic Membrane
	Q8Y4K7	lmo2431	hupD	ferrichrome ABC transporter substrate-binding protein	Inorganic ion transport and metabolism; Transport and Metabolism (ABC transporter); Lipoprotein	2.41	-0.59	Lipoprotein
	P34024	lmo0201	plcA	phosphatidylinositol-specific phospholipase c	Lipid transport and metabolism; Virulence mechanisms	3.09	-0.62	Extracellular

	Q8Y889	lmo1026	NA	LytR protein	Transcription	2.91	-0.64	Cytoplasmic Membrane
	P66248	lmo2856	rpmH	50S ribosomal protein L34	Translation	2.12	-0.66	Cytoplasmic
	Q8Y665	lmo1835	carB	carbamoyl-phosphate synthetase	Nucleotide transport and metabolism;	3.39	-0.67	Cytoplasmic
	Q8Y8F1	lmo0953	NA	hypothetical protein	Lipoprotein; Function unknown	1.49	-0.68	Extracellular
	Q8Y707	lmo1521	NA	autolysin; N-acetylmuramoyl-L-alanine amidase	Cell wall metabolism	4.53	-0.70	Cell Wall 400208
	Q8Y496	lmo2558	ami	autolysin; N-acetylmuramoyl-L-alanine amidase	Cell wall metabolism; Virulence mechanisms	2.88	-0.70	Extracellular
	Q8Y510	lmo2268	addB	ATP-dependent deoxyribonuclease subunit B	Replication, recombination and repair	2.08	-0.72	Cytoplasmic
	Q8YA11	lmo0355	NA	fumarate reductase subunit A	Carbohydrate transport and metabolism; Lipoprotein	3.84	-0.80	Lipoprotein
	Q8YA01	lmo0366	fepA	Putative lipoprotein involved in iron transport (FepA)	Inorganic ion transport and metabolism; Lipoprotein	3.24	-0.81	Lipoprotein
	P66144	lmo1816	rpmB	50S ribosomal protein L28	Translation	2.11	-0.85	Cytoplasmic
	Q8Y763	lmo1438	pbpB1	penicillin-binding protein B1; PBP3	Cell wall metabolism	4.50	-0.87	Cytoplasmic Membrane
	Q8Y7J3	lmo1284	NA	hypothetical protein	Lipid transport and metabolism; General function prediction only	1.36	-0.89	Cytoplasmic Membrane
	Q8Y5E3	lmo2121	NA	maltose phosphorylase	Carbohydrate transport and metabolism	1.51	-0.91	Cytoplasmic
	Q8Y6S7	lmo1606	NA	DNA translocase	Cell division/elongation	2.70	-0.93	Cytoplasmic
	Q8Y5C5	lmo2140	NA	ABC transporter permease	Transport and Metabolism (ABC transporter)	1.69	-0.95	Cytoplasmic Membrane
	P21171	lmo0582	iap	invasion associated secreted endopeptidase p60; ?-d-Glutamyl-l-m-Dpm peptidase; autolysin	Cell wall metabolism; Virulence mechanisms	3.73	-1.04	Extracellular
	Q8Y7P9	lmo1224	NA	hypothetical protein	Transport and Metabolism (ABC transporter); General function prediction only	2.34	-1.05	Cytoplasmic Membrane
	Q7AP49	lmo2505	spl	autolysin; peptidoglycan lytic protein P45	Cell wall metabolism	1.90	-1.08	Extracellular
	P13128	lmo0202	hly	listeriolysin O precursor	Secreted protein; Virulence mechanisms	4.67	-1.17	Extracellular
	Q8Y8Y7	lmo0755	NA	hypothetical protein	Lipid transport and metabolism; General function prediction only	1.80	-1.19	Unknown
	Q8Y436	lmo2637	pplA	peptide pheromone-encoding lipoprotein A	Lipoprotein; Virulence mechanisms	3.96	-1.22	Lipoprotein
	Q8Y5L8	lmo2039	pbpB2	penicillin-binding protein B2; PBP2	Cell wall metabolism	4.32	-1.46	Cytoplasmic Membrane
	Q8Y6L8	lmo1666	lapB	pepdidoglycan bound protein; LPXTG protein	Cell wall protein	2.85	-1.51	Cell Wall LPXTG
	Q8Y638	lmo1862	NA	hypothetical protein	Lipid transport and metabolism; General function prediction only	3.95	-1.54	Cytoplasmic Membrane
	Q8Y9P7	lmo0477	NA	secreted protein	Secreted protein; Function unknown	3.57	-1.74	Cytoplasmic Membrane
	Q8Y4J9	lmo2439	NA	hypothetical protein	Function unknown	5.11	-2.04	Unknown
	Q8Y8F4	lmo0950	NA	hypothetical protein	Cell wall metabolism; General function prediction only	1.97	-2.07	Unknown
	Q8Y9V5	lmo0415	pgdA	peptidoglycan N-deacetylase	Cell wall metabolism; Virulence mechanisms	5.65	-2.27	Cytoplasmic
	Q8Y5I3	lmo2079	NA	hypothetical protein	Lipoprotein; Function unknown	6.34	-2.51	Lipoprotein
	Q8Y5B1	lmo2156	NA	hypothetical protein	Function unknown	3.97	-3.12	Unknown
	Q8Y5W4	lmo1941	NA	hypothetical protein	Function unknown	7.07	-4.40	Cytoplasmic Membrane
	Q8Y4D2	lmo2518	TagTUV	Wall teichoic acid ligase	Cell wall metabolism	6.02	-5.57	Cytoplasmic Membrane

Table 17: Statistically significant variable proteins identified at D28 compared to D0 (D28/D0). The table presents –log(p-value) values obtained from a t-test performed using Perseus software; with higher values indicating greater statistical significance, along with log2 fold changes for each protein. Subcellular localization was determined using SignalP v5 and TOPCONS software.

	Accession Number	Locustag	Name	Product	Functional Category/COG	-Log(P-value)	Log2(D7/D0)	Localisation
UP	Q8Y9K2	lmo0525	NA	hypothetical protein	Function unknown	2.13	3.04	Cytoplasmic
	Q8Y5I4	lmo2078	NA	hypothetical protein	Function unknown	2.78	2.66	Cytoplasmic
	Q8Y5S6	lmo1979	NA	hypothetical protein	Function unknown	2.12	2.35	Cytoplasmic
	Q8Y9L5	lmo0512	NA	hypothetical protein	Function unknown	3.65	2.23	Cytoplasmic
	Q8Y892	lmo1022	liaR	two-component response regulator	Transcription; Signal transduction mechanisms; Posttranslational modification, protein turnover, chaperones; Antibiotic/Drug transport and metabolism	2.17	2.20	Cytoplasmic
	Q8Y882	lmo1035	NA	PTS beta-glucoside transporter subunit IIABC	Carbohydrate transport and metabolism	2.76	2.06	Cytoplasmic Membrane
	Q8Y8W5	lmo0777	NA	hypothetical protein	Function unknown	2.43	1.96	Cytoplasmic
	Q8Y6Y6	lmo1545	minC	septum formation inhibitor MinC	Cell division/elongation	3.01	1.92	Cytoplasmic
	Q8Y7J2	lmo1285	NA	hypothetical protein	Function unknown	4.12	1.83	Cytoplasmic
	Q8Y524	lmo2253	NA	phosphoglucomutase	Carbohydrate transport and metabolism	2.74	1.82	Cytoplasmic
	Q8Y5A6	lmo2162	NA	hypothetical protein	Carbohydrate transport and metabolism; General function prediction only	2.17	1.77	Cytoplasmic
	Q8Y8G9	lmo0935	NA	rRNA methylase	Translation	2.88	1.70	Cytoplasmic
	Q8Y5H9	lmo2083	NA	hypothetical protein	Function unknown	2.32	1.68	Cytoplasmic
	Q8Y702	lmo1528	NA	hypothetical protein	Function unknown	1.60	1.66	Cytoplasmic
	Q8Y424	lmo2651	NA	PTS mannitol transporter subunit IIA	Carbohydrate transport and metabolism	4.00	1.63	Cytoplasmic
	Q8Y9N1	lmo0494	NA	hypothetical protein	Lipid transport and metabolism; General function prediction only	1.68	1.63	Cytoplasmic
	Q927H3	lmo2666	NA	PTS galacticol transporter subunit IIB	Carbohydrate transport and metabolism	1.91	1.61	Cytoplasmic
	Q8Y7V9	lmo1160	pduL	PduL protein	Secondary metabolites biosynthesis, transport and catabolism	3.29	1.56	Cytoplasmic
	Q8Y475	lmo2580	hrtA	Heme efflux system ATPase HrtA	Transport and Metabolism (ABC transporter); Inorganic ion transport and metabolism	1.68	1.54	Cytoplasmic
	Q8Y7J5	lmo1282	NA	hypothetical protein	Function unknown	1.82	1.52	Cytoplasmic
	Q8Y401	lmo2677	NA	esterase	Lipid transport and metabolism	1.64	1.51	Cytoplasmic
	Q8Y3R8	lmo2765	NA	PTS cellbiose transporter subunit IIA	Carbohydrate transport and metabolism	2.34	1.47	Cytoplasmic
	Q8Y824	lmo1094	NA	hypothetical protein	Function unknown	3.07	1.45	Cytoplasmic
	Q8Y8J8	lmo0903	NA	hypothetical protein	Function unknown	2.92	1.45	Cytoplasmic
	Q8Y8U3	lmo0800	NA	hypothetical protein	Function unknown	1.76	1.43	Cytoplasmic
	Q8Y4F3	lmo2491	pdeE	phosphodiesterase	Nucleotide transport and metabolism	4.28	1.43	Cytoplasmic
	Q8Y7N5	lmo1239	NA	nucleoside-triphosphatase	Nucleotide transport and metabolism	3.38	1.42	Cytoplasmic
	Q8Y6Z0	lmo1541	NA	hypothetical protein	Translation; General function prediction only	1.73	1.42	Cytoplasmic
	Q8Y9X6	lmo0391	NA	hypothetical protein	Function unknown	3.13	1.42	Cytoplasmic
	Q8Y4B6	lmo2535	atpB	ATP synthase F0F1 subunit A	Energy production and conversion	2.07	1.41	Cytoplasmic Membrane
	Q9AGE7	lmo2069	groES	co-chaperonin GroES	Posttranslational modification, protein turnover, chaperones	2.49	1.40	Cytoplasmic
	Q8Y411	lmo2667	NA	PTS galacticol transporter subunit IIA	Carbohydrate transport and metabolism	3.34	1.40	Cytoplasmic
	Q8Y632	lmo1868	NA	hypothetical protein	Amino acid transport and metabolism; General function prediction only	1.93	1.33	Cytoplasmic
	Q8Y5V1	lmo1954	drm /deoB	phosphopentomutase	Nucleotide transport and metabolism	4.58	1.33	Cytoplasmic
	Q8Y560	lmo2216	NA	histidine triad (HIT) protein	Signal transduction mechanisms	3.60	1.32	Cytoplasmic
	Q8Y8G0	lmo0944	NA	hypothetical protein	Function unknown	1.84	1.30	Cytoplasmic
	Q8Y9Z0	lmo0377	NA	hypothetical protein	Function unknown	2.31	1.29	Cytoplasmic

	Q8Y4C1	lmo2529	atpD	ATP synthase F0F1 subunit beta	Energy production and conversion	4.97	1.27	Cytoplasmic
	Q8Y5U2	lmo1963	NA	hypothetical protein	Transport and Metabolism (ABC transporter); General function prediction only	1.56	1.27	Cytoplasmic Membrane
	Q92FC3	lmo0136	ctpP1	cysteine ABC transporter permease 1	Amino acid transport and metabolism; Transport and Metabolism (ABC transporter)	1.81	1.27	Cytoplasmic Membrane
	Q8Y7G0	lmo1321	NA	hypothetical protein	Function unknown	2.40	1.26	Cytoplasmic
	Q8YA59	lmo0302	NA	hypothetical protein	Function unknown	1.42	1.23	Cytoplasmic
	Q8Y6E2	lmo1745	virR	two-component response regulator	Transcription; Signal transduction mechanisms;	3.14	1.23	Cytoplasmic
	Q8Y5U5	lmo1960	fhuC	ferrichrome ABC transporter ATP-binding protein	Inorganic ion transport and metabolism; Coenzyme transport and metabolism; Transport and Metabolism (ABC transporter)	2.94	1.21	Cytoplasmic
	Q8Y6H5	lmo1709	NA	methionine aminopeptidase	Translation	1.75	1.20	Cytoplasmic
	Q8Y987	lmo0646	NA	hypothetical protein	Function unknown	2.73	1.20	Cytoplasmic
	Q8Y9Z9	lmo0368	NA	hypothetical protein	Replication, recombination and repair; General function prediction only;	1.73	1.19	Cytoplasmic
	Q8Y6S4	lmo1609	NA	thioredoxin	Energy production and conversion	2.12	1.19	Cytoplasmic
	P0DJM3	lmo1474	grpE	heat shock protein GrpE	Posttranslational modification, protein turnover, chaperones	2.04	1.18	Cytoplasmic
	Q8Y866	lmo1051	def	peptide deformylase	Translation	2.51	1.18	Cytoplasmic
	Q92C58	lmo1295	hfq	RNA-binding protein Hfq	Transcription; RNA metabolism;	2.28	1.17	Cytoplasmic
	Q8Y8S4	lmo0820	NA	acetyltransferase	Transcription; General function prediction only;	1.63	1.16	Cytoplasmic
	P0DJO9	lmo1471	prmA	ribosomal protein L11 methyltransferase	Translation	3.52	1.16	Cytoplasmic
	Q8Y8A5	lmo1005	NA	3-hydroxyisobutyrate dehydrogenase	Lipid transport and metabolism	2.65	1.15	Cytoplasmic
	Q8Y749	lmo1463	NA	cytidine deaminase	Nucleotide transport and metabolism	1.37	1.14	Cytoplasmic
	Q8Y9P0	lmo0485	NA	putative nitroreductase from NADH oxidase and arsenite oxidase family	Energy production and conversion	3.08	1.14	Cytoplasmic
	Q8Y8T3	lmo0811	NA	carbonic anhydrase	Inorganic ion transport and metabolism	3.00	1.13	Cytoplasmic
	Q8Y6D7	lmo1750	NA	hypothetical protein	Function unknown	1.70	1.11	Cytoplasmic
	Q8Y9D0	lmo0602	NA	transcripitonal regulator	Transcription; General function prediction only;	2.85	1.11	Cytoplasmic
	Q8YAG5	lmo0161	NA	hypothetical protein	Signal transduction mechanisms; General function prediction only	3.44	1.10	Cytoplasmic
	Q8Y7X9	lmo1140	NA	hypothetical protein	Function unknown	2.55	1.09	Cytoplasmic
	Q8Y6P1	lmo1643	NA	hypothetical protein	Function unknown	2.31	1.09	Cytoplasmic
	Q8Y565	lmo2211	cpfC / HemH	Coproporphyrin III ferrochelatase (HemH)	Inorganic ion transport and metabolism; Coenzyme transport and metabolism	2.37	1.08	Cytoplasmic
	Q8Y613	lmo1889	NA	hypothetical protein	Function unknown	2.28	1.07	Cytoplasmic
	Q9RGW9	lmo2190	mecA	adaptor protein	Competence	1.32	1.07	Cytoplasmic
	P28764	lmo1439	sod	superoxide dismutase	Inorganic ion transport and metabolism; Virulence mechanisms	2.94	1.07	Cytoplasmic
	Q8Y5V2	lmo1953	pnp	purine nucleoside phosphorylase	Nucleotide transport and metabolism	2.69	1.07	Cytoplasmic
	Q8Y6B6	lmo1775	purE	phosphoribosylaminoimid azole carboxylase catalytic subunit	Nucleotide transport and metabolism	1.69	1.07	Cytoplasmic
	Q8Y9U3	lmo0427	NA	PTS fructose transporter subunit IIB	Carbohydrate transport and metabolism	2.55	1.06	Unknown
	Q8Y7P4	lmo1229	NA	hypothetical protein	Cell division/elongation; General function prediction only	1.58	1.06	Cytoplasmic
	Q92CZ4	lmo1028	NA	hypothetical protein	Function unknown	2.02	1.06	Cytoplasmic
	Q8YA46	lmo0316	thiM	hydroxyethylthiazole kinase	Coenzyme transport and metabolism	3.13	1.05	Cytoplasmic
	Q8YA56	lmo0305	NA	L-allo-threonine aldolase	Amino acid transport and metabolism	2.13	1.05	Cytoplasmic
	Q8YAN3	lmo0084	NA	oxidoreductase	Energy production and conversion; General function prediction only	1.85	1.05	Cytoplasmic

	Q8YA95	lmo0260	NA	hypothetical protein	Function unknown	1.40	1.05	Cytoplasmic
	Q8Y8L0	lmo0888	mazF	endoribonuclease that cleaves mRNA at specific sites	Transcription; RNA metabolism;	1.94	1.04	Cytoplasmic
	Q8Y6R3	lmo1621	NA	hypothetical protein	Replication, recombination and repair; General function prediction only;	2.48	1.04	Cytoplasmic
	Q8Y4S4	lmo2358	gamA	N-acetylglucosamine-6-phosphate isomerase	Cell wall metabolism	4.43	1.03	Cytoplasmic
	Q92D14	lmo1008	NA	hypothetical protein	Function unknown	2.13	1.03	Cytoplasmic
	Q8Y614	lmo1888	gpsB	Cell cycle regulator GspB	Cell division/elongation; General function prediction only	2.57	1.02	Cytoplasmic
	P60357	lmo1503	reoM	regulatoráofáMurA(A) degradation	Cell wall metabolism	1.71	1.02	Cytoplasmic
	Q8Y7I9	lmo1288	luxS	S-ribosylhomocysteinase	Signal transduction mechanisms; quorum sensing	2.01	1.01	Cytoplasmic
	Q8Y4A6	lmo2545	thrB	homoserine kinase	Amino acid transport and metabolism	2.96	0.99	Cytoplasmic
	Q8Y8K6	lmo0894	rsbW	serine-protein kinase RsbW	Signal transduction mechanisms; Posttranslational modification, protein turnover, chaperones	1.78	0.99	Cytoplasmic
	Q8Y747	lmo1465	NA	metalloprotease	Translation; General function prediction only	2.54	0.98	Cytoplasmic
	Q8Y684	lmo1813	NA	phosphoglycerate dehydrogenase	Amino acid transport and metabolism	1.37	0.98	Cytoplasmic
	Q8Y9V0	lmo0420	NA	hypothetical protein	Function unknown	2.31	0.98	Cytoplasmic
	Q8Y8Q9	lmo0836	psiE	phosphate-starvation-inducible protein PsiE	Signal transduction mechanisms	2.42	0.96	Cytoplasmic Membrane
	Q8Y748	lmo1464	NA	diacylglycerol kinase	Lipid transport and metabolism	1.85	0.96	Cytoplasmic Membrane
	Q8Y9X1	lmo0397	NA	hypothetical protein	Function unknown	1.71	0.96	Cytoplasmic
	Q8Y4H7	lmo2464	NA	transcriptional regulator	Transcription	1.46	0.96	Cytoplasmic
	Q8Y9K7	lmo0520	NA	transcriptional regulator	Transcription; Carbohydrate transport and metabolism;	1.61	0.94	Cytoplasmic
	Q8Y6P6	lmo1638	NA	hypothetical protein	Function unknown	2.26	0.94	Cytoplasmic
	Q8YA86	lmo0273	NA	hypothetical protein	Posttranslational modification, protein turnover, chaperones; General function prediction only	1.41	0.94	Cytoplasmic
	Q8Y3S3	lmo2759	NA	hypothetical protein	Function unknown	2.09	0.93	Cytoplasmic
	Q8Y5Y1	lmo1922	NA	hypothetical protein	Function unknown	2.85	0.93	Cytoplasmic
	Q8Y757	lmo1448	NA	manganese-dependent inorganic pyrophosphatase	Energy production and conversion	3.18	0.93	Cytoplasmic
	Q8Y525	lmo2252	NA	aspartate aminotransferase	Amino acid transport and metabolism	2.60	0.92	Cytoplasmic
	Q8YA72	lmo0287	walR	two-component response regulator	Transcription; Signal transduction mechanisms; Cell wall metabolism	1.96	0.92	Cytoplasmic
	Q8Y494	lmo2560	rpoE	DNA-directed RNA polymerase subunit delta	Transcription	1.66	0.91	Cytoplasmic
	Q8Y4M2	lmo2415	NA	ABC transporter ATP-binding protein	Transport and Metabolism (ABC transporter); Inorganic ion transport and metabolism	4.34	0.90	Cytoplasmic
	Q8Y5B4	lmo2153	NA	flavodoxin	Energy production and conversion	3.97	0.89	Cytoplasmic
	Q8Y9X0	lmo0398	NA	PTS sugar transporter subunit IIA	Carbohydrate transport and metabolism	2.16	0.89	Cytoplasmic
	Q8Y4E5	lmo2501	phoP	two-component response phosphate regulator	Transcription; Signal transduction mechanisms;	2.61	0.89	Cytoplasmic
	Q8Y8J0	lmo0911	NA	hypothetical protein	Function unknown	1.54	0.88	Cytoplasmic
	Q8Y6Q5	lmo1629	trpF	N-(5'-phosphoribosyl)anthranilate isomerase	Amino acid transport and metabolism	2.13	0.88	Cytoplasmic
	Q8YAD3	lmo0211	ctc	50S ribosomal protein L25	Translation	3.12	0.88	Cytoplasmic
	Q8Y5L2	lmo2046	NA	2-dehydropantoate 2-reductase	Coenzyme transport and metabolism	1.90	0.87	Cytoplasmic
	Q8YAG8	lmo0158	NA	hypothetical protein	Function unknown	3.08	0.87	Cytoplasmic
	Q8Y8Y2	lmo0760	NA	hypothetical protein	Function unknown	2.84	0.86	Cytoplasmic
	Q8Y993	lmo0640	NA	oxidoreductase	Energy production and conversion; General function prediction only	1.47	0.86	Cytoplasmic
	Q8Y6A2	lmo1793	rimM	16S rRNA-processing protein RimM	Translation; RNA metabolism	1.53	0.86	Cytoplasmic
	P0A4Q8	lmo0208	NA	hypothetical protein	Function unknown	2.28	0.86	Cytoplasmic
	P64032	lmo1355	efp	elongation factor P	Translation	1.59	0.86	Cytoplasmic

	Q8Y5R1	lmo1995	dra	deoxyribose-phosphate aldolase	Nucleotide transport and metabolism	2.28	0.86	Cytoplasmic
	P58588	lmo2473	yvcK	hypothetical protein substrate of PrkA	Cell wall metabolism/metabolism of gycerol/virulence	4.36	0.85	Cytoplasmic
	Q8Y553	lmo2223	NA	hypothetical protein	Transcription; General function prediction only	1.54	0.85	Cytoplasmic
	Q8Y3T3	lmo2748	ydaG	hypothetical protein	Function unknown	2.10	0.84	Cytoplasmic
	Q8Y7N8	lmo1236	NA	hypothetical protein	Function unknown	2.47	0.84	Cytoplasmic
	Q8Y4X7	lmo2302	NA	hypothetical protein	Function unknown; Phage	2.13	0.84	Unknown
	Q8Y5R3	lmo1993	pdp	pyrimidine-nucleoside phosphorylase	Nucleotide transport and metabolism	3.25	0.83	Cytoplasmic
	Q8Y8E8	lmo0956	nagA	N-acetylglucosamine-6P-phosphate deacetylase	Cell wall metabolism	3.71	0.83	Cytoplasmic
	Q8Y5R4	lmo1992	NA	alpha-acetolactate decarboxylase	Secondary metabolites biosynthesis, transport and catabolism	1.49	0.83	Cytoplasmic
	Q8Y716	lmo1510	NA	hypothetical protein	Function unknown	1.80	0.82	Cytoplasmic
	Q8Y8Y4	lmo0758	NA	hypothetical protein	Amino acid transport and metabolism; General function prediction only	1.54	0.82	Cytoplasmic
	Q8Y844	lmo1074	tagG	teichoic acid translocation permease TagG	Cell wall metabolism	2.28	0.79	Cytoplasmic Membrane
	Q8Y681	lmo1818	NA	ribulose-phosphate 3-epimerase	Carbohydrate transport and metabolism	2.35	0.79	Cytoplasmic
	Q8YAC7	lmo0219	NA	hypothetical protein	Translation; General function prediction only	2.94	0.79	Cytoplasmic
	Q8Y6S6	lmo1607	pheT	phenylalanyl-tRNA synthetase subunit beta	Translation	2.27	0.79	Cytoplasmic
	Q8Y458	lmo2597	rplM	50S ribosomal protein L13	Translation	1.48	0.78	Cytoplasmic
	Q8Y859	lmo1059	NA	hypothetical protein	Function unknown	2.04	0.77	Cytoplasmic
	Q8Y984	lmo0649	NA	transcriptional regulator	Transcription	1.77	0.76	Cytoplasmic
	Q8Y6S5	lmo1608	NA	hypothetical protein	Function unknown	2.43	0.76	Cytoplasmic
	P64074	lmo2455	eno	phosphopyruvate hydratase; enolase	Carbohydrate transport and metabolism	4.89	0.75	Cytoplasmic
	Q8Y5W8	lmo1937	engA/der	GTP-binding protein EngA / der	Translation	3.81	0.75	Cytoplasmic
	Q8Y739	lmo1483	comEB	competence protein ComEB	Competence	2.91	0.75	Cytoplasmic
	Q8Y5F4	lmo2110	NA	mannnose-6 phospate isomerase	Carbohydrate transport and metabolism	2.69	0.75	Cytoplasmic
	Q8Y678	lmo1821	stp / prpC	phosphoprotein phosphatase	Signal transduction mechanisms; Posttranslational modification, protein turnover, chaperones; Virulence mechanisms	2.04	0.75	Cytoplasmic
	Q8Y4N7	lmo2398	ltrC	low temperature requirement protein C	Signal transduction mechanisms	2.91	0.75	Cytoplasmic
	Q927Y2	lmo2511	hpf	hibernation promoting factor	Translation	1.56	0.73	Cytoplasmic
	Q8Y741	lmo1481	holA	DNA polymerase III subunit delta	Replication, recombination and repair	2.46	0.72	Cytoplasmic
	Q8Y9N8	lmo0487	NA	hypothetical protein	Nucleotide transport and metabolism; General function prediction only	1.71	0.72	Cytoplasmic
	Q8Y9E9	lmo0580	NA	hypothetical protein	Lipid transport and metabolism; General function prediction only	2.66	0.71	Cytoplasmic
	Q8Y6Q7	lmo1627	trpA	tryptophan synthase subunit alpha	Amino acid transport and metabolism	2.42	0.71	Cytoplasmic
	Q8Y6S9	lmo1604	NA	2-cys peroxiredoxin	Posttranslational modification, protein turnover, chaperones	2.77	0.71	Cytoplasmic
	Q8Y719	lmo1507	NA	response regulator	Transcription; Signal transduction mechanisms	3.53	0.71	Cytoplasmic
	Q8Y405	lmo2673	NA	hypothetical protein	Signal transduction mechanisms; General function prediction only	1.45	0.71	Cytoplasmic
	Q8Y714	lmo1512	mnmA	tRNA-specific 2-thiouridylase	Translation; RNA metabolism	2.74	0.70	Cytoplasmic
	Q8Y520	lmo2258	NA	hypothetical protein	Function unknown	1.88	0.70	Cytoplasmic
	Q8Y5L0	lmo2049	NA	hypothetical protein	Function unknown	2.08	0.69	Cytoplasmic
	Q8Y6V2	lmo1579	NA	alanine dehydrogenase	Amino acid transport and metabolism	2.86	0.69	Cytoplasmic
	Q8Y483	lmo2572	NA	dihydrofolate reductase subunit A	Coenzyme transport and metabolism	2.50	0.69	Cytoplasmic

	Q8Y3Y1	lmo2698	NA	RpiR family transcriptional regulator	Transcription	1.52	0.69	Cytoplasmic
	Q8Y7H7	lmo1302	NA	LexA family transcriptional regulator	Transcription; Signal transduction mechanisms;	1.51	0.69	Cytoplasmic
	Q8Y9D5	lmo0595	NA	O-acetylhomoserine sulfhydrylase	Amino acid transport and metabolism	1.90	0.69	Cytoplasmic
	P0A438	lmo1002	ptsH	phosphocarrier protein HPr	Carbohydrate transport and metabolism	1.56	0.69	Cytoplasmic
	Q929B9	lmo2256	NA	hypothetical protein	Function unknown	1.98	0.68	Cytoplasmic
	Q8YAL8	lmo0100	NA	hypothetical protein	Function unknown	1.78	0.68	Cytoplasmic
	Q8Y568	lmo2208	NA	hypothetical protein	Function unknown	2.21	0.68	Cytoplasmic
	Q8Y3V1	lmo2730	NA	phosphatase	Carbohydrate transport and metabolism	1.31	0.68	Cytoplasmic
	Q8Y5Q9	lmo1997	NA	PTS mannose transporter subunit IIA	Carbohydrate transport and metabolism	1.91	0.68	Cytoplasmic
	Q8Y831	lmo1087	NA	glucitol dehydrogenase	Amino acid transport and metabolism; General function prediction only;	1.94	0.68	Cytoplasmic
	Q8Y3L0	lmo2825	serC	phosphoserine aminotransferase	Amino acid transport and metabolism; Coenzyme transport and metabolism;	3.10	0.67	Cytoplasmic
	Q8Y3Y4	lmo2695	NA	dihydroxyacetone kinase subunit DhaK	Carbohydrate transport and metabolism	2.11	0.67	Cytoplasmic
	Q8Y669	lmo1830	NA	short-chain dehydrogenase	Lipid transport and metabolism; Secondary metabolites biosynthesis, transport and catabolism; General function prediction only;	2.19	0.67	Unknown
	Q8YAM2	lmo0096	manL/mptA	PTS mannose transporter subunit IIAB	Carbohydrate transport and metabolism	3.89	0.66	Cytoplasmic
	Q8Y3Y9	lmo2690	NA	TetR family transcriptional regulator	Transcription	2.13	0.66	Cytoplasmic
	Q8Y4Q8	lmo2376	NA	peptidyl-prolyl cis-trans isomerase	Posttranslational modification, protein turnover, chaperones	2.42	0.66	Cytoplasmic
	Q8YAB3	lmo0237	gltX	glutamyl-tRNA synthetase	Translation	3.73	0.66	Cytoplasmic
	Q8Y729	lmo1494	mtnN	5'-methylthioadenosine/S-adenosylhomocysteine nucleosidase	Nucleotide transport and metabolism	3.21	0.66	Cytoplasmic
	Q8Y3Y7	lmo2692	NA	hypothetical protein	Function unknown	1.55	0.65	Cytoplasmic
	Q8Y640	lmo1860	msrA	methionine sulfoxide reductase A	Posttranslational modification, protein turnover, chaperones	2.12	0.64	Cytoplasmic
	Q8Y8F2	lmo0952	NA	hypothetical protein	Function unknown	3.63	0.64	Cytoplasmic Membrane
	Q8Y4I4	lmo2456	pgm	phosphoglyceromutase	Carbohydrate transport and metabolism	2.25	0.64	Cytoplasmic
	Q8Y3Y6	lmo2693	tmk	thymidylate kinase	Nucleotide transport and metabolism	1.44	0.64	Cytoplasmic
	Q8Y491	lmo2564	NA	4-oxalocrotonate isomerase	Lipid transport and metabolism	1.63	0.64	Cytoplasmic
	Q92CE7	lmo1257	NA	hypothetical protein	Function unknown	1.81	0.63	Cytoplasmic
	Q8Y4P9	lmo2386	yuiD	hypothetical protein	Function unknown	2.28	0.63	Cytoplasmic Membrane
	Q8Y7E7	lmo1336	NA	5-formyltetrahydrofolate cyclo-ligase	Coenzyme transport and metabolism	1.37	0.63	Cytoplasmic
	Q8Y5M2	lmo2035	murG	UDP-diphospho-muramoyl pentapeptide beta-N-acetylglucosaminyl transferase	Cell wall metabolism	2.87	0.63	Cytoplasmic
	Q8Y8G1	lmo0943	fri	non-heme iron-binding ferritin	Inorganic ion transport and metabolism; Virulence mechanisms	3.63	0.62	Cytoplasmic
	Q8YAA2	lmo0252	NA	penicilinase repressor	Transcription; Antibiotic/Drug transport and metabolism	1.65	0.61	Cytoplasmic
	P67195	lmo1457	NA	hypothetical protein	Function unknown	2.39	0.61	Cytoplasmic
	Q8Y7C9	lmo1354	NA	aminopeptidase P	Amino acid transport and metabolism	2.57	0.61	Cytoplasmic
	P58724	lmo0799	NA	hypothetical protein	Signal transduction mechanisms; General function prediction only	2.21	0.61	Cytoplasmic
	Q8Y3K5	lmo2830	NA	thioredoxin	Energy production and conversion	1.59	0.61	Cytoplasmic
	Q8Y864	lmo1053	PdhB	pyruvate dehydrogenase subunit E1 beta	Energy production and conversion	3.14	0.61	Cytoplasmic

	Q8YAT8	lmo0025	NA	phosphoheptose isomerase	Carbohydrate transport and metabolism; General function prediction only	1.73	0.61	Cytoplasmic
	Q8Y5L6	lmo2042	mraZ	transcription regulator MraZ - cell division protein MraZ	Cell division/elongation; Transcription; Antitoxin	2.79	0.60	Cytoplasmic
	Q8Y5F1	lmo2113	NA	heme peroxidase	Inorganic ion transport and metabolism	3.30	0.60	Cytoplasmic
	Q8YA85	lmo0274	NA	hypothetical protein	Function unknown	1.45	0.60	Cytoplasmic
	Q8Y3M0	lmo2815	fabG	3-ketoacyl-ACP reductase	Lipid transport and metabolism; Secondary metabolites biosynthesis, transport and catabolism; General function prediction only;	2.08	0.60	Cytoplasmic
	Q8Y6H9	lmo1705	NA	deoxyguanosine kinase/deoxyadenosine kinase	Nucleotide transport and metabolism	1.71	0.60	Cytoplasmic
	Q8Y7Q5	lmo1217	NA	endo-1,4-beta-glucanase and to aminopeptidase	Carbohydrate transport and metabolism	2.26	0.60	Cytoplasmic
	Q8Y8V8	lmo0784	mpoA	PTS mannose transporter subunit IIB	Carbohydrate transport and metabolism	1.38	0.59	Cytoplasmic
DOWN	Q9RLT9	lmo0258	rpoB	DNA-directed RNA polymerase subunit beta	Transcription	2.56	-0.59	Cytoplasmic
	Q8Y795	lmo1395	NA	hypothetical protein	Transcription; General function prediction only	2.68	-0.60	Unknwon
	Q8Y7P0	lmo1234	uvrC	excinuclease ABC subunit C	Replication, recombination and repair	3.24	-0.61	Cytoplasmic
	Q8Y9K8	lmo0519	mdrA	multidrug resistance protein	Antibiotic/Drug transport and metabolism	2.50	-0.61	Cytoplasmic Membrane
	Q8Y523	lmo2254	NA	hypothetical protein	Nucleotide transport and metabolism; General function prediction only	1.81	-0.62	Cytoplasmic Membrane
	Q8Y7F6	lmo1325	infB	translation initiation factor IF-2	Translation	2.90	-0.64	Cytoplasmic
	Q7AP54	lmo2185	hbp2	Hemoglobin binding protein 2, Hbp2	Inorganic ion transport and metabolism; Virulence mechanisms	1.47	-0.64	Cell Wall - 15924120 - SasE
	Q8YAC6	lmo0220	ftsH	cell division protein FtsH	Cell division/elongation	3.26	-0.64	Cytoplasmic Membrane
	Q8Y481	lmo2574	NA	hypothetical protein	Function unknown	2.17	-0.65	Cytoplasmic Membrane
	Q8Y4J0	lmo2449	NA	exoribonuclease RNase-R	Transcription; RNA metabolism;	2.89	-0.65	Cytoplasmic
	Q8Y7I6	lmo1291	oatA	acyltransferase	Cell wall metabolism; Lipid transport and metabolism; Virulence mechanisms	1.62	-0.67	Cytoplasmic Membrane
	Q8Y413	lmo2664	NA	sorbitol dehydrogenase	Carbohydrate transport and metabolism	3.96	-0.67	Cytoplasmic
	Q8Y510	lmo2268	addB	ATP-dependent deoxyribonuclease subunit B	Replication, recombination and repair	1.67	-0.67	Cytoplasmic
	Q8Y789	lmo1403	mutS	DNA mismatch repair protein MutS	Replication, recombination and repair	1.59	-0.67	Cytoplasmic
	Q8YAV6	lmo0007	gyrA	DNA gyrase subunit A	Replication, recombination and repair	2.46	-0.67	Cytoplasmic
	Q8Y6S7	lmo1606	NA	DNA translocase	Cell division/elongation	1.53	-0.68	Cytoplasmic
	Q8Y6G0	lmo1727	NA	LacI family transcriptional regulator	Transcription	1.76	-0.68	Cytoplasmic
	Q8Y6N9	lmo1645	NA	ATP-dependent dsDNA exonuclease SbcC	Replication, recombination and repair	2.46	-0.69	Cytoplasmic
	Q8Y983	lmo0650	NA	hypothetical protein	Function unknown; phage	2.71	-0.70	Cytoplasmic Membrane
	Q8Y3S4	lmo2757	NA	ATP-dependent DNA helicase	Replication, recombination and repair	1.92	-0.71	Cytoplasmic
	Q929L4	lmo2158	NA	hypothetical protein	Function unknown	1.38	-0.71	Cytoplasmic
	Q8YA74	lmo0285	NA	lipoprotein	Amino acid transport and metabolism; Lipoprotein	2.90	-0.72	Lipoprotein
	Q8YAD6	lmo0195	NA	ABC transporter permease	Transport and Metabolism (ABC transporter)	2.42	-0.73	Cytoplasmic Membrane
	Q8Y9I7	lmo0541	NA	ABC transporter substrate-binding protein/putative ABC-type Fe3+-hydroxamate transport system	Transport and Metabolism (ABC transporter); Lipoprotein	2.08	-0.74	Lipoprotein

	Q8Y665	lmo1835	carB	carbamoyl-phosphate synthetase	Nucleotide transport and metabolism;	1.59	-0.74	Cytoplasmic
	Q8Y769	lmo1432	NA	hypothetical protein	Function unknown	2.16	-0.75	Unknown
	Q8Y6E1	lmo1746	NA	ABC transporter permease	Transport and Metabolism (ABC transporter)	2.05	-0.77	Cytoplasmic Membrane
	Q8Y7P7	lmo1226	NA	transporter	Transport; Function unknown;	3.39	-0.78	Cytoplasmic Membrane
	Q8Y7A3	lmo1386	NA	DNA translocase	Cell division/elongation	2.49	-0.79	Cytoplasmic Membrane
	Q8YAJ0	lmo0135	ctaP	cysteine transport associated protein	Amino acid transport and metabolism; Transport and Metabolism (ABC transporter); Lipoprotein	4.08	-0.79	Cell Wall - 7531266 - dppE , Lipoprotein
	Q8Y707	lmo1521	NA	autolysin; N-acetylmuramoyl-L-alanine amidase	Cell wall metabolism	5.23	-0.80	Cell Wall - 400208 - cwlB
	Q8YA67	lmo0292	htrA	heat-shock protein htrA serine protease	Posttranslational modification, protein turnover, chaperones	1.76	-0.82	Unknown
	Q8Y7G5	lmo1316	cdsA	phosphatidate cytidylyltransferase	Lipid transport and metabolism	2.05	-0.86	Cytoplasmic Membrane
	Q929P4	lmo2125	NA	sugar ABC transporter substrate-binding protein	Carbohydrate transport and metabolism; Transport and Metabolism (ABC transporter); Lipoprotein	2.54	-0.87	Lipoprotein
	Q8Y4M0	lmo2417	NA	ABC transporter substrate-binding protein	Transport and Metabolism (ABC transporter); Amino acid transport and metabolism; Lipoprotein	3.44	-0.88	Lipoprotein
	Q8YAR7	lmo0047	NA	hypothetical protein	Lipoprotein; Function unknown	2.86	-0.88	Lipoprotein
	Q8Y4D9	lmo2508	NA	hypothetical protein	Function unknown	1.53	-0.90	Cytoplasmic Membrane
	Q8Y9T0	lmo0443	psr	repressor; LytR family transcriptional regulator	Transcription	3.75	-0.91	Cytoplasmic Membrane
	Q8Y799	lmo1391	NA	sugar ABC transporter permease	Carbohydrate transport and metabolism; Transport and Metabolism (ABC transporter)	2.00	-0.92	Cytoplasmic Membrane
	Q8Y6A4	lmo1791	NA	hypothetical protein	Function unknown	3.62	-0.92	Cytoplasmic
	Q8Y610	lmo1892	pbpA1	penicillin-binding protein A1; PBP1	Cell wall metabolism	4.86	-0.94	Cytoplasmic Membrane
	Q92EN6	lmo0399	NA	PTS fructose transporter subunit IIB	Carbohydrate transport and metabolism	1.34	-0.95	Cytoplasmic
	Q8YAE9	lmo0181	NA	sugar cycloalternan ABC transporter substrate-binding protein	Carbohydrate transport and metabolism; Transport and Metabolism (ABC transporter); Lipoprotein	2.69	-0.97	Lipoprotein
	Q8Y528	lmo2249	NA	low-affinity inorganic phosphate transporter	Inorganic ion transport and metabolism	1.40	-0.98	Cytoplasmic Membrane
	Q8Y9X4	lmo0394	NA	?-d-Glutamyl-l-m-Dpm peptidase; P60-like protein; autolysin	Cell wall metabolism	1.69	-1.02	Extracellular
	P0A355	lmo1364	cspL	cold-shock protein	Signal transduction mechanisms	1.94	-1.08	Cytoplasmic
	Q8Y5E3	lmo2121	NA	maltose phosphorylase	Carbohydrate transport and metabolism	1.52	-1.09	Cytoplasmic
	Q8Y6D1	lmo1757	NA	hypothetical protein	Function unknown; Lipoprotein	3.91	-1.11	Lipoprotein
	Q8Y5J8	lmo2062	NA	copper transporter	Inorganic ion transport and metabolism	1.68	-1.13	Cytoplasmic Membrane
	Q8Y5E9	lmo2115	anrB	ABC transporter permease / FtsX family associated with nisin resistance	Transport and Metabolism (ABC transporter); Antibiotic/Drug transport and metabolism	3.45	-1.15	Cytoplasmic Membrane
	Q8Y605	lmo1898	NA	hypothetical protein	Function unknown	4.56	-1.16	Cytoplasmic
	Q8Y6L8	lmo1666	lapB	pepdidoglycan bound protein; LPXTG protein	Cell wall protein	1.67	-1.17	Cell Wall - LPXTG
	Q8Y850	lmo1068	NA	hypothetical protein	Lipoprotein; Function unknown	5.83	-1.18	Lipoprotein
	Q8YAU8	lmo0015	qoxC	AA3-600 quinol oxidase subunit III	Energy production and conversion	1.45	-1.29	Cytoplasmic Membrane
	Q8Y4K7	lmo2431	hupD	ferrichrome ABC transporter substrate-binding protein	Inorganic ion transport and metabolism; Transport and Metabolism (ABC transporter); Lipoprotein	4.44	-1.30	Lipoprotein
	Q927C4	lmo2717	cydB	cytochrome D ubiquinol oxidase subunit II	Energy production and conversion	4.29	-1.30	Cytoplasmic Membrane
	Q8Y9N9	lmo0486	rpmF	50S ribosomal protein L32	Translation	1.96	-1.37	Cytoplasmic

	Q8Y4L1	lmo2426	NA	hypothetical protein	Inorganic ion transport and metabolism; General function prediction only	2.27	-1.44	Cytoplasmic
	Q8Y7P9	lmo1224	NA	hypothetical protein	Transport and Metabolism (ABC transporter); General function prediction only	3.94	-1.46	Cytoplasmic Membrane
	Q8Y5L8	lmo2039	pbpB2	penicillin-binding protein B2; PBP2	Cell wall metabolism	2.04	-1.47	Cytoplasmic Membrane
	Q8Y842	lmo1076	aut	autolysin; N-acetylglucosaminidase	Cell wall metabolism; Virulence mechanisms	5.91	-1.54	Extracellular
	P0DQD2	lmo0434	inlB	internalin B; class II	Cell wall protein; Virulence mechanisms	7.57	-1.54	Cell Wall - 487052 - inlA
	Q8Y649	lmo1851	NA	carboxy-terminal processing proteinase	Amino acid transport and metabolism	4.78	-1.63	Cytoplasmic Membrane
	Q8Y5I3	lmo2079	NA	hypothetical protein	Lipoprotein; Function unknown	2.70	-1.64	Lipoprotein
	Q8Y436	lmo2637	pplA	peptide pheromone-encoding lipoprotein A	Lipoprotein; Virulence mechanisms	5.79	-1.90	Lipoprotein
	Q8Y496	lmo2558	ami	autolysin; N-acetylmuramoyl-L-alanin e amidase	Cell wall metabolism; Virulence mechanisms	6.29	-1.98	Extracellular
	P21171	lmo0582	iap	invasion associated secreted endopeptidase p60; ?-d-Glutamyl-l-m-Dpm peptidase; autolysin	Cell wall metabolism; Virulence mechanisms	5.65	-2.04	Extracellular
	Q8Y4J9	lmo2439	NA	hypothetical protein	Function unknown	3.30	-2.12	Unknown
	Q7AP49	lmo2505	spl	autolysin; peptidoglycan lytic protein P45	Cell wall metabolism	2.33	-2.15	Extracellular
	Q8Y7J3	lmo1284	NA	hypothetical protein	Lipid transport and metabolism; General function prediction only	1.32	-2.16	Cytoplasmic Membrane
	Q8Y3Y8	lmo2691	murA / NamA	autolysin; N-acetylglucosaminidase	Cell wall metabolism	7.27	-2.18	Extracellular
	Q8YA01	lmo0366	fepA	Putative lipoprotein involved in iron transport (FepA)	Inorganic ion transport and metabolism; Lipoprotein	4.86	-2.34	Lipoprotein
	P34024	lmo0201	plcA	phosphatidylinositol-specif ic phospholipase c	Lipid transport and metabolism; Virulence mechanisms	5.36	-2.34	Unknown
	Q8Y5B1	lmo2156	NA	hypothetical protein	Function unknown	3.18	-2.41	Extracellular
	P13128	lmo0202	hly	listeriolysin O precursor	Secreted protein; Virulence mechanisms	5.90	-2.49	Unknown
	Q8YA11	lmo0355	NA	fumarate reductase subunit A	Carbohydrate transport and metabolism; Lipoprotein	6.23	-2.64	Lipoprotein
	Q8Y9P7	lmo0477	NA	secreted protein	Secreted protein; Function unknown	4.82	-2.79	Unknown
	Q8Y8F4	lmo0950	NA	hypothetical protein	Cell wall metabolism; General function prediction only	2.71	-2.93	Cytoplasmic Membrane
	Q8YA02	lmo0365	fepC	Putative FTR1 family high-affinity Fe2+/Pb2+ permease (FepC)	Inorganic ion transport and metabolism	4.18	-2.96	Cytoplasmic
	Q8Y9V5	lmo0415	pgdA	peptidoglycan N-deacetylase	Cell wall metabolism; Virulence mechanisms	7.48	-3.18	Cytoplasmic Membrane
	Q8Y889	lmo1026	NA	LytR protein	Transcription	4.53	-3.30	Cytoplasmic Membrane
	Q8Y763	lmo1438	pbpB1	penicillin-binding protein B1; PBP3	Cell wall metabolism	7.07	-3.46	Cytoplasmic
	Q8Y645	lmo1855	NA	D-alanyl-D-alanine carboxypeptidase	Cell wall metabolism	7.21	-3.53	Cytoplasmic
	Q8Y5W4	lmo1941	NA	hypothetical protein	Function unknown	1.92	-4.00	Cytoplasmic Membrane
	Q8Y638	lmo1862	NA	hypothetical protein	Lipid transport and metabolism; General function prediction only	3.07	-4.03	Cytoplasmic Membrane
	Q8Y4S2	lmo2360	NA	transmembrane protein	Function unknown	1.99	-4.98	Cytoplasmic Membrane
	Q8Y4D2	lmo2518	TagTUV	Wall teichoic acid ligase	Cell wall metabolism	4.60	-6.86	Cytoplasmic Membrane

3.2 Functional Analysis highlights key adaptations linked to VBNC entry and cell wall modifications

3.2.1 Subcellular localisation of variable proteins reveals cell wall proteins downregulation

The subcellular localization analysis of differentially regulated proteins across the nutrient-deprivation timeline (D7, D14, and D28) offers insights into the adaptive responses of *L. monocytogenes* under prolonged stress (Figure 37). More specifically, the analysis also categorised proteins based on their subcellular localization, as predicted by SignalP v5 and TOPCONS (described in chapter 1). Most upregulated proteins are localised in the cytoplasm, which aligns with their roles in essential cellular processes such as translation and metabolism. On the other hand, downregulated proteins, particularly those involved in virulence and cell wall metabolism, are primarily associated with the cell membrane or extracellular space. This pattern underscores the gradual adaptation of bacteria to a dormant state, where cytoplasmic functions necessary for minimal survival are preserved, while membrane-associated processes that are energetically costly or related to active growth and infection are downregulated throughout the 28-day time course.

At D7, most of the upregulated proteins were cytoplasmic, with only a few integral membrane proteins (Figure 37). Notably, LLO, an extracellular virulence factor, was downregulated as early as D7 and until the end of the time course. The loss of virulence has been observed in other foodborne and pathogenic bacteria and is believed to be an adaptation mechanism to the harsh conditions (Li et al., 2014; Zhao et al., 2017). This early and constant downregulation of LLO could reflect a shift by *L. monocytogenes* to conserve energy in response to nutrient scarcity, prioritizing survival over virulence. This suggests that even in the early stages of nutrient starvation, *L. monocytogenes* may prioritise survival mechanisms over maintaining its full virulence potential. However, what is worth of noting is the ability of *L. monocytogenes* to revert into its fully virulent potential upon infection in chicken embryonated eggs, yet the exact molecular mechanisms are to be elucidated (Cappelier et al., 2007; Carvalho et al., 2024).

By D14, the range of proteins involved in the downregulation expanded significantly. The first lipoproteins and cell wall proteins were detected at this time point, alongside other proteins across various localizations (Figure 37). This increase in identified protein localizations might suggest further bacterial adaptation during the transition into VBNC. The identification of lipoproteins and cell wall proteins downregulation could indicate that the bacteria modify their surface structures to

conserve resources. More specifically, the cell wall (CW) is considered as an energy source such as sugars, for example (Claeesen and Errington, 2019). The downregulation of the CW could thus suggest a bacterial adaptation to the nutrient limitation and therefore a bacterial mechanism to sustain themselves not only during their transition in VBNC but also during their duration in it, until the conditions for resuscitation are favourable again (Claessen and Errington, 2019; Carvalho et al., 2024). Overall, CWD has been described as a bacterial adaptation to stressful conditions that seems to allow bacteria to proliferate even without a cell wall (Claessen and Errington, 2019). Therefore, our data could suggest that *L. monocytogenes* is remodeling its cell envelope moving towards a CWD form to optimise energy storage.

Similarly, at D28, a notable but expected observation is the continuous reduction of cell wall proteins (Figure 37). This significant decrease aligns with the previous observations suggesting that CWD may be a bacterial strategy to cope with extreme stress (Claessen and Errington, 2019). The recent work by Carvalho and colleagues (Carvalho et al., 2024) on *L. monocytogenes* has documented the loss of cell wall structure as a part of the physiological and morphological modifications during *L. monocytogenes*' transition into the VBNC. Such adaptations might suggest that *L. monocytogenes* strategically minimizes structural components to conserve resources and enhance long-term survival, which may contribute to establishing persistence under harsh conditions (Claessen and Errington, 2019). Functional analyses of these variable proteins could provide further insight into the biological significance of this adaptive response and its implications for bacterial persistence in hostile environments.

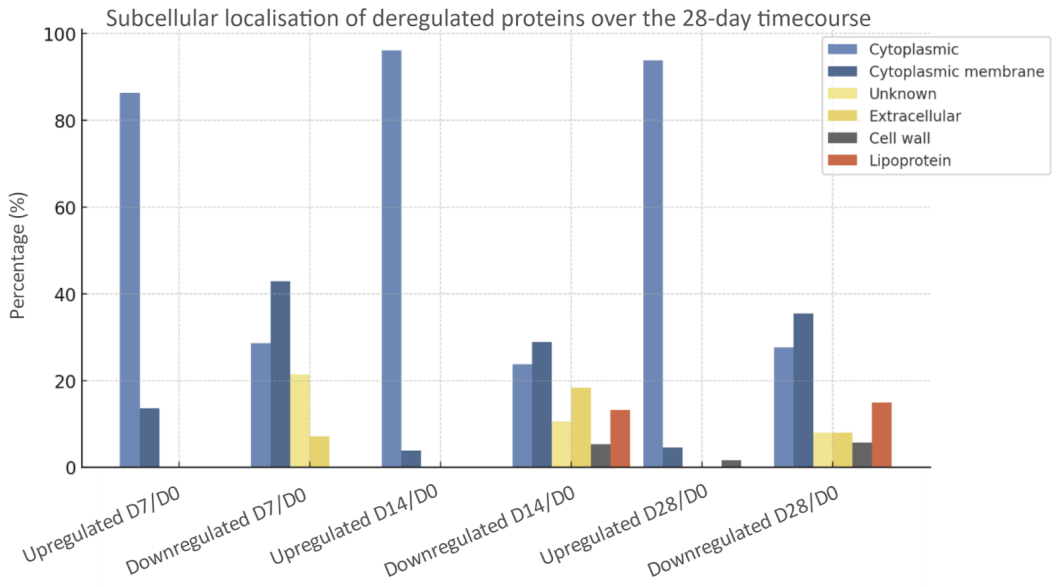

Figure 37: Bar chart illustrating the subcellular localization of deregulated proteins in *L. monocytogenes* at timepoints D7/D0, D14/D0, and D28/D0, marking its progression into the VBNC state. Subcellular localizations were determined using SignalP v.5 and TOPCONS, categorizing proteins as cytoplasmic, cytoplasmic membrane (integral membrane proteins), extracellular, lipoproteins, cell wall-associated or unknown.

3.2.2 Functional Analysis

A comparative functional analysis was performed between the initial time point (D0) and subsequent days (D7, D14, and D28) to track temporal changes in *L. monocytogenes* during its transition into VBNC state under nutrient starvation (Figure 38). At the beginning of the time course, D7, various biological functions were upregulated, particularly those related to translation, signal transduction, transport and metabolism pathways of many molecules (carbohydrates, amino acids, lipids, nucleotides) and cell wall metabolism as well. The downregulated processes mainly included ABC transporters, secondary metabolites and both cell wall metabolism and virulence. Towards the D14 and already within 1-week time there is an increased upregulation on functions associated to all transport and metabolism pathways described at D7, whereas a stronger downregulation of CW metabolism and virulence is observed. By the end of the time course, at D28, there is a similar- but stronger- to D14 pattern, with more downregulated rather than upregulated proteins involved in the CW metabolism.

The continuous upregulation of proteins involved in metabolic functions could suggest that *L. monocytogenes* utilises multiple nutrient acquisition-related mechanisms when in nutrient-limited

conditions, to scavenge nutrients from the external environment as it adapts to nutrient-deprived, stressful conditions (Claessen and Errington, 2019; Carvalho et al., 2024). Several proteins show consistent upregulation over time, particularly those involved in translation, explaining the several upregulated ribosomal proteins, such as Lmo0244 (50S ribosomal protein L33 type II) and Lmo2047 (50S ribosomal protein L32) in our dataset. An ongoing need for protein synthesis, despite the cells entering a VBNC state, could be therefore suggested, probably indicating that the bacteria maintain a baseline level of translation machinery to ensure the production of essential proteins under stress. Hypothetical proteins, such as Lmo0525 and Lmo2158, are also among the upregulated proteins. Although their exact functions remain unknown, their consistent upregulation implies potential roles in stress adaptation or survival in the VBNC state. The upregulation of Lmo2713, a GW domain-containing protein involved in cell wall integrity, might suggest an increased demand for maintaining cell structure and defence mechanisms as nutrient depletion becomes more severe. Additionally, signal transduction functions were increasingly upregulated throughout the time course, likely facilitating the regulation of metabolic shifts and stress responses (Ulrich et al., 2005). Upregulation in transcription, translation, and post-translational modifications may also be linked to these adaptive changes.

At the same time, transport and metabolism pathways were also downregulated, particularly at later time points, indicating a progressive reduction in metabolic activity as *L. monocytogenes* transitions into VBNC state (Figure 38). However, what was standing out is the downregulation of several proteins associated with virulence and cell wall metabolism. For instance, Lmo0202 (LLO), a key virulence factor in *L. monocytogenes*, shows significant downregulation, as described before. This reduction in virulence-associated proteins likely reflects the bacterium's shift from an active pathogenic state to a dormant state, conserving energy by shutting down non-essential functions such as virulence. Proteins involved in lipid transport and metabolism, such as Lmo0950 (hypothetical) and Lmo1862 (hypothetical), are also downregulated, indicating a slowdown in lipid biosynthesis and membrane modification processes. This may be part of a strategy to minimise energy expenditure. Similarly, the downregulation of cell wall-associated proteins (e.g., Lmo2518 - wall teichoic acid ligase) suggests that *L. monocytogenes* has probably started undergoing morphological adaptations such as cell wall shedding. Simultaneously, a significant downregulation of other functions; replication, recombination, repair, cell wall metabolism, virulence, and antibiotic/drug transport became more pronounced after D14 (Figure 38). This is expected, given that *L. monocytogenes* is transitioning into dormancy (Aryapetyan et al., 2018; Lotoux et al., 2022). It

has been observed that VBNC bacteria not only reduce their virulent potential, as seen in *Vibrio* species, but also exhibit decreased cell wall metabolism. This reduction in cell wall metabolism has been linked to the formation of cell wall-deficient forms in many pathogen species such as *B. subtilis*, *L. monocytogenes*, and other non-pathogenic *Listeria* specie, as well (Baker et al., 1983; Dominguez-Cuevas et al., 2012; Carvalho et al., 2024).

Overall, many of the functions seem to be the same between upregulated and downregulated but with different numbers and proteins involved in each case (Figure 38, Tables 15-17). This phenotype could be explained by the fact that bacteria cells might be in different transitional states due to the different culturable states (Carvalho et al., 2024). More specifically, the downregulated functions could indicate the transition of *L. monocytogenes* from culturable into the VBNC state, whereas the processes involved with upregulation might reflect the bacterial adaptation mechanisms under harsh environmental conditions including nutrient scarcity (Carvalho et al., 2024).

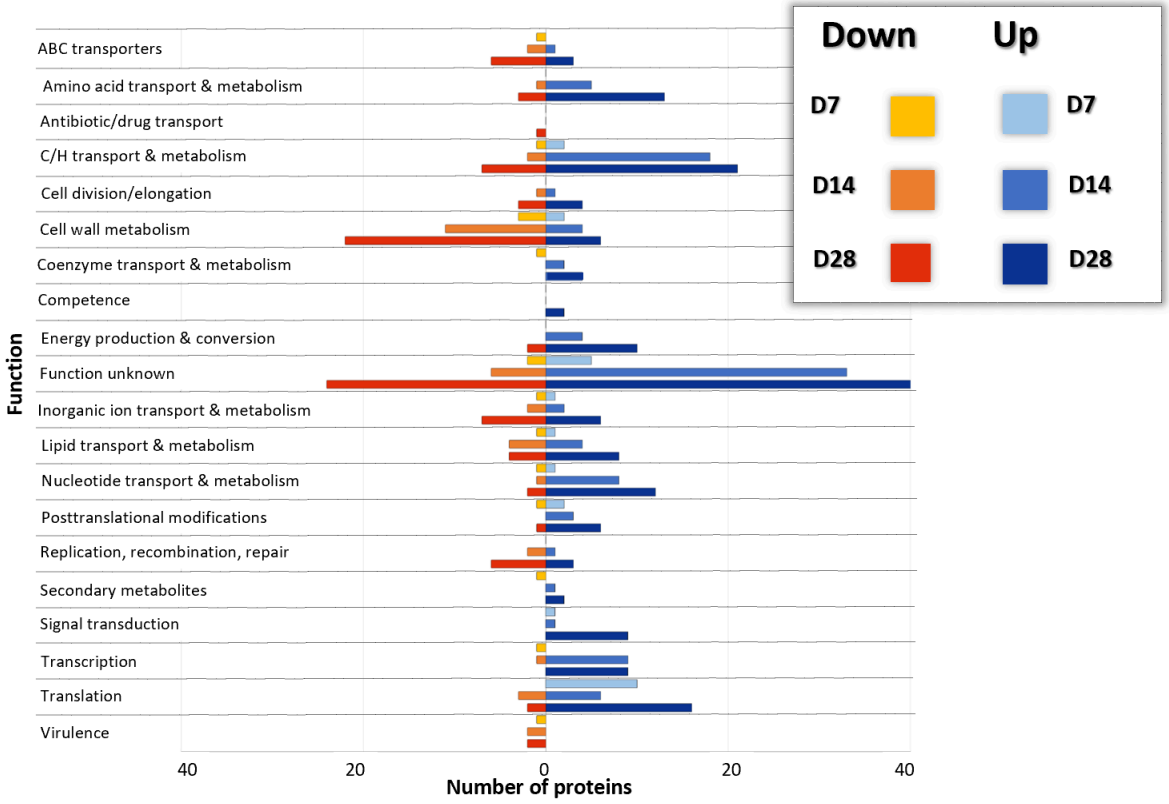

Figure 38: Functional analysis of significantly variable proteins identified over the 28-day time course (D7, D14, D28). The x-axis represents the number of deregulated proteins, while the y-axis corresponds to their associated functions.

3.3 A subset of proteins maintain their up- or downregulation trend over the complete time course

While many proteins showed variable expression, with significant changes emerging after the second week, D14, and continuing until D28, a few proteins exhibited a stable trend in their regulation as early as D7 (Figure 39, Table 18). These consistently upregulated or downregulated proteins might suggest an early and sustained adaptation response by *L. monocytogenes* to the nutrient-deprived environment, underscoring their potential importance in the bacterium's long-term survival strategy.

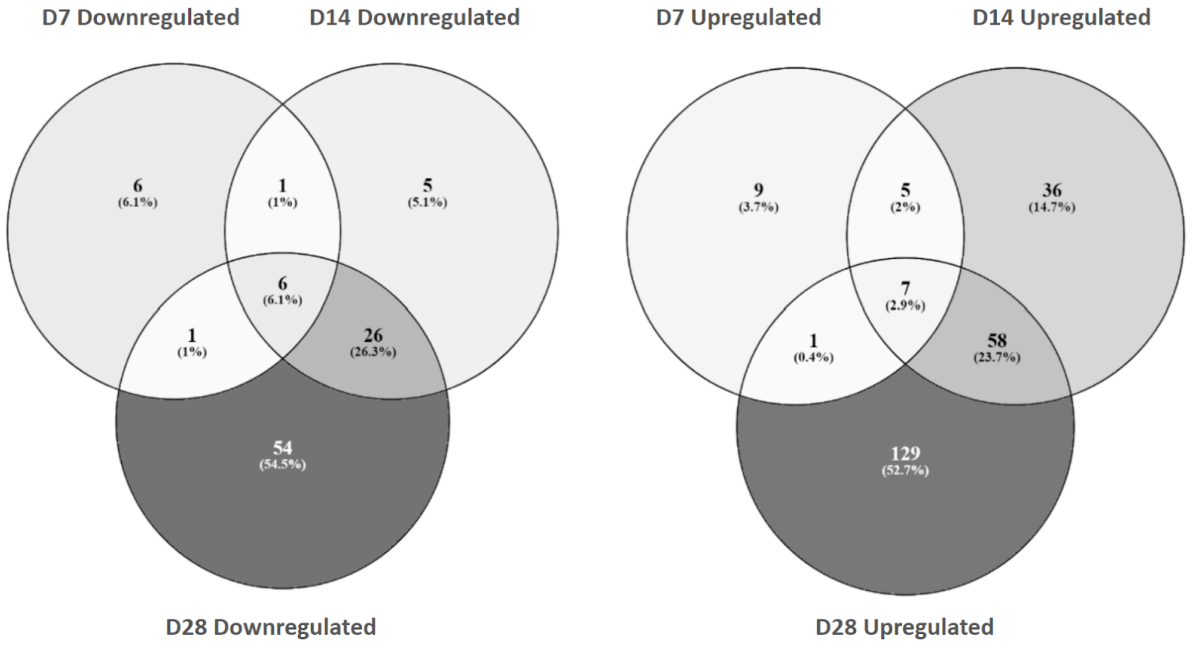

Figure 39: Venn diagrams showing the number of shared variable proteins; upregulated (left) and downregulated (right), over the 28-day time course (D7, D14, D28).

Table 18: Variable proteins maintaining up- or down- regulation effect during the 28-day time course. Fold change (FC) and p-value based on the statistical analysis (t-test) with Perseus.

	Accession Number	Locustag	Name	Product	Functional Category/COG	-Log(P-value) D7/D0	FC Log2(D7/D0)	-Log(P-value) D14/D0	FC Log2(D14/D0)	-Log(P-value) D28/D0	FC Log2(D28/D0)	Localisation
UP	Q8Y9K2	lmo0525	NA	hypothetical protein	Function unknown	2.36	3.24	2.89	3.72	2.13	3.04	Cytoplasmic
	Q8Y702	lmo1528	NA	hypothetical protein	Function unknown	1.30	1.15	1.89	1.68	1.60	1.66	Cytoplasmic
	Q927H3	lmo2666	NA	PTS galacticol transporter subunit IIB	Carbohydrate transport and metabolism	2.06	0.98	3.07	1.22	1.91	1.61	Cytoplasmic
	Q8Y9E9	lmo0580	NA	hypothetical protein	Lipid transport and metabolism; General function prediction only	1.73	0.86	2.18	0.77	2.66	0.71	Cytoplasmic
	Q8Y8Q9	lmo0836	psiE	phosphate-starvation-inducible protein PsiE	Signal transduction mechanisms	1.72	0.78	-	-	2.42	0.96	Cytoplasmic Membrane
	P64032	lmo1355	efp	elongation factor P	Translation	1.42	0.77	1.87	1.00	1.59	0.86	Cytoplasmic
	Q8Y9U3	lmo0427	NA	PTS fructose transporter subunit IIB	Carbohydrate transport and metabolism	1.48	0.72	3.03	1.26	2.55	1.06	Cytoplasmic
	Q8Y7N5	lmo1239	NA	nucleoside-triphosphatase	Nucleotide transport and metabolism	2.27	0.67	2.47	0.83	3.38	1.42	Cytoplasmic
DOWN	P13128	lmo0202	hly	listeriolysin O precursor	Secreted protein; Virulence mechanisms	3.87	-0.76	4.67	-1.17	5.90	-2.49	Extracellular
	Q8Y5E3	lmo2121	NA	maltose phosphorylase	Carbohydrate transport and metabolism	2.78	-0.89	1.51	-0.91	1.52	-1.09	Cytoplasmic
	Q8Y7P9	lmo1224	NA	hypothetical protein	Transport and Metabolism (ABC transporter); General function prediction only	2.56	-0.91	2.34	-1.05	3.94	-1.46	Cytoplasmic Membrane
	Q8Y5J8	lmo2062	NA	copper transporter	Inorganic ion transport and metabolism	1.46	-1.19	-	-	1.68	-1.13	Cytoplasmic Membrane
	Q8Y5W4	lmo1941	NA	hypothetical protein	Function unknown	3.62	-1.62	7.07	-4.40	1.92	-4.00	Cytoplasmic Membrane
	Q8Y8F4	lmo0950	NA	hypothetical protein	Cell wall metabolism; General function prediction only	2.64	-2.69	1.97	-2.07	2.71	-2.93	Unknown
	Q8Y4D2	lmo2518	TagTUV	Wall teichoic acid ligase	Cell wall metabolism	3.45	-2.73	6.02	-5.57	4.60	-6.86	Cytoplasmic Membrane

In the nutrient-deprived environment of mineral water, *L. monocytogenes* experiences significant physiological stress over the 28-day time course, as reflected in the consistent upregulation or

downregulation of key proteins. The proteins that are consistently upregulated, particularly those related to metabolism, such as the phosphotransferase system (PTS transporter systems) (e.g., Lmo2666 and Lmo0427), likely represent critical components of the bacterium's stress response, enabling it to adapt to harsh condition of nutrient limitations. This upregulation suggests that *L. monocytogenes* optimises nutrient uptake mechanisms early in the process, sustaining metabolic activity even in prolonged nutrient deprivation. Similarly, research on biofilm formation in FPEs has shown the PTS system's pivotal role in nutrient scavenging and metabolic adaptation (Gray et al., 2021). In both contexts, *L. monocytogenes* might employ the PTS system to thrive under challenging conditions whether by forming biofilms or persisting in low-nutrient environments like mineral water (Gray et al., 2021). This parallel highlights the PTS system as a fundamental adaptive mechanism for survival, allowing the bacterium to respond efficiently to environmental stress and nutrient scarcity.

The downregulation of certain proteins, particularly those associated with virulence such as LLO (Lmo0202) (Zhao et al., 2017; Aryapetyan et al., 2018; Lotoux et al., 2022) along with TagTUV (Lmo2518), a wall teichoic ligase linked to cell wall metabolism, suggests a strategic shift in *L. monocytogenes* towards survival-focused mechanisms. The marked reduction in TagTUV, in particular, could indicate an early role for teichoic acid in facilitating cell wall modifications that promote persistence under these conditions (Kawai et al., 2011). In the absence of abundant nutrients, *L. monocytogenes* appears to deprioritize virulence, redirecting its resources to support essential survival processes. This adaptive strategy, observed in other studies could indicate an energy-conserving response whereby the bacterium focuses on nutrient uptake and stress resistance rather than on energy-intensive virulence pathways (Oliver et al., 2005; Li et al., 2014; Zhao et al., 2017).

The consistency in deregulation of specific proteins could suggest that *L. monocytogenes* undergoes a stable adaptation to long-term nutrient starvation. The proteins involved in nutrient transport, metabolism, and stress response could be upregulated as they are necessary for prolonged survival, while the downregulation of other functions reflects a deprioritization of growth or pathogenicity in favour of persistence (Carvalho et al., 2024). Therefore, these proteomic shifts offer insights into how *L. monocytogenes* manages its resources and maintains viability under prolonged stress, potentially leading to the VBNC state and enhancing its persistence.

3.4 Emergence of variable proteins after the second week in mineral water

A notable increase in downregulated proteins was observed after D14, with the majority of proteins diminishing by D28 (Tables 15-17) and many autolysins within the dataset. Autolysins are a family of peptidoglycan hydrolases, cleaving different types of bonds in the peptidoglycan (Holtje, 1998). Their role is essential for the biogenesis, maintenance and stability of the peptidoglycan (Holtje, 1998). In our study, several autolysins including NamA, Ami, Aut, and Spl were significantly downregulated by D14 and sustained low fold changes by D28. Given the role of autolysins in cell wall degradation, their downregulation suggests that *L. monocytogenes* may be stabilising its cell wall structure to adapt to the VBNC state. This aligns with findings by Carvalho and colleagues (Carvalho et al., 2024), who identified autolysin NamA as a pivotal player in this transition. The observed decrease in overall autolysin abundance and in accordance to the many characterised autolysins in *L. monocytogenes* (Bierne and Cossart, 2007) may indicate an adaptive mechanism to preserve cell wall integrity, facilitating *L. monocytogenes*' survival under nutrient limitations and further indicating that reduced autolysin activity plays a role in the transition toward a VBNC state in this environment.

Additionally, many proteins in our dataset that are associated with peptidoglycan maturation and turnover were found downregulated already at D14. More specifically, cell wall-associated proteins, including penicillin-binding proteins (PbpB1, PbpB2) and peptidoglycan-associated proteins (PgdA, LapB), were found to be consistently downregulated by D28 (Tables 15-17). These proteins play essential roles in maintaining cell wall integrity and peptidoglycan synthesis, and their downregulation could support transition towards cell wall loss, facilitating *L. monocytogenes* entry into the VBNC state. Overall, it could be an indication that *L. monocytogenes* is adapting to the harsh conditions through morphological and physiological modifications. Therefore, its survival and adaptation could depend on acquiring energy through their own cell wall shedding mechanism to maintain and sustain their metabolism (Claessen and Errington, 2019; Carvalho et al., 2024).

Simultaneously, proteins involved in signal transduction, such as Stp (a serine/threonine phosphatase that is discussed in detail in the following section) and two-component system regulators like LiaR and VirR, were significantly upregulated from D14 to D28. Stp is responsible for the dephosphorylation of key proteins that regulate stress responses, and the upregulation of these signalling proteins might suggest that *L. monocytogenes* is actively modulating its stress response pathways during nutrient deprivation (Archambaud et al., 2005). For instance, LiaR part of the LiaSR

two component system is a protein associated to cell wall stress responses and its role has been monitored in other gram-positive species such *B. subtilis* and *S. agalactiae* (Masher et al., 2004; Jordan et al., 2006; Klinzing et al., 2013). Identifying LiaR in our dataset and taking into account the loss of the cell wall during *L. monocytogenes*' transition into the VBNC, is an interesting finding since its upregulation could suggest a bacterial adaptation mechanism to the harsh conditions encountered during the transition from the vegetative state. Similarly, VirR is another protein part of the two-component system VirSR, which is critical for responding to environmental stress, including changes in external conditions. Recent studies have shown that VirSR is involved in the biofilm formation of *L. monocytogenes* (Guo et al., 2023). Overall, signal transduction is vital for *L. monocytogenes* adaptation in the environment and especially under harsh conditions where *L. monocytogenes* tries to adapt and establish a silent and persistent niche.

Many microbes have developed mechanisms to combat oxidative stress that might result from the host or the environment (Cheng et al., 2017; Anjou et al., 2024). One such example is the thioredoxin system which contributes in preventing bacteria from oxidative damage and maintaining protein function (Cheng et al., 2017; Anjou et al., 2024). In *L. monocytogenes* it has been suggested that the TrxA helps bacteria to proliferate contributing not only to its protein function, but its virulence and motility as well (Cheng et al., 2017). In our study, proteins involved in oxidative stress defence, such as superoxide dismutase (Sod) and thioredoxins (Lmo1609, TrxA, Lmo2830), were also upregulated throughout the complete time course. This could suggest a critical role in mitigating oxidative damage from the environment and thus protecting *L. monocytogenes* during its transition to the VBNC state. Overall, the upregulation of these defence systems might suggest that *L. monocytogenes* is attempting to survive in the nutrient-deprived environment over the 28-day time course.

Lastly, the upregulation of certain stress-related proteins, such as the chaperone GroES, which assists in preventing protein aggregation, suggests that protein misfolding and aggregation are occurring as the bacteria enter the VBNC state. Research has shown that protein aggregation is a hallmark of cells undergoing stress, including those entering dormancy (Bollen et al., 2021; Dewachter et al., 2021). Additionally, the toxin-antitoxin system MazEF, specifically MazF, which is linked to bacterial persistence and dormancy, was also upregulated. This implies that the MazEF system could be contributing to the persistence of *L. monocytogenes* in the VBNC state by inhibiting cell growth and promoting dormancy (Curtis et al., 2017).

3.5 Molecular mechanisms of VBNC transition and interpretation of selected mutants.

Based on our proteomic and functional analyses, we tested deletion mutants of deregulated proteins that were either upregulated or downregulated over the complete 28-day-time course. The proteins were selected for their subcellular localization, abundance, and biological relevance, as indicated in the literature and further discussed later on. Although we aimed to assess the effects of several identified proteomic markers throughout the time course, time constraints allowed us to focus on only a subset (Table 19). The selected candidates showed no significant impact on growth in mineral water and therefore no significant phenotypic changes in terms of culturability were observed when compared to the *L. monocytogenes* EGDe wild-type strain (Figure 40-46). However, further validation experiments are needed to confirm whether there is truly an effect or not. In addition to the proteins tested in Table 19, we also included *ptsI*, the enzyme key regulator of all PTS systems. The reason for selecting *ptsI* is based on the fact that, in our dataset, several upregulated proteins are associated with PTS systems (Table 16-18). Notably, the number of PTS-associated proteins increases progressively towards the end of the time course. By day 28, there are approximately three times more PTS-associated proteins compared to day 7, probably suggesting a significant shift in metabolic adaptation during the course of infection.

Table 19: Protein markers selected for generation of deletion mutants. Blue; Upregulated, Red; Downregulated

Uniprot Accession Number	Locustag	Protein Name	Function	Localization	Potential relevance
Q8Y8L0	lmo0888	mazF	endoribonuclease that cleaves mRNA at specific sites; Transcription ; RNA metabolism	Cytoplasmic	Mediates stress response; conserves energy during VBNC.
Q8Y8E0	lmo0964	yjbH	Protease adaptor; involved in secondary metabolism (transport & catabolism)	Cytoplasmic	Regulates protein degradation; energy conservation in VBNC.
Q8Y3W6	lmo2713	-	GW domain-containing glycosaminoglycan-binding protein; cell wall metabolism	Cytoplasmic Membrane	May stabilize cell wall structure under stress.
Q8Y678	lmo1821	stp / prpC	Phosphoprotein phosphatase; Signal transduction, Virulence, PTS modifications	Cytoplasmic	Adjusts signaling networks for survival in VBNC.
Q8Y4E5	lmo2501	phoP	Two-component response regulator; transcription; Signal transduction	Cytoplasmic	Responds to environmental stress; modulates gene expression.
Q929L4	lmo2158	Hypothetical	Unknown function	Cytoplasmic	Potential role in stress adaptation during VBNC.

3.5.1 Lmo0888, MazF

Our first target was the Lmo0888 or MazF, an endoribonuclease that that plays a crucial role in regulating mRNA stability by cleaving specific mRNA sites and is part of the Toxin/Antitoxin (TA) system Lmo0888/Lmo0889 or MazEF. TA systems have been described for their effect in regulating bacterial survival and even participating in the generation of persister cells (Curtis et al., 2017). In *L. monocytogenes*, it has been shown that this TA system has an effect on proteins dependent on the stress regulator SigB (Curtis et al., 2017). Therefore, we were interested in finding out whether the MazF could suggest a mechanism by which *L. monocytogenes* can manage protein synthesis during environmental stressors. In the context of the VBNC state, this regulation might allow the bacteria to conserve resources under nutrient deprivation conditions. affect the transition of *L. monocytogenes* into the VBNC state. However, our results did not indicate such an effect of MazF on the transition of *L. monocytogenes* into a VBNC state (Figure 40).

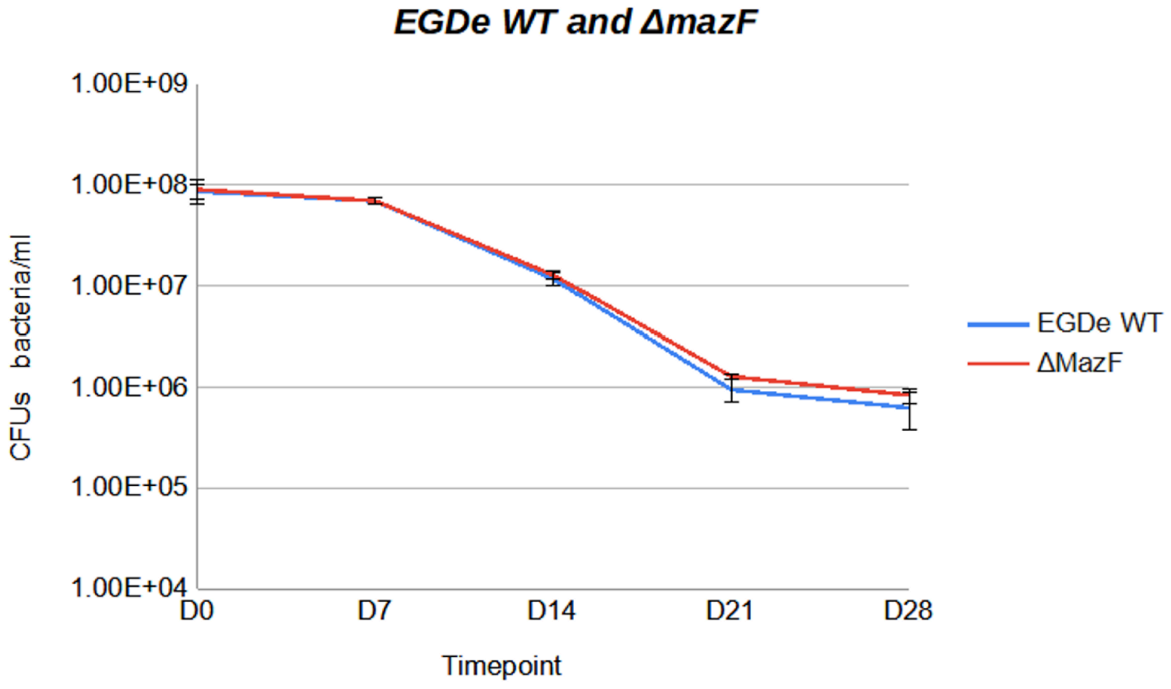

Figure 40 : Culturable cell numbers of EGDe wild-type *L. monocytogenes* (EGDe WT, blue) and MazF-deficient (Δ*mazF*, red) in mineral water that were quantified by CFU enumeration in BHI agar and monitored over the 28-day time course.

3.5.2 Lmo0964, yjbH

Secondly, Lmo0964 (yjbH) is a thioredoxin protease adaptor that interacts with proteases, thereby regulating the degradation of specific proteins. Lmo0964 is associated with roles in secondary metabolism, biosynthesis and transport & catabolism (Cheng et al., 2021). *In vivo* studies have shown that YjbH is essential for translational activation of the ActA protein but exact molecular players are not yet elucidated (Cheng et al., 2021). Studies in other species like in *B. subtilis* have shown that YjbH interacts with Spx resulting in regulations of oxidative stress (Cheng et al., 2021). In *L. monocytogenes* the YjbH protein interacts with SpxA1; an arsenate reductase transcriptional regulator, to help the bacteria defend against oxidative stress and regulate virulence factors within LIPI-1 (Cheng et al., 2021). Additionally, the Δ*yjbH* leads to the downregulation of certain genes involved in sugar transport (PTS) when exposed to oxidative stress (Cheng et al., 2021). However, in nonstress conditions, the Δ*yjbH* results in increased expression of the PrfA protein, crucial for *L. monocytogenes* virulence (Cheng et al., 2021). Overall, YjbH is essential for managing stress responses. In the VBNC context, we were interested in whether the downregulation of this protein might indicate a strategy to conserve energy when faced with nutritional limitations. However, our deletion studies revealed no significant change when compared to the *L. monocytogenes* EGDe WT strain (Figure 41).

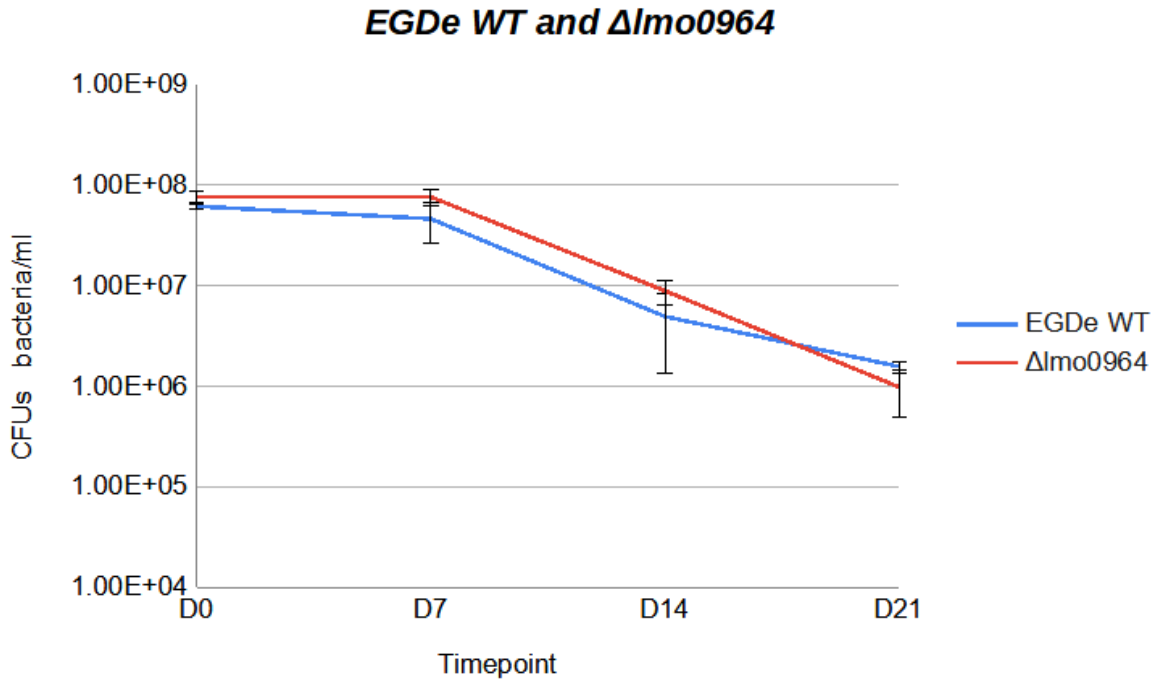

Figure 41: Culturable cell numbers of EGDe wild-type *L. monocytogenes* (EGDe WT, blue) and Lmo0964-deficient (Δ*lmo094*, red) in mineral water that were quantified by CFU enumeration in BHI agar and monitored over the complete 28-day time course.

3.5.3 Lmo2713, hypothetical GW domain protein

Additionally, another protein that we tested in the context of cell wall teichoic acids modulations was the Lmo2713, a GW domain-containing glycosaminoglycan-binding protein. Although its exact function remains unidentified, the presence of the GW domain suggests a potential role in interactions with the cell wall and showing a potential uncharacterised autolytic activity (Cabanes et al., 2002; Bierne and Cossart, 2007; Carvalho et al., 2018). The upregulation of this protein may be vital for maintaining cellular integrity during the prolonged survival of the bacteria in a VBNC state. Nevertheless, its assessment over the wild type did not show any significant change, thus, no effect of Δ*lmo2713* during the transition of the *L. monocytogenes* into the VBNC state (Figure 42).

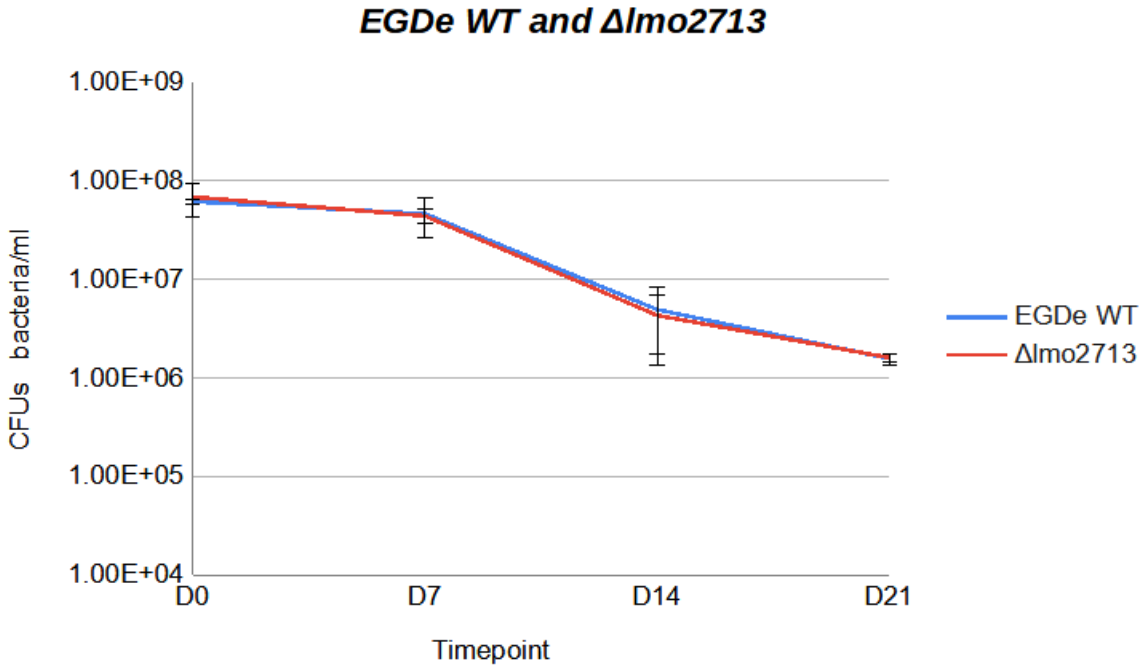

Figure 42: Culturable cell numbers of EGDe wild-type *L. monocytogenes* (EGDe WT, blue) and Lmo2713-deficient (Δ*lmo2713*, red) in mineral water that were quantified by CFU enumeration in BHI agar and monitored over the complete 28-day time course.

3.5.4 Lmo1821, Stp

Another protein of interest was the Lmo1821 (stp / prpC), a serine-threonine phosphatase with roles not only in signal transduction and virulence but stress response, too (Archambaud et al., 2005). Many studies in bacteria including *L. monocytogenes* have characterised the importance of

phosphorylation as mechanisms for adapting and proliferating under adverse conditions (Archambaud et al., 2005). The importance of Stp in various signalling pathways led us to think that its upregulation during the VBNC state may facilitate necessary adjustments in signalling networks, allowing the bacteria to optimise survival without actively expressing virulence. However, the *Δstp* mutant revealed no effect when tested against the EGDe WT suggesting that phosphorylation might have no effect in the VBNC phenotype. Nevertheless, more markers should be tested to draw any relevant conclusions (Figure 43).

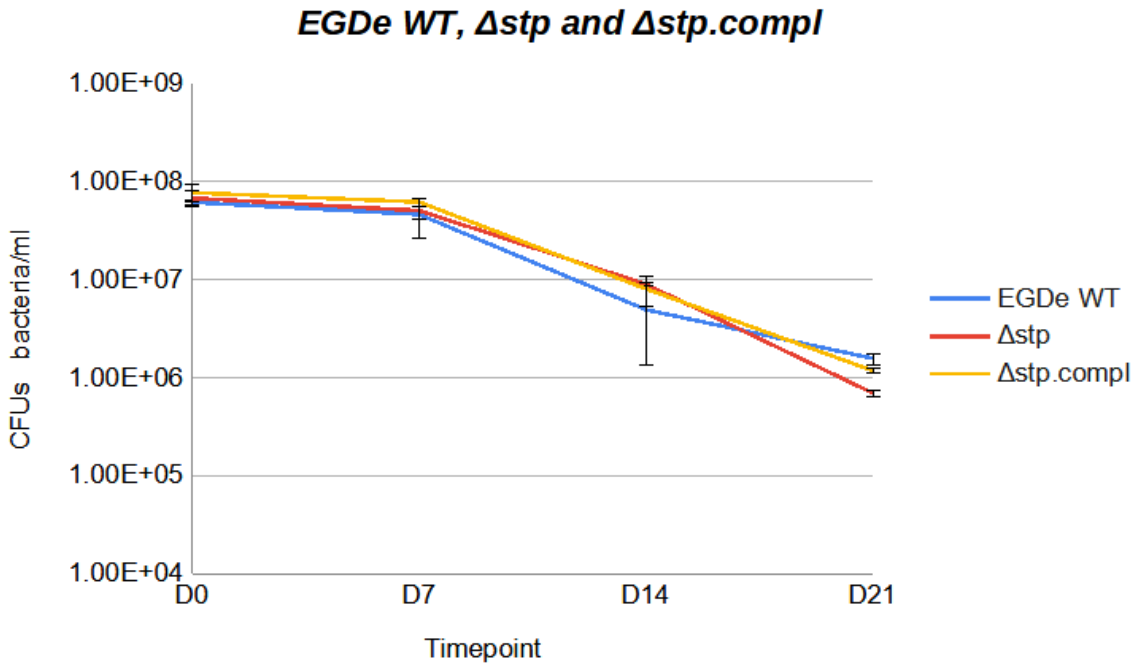

Figure 43: Culturable cell numbers of EGDe wild-type *L. monocytogenes* (EGDe WT, blue), Stp-deficient (Δ*stp*, red) and complemented Δ*stp* (Δ*stp*. compl, yellow) strain expressing the *stp,* in mineral water, that were quantified by CFU enumeration in BHI agar and monitored over the 28-day time course.

3.5.5 Lmo2501, PhoP

Similarly, Lmo2501 (PhoP) is a two-component response regulator involved in signal transduction and transcription. More specifically, the PhoP is a homolog of the two component system of *B. subtilis* and it has been shown to contribute in the biosynthesis of cell wall teichoic acids (Krawczyk-Balska et al., 2012). Studies have shown that *ΔphoR* could result in altered tolerance to ethanol stress and *ΔphoP* has been shown to affect cell growth of bacteria under unfavourable conditions (Krawczyk-Balska et al., 2012). The upregulation of PhoP in the context of VBNC state might indicate an adaptive response that modulates gene expression, ensuring survival environmental stressors, including nutrient limitation. However, when we tested the *ΔPhoP* against the EGDe WT there was no significant effect observed during the transition of *L. monocytogenes* into VBNC (Figure 44).

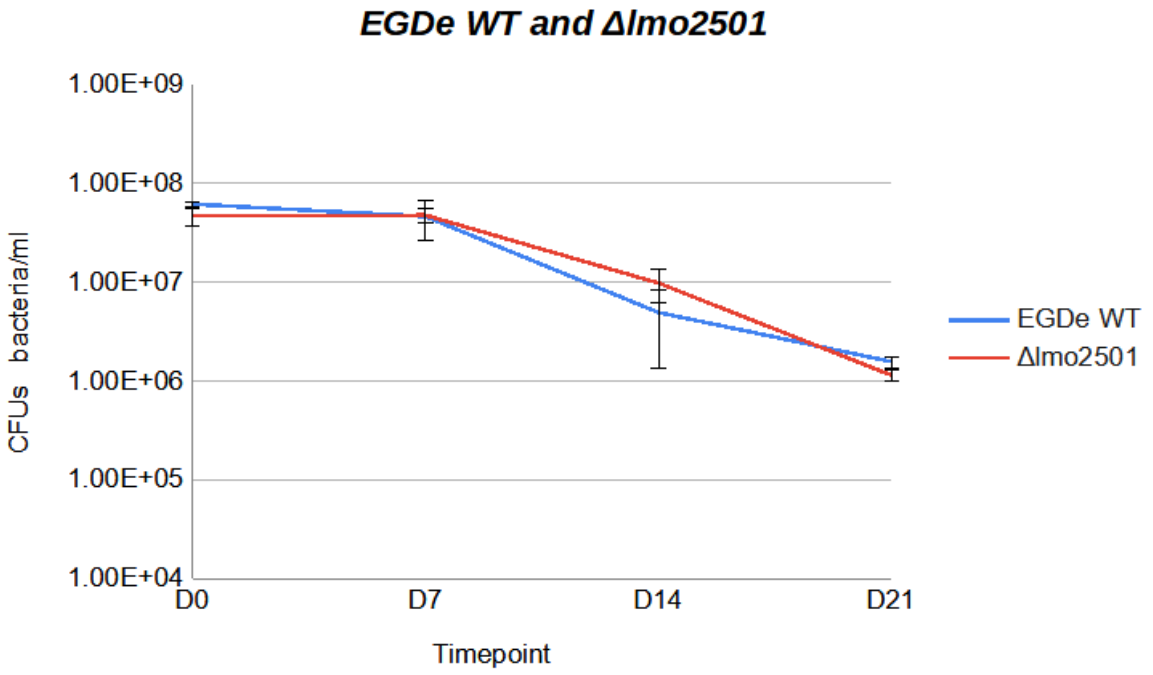

Figure 44: Culturable cell numbers of EGDe wild-type *L. monocytogenes* (EGDe WT, blue) and Lmo2501-deficient (Δ*lmo2501,* red) in mineral water that were quantified by CFU enumeration in BHI agar and monitored over the 28-day time course.

3.5.6 Lmo2158, hypothetical protein

Lmo2158 is a hypothetical protein of uncharacterised functions. It is a homolog to the YwmG, recently renamed to CsbD of *B. subtilis* and *Streptococcus* species (Jia et al., 2023). Studies of *Streptococcus* species have shown that CsbD contributes to bacterial resistance against bile stresses (Jia et al., 2023. Therefore, we were interested whether Lmo2158 could benefit *L. monocytogenes* adaptability due to the nutrient deprived conditions of our experiment. Despite its continuous downregulation during the time course that triggered our interest, there was no noticeable significance when we compared the Δ*lmo2158* to the wild type EGDe (Figure 45).

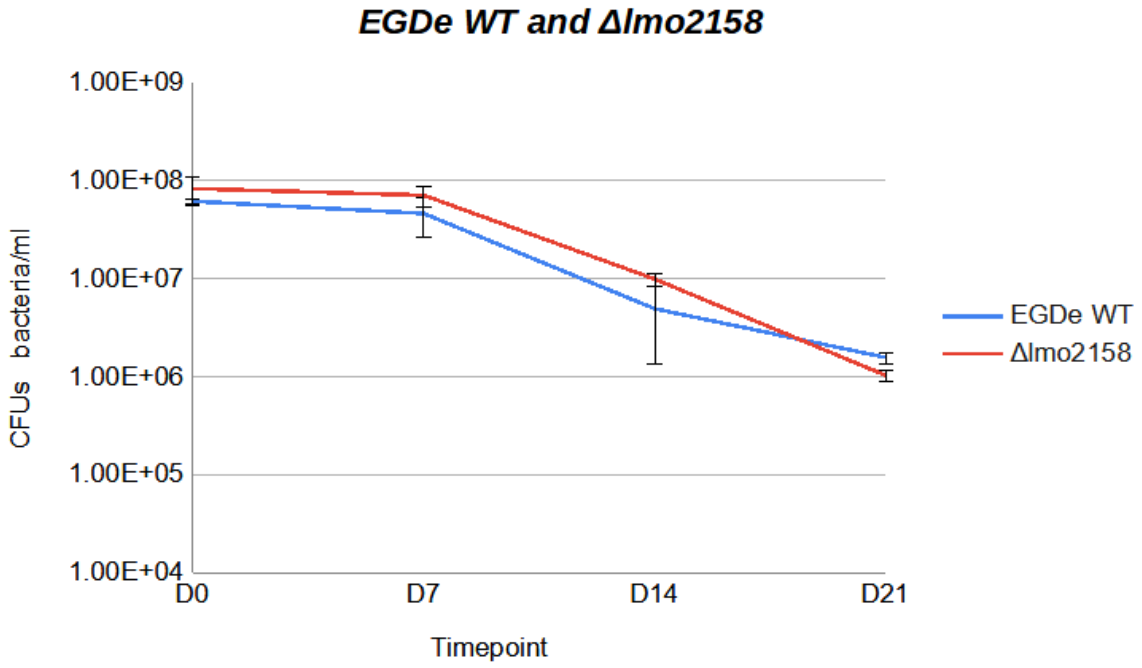

Figure 45: Culturable cell numbers of EGDe wild-type *L. monocytogenes* (EGDe WT, blue) and lmo2158-deficient (Δ*lmo2158,* red) in mineral water that were quantified by CFU enumeration in BHI agar and monitored over the complete 28-day time course.

3.5.7 PtsI

An additional deletion mutant tested was *ΔptsI*, encoding an enzyme responsible for the activation of the phosphoenolpyruvate carbohydrate phosphotransferase system (PTS). Having observed a global upregulation of the PTS, we were interested to identify whether the deletion of the PTS system impacts the energy production and thus having an impact on *L. monocytogenes* transition into the VBNC state (Figure 46).

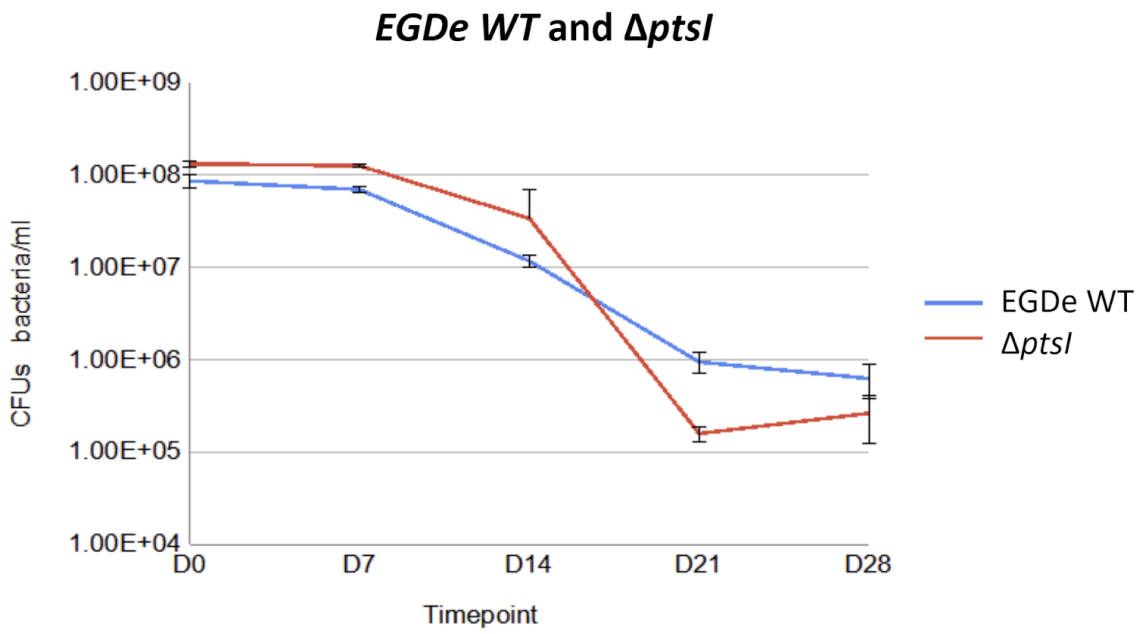

Figure 46: Culturable cell numbers of EGDe wild-type *L. monocytogenes* (EGDe WT, blue) and PtsI-deficient (Δ*pts*I, red) in mineral water that were quantified by CFU enumeration and monitored over the complete 28-day time course.

Overall, from all the tested mutants (Table 19, Figures 40-46) none of them revealed a distinct phenotype that could have an effect in the transition of *L. monocytogenes* into the VBNC state. However, extra validation tests including immunofluorescence and viability assays such as flow cytometry with CFDA and/or LIVE/DEAD assays are essential to confirm the absence or presence of any potential effect.

IV. Summary

To begin with, the physiological adaptation of bacteria into VBNC through cell wall modifications is believed to be associated with reduced demands for energy and more specifically with the need of bacteria to find alternative and less costly ways to maintain and sustain themselves both during their transition and while in VBNC state (Baker et al., 1983). Environmental stressors, such as nutrient deprivation, commonly drive bacteria into latency (Jia et al., 2020), and a hallmark of the VBNC state is cell wall modification, often resulting in the formation of CWD variants that maintain viability without a fully intact cell wall (Klieneberger, 1935). Alterations in the cell wall and in the overall morphology have been described in many other bacterial species as well, such as *E. coli, E. faecalis and H. pylori* (Signoretoo et al., 2000; Signoretto et al., 2002; Li et al., 2014). The morphological transition of *L. monocytogenes* into the VBNC state has been described recently, highlighting the CWD of bacteria as a mechanism of adaptability (Carvalho et al., 2024). Carvalho et al., 2024 identified the autolysin NamA and the stress response regulator SigB as key players for this transition. Therefore, we were interested in pursuing a proteomics analysis to identify further protein players that could have a role in the CWD form and in the transition of *L. monocytogenes* into VBNC in general.

The proteomic characterization of the VBNC state of *L. monocytogenes* presented in this chapter highlighted key adaptive responses during its transition into the VBNC state and under nutrient deprivation in mineral water over a 28-day period, addressing an aspect of bacterial persistence under environmental stress similarly to Carvalho et al., 2024 observations. The VBNC state represents a survival mechanism where bacteria remain viable but are unable to grow on standard culture media, posing significant challenges for detection and control in food safety contexts (Oliver, 2005; Aryapetyan et al., 2018; Lotoux et al., 2022). This phenomenon is particularly relevant in food safety and public health due to the risk of VBNC cells reactivating under favourable conditions (Oliver 2005; Lotoux et al., 2022).

More specifically, our proteomic analysis studies the survival strategies of *L. monocytogenes* as it adapts to prolonged starvation. LC-MS/MS analyses identified proteins involved in nutrient uptake, cellular repair, and metabolic shifts characteristic of the VBNC state, revealing a collaborative nutrient starvation response. Notably, proteins related to stress responses were upregulated, reflecting a focus on cellular repair mechanisms that allow *L. monocytogenes* to preserve viability

despite growth inhibition (Carvalho et al., 2024). A significant metabolic downshift was observed, with a marked reduction in proteins associated with central metabolic processes, indicative of an energy-conservation strategy aligning with dormancy (Lotoux et al., 2022). Interestingly, the analysis also revealed substantial downregulation in proteins linked to cell wall metabolism, particularly those involved in peptidoglycan synthesis and cell wall remodelling (Claessen and Errington, 2019; Carvalho et al., 2024). This downregulation suggests that *L. monocytogenes* is minimising energy expenditure on cell wall maintenance as it transitions into a VBNC state (Claessen and Errington, 2019; Carvalho et al., 2024). Consistent with other studies, the findings support that *L. monocytogenes* reduces metabolic demands by altering its cell wall properties, facilitating survival under nutrient-limited conditions through a potential shift towards a cell wall-deficient (CWD) form (Claessen and Errington, 2019; Carvalho et al., 2024). Our data show strong downregulation of autolysins, penicillin-binding proteins, and peptidoglycan-associated proteins over the time course, supporting a progressive downregulation in cell wall integrity as the bacterium enters the VBNC state, as well (Claessen and Errington, 2019; Carvalho et al., 2024). This cell wall remodelling could also provide a nutrient source, as breakdown products from peptidoglycan degradation may be repurposed to sustain energy needs under starvation conditions (Claessen & Errington, 2019; Carvalho et al., 2024).

Finally, to investigate the roles of specific proteins, we conducted deletion studies targeting mutants: Δ*mazF*, Δ*lmo0964*, Δ*lmo2713*, Δ*stp*, Δ*phoP*, Δ*ptsI* and Δ*lmo2158*. These proteins are involved in energy conservation and conversion, cell wall metabolism, and signal transduction, and are thought to play essential roles in responding to environmental stresses. Culturability studies (CFUs) showed no significant differences in the ability of these mutants to enter the VBNC state compared to the control EGDe WT strain. As previously discussed, the VBNC state is marked by a loss of culturability in growth media while retaining metabolic activity, typically assessed through viability assays like LIVE/DEAD and CFDA, which target damaged membranes and metabolic function, respectively (Wideman et al., 2021). In our study, all culturability assays were conducted in triplicate. Although no differences were observed in culturability, additional viability assays could be valuable to further exclude these proteins as candidates. Additionally, generation and testing of other mutants would be useful to identify proteins associated with entry into the VBNC state.

In conclusion, our findings suggest that *L. monocytogenes* initiates a nutrient-starvation response to survive prolonged nutrient scarcity, prioritising nutrient scavenging, import, and minimal metabolic activity, while downregulating pathways associated with virulence and cell wall synthesis. These

adaptations allow for an efficient and energy-conserving survival strategy that enhances its persistence in harsh environments (Oliver 2005, Li et al., 2014; Zhao et al., 2017; Claessen and Errington, 2019; Carvalho et al., 2024). Our proteomic data provide insights into the molecular mechanisms driving the VBNC phenotype, contributing to a broader understanding of *L. monocytogenes* VBNC persistence and survival, particularly in food safety contexts where reactivation risks remain a public health concern (Oliver, 2005; Gray et al., 2021).

V. Material & Methods

5.1 Bacteria and preparation of VBNC cultures

Stationary phase bacteria grown overnight at 37℃ in BHI with agitation were prepared in mineral water. The bacterial concentration for our experiment in order to reach VBNC in a one-month course was 10^8 bacteria/ml. The concentration of all the tested species was determined by CFUs. For preparation of the VBNC cultures, the bacteria were washed three times and finally resuspended with sterile filtered water. The washed bacteria were then transferred in vented-cap flasks containing 100 ml of mineral water and were left for incubation at RT, in ambient light and without agitation. Samples were extracted for further proteomic analyses at D0, D4, D14 and D28. The deletion mutants were constructed based on pMAD mutagenesis and/or were provided to us by collaborators, as in the case of the Δ*stp* mutant and its complemented strain. The VBNC cultures of the deletion mutants were generated following the same protocol as for the wild type cultures (WT).

5.2 Sample preparation for bacterial supernatant proteins recovery

All samples were prepared in triplicate and aliquots were collected from each culture. Samples were centrifuged at 8000g x 5min, the bacterial pellets were resuspended in 1 ml of lysis buffer (10mM TrisCl pH 8.0, 1mM EDTA, 0.1% RapiGest SF and 1X Protease phosphatase inhibitors) and transferred to 2ml screw-cap tubes containing 0.5g glass beads for bacterial lysis (5 cycles, 6m/s, 30sec) and incubated in ice for 1 min. The samples were then centrifuged (16000g, 4℃, 10min) and the supernatant was collected and concentrated with Ultrafiltration Amicon 3 kDa cut-off centrifugal filters (10000g, 4℃). Protein concentration was assessed with BCA assay and the samples were then prepared for in-gel digestion and LC-MS/MS injection.

5.3 Sample preparation for proteomics and LC-MS/MS

For the proteome analysis, 10 µg of protein extract were loaded for short migration 1D gel electrophoresis (NuPAGE® 4-12 % Bis-Tris 1.5mm Gel, Novex). Proteins were stained using Coomassie G-250 (SimplyBlue™ SafeStain, Invitrogen) and the protein lane (7mm*8mm) was cut into 1 mm pieces. The gel pieces were then discoloured using Solvent A (10 % v/v acetic acid, 40 % v/v ethanol) and Solvent B (50 % v/v 50 mM ammonium bicarbonate, 50 % v/v acetonitrile) followed by reduction with freshly made 10 mM dithiothreitol (DTT) (Sigma) and alkylation with 55 mM iodoacetamide (IAA) (Sigma). The prepared protein extracts were digested overnight at 37 ℃ with 100 ng of trypsin

(Promega) and the overnight peptides were extracted using an extraction buffer (0.5 % v/v trifluoroacetic acid, 50 % v/v acetonitrile). The peptides were dried completely using a SpeedVac concentrator (Savant™ SPD121D, Thermo Fisher Scientific) and then resuspended in 23µl loading buffer (0.5 % Formic Acid , 2 % v/v Acetonitrile) for LC-MS/MS with TimsTOF Pro mass spectrometer (Bruker) proteome analysis.

5.4 Subcellular localisation

The identified variable proteins were subjected to a subcellular localisation with various complementary online topological tools; SIgnalP v.5.0 for signal peptide prediction based on Hidden Markov Model or Neural Networks, TOPCONS for transmembrane domains and N-topology, PRED-LIPO for lipoproteins, CW-PRED for cell wall proteins based on the SrtA and SrtB proteins and PSORTb as an extra tool. The final subcellular prediction verdicts were then concluded based on the information of all the above tools.

5.5 Bioinformatic analysis

MaxQuant and the reference genome *L. monocytogenes* EGDe WT from the NCBI database were used for the protein identification of our samples (FDR 1%, 1 peptide) and LFQ including reversed sequences and contaminants automatically generated by MaxQuant were the main parameters used in our analysis. The output tables were statistically analysed with the Perseus software and the significant variable proteins underwent functional annotations to assess the overall properties of bacteria during their entry into VBNC.

Conclusions

Chapter 1 - Conclusions on the Chronic Phase of *L. monocytogenes* Infection in Trophoblast Cells

This study could provide insights into the mechanisms through which *L. monocytogenes* may establish and maintain chronic infection within trophoblast cells. Through proteomic analysis, strategies employed by *L. monocytogenes* to manipulate host cellular environments were suggested, offering an understanding of how this pathogen might persist in dormancy.

Downregulation and Upregulation of Key Biological Processes

One of the most notable findings is the significant downregulation of angiogenesis and the HIF-1α signalling pathway during chronic infection. Angiogenesis is closely regulated by the HIF-1α and the observed suppression of both pathways could likely disrupt normal cellular homeostasis, impairing immune surveillance and enabling *L. monocytogenes* to evade detection (Osherov and Ben-Ami, 2016; Knight and Stanley, 2019). By inhibiting angiogenesis, *L. monocytogenes* may limit blood vessel formation and immune cell infiltration into infected tissues, reducing immune-mediated clearance (Osherov and Ben-Ami, 2016).

Additionally, pathways involved in cellular signalling and immune regulation, such as the MAPK signalling cascade, were also altered. The MAPK signalling pathway, critical for inflammation and immune responses, was specifically downregulated at the chronic phase of infection, potentially promoting cell survival in infected trophoblasts by inhibiting pro-inflammatory responses (Zhong and Kyriakis, 2017; Nandi and Aroeti, 2023). Overall, it has been shown that bacteria might behave differently in the acute or chronic phase of the infections and many pathogens, such as enteropathogens or pathogens like *Mtb* and *Helicobacter pylori*, have been shown to manipulate MAPK and signalling pathways to establish a favourable environment for long-term infection (Koul et al., 2004; Brodsky and Medzhitov, 2009; Muller et al., 2011; Hashino et al., 2015).

Modulation of Host Immune Responses

The study highlights *L. monocytogenes* ability to modulate immune responses within trophoblast cells during chronic infection. Similarities were noted between this infection model and chronic infection in hepatocytes, as described by Descoeudres et al., 2021, particularly in the manipulation of immune pathways like the complement and coagulation cascades. However, in trophoblast cells,

these pathways were strongly downregulated during the acute phase, followed by a continuous but less intense downregulation towards the chronic phase. This could suggest that the dynamics of immune response modulation might differ depending on the infected tissue. The downregulation of immune pathways; complement and coagulation during acute infection may help *L. monocytogenes* to avoid early immune detection, while a slighter reactivation during chronic infection could potentially allow the pathogen to persist without inducing a robust inflammatory response.

Moreover, the data suggest that *L. monocytogenes* may modulate its interaction with the host's immune system to maintain a balance that avoids complete immune evasion but limits host defences. In particular, the potential suppression of angiogenesis and immune signalling pathways could demonstrate a strategy aimed at minimising immune cell recruitment to the infected tissue, facilitating the establishment of a favourable environment for persistent infection that could acts as a reservoir for recurrent infections in maternal tissues (Bakardiev et al., 2005). Transcriptomic analyses of preterm placentas infected with *L. monocytogenes* also highlight alterations in inflammatory signatures, emphasising the pathogen's impact on maternal-foetal immune balance (Johnson et al., 2020). Understanding these immune dynamics could be critical for developing therapeutic interventions aimed at reducing the pathogen's ability to persist, preventing both the mother and the foetus from complications during pregnancy.

Summary of Chronic *L. monocytogenes* Infection

Chronic infection by *L. monocytogenes* in trophoblast cells reveals a potential manipulation of host processes, including the downregulation of angiogenesis, immune signalling and cellular communication pathways, which are crucial for immune surveillance and tissue homeostasis. The pathogen's ability to suppress these key processes likely contributes to its capacity to establish a dormant, persistent infection within the host. These findings pose significant challenges for the treatment and eradication of *L. monocytogenes*, especially in vulnerable tissues. Understanding the molecular mechanisms behind *L. monocytogenes* persistence, including its modulation of angiogenesis and immune signalling pathways, could be essential for the development of strategies to combat chronic infections.

Chapter 2 - Conclusions on the VBNC state of *L. monocytogenes*

Our study provides insights into the potential entry of *L. monocytogenes* into a VBNC state, especially under nutrient-deprived conditions. This phenomenon has critical implications for understanding the persistence and pathogenicity of *L. monocytogenes*, particularly in environments where the bacteria are exposed to stress conditions that could otherwise be lethal such as in FPEs.

Proteomic evidence of VBNC state transition

The proteomic analysis conducted over a 28-day time course in nutrient-deprived conditions revealed distinct patterns that suggest *L. monocytogenes* may enter a VBNC state as a survival strategy (Claessen and Errington, 2019; Carvalho et al., 2024). The observation of significant up- and downregulation of various proteins, especially after the D14, points to a dynamic response to prolonged environmental stress. The downregulation of proteins involved in cell wall metabolism is particularly noteworthy. This downregulation aligns with previous findings that cell wall modification is a hallmark of bacteria entering a VBNC state, as seen in other species such as *Bacillus, Vibrio, Enterococci species* and *E. coli* (Baker et al., 1983; Signoretto et al., 2000; Signoretto et al., 2002; Dominguez-Cuevas et al., 2012; Kawai and Errington, 2023). The study's data suggest that *L. monocytogenes* may similarly employ a strategy of cell wall alteration, potentially leading to the formation of cell wall-deficient (CWD) bacteria, which are more resistant to environmental stresses (Claessen and Errington, 2019; Carvalho et al., 2024). This state of reduced metabolic activity and altered cell structure may help *L. monocytogenes* conserve energy and resources, thereby sustaining viability over extended periods in adverse environments (Claessen and Errington, 2019; Carvalho et al., 2024).

Role of autolysins in VBNC entry

The study highlights the downregulation of autolysins, including NamA, which are enzymes responsible for breaking down the peptidoglycan (Holtje et al., 1998; Bierne and Cossart, 2017). The reduced activity, namely downregulation, of these proteins could facilitate the transition into a VBNC state by allowing morphological transitions in shape e.g. from rod-shaped to cocci, acting as a bacterial adaptation mechanism (Claessen and Errington, 2019; Carvalho et al., 2024). For example, the connection between NamA and the slower transition into a VBNC state suggests a regulatory role for this protein in maintaining the integrity of *L. monocytogenes* during stress (Carvalho et al., 2024).

The potential involvement of other autolytic regulators and transcription factors, as discussed in the thesis, further supports the idea that *L. monocytogenes* may be modulating its cell wall metabolism in response to prolonged stress, potentially entering a dormant state (Carvalho et al., 2024). The proteomic data show a consistent downregulation of proteins associated with cell wall metabolism throughout the study, reinforcing the hypothesis that these changes are integral to the bacteria's survival strategy under nutrient deprivation.

Implications of the VBNC state for pathogenicity and survival

The transition into a VBNC state has profound implications for *L. monocytogenes*'s pathogenicity. In this dormant form, the bacteria are less detectable by standard culturing techniques, which poses a significant challenge for food safety (Wideman et al., 2021; Aryapetyan et al., 2018; Lotoux et al., 2022). This persistence is particularly concerning in FPEs, where *L. monocytogenes* can survive in a dormant state until conditions become favourable for reactivation and growth, potentially leading to contamination and outbreaks of listeriosis. Our study also observed the global upregulation of the PTS system, which is associated with energy conservation and stress adaptation. This involvement of PTS in the transition to a VBNC state highlights the sophisticated regulatory mechanisms that *L. monocytogenes* employs to survive under nutrient-deprived conditions (Gray et al., 2021). However, our study's deletion mutant showed no significant effect regarding the entry of *L. monocytogenes* into the VBNC state.

Summary of *L. monocytogenes* VBNC state

In conclusion, our proteomic analysis studied the *L. monocytogenes'* behaviour towards its transition into VBNC state under nutrient-deprived conditions. Specifically, the bacterium downregulates virulence and cell wall synthesis proteins while upregulating proteins involved in nutrient scavenging and stress response pathways. This strategic modulation allows *L. monocytogenes* to optimize survival in nutrient-scarce environments, suggesting that the VBNC state functions as a key persistence mechanism. Future research should aim to identify additional proteomic markers critical for this transition and examine interventions that could inhibit entry or maintenance of the VBNC state, with significant implications for public health and food safety.

Conclusions on the dormant state of *L. monocytogenes* both in host and environmental contexts - Chapter 1 & 2

To begin with, the combined findings from Chapters 1 and 2 offer a comprehensive view of *L. monocytogenes* survival strategies under both infection conditions and nutrient starvation, with a focus on the pathogen's ability to persist in host cells and the environment. Taken together, these two chapters provide proteomics insights about the possibility that *L. monocytogenes* could a) evade immune responses and b) enter a VBNC state under stress.

In Chapter 1, we explored the secretome of infected trophoblast cells. The data revealed that during both the acute (24h p.i.) and chronic (96h p.i.) phases the host secretion is downregulated. In particular, many intermediate signal transduction systems, such as MAPK, Ras, Rap1, EGFR and Shear stress signalling pathways are downregulated specifically at 96h p.i., probably allowing *L. monocytogenes* to evade detection and establish persistent infection within the trophoblast niche (Nandi and Aroeti, 2023). Similarly, pathogens such as *Mtb and H. pylori* are thought to manipulate host immune responses to establish a persistent state of infection (Koul et al., 2004; Muller et al., 2011). In chapter 2 shifts the focus to the VBNC state of *L. monocytogenes*, a non-culturable but viable form that allows the pathogen to survive in nutrient-starved environments such as filtered and autoclaved mineral water. The proteomic analysis of *L. monocytogenes* under these conditions highlights the pathogen's ability to conserve energy and enhance stress response mechanisms to maintain viability over an extended period. *L. monocytogenes'* low metabolic activity, combined with the upregulation of stress proteins, reflects a dormancy-like survival strategy that poses a significant challenge for bacterial detection and control (Claessen and Errington, 2019; Carvalho et al., 2024).

Both chapters underscore the adaptability of *L. monocytogenes*, whether in the context of host infection or in response to environmental stresses. In Chapter 1, it is hypothesized that the pathogen not only evades immune detection but also manipulates host cellular processes to proliferate over time. Similarly, in Chapter 2, the VBNC state of *L. monocytogenes* represents not only a proteomic approach of the survival strategy of the VBNC state, but it also offers a validation of previous studies where it is confirmed that both stress responses and cell wall modifications, specifically the cell wall loss, contribute to the transition of *L. monocytogenes* into the VBNC state (Claessen and Errington, 2019; Carvalho et al., 2024).

The integration of the findings from these two chapters could highlight several aspects of *L. monocytogenes* persistence. First, the pathogen's ability to modulate both its metabolic and immune evasion strategies is central to its long-term survival. In Chapter 1, *L. monocytogenes* could lead to immune suppression and secretory modulation to maintain a chronic infection, while in Chapter 2, it conserves energy, enhances stress responses and it manages to adapt to the new environmental challenges via phenotypic changes. These parallel strategies suggest that *L. monocytogenes* is highly adaptable, capable of adjusting to both intracellular and extracellular conditions to ensure survival. Additionally, the identification of potential biomarkers in both the infection and VBNC states offers new possibilities for detecting and combating *L. monocytogenes*. In infected trophoblast cells, proteins specific to the chronic infection phase may serve as diagnostic markers for persistent infections, aiding in the development of targeted therapies. Meanwhile, the stress proteins identified in the VBNC state might provide appropriate candidates for developing more sensitive detection methods for food and water safety monitoring.

Finally, the combined insights from these chapters underscore the importance of developing comprehensive strategies to address *L. monocytogenes* persistence in both clinical and environmental settings. In clinical infections, targeting the pathogen’s immune evasion mechanisms may offer new therapeutic approaches to clearing chronic infections. In environmental systems, improving detection methods for VBNC *Listeria* populations could enhance food safety protocols and reduce the risk of outbreaks.

In conclusion, the work presented in Chapters 1 and 2 provides a detailed understanding of *L. monocytogenes* persistence mechanisms across different niches. Notably, this research demonstrates the organism can fine-tune its molecular response to different environmental conditions, to effect a persistent phenotype. This facilitates persistence in diverse environments, from intracellular host where immunosuppression is critical to prolonged persistence, to extracellular nutrient-starved environments, where nutrient scavenging and stress resistance are prioritised. By examining both the host-pathogen interaction in infected trophoblast cells and the adaptive responses in the VBNC state, this research highlights the pathogen’s remarkable ability to survive and thrive under diverse conditions. These findings have important implications for both public health and clinical management of *L. monocytogenes* infections, offering new insights into detection, diagnosis, and treatment strategies for persistent bacterial states.

Future perspectives

The findings of this study should be further explored in order to figure out both the complexity of host- *L. monocytogenes* interphase and additional mechanisms assisting the entry/exit of *L. monocytogenes* into/out of the VBNC state. Future research could delve deeper into understanding the molecular and cellular dynamics observed in both the secretome and VBNC phenotypes by using the proteomics data of this study as a foundational step.

Firstly, to validate the proteomic changes observed in the secretome study, alternative approaches such as western blotting and ELISA can be employed. These techniques not only provide an opportunity to verify the findings but also enable quantitative assessment of key proteins of interest. Secondly, whole cell lysate analysis is crucial to gain a more comprehensive understanding of the intracellular proteomic profile. Thirdly, functional studies, including overexpression experiments and RNA analysis, could further elucidate the role of specific proteins in modulating infection outcomes. Additionally, profiling variable cytokine levels using cytokine profilers would help identify cytokines that might have been overlooked during secretome recovery and provide deeper insights into host immune responses and the signaling pathways potentially influenced by infection. Finally, investigating the involvement of specific virulence factors in host secretion modulation, particularly through the use of deletion mutants, could yield valuable information about their contributions to the infection process.

Future research on the VBNC phenotype could focus on, firstly, identifying additional deletion mutants to explore their roles in the entry into the VBNC state. An initial focus could be on mutants associated with cell wall metabolism, particularly peptidoglycan-synthesizing enzymes, to investigate whether cell wall inhibition plays a role in this process. Secondly, the role of these mutants in exiting the VBNC state could be investigated by introducing deletion mutants into embryonated eggs to assess their impact on the transition and subsequent viability of *L. monocytogenes* (Carvalho et al., 2024). Thirdly, expanding these studies to include multiple deletion mutants would provide insights into potential interaction among pathways involved in the entry or exit process from the VBNC state. Additionally, phosphoproteomic analysis could be employed to investigate phosphorylation changes during the transitions into and out of the VBNC state, offering a deeper understanding of post-translational modifications.

References

1. Adnan M, Siddiqui AJ, Noumi E, Hannachi S, Ashraf SA, Awadelkareem AM, Snoussi M, Badraoui R, Bardakci F, Sachidanandan M, Patel M & Patel M (2023). Integrating network pharmacology approaches to decipher the multi-target pharmacological mechanism of microbial biosurfactants as novel green antimicrobials against Listeriosis. Antibiotics, 12(1), Article 1. https://doi.org/10.3390/antibiotics12010005.
2. Anjou C, Lotoux A, Zhukova A, Royer M, Caulat LC, Capuzzo E, Morvan C & Martin-Verstraete I (2024). The multiplicity of thioredoxin systems meets the specific lifestyles of *Clostridia*. PLOS Pathogens, 20(2), e1012001. https://doi.org/10.1371/journal.ppat.1012001
3. Anses, 2011 (Updated 2020). (n.d.). Retrieved 6 November 2024, from https://www.anses.fr/en/system/files/BIORISK2016SA0081FiEN.pdf
4. Archambaud C, Gouin E, Pizarro-Cerda J, Cossart P & Dussurget O (2005). Translation elongation factor EF-Tu is a target for Stp, a serine-threonine phosphatase involved in virulence of *Listeria monocytogenes.* Molecular Microbiology, 56(2), 383–396. https://doi.org/10.1111/j.1365-2958.2005.04551.x
5. Arora N, Sadovsky Y, Dermody TS & Coyne CB (2017). Microbial vertical transmission during human pregnancy. Cell Host & Microbe, 21(5), 561–567. https://doi.org/10.1016/j.chom.2017.04.007
6. Ayrapetyan M, Williams T, Oliver JD (2018). Relationship between the viable but nonculturable state and antibiotic persister cells. J Bacteriol. 2018;200(13):e00253-18.
7. Bakardjiev AI, Stacy BA & Portnoy DA (2005). Growth of *Listeria monocytogenes* in the guinea pig placenta and role of cell-to-cell spread in fetal infection. The Journal of Infectious Diseases, 191(11), 1889–1897. https://doi.org/10.1086/430090
8. Baker RM, Singleton FL & Hood MA (1983). Effects of nutrient deprivation on *Vibrio cholerae*. Applied and Environmental Microbiology, 46(4), 930–940. https://doi.org/10.1128/aem.46.4.930-940.1983
9. Banerjee M, Copp J, Vuga D, Marino M, Chapman T, Van Der Geer P & Ghosh P (2004). GW domains of the *Listeria monocytogenes* invasion protein InlB are required for potentiation of Met activation. Molecular Microbiology, 52(1), 257–271. https://doi.org/10.1111/j.1365-2958.2003.03968.x
10. Bardin N, Murthi P & Alfaidy N (2015). Normal and pathological placental angiogenesis. BioMed Research International, 2015(1), 354359. https://doi.org/10.1155/2015/354359
11. Bayles DO, Annous BA, Wilkinson BJ (1996). Cold stress proteins induced in *Listeria monocytogenes* in response to temperature downshock and growth at low temperatures. Appl Environ Microbiol. 1996;62(3):1116-1119. doi:10.1128/aem.62.3.1116-1119.1996.
12. Besnard V, Federighi M, Cappelier JM (2000). Development of a direct viable count procedure for the investigation of VBNC state in *Listeria monocytogenes*: dvc procedure in *Listeria monocytogenes*. Lett Appl Microbiol. 2000;31(1):77–81.
13. Bhardwaj V, Kanagawa O, Swanson PE, Unanue ER (1998). Chronic Listeria infection in SCID mice: requirements for the carrier state and the dual role of T cells in transferring protection or suppression. J Immunol. 1998;160(1):376–384.
14. Bhavsar AP, Guttman JA & Finlay BB (2007). Manipulation of host-cell pathways by bacterial pathogens. Nature, 449(7164), 827–834. https://doi.org/10.1038/nature06247

15. Bierne H & Cossart P (2007). *Listeria monocytogenes* surface proteins: from genome predictions to function. Microbiology and Molecular Biology Reviews, 71(2), 377–397. https://doi.org/10.1128/mmbr.00039-06
16. Bierne H, Milohanic E, Kortebi M (2018). To be cytosolic or vacuolar: the double life of *Listeria monocytogenes.* Front Cell Infect Microbiol. 2018;8:136.
17. Birmingham CL, Canadien V, Kaniuk NA, Steinberg R, Higgins DE & Brumell JH (2008). Listeriolysin O allows *Listeria monocytogenes* replication in macrophage vacuoles. Nature. 2008;451(7176):350–354.
18. Blein-Nicolas M & Zivy M (2016). Thousand and one ways to quantify and compare protein abundances in label-free bottom-up proteomics. Biochimica et Biophysica Acta (BBA) - Proteins and Proteomics, 1864(8), 883–895. https://doi.org/10.1016/j.bbapap.2016.02.019
19. Bollen C, Dewachter L & Michiels J (2021). Protein aggregation as a bacterial strategy to survive antibiotic treatment. Frontiers in Molecular Biosciences, 8. https://doi.org/10.3389/fmolb.2021.669664.
20. Bridier A, Briandet R, Thomas V, Dubois-Brissonnet F (2011). Comparative biocidal activity of peracetic acid, benzalkonium chloride and ortho-phthalaldehyde on 77 bacterial strains. J Hosp Infect. 2011;78(3):208–213.
21. Brodsky IE & Medzhitov R (2009). Targeting of immune signalling networks by bacterial pathogens. Nature Cell Biology, 11(5), 521–526. https://doi.org/10.1038/ncb0509-521
22. Bruderer R, Bernhardt OM, Gandhi T, Miladinović SM, Cheng LY, Messner S, Ehrenberger T, Zanotelli V, Butscheid Y, Escher C, Vitek O, Rinner O & Reiter L (2015). Extending the limits of quantitative proteome profiling with data-independent acquisition and application to acetaminophen-treated three-dimensional liver microtissues. Molecular & Cellular Proteomics, 14(5), 1400–1410. https://doi.org/10.1074/mcp.M114.044305
23. Bucur FI, Grigore-Gurgu L, Crauwels P, Riedel CU & Nicolau AI (2018). Resistance of *Listeria monocytogenes* to stress conditions encountered in food and food processing environments. Frontiers in Microbiology, 9. https://doi.org/10.3389/fmicb.2018.02700
24. Cabanes D, Dehoux P, Dussurget O, Frangeul L, Cossart P (2002). Surface proteins and the pathogenic potential of *Listeria monocytogenes*. Trends Microbiol. 2002;10(6):238–245.
25. Camejo A, Reis O, Leitão E, Sousa S, Cabanes D (2011). The arsenal of virulence factors deployed by *Listeria monocytogenes* to promote its cell infection cycle. Virulence. 2011;2(5):379–394.
26. Cappelier J, Besnard V, Roche S, Velge P & Federighi MM (2007). Avirulent Viable But Non Culturable cells of *Listeria monocytogenes* need the presence of an embryo to be recovered in egg yolk and regain virulence after recovery. Veterinary Research, 38(4), 573–583. https://doi.org/10.1051/vetres:2007017
27. Carlin CR, Liao J, Weller D, Guo X, Orsi RH, Wiedmann M (2021). *Listeria cossartiae sp. nov., Listeria immobilis sp. nov., Listeria portnoyi sp. nov.,* and *Listeria rustica sp. nov*., isolated from agricultural water and natural environments. Int J Syst Evol Microbiol. 2021;71(1):004717.
28. Carvalho F, Carreaux A, Sartori-Rupp A, Tachon S, Gazi AD, Courtin P, Nicolas P, Dubois-Brissonnet F, Barbotin A, Desgranges E, Bertrand M, Gloux K, Schouler C, Carballido-López R, Chapot-Chartier M-P, Milohanic E, Bierne H & Pagliuso A (2024). Aquatic environment drives the emergence of cell wall-deficient dormant forms in Listeria. Nature Communications, 15(1), 8499. https://doi.org/10.1038/s41467-024-52633-7
29. Carvalho F, Sousa S & Cabanes D (2018). L-Rhamnosylation of wall teichoic acids promotes efficient surface association of virulence factors InlB and Ami through interaction with GW domains. Environmental Microbiology, 20(11), 3941–3951. https://doi.org/10.1111/1462-2920.14351

30. Chait BT (2006). Mass Spectrometry: Bottom-up or top-down? Science, 314(5796), 65–66. https://doi.org/10.1126/science.1133987
31. Chao T-C & Hansmeier N (2012). The current state of microbial proteomics: Where we are and where we want to go. PROTEOMICS, 12(4–5), 638–650. https://doi.org/10.1002/pmic.201100381
32. Charlier C, Disson O & Lecuit M (2020). Maternal-neonatal listeriosis. Virulence, 11(1), 391–397. https://doi.org/10.1080/21505594.2020.1759287
33. Chávez-Arroyo A & Portnoy DA (2020). Why is *Listeria monocytogenes* such a potent inducer of CD8+ T-cells? Cellular Microbiology, 22(4), e13175. https://doi.org/10.1111/cmi.13175
34. Chelius D & Bondarenko PV (2002). Quantitative profiling of proteins in complex mixtures using liquid chromatography and mass spectrometry. Journal of Proteome Research, 1(4), 317–323. https://doi.org/10.1021/pr025517j
35. Chen D-B & Zheng J (2014). Regulation of placental angiogenesis. Microcirculation (New York, N.Y.: 1994), 21(1), 15–25. https://doi.org/10.1111/micc.12093
36. Cheng C, Dong Z, Han X, Wang H, Jiang L, Sun J, Yang Y, Ma T, Shao C, Wang X, Chen Z, Fang W, Freitag NE, Huang H & Song H (2017). Thioredoxin A is essential for motility and contributes to host infection of *Listeria monocytogenes* via redox interactions. Frontiers in Cellular and Infection Microbiology, 7. https://doi.org/10.3389/fcimb.2017.00287
37. Cheng C, Sun J, Yu H, Ma T, Guan C, Zeng H, Zhang X, Chen Z & Song H (2020). Listeriolysin O pore-forming activity Is required for ERK1/2 phosphorylation during *Listeria monocytogenes* infection. Frontiers in Immunology, 11, 1146. https://doi.org/10.3389/fimmu.2020.01146
38. Cherifi T, Carrilloo C, Lambert D, Miniai I, Quessy S, Lariviere-Gauthier G, Blais B & Fravalo Ph (2018). Genomic characterization of *Listeria monocytogenes* isolates reveals that their persistence in a pig slaughterhouse is linked to the presence of benzalkonium chloride resistance genes. BMC Microbiol. 2018;18(1):220. doi:10.1186/s12866-018-1363-9.
39. Cindrova-Davies T & Sferruzzi-Perri AN (2022). Human placental development and function. Seminars in Cell & Developmental Biology, 131, 66–77. https://doi.org/10.1016/j.semcdb.2022.03.039
40. Claessen D & Errington J (2019). Cell wall deficiency as a coping strategy for stress. Trends in Microbiology, 27(12), 1025–1033. https://doi.org/10.1016/j.tim.2019.07.008
41. Cobb CA, Curtis GD, Bansi DS, Slade E, Mehal W, Mitchell RG & Chapman RW (1996). Increased prevalence of *Listeria monocytogenes* in the faeces of patients receiving long-term H2-antagonists. European Journal of Gastroenterology & Hepatology, 8(11), 1071–1074. https://doi.org/10.1097/00042737-199611000-00008
42. Copp J, Marino M, Banerjee M, Ghosh P & Geer P van der (2003). Multiple regions of Internalin B contribute to its ability to turn on the Ras-mitogen-activated protein kinase pathway. Journal of Biological Chemistry, 278(10), 7783–7789. https://doi.org/10.1074/jbc.M211666200
43. Corr SC & O'Neill LAJ (2009). *Listeria monocytogenes* infection in the face of innate immunity. Cellular Microbiology, 11(5), 703–709. https://doi.org/10.1111/j.1462-5822.2009.01294.x
44. Costa K, Bacher G, Allmaier G, Dominguez-Bello MG, Engstrand L, Falk P, de Pedro MA & García-del Portillo F (1999). The Morphological transition of Helicobacter pylori cells from spiral to coccoid is preceded by a substantial modification of the cell wall. Journal of Bacteriology, 181(12), 3710–3715. https://doi.org/10.1128/jb.181.12.3710-3715.1999
45. Costa A, Bertolotti L, Brito L, Civera T (2016). Biofilm formation and disinfectant susceptibility of persistent and nonpersistent *Listeria monocytogenes* isolates from Gorgonzola cheese processing plants. Foodborne Pathog Dis. 2016;13(9):602–609.

46. Cramer T, Yamanishi Y, Clausen BE, Förster I, Pawlinski R, Mackman N, Haase VH, Jaenisch R, Corr M, Nizet V, Firestein GS, Gerber HP, Ferrara N & Johnson RS (2003). HIF-1alpha is essential for myeloid cell-mediated inflammation. Cell, 112(5), 645–657. https://doi.org/10.1016/s0092-8674(03)00154-5
47. Crick FHC (1958) On protein synthesis.
48. Cullen and Lockyer (2002). Integration of calcium and RAS signalling. Nature Reviews Molecular Cell Biology. Retrieved 28 October 2024, from https://www.nature.com/articles/nrm808
49. Curtis TD, Takeuchi I, Gram L & Knudsen GM (2017). The influence of the toxin/antitoxin mazEF on growth and survival of *Listeria monocytogenes* under stress. Toxins, 9(1), 31. https://doi.org/10.3390/toxins9010031
50. Demichev V, Messner CB, Vernardis SI, Lilley KS & Ralser M (2019). DIA-NN: Neural networks and interference correction enable deep proteome coverage in high throughput. Nature Methods, 17(1), 41. https://doi.org/10.1038/s41592-019-0638-x
51. Descoeudres N, Jouneau L, Henry C, Gorrichon K, Derre-Bobillot A, Serror P, Gillespie LL, Archambaud C, Pagliuso A & Bierne H (2021). An immunomodulatory transcriptional signature associated with persistent Listeria infection in hepatocytes. Front Cell Infect Microbiol. 2021;11:761945.
52. Descoeudres N (2021). Characterisation of the hepatocyte response to long-term *Listeria monocytogenes* infection. Infectious diseases. Université Paris-Saclay, 2021. English. ffNNT : 2021UPASL115ff. Fftel03917510f
53. Dewachter L, Bollen C, Wilmaerts D, Louwagie E, Herpels P, Matthay P, Khodaparast L, Khodaparast L, Rousseau F, Schymkowitz J & Michiels J (2021). The dynamic transition of persistence toward the viable but non culturable state during stationary phase is driven by protein aggregation. mBio, 12(4), 10.1128/mbio.00703-21. https://doi.org/10.1128/mbio.00703-21
54. Diacovich L & Gorvel J-P (2010). Bacterial manipulation of innate immunity to promote infection. Nature Reviews Microbiology, 8(2), 117–128. https://doi.org/10.1038/nrmicro2295
55. Domínguez-Cuevas P, Mercier R, Leaver M, Kawai Y & Errington J (2012). The rod to L-form transition of Bacillus subtilis is limited by a requirement for the protoplast to escape from the cell wall sacculus. Molecular Microbiology, 83(1), 52–66. https://doi.org/10.1111/j.1365-2958.2011.07920.x
56. Donaldson JR, Nanduri B, Burgess SC, Lawrence ML (2009). Comparative proteomic analysis of *Listeria monocytogenes* strains F2365 and EGD. Appl Environ Microbiol. 2009;75(2):366-373. doi:10.1128/AEM.01847-08.
57. Doyle ME, Mazzotta AS, Wang T, Wiseman DW, Scott VN (2001). Heat resistance of *Listeria monocytogenes.* J Food Prot. 2001;64(3):410-429. doi:10.4315/0362-028x-64.3.410.
58. Dreyer M, Aguilar-Bultet L, Rupp S, Guldimann C, Stephan R, Schock A, Otter A, Schupbach G, Brisse S, Lecuit M, Frey J & Oevermann A (2016). *Listeria monocytogenes* sequence type 1 is predominant in ruminant rhombencephalitis. Nat Commun. 2016;7:11369.
59. Dumas E, Meunier B, Berdagué JL, Chambon C, Desvaux M, Hébraud M (2008). Comparative analysis of extracellular and intracellular proteomes of *Listeria monocytogenes* strains reveals a correlation between protein expression and serovar. Appl Environ Microbiol. 2008;74(23):7399-7409. doi:10.1128/AEM.00594-08.
60. Dussurget O, Bierne H & Cossart P (2014). The bacterial pathogen *Listeria monocytogenes* and the interferon family: Type I, type II and type III interferons. Frontiers in Cellular and Infection Microbiology, 4, 50. https://doi.org/10.3389/fcimb.2014.00050
61. Eshwar AK, Guldimann C, Oevermann A, Tasara T (2017). Cold-shock domain family proteins (Csps) are involved in regulation of virulence, cellular aggregation, and flagella-based motility in *Listeria monocytogenes*—Front Cell Infect Microbiol. 2017;7:453. doi:10.3389/fcimb.2017.00453.

62. Espina JA, Cordeiro MH, Milivojevic M, Pajić-Lijaković I & Barriga EH (2023). Response of cells and tissues to shear stress. Journal of Cell Science, 136(18), jcs260985. https://doi.org/10.1242/jcs.260985
63. Evani SJ & Ramasubramanian AK (2016). Biophysical regulation of *Chlamydia pneumoniae*-infected monocyte recruitment to atherosclerotic foci. Scientific Reports, 6(1), 19058. https://doi.org/10.1038/srep19058
64. Fernández-Costa C, Martínez-Bartolomé S, McClatchy DB, Saviola AJ, Yu N-K & Yates JRI (2020). Impact of the identification strategy on the reproducibility of the DDA and DIA results. Journal of Proteome Research, 19(8), 3153–3161. https://doi.org/10.1021/acs.jproteome.0c00153
65. Ferreira V, Wiedmann M, Teixeira P, Stasiewicz MJ (2014). *Listeria monocytogenes* persistence in food-associated environments: epidemiology, strain characteristics, and implications for public health. J Food Prot. 2014;77(1):150–170.
66. Filipello V, Gallina S, Amato E, Losio MN, Pontello M, Decastelli L & Lomonaco S (2017). Diversity and persistence of *Listeria monocytogenes* within the Gorgonzola PDO production chain and comparison with clinical isolates from the same area. Int J Food Microbiol. 2017;245:73–78. doi:10.1016/j.ijfoodmicro.2017.01.012.
67. Fox EM, Allnutt T, Bradbury MI, Fanning S, Chandry PS (2016). Comparative genomics of the *Listeria monocytogenes* ST204 subgroup. Front Microbiol. 2016;7:2057. doi:10.3389/fmicb.2016.02057.
68. Fox EM, Leonard N, Jordan K (2011). Physiological and transcriptional characterization of persistent and nonpersistent *Listeria monocytogenes* isolates. Appl Environ Microbiol. 2011;77(18):6559–6569.
69. Fox EM, Wall PG, Fanning S (2015). Control of Listeria species food safety at a poultry food production facility. Food Microbiol. 2015;51:81–86. doi:10.1016/j.fm.2015.05.002.
70. Gandhi M, Chikindas ML (2007). Listeria: A foodborne pathogen that knows how to survive. Int J Food Microbiol. 2007;113(1):1–15.
71. Garrett TPJ, McKern NM, Lou M, Elleman TC, Adams TE, Lovrecz GO, Zhu H-J, Walker F, Frenkel MJ, Hoyne PA, Jorissen RN, Nice EC, Burgess AW & Ward CW (2002). Crystal structure of a truncated epidermal growth factor receptor extracellular domain bound to transforming growth factor α. Cell, 110(6), 763–773. https://doi.org/10.1016/S0092-8674(02)00940-6
72. Ghosh BK & Carroll KK (1968). Isolation, composition, and structure of membrane of *Listeria monocytogenes.* Journal of Bacteriology, 95(2), 688–699. https://doi.org/10.1128/jb.95.2.688-699.1968
73. Gilmore JM & Washburn MP (2010). Advances in shotgun proteomics and the analysis of membrane proteomes. Journal of Proteomics, 73(11), 2078–2091. https://doi.org/10.1016/j.jprot.2010.08.005
74. Giotis ES, Blair IS, McDowell DA (2009). Effects of short-term alkaline adaptation on surface properties of *Listeria monocytogenes* 10403S. Open Food Sci J. 2009;3:62–65. doi:10.2174/1874256400903010062.
75. Giotis ES, McDowell DA, Blair IS, Wilkinson BJ (2007). Role of branched-chain fatty acids in pH stress tolerance in *Listeria monocytogenes.* Appl Environ Microbiol. 2007;73(3):997–1001. doi:10.1128/AEM.00865-06.
76. Goulet V, Hebert M, Hedberg C, Laurent E, Vaillant V, De Valk H & Desenclos J-D (2012). Incidence of listeriosis and related mortality among groups at risk of acquiring listeriosis. Clin Infect Dis. 2012;54(5):652–660.
77. Granholm V & Käll L (2011). Quality assessments of peptide-spectrum matches in shotgun proteomics. Proteomics, 11(6), 1086–1093. https://doi.org/10.1002/pmic.201000432

78. Gray J, Chandry PS, Kaur M, Kocharunchitt C, Fanning S, Bowman JP & Fox EM. (2021). Colonisation dynamics of *Listeria monocytogenes* strains isolated from food production environments. Scientific Reports, 11, 12195. https://doi.org/10.1038/s41598-021-91503-w
79. Grif K, Hein I, Wagner M, Brandl E, Mpamugo O, McLauchlin J, Dierich MP & Allerberger F (2001). Prevalence and characterization of *Listeria monocytogenes* in the faeces of healthy Austrians. Wien Klin Wochenschr. 2001;113(20):737–742.
80. Grif K, Patscheider G, Dierich MP, Allerberger F (2003). Incidence of faecal carriage of *Listeria monocytogenes* in three healthy volunteers: a one-year prospective stool survey. Eur J Clin Microbiol Infect Dis. 2003;22(1):16–20.
81. Guo Q, Zhang Y, Fang X, Yang Y, Liang X, Liu J & Fang C (2023). Two-component system virS/virR regulated biofilm formation of *Listeria monocytogenes* 10403S. Food Bioscience, 55, 102973. https://doi.org/10.1016/j.fbio.2023.102973
82. Hackett M. (2008). Science, marketing and wishful thinking in quantitative proteomics. Proteomics, 8(22), 4618–4623. https://doi.org/10.1002/pmic.200800358
83. Hafner L, Pichon M, Burucoa C, Nusser SHA, Moura A, Garcia-Garcera M & Lecuit M (2021). *Listeria monocytogenes* faecal carriage is common and depends on the gut microbiota. Nat Commun. 2021;12(1):6826.
84. Harter EM, Wagner EM, Zaiser A, Halecker S, Wagner M, Rychli K (2017). Stress Survival Islet 2, predominantly present in *Listeria monocytogenes* strains of sequence type 121, is involved in the alkaline and oxidative stress responses. Appl Environ Microbiol. 2017;83(8):e00319-17.
85. Hashino M, Tachibana M, Nishida T, Hara H, Tsuchiya K, Mitsuyama M, Watanabe K, Shimizu T & Watarai M (2015). Inactivation of the MAPK signaling pathway by *Listeria monocytogenes* infection promotes trophoblast giant cell death. Frontiers in Microbiology, 6. https://doi.org/10.3389/fmicb.2015.01145
86. Hein I, Klinger S, Dooms M, Flekna G, Stressl B, Leclerq A, Hill C, Allerberger F & Wagner M (2011). Stress survival islet 1 (SSI-1) survey in *Listeria monocytogenes* reveals an insert common to *Listeria innocua* in sequence type 121 *L. monocytogenes* strains. Appl Environ Microbiol. 2011;77(7):2169–2173. doi:10.1128/AEM.02159-10.
87. Hein I, Klinger S, Dooms M, Flekna G, Stessl B, Leclercq A, Hill C, Allerberger F, Wagner M (2011). Stress Survival Islet 1 (SSI-1) survey in *Listeria monocytogenes* reveals an insert common to *Listeria innocua* in sequence type 121 *L. monocytogenes* strains. Appl Environ Microbiol. 2011;77(7):2169–2173.
88. Herradon G, Ramos-Alvarez MP & Gramage E (2019). Connecting metainflammation and neuroinflammation through the PTN-MK-RPTPβ/ζ Axis: relevance in therapeutic development. Frontiers in Pharmacology, 10. https://doi.org/10.3389/fphar.2019.00377
89. Hilbi H & Kortholt A (2019). Role of the small GTPase Rap1 in signal transduction, cell dynamics and bacterial infection. Small GTPases, 10(5), 336–342. https://doi.org/10.1080/21541248.2017.1331721
90. Hoffmann I, Eugène E, Nassif X, Couraud P-O & Bourdoulous S (2001). Activation of ErbB2 receptor tyrosine kinase supports invasion of endothelial cells by Neisseria meningitidis. The Journal of Cell Biology, 155(1), 133. https://doi.org/10.1083/jcb.200106148
91. Holah JT, Taylor JH, Dawson DJ, Hall KE (2002). Biocide use in the food industry and the disinfectant resistance of persistent strains of *Listeria monocytogenes* and Escherichia coli. J Appl Microbiol. 2002;92(S1):111S–120S.

92. Höltje J-V (1998). Growth of the stress-bearing and shape-maintaining murein sacculus *of Escherichia coli.* Microbiology and Molecular Biology Reviews, 62(1), 181–203. https://doi.org/10.1128/mmbr.62.1.181-203.1998
93. Huang C, Lu T-L & Yang Y (2023). Mortality risk factors related to listeriosis—A meta-analysis. Journal of Infection and Public Health, 16(5), 771–783. https://doi.org/10.1016/j.jiph.2023.03.013
94. Hurley D, Luque-Sastre L, Parker CT, Huynh S, Eshwar AK, Nguyen SV, Andrews N, Moura A, Fox ME, Jordan K, Lehner A, Stephan R & Fanning S (2019) Whole-genome sequencing-based characterization of 100 *Listeria monocytogenes* isolates collected from food processing environments over a four-year period. mSphere. 2019;4(2)
95. Irikura VM, Hirsch E & Hirsh D (1999). Effects of interleukin-1 receptor antagonist overexpression on infection by *Listeria monocytogenes.* Infection and Immunity, 67(4), 1901–1909. https://doi.org/10.1128/iai.67.4.1901-1909.1999
96. Jia L, Yuan C, Pan F, Zhou X, Fan H & Ma Z (2023). CsbD, a novel group B Streptococcal stress response factor that contributes to bacterial resistance against environmental bile salts. Journal of Bacteriology, 205(6), e00448-22. https://doi.org/10.1128/jb.00448-22
97. Johnson LJ, Azari S, Webb A, Zhang X, Gavrilin MA, Marshall JM, Rood K & Seveau S (2021). Human placental trophoblasts infected by *Listeria monocytogenes* undergo a pro-inflammatory switch associated with poor pregnancy outcomes. Frontiers in Immunology, 12. https://doi.org/10.3389/fimmu.2021.709466
98. Jordan S, Rietkötter E, Strauch MA, Kalamorz F, Butcher BG, Helmann JD & Mascher T (2007). LiaRS-dependent gene expression is embedded in transition state regulation in Bacillus subtilis. Microbiology, 153(8), 2530–2540. https://doi.org/10.1099/mic.0.2007/006817-0
99. Kastbjerg VG, Gram L (2009). Model systems allowing quantification of sensitivity to disinfectants and comparison of disinfectant susceptibility of persistent and presumed nonpersistent *Listeria monocytogenes.* J Appl Microbiol. 2009;106(5):1667–1681.
100. Katz M, Amit I & Yarden Y (2007a). Regulation of MAPKs by growth factors and receptor tyrosine kinases. Biochimica et Biophysica Acta (BBA) - Molecular Cell Research, 1773(8), 1161–1176. https://doi.org/10.1016/j.bbamcr.2007.01.002
101. Kawai Y, Marles-Wright J, Cleverley RM, Emmins R, Ishikawa S, Kuwano M, Heinz N, Bui NK, Hoyland CN, Ogasawara N, Lewis RJ, Vollmer W, Daniel RA & Errington J (2011). A widespread family of bacterial cell wall assembly proteins. The EMBO Journal, 30(24), 4931. https://doi.org/10.1038/emboj.2011.358
102. Kayal S, Lilienbaum A, Join-Lambert O, Li X, Israël A & Berche P (2002). Listeriolysin O secreted by *Listeria monocytogenes* induces NF-κB signalling by activating the IκB kinase complex. Molecular Microbiology, 44(5), 1407–1419. https://doi.org/10.1046/j.1365-2958.2002.02973.x
103. Khorami-Sarvestani S, Vanaki N, Shojaeian S, Zarnani K, Stensballe A, Jeddi-Tehrani M & Zarnani A-H (2024). Placenta: An old organ with new functions. Frontiers in Immunology, 15. https://doi.org/10.3389/fimmu.2024.1385762
104. Klieneberger E (1935). The natural occurrence of pleuropneumonia-like organism in apparent symbiosis with Strrptobacillus moniliformis and other bacteria. The Journal of Pathology and Bacteriology, 40(1), 93–105. https://doi.org/10.1002/path.1700400108
105. Klinzing DC, Ishmael N, Hotopp JCD, Tettelin H, Shields KR, Madoff LC & Puopolo KM (2013). The two-component response regulator LiaR regulates cell wall stress responses, pili expression and virulence in group B Streptococcus. Microbiology, 159(Pt_7), 1521–1534. https://doi.org/10.1099/mic.0.064444-0

106. Knight M & Stanley S (2019). HIF-1α as a central mediator of cellular resistance to intracellular pathogens. Current Opinion in Immunology, 60, 111–116. https://doi.org/10.1016/j.coi.2019.05.005
107. Kode DS (2021). Homologous and heterologous stress adaptation in *Listeria monocytogenes* after sublethal exposure to quaternary ammonium compound [dissertation]. Mississippi State University; 2021. Available from: https://scholarsjunction.msstate.edu/td/5117.
108. Kogut MH, Genovese KJ & He H (2007). Flagellin and lipopolysaccharide stimulate the MEK-ERK signaling pathway in chicken heterophils through differential activation of the small GTPases, Ras and Rap1. Molecular Immunology, 44(7), 1729–1736. https://doi.org/10.1016/j.molimm.2006.07.292
109. Kortebi M, Milohanic E, Mitchell G, Pechoux C, Prevost MC, Cossart P & Bierne H (2017) *Listeria monocytogenes* switches from dissemination to persistence by adopting a vacuolar lifestyle in epithelial cells. PLoS Pathog. 2017;13(11):e1006734.
110. Kortebi M (2018). Caractérisation d'une phase de persistance intracellulaire du pathogène *Listeria monocytogenes*. Biologie cellulaire. Université Paris-Saclay, 2018. Français. ffNNT : 2018SACLS477ff. Fftel-02422223v2f
111. Koul A, Herget T, Klebl B & Ullrich A (2004). Interplay between mycobacteria and host signalling pathways. Nature Reviews. Microbiology, 2(3), 189–202. https://doi.org/10.1038/nrmicro840
112. Krawczyk-Balska A, Marchlewicz J, Dudek D, Wasiak K & Samluk A (2012). Identification of a ferritin-like protein of *Listeria monocytogenes* as a mediator of β-lactam tolerance and innate resistance to cephalosporins. BMC Microbiology, 12(1), 278. https://doi.org/10.1186/1471-2180-12-278
113. Lam GY, Cemma M, Muise AM, Higgins DE, Brumell JH (2013). Host and bacterial factors that regulate LC3 recruitment to *Listeria monocytogenes* during the early stages of macrophage infection. Autophagy. 2013;9(7):985–995.
114. Lamont RJ, Postlethwaite R (1986). Carriage of *Listeria monocytogenes* and related species in pregnant and non-pregnant women in Aberdeen, Scotland. J Infect. 1986;13(3):187–193.
115. Li J, Smith LS & Zhu H-J (2021). Data-independent acquisition (DIA): An emerging proteomics technology for analysis of drug-metabolizing enzymes and transporters. Drug Discovery Today: Technologies, 39, 49–56. https://doi.org/10.1016/j.ddtec.2021.06.006
116. Li L, Mendis N, Trigui H, Oliver JD & Faucher SP (2014). The importance of the viable but non-culturable state in human bacterial pathogens. Frontiers in Microbiology, 5. https://doi.org/10.3389/fmicb.2014.00258
117. Li Q, Ali MA & Cohen JI (2006). Insulin degrading enzyme is a cellular receptor mediating Varicella-zoster virus infection and cell-to-cell spread. Cell, 127(2), 305. https://doi.org/10.1016/j.cell.2006.08.046
118. Liu H, Sadygov RG & Yates JR (2004). A model for random sampling and estimation of relative protein abundance in shotgun proteomics. Analytical Chemistry, 76(14), 4193–4201. https://doi.org/10.1021/ac0498563
119. Liu D (2006). Identification, subtyping and virulence determination of *Listeria monocytogenes*, an important foodborne pathogen. J Med Microbiol. 2006;55(6):645–659.
120. Lotoux A, Milohanic E, Bierne H (2022). The viable but non-culturable state of *Listeria monocytogenes* in the one-health continuum. Front Cell Infect Microbiol. 2022;12:849915. doi:10.3389/fcimb.2022.849915.
121. Målen H, Berven FS, Fladmark KE & Wiker HG (2007). Comprehensive analysis of exported proteins from Mycobacterium tuberculosis H37Rv. Proteomics, 7(10), 1702–1718. https://doi.org/10.1002/pmic.200600853

122. Maltepe E & Fisher SJ (2015). Placenta: the forgotten organ. Annual Review of Cell and Developmental Biology, 31(Volume 31, 2015), 523–552. https://doi.org/10.1146/annurev-cellbio-100814-125620
123. Marchetti-Deschmann M & Allmaier G (2011). Mass spectrometry—one of the pillars of proteomics. Journal of Proteomics, 74(7), 915–919. https://doi.org/10.1016/j.jprot.2011.04.024
124. Mascher T, Zimmer SL, Smith T-A & Helmann JD (2004). Antibiotic-inducible promoter regulated by the cell envelope stress-sensing two-component system LiaRS of Bacillus subtilis. Antimicrobial Agents and Chemotherapy, 48(8), 2888–2896. https://doi.org/10.1128/aac.48.8.2888-2896.2004
125. Maudet C, Levallois S, Disson O, Lecuit M (2021). Innate immune responses to Listeria in vivo. Curr Opin Microbiol. 2021;59:95–101.
126. Maury MM, Tsai Y-H, Charlier C, Touchon M, Chenal-Francisque V, Leclercq A, Criscuolo A, Gaultier C, Roussel S, Brisabois A, Disson O, Rocha EPC, Brisse S & Lecuit M (2016). Uncovering *Listeria monocytogenes* hypervirulence by harnessing its biodiversity. Nature Genetics, 48(3), 308. https://doi.org/10.1038/ng.3501
127. McArdle AJ & Menikou S (2021). What is proteomics? Archives of Disease in Childhood - Education and Practice, 106(3), 178–181. https://doi.org/10.1136/archdischild-2019-317434
128. McDonnell G, Russell AD (1999). Antiseptics and disinfectants: activity, action, and resistance. Clin Microbiol Rev. 1999;12(1):147–179.
129. McDonnell GE (2017). Antisepsis, disinfection, and sterilisation. In: Types, Action, and Resistance. 2nd ed. Washington, DC: ASM Press; 2017:432.
130. McVey JH, Michaelides K, Hansen LP, Ferguson-Smith M, Tilghman S, Krumlauf R & Tuddenham EG (1993). A G-->A substitution in an HNF I binding site in the human alpha-fetoprotein gene is associated with hereditary persistence of alpha-fetoprotein (HPAFP). Human Molecular Genetics, 2(4), 379–384. https://doi.org/10.1093/hmg/2.4.379
131. Megli C, Morosky S, Rajasundaram D & Coyne CB (2020). Inflammasome signaling in human placental trophoblasts regulates immune defense against *Listeria monocytogenes* infection. Journal of Experimental Medicine, 218(1), e20200649. https://doi.org/10.1084/jem.20200649
132. Megli CJ & Coyne CB (2022). Infections at the maternal–fetal interface: An overview of pathogenesis and defence. Nature Reviews Microbiology, 20(2), 67–82. https://doi.org/10.1038/s41579-021-00610-y
133. Mehrabadi A, Aghamohamadi N, Khoshmirsafa M, Aghamajidi A, Pilehforoshha M, Massoumi R, & Falak R (2022). The roles of interleukin-1 receptor accessory protein in certain inflammatory conditions. Immunology, 166(1), 38–46. https://doi.org/10.1111/imm.13462
134. Melton-Witt JA, Rafelski SM, Portnoy DA, Bakardjiev AI (2012). Oral infection with signature-tagged *Listeria monocytogenes* reveals organ-specific growth and dissemination routes in guinea pigs. Infect Immun. 2012;80(2):720–732.
135. Molina JR & Adjei AA (2006). The Ras/Raf/MAPK pathway. Journal of Thoracic Oncology, 1(1), 7–9. https://doi.org/10.1016/S1556-0864(15)31506-9
136. Moon B, Yang S-J, Park SM, Lee S-H, Song KS, Jeong E-J, Park M, Kim J-S, Yeom YI & Kim J-A. (2020). LAD1 expression is associated with the metastatic potential of colorectal cancer cells. BMC Cancer, 20(1), 1180. https://doi.org/10.1186/s12885-020-07660-0
137. Moura A, Tourdjman M, Leclercq A, Hamelin E, Laurent E, Fredriksen N, Van Cauteren D, Bracq-Dieye H, Thouvenot P, Vales G, Tessaud-Rita N, Maury MM, Alexandru A, Criscuolo A, Quevillon E, Donguy MP, Enouf V, de Valk H, Brisse S & Lecuit M (2017). Real-time whole-genome sequencing for surveillance of *Listeria monocytogenes*, France. Emerg Infect Dis. 2017;23(9):1462–1470.

138.Muchaamba F, Eshwar AK, Stevens MJA, von Ah U, Tasara T (2019). Variable carbon source utilisation, stress resistance, and virulence profiles among *Listeria monocytogenes* strains responsible for listeriosis outbreaks in Switzerland. Front Microbiol. 2019;10:957. doi:10.3389/fmicb.2019.00957.
139.Müller A, Oertli M & Arnold IC (2011). H. pylori exploits and manipulates innate and adaptive immune cell signaling pathways to establish persistent infection. Cell Communication and Signaling, 9(1), 25. https://doi.org/10.1186/1478-811X-9-25
140.Murray EGD, Webb RA, Swann MBR (1926). A disease of rabbits characterised by a large mononuclear leukocytosis, caused by a hitherto undescribed bacillus Bacterium monocytogenes. J Pathol. 1926;29:407–439.
141.Nandi I & Aroeti B (2023). Mitogen-Activated Protein Kinases (MAPKs) and enteric bacterial pathogens: a complex interplay. International Journal of Molecular Sciences, 24(15), 11905. https://doi.org/10.3390/ijms241511905.
142.Nikitas G, Deschamps C, Disson O, Niault T, Cossart P & Lecuit M (2011). Transcytosis of Listeria monocytogenes across the intestinal barrier upon specific targeting of goblet cell accessible E-cadherin. J Exp Med. 2011;208(11):2263–2277.
143.Nilsson RE, Ross T, Bowman JP (2011). Variability in biofilm production by *Listeria monocytogenes* correlated to strain origin and growth conditions. Int J Food Microbiol. 2011;150(1):14–24.
144.Noinaj N, Easley NC, Oke M, Mizuno N, Gumbart J, Boura E, Steere AN, Zak O, Aisen P, Tajkhorshid E, Evans RW, Gorringe AR, Mason AB, Steven AC & Buchanan SK (2012). Structural basis for iron piracy by pathogenic Neisseria. Nature, 483(7387), 53. https://doi.org/10.1038/nature10823
145.Oddo M, Calandra T, Bucala R & Meylan PRA (2005). Macrophage migration inhibitory factor reduces the growth of virulent Mycobacterium tuberculosis in human macrophages. Infection and Immunity, 73(6), 3783–3786. https://doi.org/10.1128/IAI.73.6.3783-3786.2005
146.Olaya-Abril A, Jiménez-Munguía I, Gómez-Gascón L & Rodríguez-Ortega M J (2014). Surfomics: Shaving live organisms for a fast proteomic identification of surface proteins. Journal of Proteomics, 97, 164–176. https://doi.org/10.1016/j.jprot.2013.03.035
147.Oliver JD (2005). The viable but nonculturable state in bacteria. Journal of Microbiology (Seoul, Korea), 43 Spec No, 93–100.
148.Oliver JD (2010). Recent findings on the viable but nonculturable state in pathogenic bacteria. FEMS Microbiol Rev. 2010;34(4):415–425.
149.Orsi RH & Wiedmann M.(2016). Characteristics and distribution of Listeria spp., including Listeria species newly described since 2009. Applied Microbiology and Biotechnology, 100(12), 5273–5287. https://doi.org/10.1007/s00253-016-7552-2
150.Orsi RH, den Bakker HC, Wiedmann M (2011). *Listeria monocytogenes* lineages: genomics, evolution, ecology, and phenotypic characteristics. Int J Med Microbiol. 2011;301(1):79–96.
151.Orsi RH, Wiedmann M (2016). Characteristics and distribution of Listeria spp., including Listeria species newly described since 2009. Appl Microbiol Biotechnol. 2016;100(12):5273–5287.
152.Ortega MA, Fraile-Martínez O, García-Montero C, Sáez MA, Álvarez-Mon MA, Torres-Carranza D, Álvarez-Mon M, Bujan J, García-Honduvilla N, Bravo C, Guijarro LG & León-Luis JAD (2022). The pivotal role of the placenta in normal and pathological pregnancies: a focus on preeclampsia, fetal growth restriction, and maternal chronic venous disease. Cells, 11(3), 568. https://doi.org/10.3390/cells11030568
153.Osek J, Lachtara B, Wieczorek K (2022). *Listeria monocytogenes* - how this pathogen survives in food-production environments? Front Microbiol. 2022;13:866462. doi:10.3389/fmicb.2022.866462.
154.Osherov N & Ben-Ami R (2016). Modulation of host angiogenesis as a microbial survival strategy and therapeutic target. PLOS Pathogens, 12(4), e1005479. https://doi.org/10.1371/journal.ppat.1005479

155. Palaiodimou L, Fanning S & Fox EM (2021). Genomic insights into persistence of Listeria species in the food processing environment. Journal of Applied Microbiology, 131(5), 2082–2094. https://doi.org/10.1111/jam.15089
156. Paoletti AC, Parmely TJ, Tomomori-Sato C, Sato S, Zhu D, Conaway RC, Conaway JW, Florens L & Washburn MP (2006). Quantitative proteomic analysis of distinct mammalian mediator complexes using normalized spectral abundance factors. Proceedings of the National Academy of Sciences, 103(50), 18928–18933. https://doi.org/10.1073/pnas.0606379103
157. Parsons C, Lee S & Kathariou S (2019). Heavy metal resistance determinants of the foodborne pathogen *Listeria monocytogenes.* Genes, 10(1), Article 1. https://doi.org/10.3390/genes10010011
158. Parsons C, Lee S & Kathariou S (2020). Dissemination and conservation of cadmium and arsenic resistance determinants in Listeria and other Gram-positive bacteria. Molecular Microbiology, 113(3), 560–569. https://doi.org/10.1111/mmi.14470
159. Paterson JS (1940). The antigenic structure of organisms of the genus Listerella. J Pathol Bacteriol. 1940;51:427–436.
160. Pentecost M, Kumaran J, Ghosh P, Amieva MR (2006). *Listeria monocytogenes* internalin B activates junctional endocytosis to accelerate intestinal invasion. PLoS Pathog. 2010;6(3).
161. Pentecost M, Otto G, Theriot JA, Amieva MR . *Listeria monocytogenes* invades the epithelial junctions at sites of cell extrusion. PLoS Pathog. 2006;2(1).
162. Peron-Cane C, Fernandez JC, Leblanc J, Wingertsmann L, Gautier A, Desprat N, Lebreton A (2020). Fluorescent secreted bacterial effectors reveal active intravacuolar proliferation of *Listeria monocytogenes* in epithelial cells. PLoS Pathog. 2020;16(5):e1009001.
163. Petit FM, Hébert M, Picone O, Brisset S, Maurin M-L, Parisot F, Capel L, Benattar C, Sénat M-V, Tachdjian G & Labrune P (2008). A new mutation in the AFP gene responsible for a total absence of alpha feto-protein on second trimester maternal serum screening for Down syndrome. European Journal of Human Genetics, 17(3), 387. https://doi.org/10.1038/ejhg.2008.186
164. Pirie JHH (1940). Listeria: change of name for a genus bacteria. Nature. 1940;145:264.
165. Pizarro-Cerdá J & Cossart P (2018). *Listeria monocytogenes*: Cell biology of invasion and intracellular growth. Microbiology Spectrum, 6(6), 10.1128/microbiolspec.gpp3-0013–2018. https://doi.org/10.1128/microbiolspec.gpp3-0013-2018
166. Rabilloud T & Lelong C (2011). Two-dimensional gel electrophoresis in proteomics: A tutorial. Journal of Proteomics, 74(10), 1829–1841. https://doi.org/10.1016/j.jprot.2011.05.040
167. Radoshevich L, Cossart P (2017). *Listeria monocytogenes*: towards a complete picture of its physiology and pathogenesis. Nat Rev Microbiol. 2017;15(5):312–328.
168. Ragon M, Wirth T, Hollandt F, Lavenir R, Lecuit M, Monnier AL & Brisse S (2008). A new perspective on *Listeria monocytogenes* evolution. PLOS Pathogens, 4(9), e1000146. https://doi.org/10.1371/journal.ppat.1000146
169. Resing KA & Ahn NG (2005). Proteomics strategies for protein identification. FEBS Letters, 579(4), 885–889. https://doi.org/10.1016/j.febslet.2004.12.001
170. Reynolds LP & Redmer DA (2001). Angiogenesis in the placenta. Biology of Reproduction, 64(4), 1033–1040. https://doi.org/10.1095/biolreprod64.4.1033
171. Robbins JR & Bakardjiev AI (2011). Pathogens and the placental fortress. Current Opinion in Microbiology, 15(1), 36. https://doi.org/10.1016/j.mib.2011.11.006
172. Robbins JR, Zeldovich VB, Poukchanski A, Boothroyd JC & Bakardjiev AI (2012). Tissue barriers of the human placenta to infection with *Toxoplasma gondii*. Infection and Immunity, 80(1), 418–428. https://doi.org/10.1128/iai.05899-11

173. Rodríguez-Campos D, Rodríguez-Melcón C, Alonso-Calleja C, Capita R (2019). Persistent *Listeria monocytogenes* isolates from a poultry-processing facility form more biofilm but do not have a greater resistance to disinfectants than sporadic strains. Pathogens. 2019;8(4):250. doi:10.3390/pathogens8040250.
174. Roth L, Srivastava S, Lindzen M, Sas-Chen A, Sheffer M, Lauriola M, Enuka Y, Noronha A, Mancini M, Lavi S, Tarcic G, Pines G, Nevo N, Heyman O, Ziv T, Rueda OM, Gnocchi D, Pikarsky E, Admon A, Caldas C & Yarden, Y. (2018). SILAC identifies LAD1 as a filamin-binding regulator of actin dynamics in response to EGF and a marker of aggressive breast tumors. Science Signaling, 11(515), eaan0949. https://doi.org/10.1126/scisignal.aan0949
175. Ruppitsch W, Pietzka A, Prior K, Bletz S, Fernandez HL, Allerberger F, Harmsen D & Mellmann A (2015). Defining and evaluating a core genome multilocus sequence typing scheme for whole-genome sequence-based typing of *Listeria monocytogenes*. J Clin Microbiol. 2015;53(9):2869–2876.
176. Ryan S, Begley M, Hill C, Gahan CGM (2010). A five-gene stress survival islet (SSI-1) that contributes to the growth of *Listeria monocytogenes* in suboptimal conditions. J Appl Microbiol. 2010;109(3):984–995.
177. Ryan S, Hill C, Gahan CG (2008). Acid stress responses in *Listeria monocytogenes*. Adv Appl Microbiol. 2008;65:67-91. doi:10.1016/S0065-2164(08)00603-5.
178. Ryser E & Marth EH (2007). Listeria, listeriosis, and food safety: Third edition. In Listeria, Listeriosis, and Food Safety, Third Edition (p. 875).
179. Salcedo C, Arreaza L, Alcalá B, de la Fuente L, & Vázquez JA (2003). Development of a multilocus sequence typing method for analysis of *Listeria monocytogenes* clones. Journal of Clinical Microbiology, 41(2), 757–762. https://doi.org/10.1128/jcm.41.2.757-762.2003
180. Sanders KL & Edwards JL (2020). Nano-liquid chromatography-mass spectrometry and recent applications in omics investigations. Analytical Methods, 12(36), 4404–4417. https://doi.org/10.1039/D0AY01194K
181. Sangiorgio G, Nicitra E, Bivona D, Bonomo C, Bonacci P, Santagati M, Musso N, Bongiorno D, & Stefani S (2024). Interactions of Gram-positive bacterial membrane vesicles and hosts: updates and future directions. International Journal of Molecular Sciences, 25(5), 2904. https://doi.org/10.3390/ijms25052904
182. Santos T (2019). Role of proteome in biofilm development and adaptation of *Listeria monocytogenes* to controlled environments. Bacteriology. Université Clermont Auvergne [2017-2020], 2019. English. ffNNT : 2019CLFAC027ff. Fftel-02426255f
183. Sashinami H, Sakuraba H, Ishiguro Y, Munakata A, Nishihira J, & Nakane A (2006). The role of macrophage migration inhibitory factor in lethal *Listeria monocytogenes* infection in mice. Microbial Pathogenesis, 41(2–3), 111–118. https://doi.org/10.1016/j.micpath.2006.06.001
184. Sauders BD, Pettit D, Currie Bm Suits P, Evans A, Stellrecht K, Dryja DM, Slate D & Wiedmann M (2005). Low prevalence of *Listeria monocytogenes* in human stool. J Food Prot. 2005;68(1):178–181.
185. Schille S, Crauwels P, Bohn R, Bagola K, Walther P, van Zandbergen G (2018). LC3-associated phagocytosis in microbial pathogenesis. Int J Med Microbiol. 2018;308(3):228–236.
186. Schlech WF 3rd, Lavigne PM, Bortolussi RA, Allen AC, Haldane EV, Wort AJ, Hightower AW, Johnson SE, King SH, Nicholls ES & Broome CV (1983). Epidemic listeriosis—evidence for transmission by food. N Engl J Med. 1983;308(4):203–206.
187. Schmitz-Esser S, Müller A, Stessl B, Wagner M (2015). Genomes of sequence type 121 *Listeria monocytogenes* strains harbour highly conserved plasmids and prophages. Front Microbiol. 2015;6:380. doi:10.3389/fmicb.2015.00380.

188. Schroder D, Guldimann C, Märtlbauer E (2022). Asymptomatic carriage of *Listeria monocytogenes* by animals and humans and its impact on the food chain. Foods. 2022;11(22):3472.
189. Seeliger HPR, Höhne K (1979). Chapter II: serotyping of *Listeria monocytogenes* and related species. Methods in Microbiology. Academic Press; 1979:31–49.
190. Signoretto C, del Mar Lleò M, Tafi MC, & Canepari P (2000). Cell wall chemical composition of *Enterococcus faecalis* in the viable but non culturable state. Applied and Environmental Microbiology, 66(5), 1953–1959. https://doi.org/10.1128/AEM.66.5.1953-1959.2000
191. Signoretto C, Lleò M del M & Canepari P (2002). Modification of the peptidoglycan of *Escherichia coli* in the viable but non culturable state. Current Microbiology, 44(2), 125–131. https://doi.org/10.1007/s00284-001-0062-0
192. Smith A, Hearn J, Taylor C, Wheelhouse N, Kaczmarek M, Moorhouse E & Singleton I (2019) *Listeria monocytogenes* isolates from ready-to-eat plant produce are diverse and have virulence potential. Int J Food Microbiol. 2019;299:23–32. doi:10.1016/j.ijfoodmicro.2019.03.013.
193. Sperry KEV, Kathariou S, Edwards JS, Wolf LA (2008). Multiple-locus variable-number tandem-repeat analysis as a tool for subtyping *Listeria monocytogenes* strains. J Clin Microbiol. 2008;46(5):1435–1444. doi:10.1128/JCM.02207-07.
194. Steckler AJ, Cardenas-Alvarez MX, Townsend Ramsett MK, Dyer N, Bergholz TM (2018). Genetic characterization of *Listeria monocytogenes* from ruminant listeriosis from different geographical regions in the U.S. Vet Microbiol. 2018;215:93–97.
195. Tang P, Rosenshine I & Finlay BB (1994). *Listeria monocytogenes*, an invasive bacterium, stimulates MAP kinase upon attachment to epithelial cells. Molecular Biology of the Cell, 5(4), 455. https://doi.org/10.1091/mbc.5.4.455
196. Tang P, Rosenshine I, Cossart P & Finlay BB (1996). Listeriolysin O activates mitogen-activated protein kinase in eucaryotic cells. https://doi.org/10.1128/iai.64.6.2359-2361.1996
197. Tang P, Sutherland CL, Gold MR & Finlay BB (1998). *Listeria monocytogenes* invasion of epithelial cells requires the MEK-1/ERK-2 mitogen-activated protein kinase pathway. https://doi.org/10.1128/iai.66.3.1106-1112.1998
198. Tasara T, Stephan R. Evaluation of housekeeping genes in *Listeria monocytogenes* as potential internal control references for normalising mRNA expression levels in stress adaptation models using real-time PCR (2007). FEMS Microbiol Lett. 2007;269(2):265–272.
199. Thakur A, Mikkelsen H & Jungersen G (2019). Intracellular pathogens: host immunity and microbial persistence strategies. Journal of Immunology Research, 2019(1), 1356540. https://doi.org/10.1155/2019/1356540
200. Théry C, Ostrowski M & Segura E (2009). Membrane vesicles as conveyors of immune responses. Nature Reviews. Immunology, 9(8), 581–593. https://doi.org/10.1038/nri2567
201. Tran TT, Mathmann CD, Gatica-Andrades M, Rollo RF, Oelker M, Ljungberg JK, Nguyen TTK, Zamoshnikova A, Kummari LK, Wyer OJK, Irvine KM, Melo-Bolívar J, Gross A, Brown D, Mak JYW, Fairlie DP, Hansford KA, Cooper MA, Giri R, Schreiber V, Joseph SR, Simpson F, Barnett TC, Johansson J, Dankers W, Harris J, Wells TJ, Kapetanovic R, Sweet MJ, Latomanski EA, Newton HJ, Guérillot RJR, Hachani A, Stinear TP, Ong SY, Chandran Y, Hartland EL, Kobe B, Stow JL, Sauer-Eriksson AE, Begun J, Kling JC, Blumenthal A (2022). Inhibition of the master regulator of *Listeria monocytogenes* virulence enables bacterial clearance from spacious replication vacuoles in infected macrophages. PLoS Pathog. 2022;18(1):e1010166. doi:10.1371/journal.ppat.1010166.
202. Trevor CE, Gonzalez-Munoz AL, Macleod OJS, Woodcock PG, Rust S, Vaughan T J, Garman EF, Minter R, Carrington M & Higgins MK (2019). Structure of the trypanosome transferrin receptor reveals

mechanisms of ligand recognition and immune evasion. Nature Microbiology, 4(12), 2074–2081. https://doi.org/10.1038/s41564-019-0589-0

203. Trost M, Wehmhöner D, Kärst U, Dieterich G, Wehland J, & Jänsch L (2005). Comparative proteome analysis of secretory proteins from pathogenic and nonpathogenic species. PROTEOMICS, 5(6), 1544–1557. https://doi.org/10.1002/pmic.200401024
204. Tsou C-C, Avtonomov D, Larsen B, Tucholska M, Choi H, Gingras A-C & Nesvizhskii AI (2015). DIA-Umpire: Comprehensive computational framework for data-independent acquisition proteomics. Nature Methods, 12(3), 258–264. https://doi.org/10.1038/nmeth.3255
205. Turco MY, & Moffett A (2019). Development of the human placenta. Development, 146(22), dev163428. https://doi.org/10.1242/dev.163428
206. Ulrich LE, Koonin EV & Zhulin IB (2005). One-component systems dominate signal transduction in prokaryotes. Trends in Microbiology, 13(2), 52–56. https://doi.org/10.1016/j.tim.2004.12.006
207. Van Oudenhove L, & Devreese B (2013). A review on recent developments in mass spectrometry instrumentation and quantitative tools advancing bacterial proteomics. Applied Microbiology and Biotechnology, 97(11), 4749–4762. https://doi.org/10.1007/s00253-013-4897-7
208. Vázquez-Boland JA, Krypotou E, & Scortti M (2017). Listeria placental infection. mBio, 8(3), 10.1128/mbio.00949-17. https://doi.org/10.1128/mbio.00949-17
209. Velge Ph, Bottreau E, Kaeffer B, Yurduse N, Pardon P & Van Langendonck N (1994). Protein tyrosine kinase inhibitors block the entries of *Listeria monocytogenes* and *Listeria ivanovii* into epithelial cells. Microbial Pathogenesis, 17(1), 37–50. https://doi.org/10.1006/mpat.1994.1050
210. Wang J, Ray AJ, Hammons SR, Oliver HF (2015). Persistent and transient *Listeria monocytogenes* strains from retail deli environments vary in their ability to adhere and form biofilms and rarely have inlA premature stop codons. Foodborne Pathog Dis. 2015;12(2):151–158. doi:10.1089/fpd.2014.1837.
211. Wang Y, Li T, Chen Y, Wei H, Sun R, Tian Z (2017). Involvement of NK cells in IL-28B-mediated immunity against influenza virus infection. J Immunol. 2017;199(3):1012–1020.
212. Ward TJ, Ducey TF, Usgaard T, Dunn KA, Bielawski JP (2008). Multilocus genotyping assays for single nucleotide polymorphism-based subtyping of *Listeria monocytogenes* isolates. Appl Environ Microbiol. 2008;74(24):7629–7642.
213. Weiglein I, Goebel W, Troppmair J, Rapp UR, Demuth A, & Kuhn M (1997). *Listeria monocytogenes* infection of HeLa cells results in listeriolysinO-mediated transient activation of the Raf-MEK-MAP kinase pathway. FEMS Microbiology Letters, 148(2), 189–195. https://doi.org/10.1111/j.1574-6968.1997.tb10287.x
214. Wideman NE, Oliver JD, Crandall PG, & Jarvis NA (2021). Detection and potential virulence of viable but non culturable (VBNC) *Listeria monocytogenes*: a review. Microorganisms, 9(1), 194. https://doi.org/10.3390/microorganisms9010194
215. Wilkins MR, Pasquali C, Appel RD, Ou K, Golaz O, Sanchez J-C., Yan JX, Gooley AA, Hughes G, Humphery-Smith I, Williams KL, & Hochstrasser DF. (1996). From proteins to proteomes: large scale protein identification by two-dimensional electrophoresis and arnino acid analysis. Bio/Technology, 14(1), 61–65. https://doi.org/10.1038/nbt0196-61
216. Yamashita T, Nakane A, Watanabe T, Miyoshi I, & Kasai N. (1994). Evidence that alpha-fetoprotein suppresses the immunological function in transgenic mice. Biochemical and Biophysical Research Communications, 201(3), 1154–1159. https://doi.org/10.1006/bbrc.1994.1826
217. Zhang W, Jayarao BM, & Knabel SJ. (2004). Multi-virulence-locus sequence typing of *Listeria monocytogenes*. Applied and Environmental Microbiology, 70(2), 913–920. https://doi.org/10.1128/AEM.70.2.913-920.2004

218. Zhao X, Zhong J, Wei C, Lin C-W, & Ding T. (2017). Current perspectives on viable but non culturable state in foodborne pathogens. Frontiers in Microbiology, 8. https://doi.org/10.3389/fmicb.2017.00580
219.Zhao X, Zhong J, Wei C, Lin CW, Ding T (2017). Current perspectives on viable but nonculturable state in foodborne pathogens. Front Microbiol. 2017;8:1260.
220.Zhong, J, & Kyriakis JM. (2007). Dissection of a signaling pathway by which pathogen-associated molecular patterns recruit the JNK and p38 MAPKs and trigger cytokine release. Journal of Biological Chemistry, 282(33), 24246–24254. https://doi.org/10.1074/jbc.M703422200
221.Zhu W, Smith JW, & Huang, C-M. (2010). Mass spectrometry-based label-free quantitative proteomics. BioMed Research International, 2010(1), 840518. https://doi.org/10.1155/2010/840518.
222. Zinchenko AA, Sergeyev VG, Yamabe K, Murata S, Yoshikawa K (2004). DNA compaction by divalent cations: structural specificity revealed by the potentiality of designed quaternary ammonium salts. Chem biochem. 2004;5(8):1014–1020. doi:10.1002/cbic.200300797.

Supplementary Material

Chapter 1

Supplementary Table 1-A: Differentially regulated secreted proteins identified with SC at I/NI 24h.
Total: 36 proteins- Red; Downregulated proteins: 4 proteins - Green; Upregulated proteins: 32 proteins

Uniprot	Protein	p-value	Ratio I/NI24H
P00450	Ceruloplasmin	6.79E-04	0.20
P24043	Laminin subunit alpha-2	1.66E-02	0.25
P01706	Immunoglobulin lambda variable 2-11	4.14E-02	0.33
P00747	Plasminogen	1.54E-03	0.57
P10909	Clusterin	6.17E-03	2.27
P14174	Macrophage migration inhibitory factor	6.10E-03	2.38
Q969H8	Myeloid-derived growth factor	4.56E-03	2.70
P30740	Leukocyte elastase inhibitor	5.65E-12	3.07
O76061	Stanniocalcin-2	7.52E-08	3.16
Q9H4A4	Aminopeptidase B	1.05E-61	3.93
P31947	14-3-3 protein sigma	2.00E-03	4.00
Q10471	Polypeptide N-acetylgalactosaminyltransferase 2	4.28E-04	4.17
P27797	Calreticulin	6.79E-35	4.40
Q9NZV1	Cysteine-rich motor neuron 1 protein	5.60E-05	4.43
O43852	Calumenin	1.32E-09	4.44
Q99542	Matrix metalloproteinase-19	4.26E-06	5.14
Q02818	Nucleobindin-1	1.12E-08	5.40
P17693	HLA class I histocompatibility antigen, alpha chain G	3.78E-06	5.67
M5A8F1	Suppressyn	6.18E-08	7.80
Q8WUM4	Programmed cell death 6-interacting protein	1.28E-54	8.41
P06744	Glucose-6-phosphate isomerase	2.10E-106	8.41
Q99988	Growth/differentiation factor 15	3.31E-10	14.00
P05121	Plasminogen activator inhibitor 1	6.95E-05	16.00
Q00796	Sorbitol dehydrogenase	5.17E-08	27.00
P09429	High mobility group protein B1	4.41E-108	38.18
P53621	Coatomer subunit alpha	7.68E-58	101.50
P26583	High mobility group protein B2	3.91E-102	346.00
O00515	Ladinin-1	2.37E-17	Inf
P19883	Follistatin	2.09E-04	Inf
P43490	Nicotinamide phosphoribosyltransferase	6.87E-27	Inf

P67809	Y-box-binding protein 1	2.17E-59	Inf
Q08J23	RNA cytosine C(5)-methyltransferase NSUN2	3.50E-10	Inf
Q66K79	Carboxypeptidase Z	7.09E-13	Inf
Q8N474	Secreted frizzled-related protein 1	3.50E-10	Inf
Q8NCW5	NAD(P)H-hydrate epimerase	1.10E-08	Inf
Q9BXX0	EMILIN-2	7.02E-07	Inf

Supplementary Table 1-B: Differentially regulated secreted identified both with SC and XIC at I/NI 24h.
Total: 62 proteins- Red; Downregulated proteins: 53 proteins - Green; Upregulated proteins: 9 proteins

Uniprot	Protein	p-value	Ratio I/NI 24H
P43652	Afamin	1.31E-03	0.02
P05543	Thyroxine-binding globulin	7.14E-06	0.03
P36955	Pigment epithelium-derived factor	1.23E-07	0.03
Q04756	Hepatocyte growth factor activator	6.12E-06	0.03
P05155	Plasma protease C1 inhibitor	1.44E-05	0.05
P01023	Alpha-2-macroglobulin	1.16E-04	0.05
P08697	Alpha-2-antiplasmin	1.88E-06	0.05
Q12884	Prolyl endopeptidase FAP	6.16E-05	0.06
P04746	Pancreatic alpha-amylase	1.24E-06	0.06
P01031	Complement C5	2.88E-05	0.06
Q9BTY2	Plasma alpha-L-fucosidase	1.46E-05	0.07
Q9NPH3	Interleukin-1 receptor accessory protein	7.14E-06	0.07
P02787	Serotransferrin	2.54E-06	0.07
P01024	Complement C3	3.37E-06	0.07
P04114	Apolipoprotein B-100	7.14E-06	0.07
Q08380	Galectin-3-binding protein	2.21E-06	0.07
P01034	Cystatin-C	6.87E-04	0.07
P02452	Collagen alpha-1(I) chain	2.02E-05	0.08
P12109	Collagen alpha-1(VI) chain	1.42E-04	0.08
P08123	Collagen alpha-2(I) chain	1.46E-05	0.08
P49747	Cartilage oligomeric matrix protein	2.88E-05	0.08
P19823	Inter-alpha-trypsin inhibitor heavy chain H2	1.24E-06	0.08
P35443	Thrombospondin-4	5.43E-06	0.08
P0C0L4	Complement C4-A	8.06E-05	0.09

P01008	Antithrombin-III	9.48E-05	0.1
Q8NCC3	Phospholipase A2 group XV	4.06E-05	0.11
Q96PD5	N-acetylmuramoyl-L-alanine amidase	2.93E-02	0.12
O00391	Sulfhydryl oxidase 1	2.21E-06	0.12
Q6ZRP7	Sulfhydryl oxidase 2	7.14E-06	0.13
P07711	Procathepsin L	4.34E-04	0.13
P35052	Glypican-1	7.06E-05	0.13
Q9BWS9	Chitinase domain-containing protein 1	2.46E-04	0.13
P19021	Peptidyl-glycine alpha-amidating monooxygenase	2.25E-05	0.15
Q15582	Transforming growth factor-beta-induced protein ig-h3	3.26E-05	0.16
Q6H9L7	Isthmin-2	2.21E-06	0.16
Q14050	Collagen alpha-3(IX) chain	5.12E-03	0.16
P02748	Complement component C9	1.48E-03	0.17
Q8WVQ1	Soluble calcium-activated nucleotidase 1	7.53E-04	0.17
P16035	Metalloproteinase inhibitor 2	8.68E-05	0.19
P50897	Palmitoyl-protein thioesterase 1	2.58E-04	0.2
Q92876	Kallikrein-6	8.96E-04	0.21
P07858	Cathepsin B	4.06E-05	0.21
P07996	Thrombospondin-1	2.39E-03	0.23
P02771	Alpha-fetoprotein	1.38E-02	0.25
P07602	Prosaposin	6.00E-04	0.31
Q9GZN4	Brain-specific serine protease 4	3.05E-02	0.36
O75882	Attractin	2.77E-02	0.46
Q13361	Microfibrillar-associated protein 5	1.41E-02	0.5
P08572	Collagen alpha-2(IV) chain	7.46E-03	0.52
P07237	Protein disulfide-isomerase	1.93E-03	1.6
P41250	Glycine--tRNA ligase	1.19E-02	2.02
Q07021	Complement component 1 Q subcomponent-binding protein	2.95E-02	2.36
P10599	Thioredoxin	7.20E-04	2.47
P07355	Annexin A2	9.69E-03	2.64
P04083	Annexin A1	5.21E-03	2.73
P14735	Insulin-degrading enzyme	1.02E-03	2.88
P55145	Mesencephalic astrocyte-derived neurotrophic factor	1.21E-03	3.56
Q96HE7	ERO1-like protein alpha	1.24E-04	4.69

Q12904	Aminoacyl tRNA synthase complex-interacting multifunctional protein 1	7.10E-06	4.89
P51858	Hepatoma-derived growth factor	3.90E-05	6.3
P22626	Heterogeneous nuclear ribonucleoproteins A2/B1	1.24E-06	10.32
Q15046	Lysine--tRNA ligase	3.19E-05	12.39

Supplementary Table 1-C: Differentially regulated secreted identified with XIC at I/NI 24h.
Total: 88 proteins- Red; Downregulated proteins: 86 proteins - Green; Upregulated proteins: 2 proteins

Uniprot	Protein	p-value	Ratio I/NI 24H
P51884	Lumican	2.21E-06	0.03
P02461	Collagen alpha-1(III) chain	4.25E-05	0.03
P20827	Ephrin-A1	1.83E-05	0.03
P13591	Neural cell adhesion molecule 1	6.12E-06	0.03
P12111	Collagen alpha-3(VI) chain	1.70E-03	0.04
P20849	Collagen alpha-1(IX) chain	8.30E-04	0.04
Q8IUL8	Cartilage intermediate layer protein 2	7.10E-06	0.05
Q13822	Ectonucleotide pyrophosphatase/phosphodiesterase family member 2	2.37E-04	0.05
P10915	Hyaluronan and proteoglycan link protein 1	1.11E-05	0.05
Q14520	Hyaluronan-binding protein 2	6.13E-05	0.06
P02790	Hemopexin	2.17E-04	0.06
P31431	Syndecan-4	3.90E-05	0.06
P20742	Pregnancy zone protein	2.58E-04	0.07
P98095	Fibulin-2	1.36E-03	0.07
P04004	Vitronectin	2.19E-04	0.07
Q14624	Inter-alpha-trypsin inhibitor heavy chain H4	6.37E-06	0.07
Q9UBX5	Fibulin-5	9.48E-05	0.07
P12107	Collagen alpha-1(XI) chain	5.03E-06	0.08
P00734	Prothrombin	1.71E-05	0.08
Q9Y2E5	Epididymis-specific alpha-mannosidase	4.31E-05	0.08
P00746	Complement factor D	4.06E-05	0.08
Q6EMK4	Vasorin	5.70E-05	0.09
Q9UBQ6	Exostosin-like 2	1.30E-04	0.09
P02774	Vitamin D-binding protein	1.83E-05	0.09
P02753	Retinol-binding protein 4	1.71E-05	0.09
P02749	Beta-2-glycoprotein 1	6.55E-05	0.1

O00584	Ribonuclease T2	5.03E-06	0.1
P19827	Inter-alpha-trypsin inhibitor heavy chain H1	2.62E-04	0.1
P20908	Collagen alpha-1(V) chain	1.44E-05	0.11
O60462	Neuropilin-2	6.11E-06	0.11
Q92820	Gamma-glutamyl hydrolase	7.14E-06	0.11
P15291	Beta-1,4-galactosyltransferase 1	7.65E-06	0.12
O43278	Kunitz-type protease inhibitor 1	5.03E-06	0.12
P35858	Insulin-like growth factor-binding protein complex acid labile subunit	3.52E-03	0.12
P23142	Fibulin-1	1.90E-05	0.12
P98160	Basement membrane-specific heparan sulfate proteoglycan core protein	3.66E-05	0.12
P14543	Nidogen-1	8.94E-06	0.12
O00468	Agrin	1.96E-04	0.13
P05156	Complement factor I	1.35E-04	0.13
P61916	NPC intracellular cholesterol transporter 2	6.37E-06	0.13
P02788	Lactotransferrin	1.08E-03	0.13
O75487	Glypican-4	2.54E-06	0.15
P08174	Complement decay-accelerating factor	4.24E-05	0.15
Q08345	Epithelial discoidin domain-containing receptor 1	1.86E-04	0.15
P09486	SPARC	1.78E-05	0.15
O15230	Laminin subunit alpha-5	2.21E-06	0.15
P02786	Transferrin receptor protein 1	5.13E-04	0.16
Q03167	Transforming growth factor beta receptor type 3	1.99E-05	0.17
Q16651	Prostasin	5.46E-04	0.17
P61769	Beta-2-microglobulin	6.55E-05	0.18
Q92484	Acid sphingomyelinase-like phosphodiesterase 3a	3.68E-05	0.18
P02750	Leucine-rich alpha-2-glycoprotein	8.17E-05	0.18
Q06033	Inter-alpha-trypsin inhibitor heavy chain H3	4.34E-04	0.18
P02765	Alpha-2-HS-glycoprotein	8.75E-04	0.19
P00533	Epidermal growth factor receptor	9.48E-05	0.19
P15509	Granulocyte-macrophage colony-stimulating factor receptor subunit alpha	3.37E-06	0.2
Q9Y653	Adhesion G-protein coupled receptor G1	3.41E-05	0.2
P02462	Collagen alpha-1(IV) chain	3.95E-05	0.2
P06396	Gelsolin	1.35E-03	0.21
P02458	Collagen alpha-1(II) chain	3.29E-03	0.21

Q9BXJ4	Complement C1q tumor necrosis factor-related protein 3	4.29E-04	0.22
P11047	Laminin subunit gamma-1	3.23E-04	0.22
Q15063	Periostin	3.25E-03	0.22
Q96P44	Collagen alpha-1(XXI) chain	7.29E-05	0.22
Q96NY8	Nectin-4	3.15E-05	0.23
P15328	Folate receptor alpha	2.73E-04	0.23
Q6PCB0	von Willebrand factor A domain-containing protein 1	3.44E-05	0.23
P02675	Fibrinogen beta chain	3.89E-02	0.24
P05067	Amyloid-beta precursor protein	7.75E-04	0.25
P49763	Placenta growth factor	1.23E-02	0.25
Q92673	Sortilin-related receptor	2.45E-03	0.26
O60568	Multifunctional procollagen lysine hydroxylase and glycosyltransferase LH3	1.59E-04	0.26
Q9GZM7	Tubulointerstitial nephritis antigen-like	1.02E-03	0.27
P55268	Laminin subunit beta-2	2.27E-03	0.27
P02751	Fibronectin	1.86E-04	0.27
P07339	Cathepsin D	8.68E-05	0.29
P40189	Interleukin-6 receptor subunit beta	7.53E-04	0.3
P25391	Laminin subunit alpha-1	9.22E-03	0.3
A6NKQ9	Choriogonadotropin subunit beta variant 1	2.25E-03	0.3
P12259	Coagulation factor V	7.91E-05	0.3
Q16610	Extracellular matrix protein 1	2.14E-02	0.33
P27487	Dipeptidyl peptidase 4	9.00E-03	0.35
Q14118	Dystroglycan 1	2.94E-03	0.36
P07942	Laminin subunit beta-1	1.58E-02	0.36
Q5JS37	NHL repeat-containing protein 3	7.36E-03	0.43
Q99715	Collagen alpha-1(XII) chain	6.56E-05	0.5
Q01469	Fatty acid-binding protein 5	3.79E-02	2.24
P08238	Heat shock protein HSP 90-beta	2.66E-03	13.89

Supplementary Table 2-A: Differentially regulated secreted identified with SC at I/NI 96h.
Total: 27 proteins- Red; Downregulated proteins: 9 proteins - Green; Upregulated proteins: 18 proteins

Uniprot	Protein	p-value	Ratio I/NI 96H
P29508	Serpin B3	1.86E-02	0.00
Q92673	Sortilin-related receptor	1.85E-11	0.03
Q6ZRP7	Sulfhydryl oxidase 2	5.64E-06	0.16
O00560	Syntenin-1	9.09E-07	0.16
O00584	Ribonuclease T2	1.26E-03	0.24
P36955	Pigment epithelium-derived factor	9.83E-15	0.27
Q15109	Advanced glycosylation end product-specific receptor	2.28E-02	0.27
P98160	Basement membrane-specific heparan sulfate proteoglycan core protein	2.32E-16	0.37
Q9GZN4	Brain-specific serine protease 4	3.59E-02	0.43
P27797	Calreticulin	1.97E-05	1.54
P62937	Peptidyl-prolyl cis-trans isomerase A	1.97E-06	1.56
Q01469	Fatty acid-binding protein 5	1.49E-02	1.64
P53621	Coatomer subunit alpha	2.15E-02	1.75
P04083	Annexin A1	5.20E-03	1.76
P43490	Nicotinamide phosphoribosyltransferase	3.47E-02	1.77
P05121	Plasminogen activator inhibitor 1	5.01E-03	1.79
P06744	Glucose-6-phosphate isomerase	4.17E-14	1.89
P10599	Thioredoxin	4.86E-03	1.96
P51858	Hepatoma-derived growth factor	3.19E-04	1.96
Q99988	Growth/differentiation factor 15	7.57E-04	2.02
P31947	14-3-3 protein sigma	9.86E-03	2.21
Q969H8	Myeloid-derived growth factor	3.05E-03	2.69
Q66K79	Carboxypeptidase Z	4.09E-05	3.48
Q8N474	Secreted frizzled-related protein 1	6.48E-03	5.00
P21246	Pleiotrophin	6.98E-07	15.00
Q9BXX0	EMILIN-2	5.08E-05	18.75
Q12904	Aminoacyl tRNA synthase complex-interacting multifunctional protein 1	1.16E-11	45.00

Supplementary Table 2-B: Differentially regulated secreted identified with SC and XIC at I/NI 96h.
Total: 51 proteins- Red; Downregulated proteins: 39 -proteins - Green; Upregulated proteins: 12 proteins

Uniprot	Protein	p-value	Ratio I/NI 96H
P08253	72 kDa type IV collagenase	7.79E-04	0.09
A6NKQ9	Choriogonadotropin subunit beta variant 1	1.20E-04	0.1
P10915	Hyaluronan and proteoglycan link protein 1	7.68E-06	0.14
O75882	Attractin	8.04E-04	0.17
Q9BTY2	Plasma alpha-L-fucosidase	9.85E-04	0.17
Q16651	Prostasin	3.68E-04	0.18
Q9UBQ6	Exostosin-like 2	7.58E-04	0.19
O75487	Glypican-4	3.93E-04	0.2
Q9H1B5	Xylosyltransferase 2	1.63E-04	0.2
P05155	Plasma protease C1 inhibitor	1.23E-03	0.22
P35052	Glypican-1	1.20E-04	0.22
O00391	Sulfhydryl oxidase 1	1.48E-05	0.25
Q14050	Collagen alpha-3(IX) chain	3.64E-02	0.27
P09958	Furin	1.05E-02	0.28
Q8WVQ1	Soluble calcium-activated nucleotidase 1	1.35E-02	0.28
P14543	Nidogen-1	3.73E-04	0.29
P19021	Peptidyl-glycine alpha-amidating monooxygenase	4.97E-04	0.29
Q6EMK4	Vasorin	1.02E-02	0.29
P00746	Complement factor D	1.40E-03	0.3
Q92820	Gamma-glutamyl hydrolase	1.63E-04	0.3
P02786	Transferrin receptor protein 1	9.37E-04	0.31
P15291	Beta-1,4-galactosyltransferase 1	2.22E-03	0.31
Q03167	Transforming growth factor beta receptor type 3	6.44E-03	0.32
P50897	Palmitoyl-protein thioesterase 1	4.22E-03	0.33
P31431	Syndecan-4	1.50E-04	0.34
P05067	Amyloid-beta precursor protein	1.14E-03	0.37
P01034	Cystatin-C	5.13E-03	0.39
Q16610	Extracellular matrix protein 1	1.87E-02	0.39
Q8NCC3	Phospholipase A2 group XV	8.67E-03	0.41
P02462	Collagen alpha-1(IV) chain	6.74E-04	0.42
P07339	Cathepsin D	1.53E-02	0.43
P20908	Collagen alpha-1(V) chain	5.13E-03	0.43

O00468	Agrin	1.11E-02	0.44
P61916	NPC intracellular cholesterol transporter 2	8.40E-03	0.44
O43278	Kunitz-type protease inhibitor 1	2.23E-02	0.45
P07858	Cathepsin B	1.77E-02	0.48
Q14118	Dystroglycan 1	1.74E-02	0.49
P08572	Collagen alpha-2(IV) chain	6.30E-03	0.53
P40189	Interleukin-6 receptor subunit beta	2.26E-02	0.57
P19883	Follistatin	1.08E-02	2.02
Q8NCW5	NAD(P)H-hydrate epimerase	1.73E-02	2.02
Q96HE7	ERO1-like protein alpha	7.11E-03	2.03
P07355	Annexin A2	1.19E-02	2.06
P67809	Y-box-binding protein 1	7.11E-03	2.79
P22626	Heterogeneous nuclear ribonucleoproteins A2/B1	3.60E-04	2.94
Q07021	Complement component 1 Q subcomponent-binding protein	2.53E-04	3.04
Q15046	Lysine--tRNA ligase	1.52E-04	3.66
Q86Y38	Xylosyltransferase 1	1.08E-03	4.76
P55145	Mesencephalic astrocyte-derived neurotrophic factor	3.68E-04	5.44
O00515	Ladinin-1	2.01E-04	6.92
P05161	Ubiquitin-like protein ISG15	1.20E-04	23.71

Supplementary Table 2-C: Differentially regulated secreted identified with XIC at I/NI 96h.
Total: 64 proteins- Red; Downregulated proteins: 58 proteins - Green; Upregulated proteins: 6 proteins

Uniprot	Protein	p-value	Ratio I/NI 96H
Q14393	Growth arrest-specific protein 6	2.25E-03	0.16
P43251	Biotinidase	7.17E-03	0.24
P02751	Fibronectin	1.45E-02	0.26
Q6ISS4	Leukocyte-associated immunoglobulin-like receptor 2	1.80E-02	0.26
P02787	Serotransferrin	7.64E-03	0.27
P21926	CD9 antigen	1.07E-02	0.28
P08174	Complement decay-accelerating factor	1.01E-03	0.29
Q92484	Acid sphingomyelinase-like phosphodiesterase 3a	9.47E-03	0.29
Q9Y2E5	Epididymis-specific alpha-mannosidase	1.12E-03	0.29
P21860	Receptor tyrosine-protein kinase erbB-3	1.10E-02	0.30
Q08345	Epithelial discoidin domain-containing receptor 1	2.55E-03	0.30
P02750	Leucine-rich alpha-2-glycoprotein	2.44E-02	0.31
Q9UHI8	A disintegrin and metalloproteinase with thrombospondin motifs 1	1.91E-02	0.31
P98095	Fibulin-2	2.01E-04	0.34
O14786	Neuropilin-1	8.41E-04	0.35
O75503	Ceroid-lipofuscinosis neuronal protein 5	1.49E-02	0.35
P03973	Antileukoproteinase	3.90E-03	0.35
P20827	Ephrin-A1	2.63E-03	0.35
O75629	Protein CREG1	5.41E-03	0.37
P02771	Alpha-fetoprotein	3.50E-03	0.37
P00533	Epidermal growth factor receptor	2.12E-03	0.38
P23142	Fibulin-1	3.73E-04	0.38
P19827	Inter-alpha-trypsin inhibitor heavy chain H1	3.20E-03	0.39
P55058	Phospholipid transfer protein	3.88E-03	0.40
Q9HAT2	Sialate O-acetylesterase	7.52E-04	0.40
Q9Y264	Angiopoietin-4	2.91E-02	0.40
P01033	Metalloproteinase inhibitor 1	1.56E-03	0.41
P61769	Beta-2-microglobulin	1.80E-02	0.41
Q6H9L7	Isthmin-2	2.11E-03	0.42
Q14520	Hyaluronan-binding protein 2	9.22E-03	0.43
O60462	Neuropilin-2	3.20E-03	0.45
P04085	Platelet-derived growth factor subunit A	1.97E-02	0.46

Q9Y653	Adhesion G-protein coupled receptor G1	6.51E-03	0.46
P07711	Procathepsin L	4.15E-02	0.47
P15692	Vascular endothelial growth factor A	6.84E-03	0.47
Q96NY8	Nectin-4	1.38E-02	0.48
Q9GZM7	Tubulointerstitial nephritis antigen-like	1.04E-03	0.48
P01023	Alpha-2-macroglobulin	1.24E-02	0.49
P07942	Laminin subunit beta-1	2.18E-04	0.49
Q9NPH3	Interleukin-1 receptor accessory protein	3.15E-03	0.49
P02788	Lactotransferrin	1.20E-02	0.50
Q6PCB0	von Willebrand factor A domain-containing protein 1	2.40E-02	0.51
P22455	Fibroblast growth factor receptor 4	3.71E-02	0.52
Q5JS37	NHL repeat-containing protein 3	2.44E-02	0.52
P12111	Collagen alpha-3(VI) chain	1.47E-02	0.53
P16112	Aggrecan core protein	3.26E-02	0.53
Q96P44	Collagen alpha-1(XXI) chain	2.12E-03	0.53
P01024	Complement C3	7.19E-03	0.56
Q12884	Prolyl endopeptidase FAP	2.27E-02	0.56
Q8WUM4	Programmed cell death 6-interacting protein	1.17E-03	0.57
P04746	Pancreatic alpha-amylase	9.51E-03	0.59
P25391	Laminin subunit alpha-1	1.09E-02	0.59
Q04756	Hepatocyte growth factor activator	8.85E-04	0.61
P02774	Vitamin D-binding protein	2.65E-02	0.62
P49747	Cartilage oligomeric matrix protein	1.10E-02	0.62
P01031	Complement C5	9.22E-03	0.63
P49763	Placenta growth factor	1.53E-02	0.63
Q14624	Inter-alpha-trypsin inhibitor heavy chain H4	2.47E-02	0.63
P0DMV8	Heat shock 70 kDa protein 1A	2.26E-02	1.50
M5A8F1	Suppressyn	2.36E-02	1.61
P08238	Heat shock protein HSP 90-beta	4.49E-02	1.65
Q9NZV1	Cysteine-rich motor neuron 1 protein	2.24E-02	1.94
P09429	High mobility group protein B1	1.25E-02	3.29
P26583	High mobility group protein B2 (High mobility group protein 2) (HMG-2)	1.77E-02	3.76

Supplementary Table 3-A: Differentially regulated secreted identified both with SC at I 96h/24h.
Total: 23 proteins- Red; Downregulated proteins: 21 proteins - Green; Upregulated proteins: 2 proteins

Uniprot	Protein	p-value	Ratio I 96H/24H
Q92673	Sortilin-related receptor	3.14E-06	0.05
Q14050	Collagen alpha-3(IX) chain	4.51E-03	0.17
O75882	Attractin	2.77E-04	0.23
P53621	Coatomer subunit alpha	2.03E-18	0.26
O00560	Syntenin-1	1.34E-03	0.27
Q8WUM4	Programmed cell death 6-interacting protein	3.14E-15	0.42
Q01469	Fatty acid-binding protein 5	2.01E-08	0.43
P22626	Heterogeneous nuclear ribonucleoproteins A2/B1	9.23E-28	0.48
Q96HE7	ERO1-like protein alpha	9.33E-06	0.48
P09429	High mobility group protein B1	1.67E-14	0.5
P43490	Nicotinamide phosphoribosyltransferase	5.83E-04	0.5
Q12904	Aminoacyl tRNA synthase complex-interacting multifunctional protein 1	6.56E-04	0.51
Q15046	Lysine--tRNA ligase	4.09E-06	0.52
O60568	Multifunctional procollagen lysine hydroxylase and glycosyltransferase LH3	1.26E-02	0.55
P07355	Annexin A2	7.74E-14	0.55
P26583	High mobility group protein B2	4.07E-09	0.56
P62937	Peptidyl-prolyl cis-trans isomerase A	1.17E-14	0.57
P61916	NPC intracellular cholesterol transporter 2	6.86E-04	0.59
P67809	Y-box-binding protein 1	8.31E-05	0.61
P07237	Protein disulfide-isomerase	2.17E-09	0.64
Q16651	Prostasin	4.56E-02	0.66
P31947	14-3-3 protein sigma	3.09E-02	1.88
P03952	Plasma kallikrein	1.29E-02	5.63

Supplementary Table 3-B: Differentially regulated secreted identified both with SC and XIC at I 96h/24h. Total: 24 proteins- Red; Downregulated proteins: 2 - Green; Upregulated proteins: 22 proteins

Uniprot	Protein	p-value	Ratio I 96H/24H
Q08J23	RNA cytosine C(5)-methyltransferase NSUN2	5.70E-04	0.18
P14735	Insulin-degrading enzyme	4.10E-03	0.55
P19021	Peptidyl-glycine alpha-amidating monooxygenase	2.57E-03	2.37
Q15063	Periostin	1.62E-03	3.14
Q15582	Transforming growth factor-beta-induced protein ig-h3	3.60E-02	3.34
Q99988	Growth/differentiation factor 15	5.34E-04	3.37
Q96NY8	Nectin-4	1.24E-03	3.39
P02787	Serotransferrin	1.28E-03	3.42
P16035	Metalloproteinase inhibitor 2	3.54E-04	3.67
Q8NCC3	Phospholipase A2 group XV	1.14E-02	3.84
P07711	Procathepsin L	1.63E-03	4.28
P01008	Antithrombin-III	3.54E-04	4.47
P06396	Gelsolin	4.38E-04	4.55
O00391	Sulfhydryl oxidase 1	5.14E-04	4.73
P01031	Complement C5	1.55E-04	4.93
P01024	Complement C3	4.00E-04	5.05
P07996	Thrombospondin-1	6.69E-04	5.1
P02788	Lactotransferrin	2.62E-04	5.15
P0C0L4	Complement C4-A	7.25E-04	5.28
P04004	Vitronectin	1.01E-02	5.76
Q04756	Hepatocyte growth factor activator	1.55E-04	5.9
P05121	Plasminogen activator inhibitor 1	2.07E-04	9.8
Q08380	Galectin-3-binding protein	2.91E-04	12.14
P05161	Ubiquitin-like protein ISG15	4.97E-05	23.42

Supplementary Table 3-C: Differentially regulated secreted identified with XIC at I 96h/24h.
Total: 116 proteins- Red; Downregulated proteins: 0 - Green; Upregulated proteins: 116 proteins

Uniprot	Protein	p-value	Ratio I 96H/24H
Q00796	Sorbitol dehydrogenase	1.74E-02	1.58
Q5JS37	NHL repeat-containing protein 3	1.04E-02	1.6
P30740	Leukocyte elastase inhibitor	3.00E-02	1.62
Q99542	Matrix metalloproteinase-19	3.15E-02	1.69
Q07021	Complement component 1 Q subcomponent-binding protein	4.32E-02	1.7
Q9UBQ6	Exostosin-like 2	3.94E-02	1.71
O75487	Glypican-4	3.01E-02	1.75
Q9HAT2	Sialate O-acetylesterase	4.75E-02	1.77
O43278	Kunitz-type protease inhibitor 1	7.50E-03	1.91
P98095	Fibulin-2	6.63E-03	1.91
P20827	Ephrin-A1	3.64E-02	1.91
Q6PCB0	von Willebrand factor A domain-containing protein 1	1.39E-02	1.92
Q92820	Gamma-glutamyl hydrolase	4.54E-02	1.92
P10909	Clusterin	1.63E-02	1.92
P21741	Midkine	1.67E-02	1.93
P17693	HLA class I histocompatibility antigen, alpha chain G	4.59E-03	1.98
O43852	Calumenin	2.06E-02	1.99
P23142	Fibulin-1	5.45E-03	2.03
Q99715	Collagen alpha-1(XII) chain	2.09E-03	2.04
Q08345	Epithelial discoidin domain-containing receptor 1	2.07E-02	2.1
Q9GZM7	Tubulointerstitial nephritis antigen-like	4.77E-03	2.21
P35052	Glypican-1	1.14E-02	2.22
Q9Y240	C-type lectin domain family 11 member A	2.32E-03	2.23
P14543	Nidogen-1	5.20E-03	2.23
P15509	Granulocyte-macrophage colony-stimulating factor receptor subunit alpha	3.22E-03	2.23
Q969H8	Myeloid-derived growth factor	2.09E-02	2.23
P21246	Pleiotrophin	5.45E-03	2.29
P31431	Syndecan-4	2.96E-02	2.31
P02786	Transferrin receptor protein 1	1.13E-02	2.32
Q6H9L7	Isthmin-2	1.09E-02	2.36
P02790	Hemopexin	2.18E-02	2.4
P02461	Collagen alpha-1(III) chain	8.67E-03	2.4

Q03167	Transforming growth factor beta receptor type 3	1.98E-03	2.4
P00746	Complement factor D	2.02E-02	2.42
P08174	Complement decay-accelerating factor	4.00E-03	2.5
P20908	Collagen alpha-1(V) chain	8.82E-03	2.51
Q14624	Inter-alpha-trypsin inhibitor heavy chain H4	1.97E-02	2.51
P27797	Calreticulin	9.22E-04	2.52
P02765	Alpha-2-HS-glycoprotein	1.11E-02	2.59
P07942	Laminin subunit beta-1	1.66E-02	2.66
P10915	Hyaluronan and proteoglycan link protein 1	7.24E-03	2.69
P02649	Apolipoprotein E	7.25E-04	2.7
Q9BXJ4	Complement C1q tumor necrosis factor-related protein 3	8.25E-03	2.7
O00515	Ladinin-1	2.34E-04	2.72
P51858	Hepatoma-derived growth factor	2.89E-03	2.72
P03973	Antileukoproteinase	4.52E-02	2.77
Q02818	Nucleobindin-1	9.00E-03	2.79
P09486	SPARC	5.57E-03	2.79
P04083	Annexin A1	1.54E-03	2.8
Q96P44	Collagen alpha-1(XXI) chain	4.58E-02	2.82
P25391	Laminin subunit alpha-1	4.75E-03	2.82
Q641Q3	Meteorin-like protein	3.96E-03	2.92
P08572	Collagen alpha-2(IV) chain	1.28E-03	2.92
Q10471	Polypeptide N-acetylgalactosaminyltransferase 2	5.31E-04	2.97
P19827	Inter-alpha-trypsin inhibitor heavy chain H1	7.81E-04	2.98
P05155	Plasma protease C1 inhibitor	2.49E-02	3.02
P55145	Mesencephalic astrocyte-derived neurotrophic factor	5.69E-03	3.04
Q16610	Extracellular matrix protein 1	5.55E-03	3.06
P28799	Progranulin	8.92E-03	3.11
P55058	Phospholipid transfer protein	1.76E-03	3.14
P02749	Beta-2-glycoprotein 1	2.34E-03	3.17
P32455	Guanylate-binding protein 1	3.67E-02	3.18
P61769	Beta-2-microglobulin	8.84E-03	3.19
P19883	Follistatin	1.24E-03	3.2
P00533	Epidermal growth factor receptor	5.43E-03	3.2
P20849	Collagen alpha-1(IX) chain	2.32E-03	3.2

Q06033	Inter-alpha-trypsin inhibitor heavy chain H3	6.57E-04	3.28
P15692	Vascular endothelial growth factor A	3.57E-02	3.32
Q6UY14	ADAMTS-like protein 4	3.64E-03	3.36
P35443	Thrombospondin-4	5.36E-05	3.44
Q66K79	Carboxypeptidase Z	3.98E-04	3.44
Q92824	Proprotein convertase subtilisin/kexin type 5	1.55E-03	3.47
O60462	Neuropilin-2	1.75E-03	3.59
P20742	Pregnancy zone protein	2.21E-02	3.6
P00747	Plasminogen	6.97E-04	3.6
Q9NPH3	Interleukin-1 receptor accessory protein	2.66E-03	3.63
P12109	Collagen alpha-1(VI) chain	4.70E-03	3.69
Q13361	Microfibrillar-associated protein 5	1.67E-02	3.7
P19823	Inter-alpha-trypsin inhibitor heavy chain H2	4.20E-04	3.75
P49763	Placenta growth factor	4.00E-04	3.78
P36955	Pigment epithelium-derived factor	2.70E-03	3.79
P05452	Tetranectin	4.06E-04	3.92
Q9NZV1	Cysteine-rich motor neuron 1 protein	1.98E-03	3.95
P08123	Collagen alpha-2(I) chain	1.61E-02	3.96
Q12805	EGF-containing fibulin-like extracellular matrix protein 1	1.54E-02	4
Q12884	Prolyl endopeptidase FAP	6.71E-03	4.08
P02452	Collagen alpha-1(I) chain	2.48E-03	4.1
P18065	Insulin-like growth factor-binding protein 2	1.00E-03	4.1
P10643	Complement component C7	1.55E-03	4.14
M5A8F1	Suppressyn	2.39E-04	4.18
O76061	Stanniocalcin-2	2.81E-03	4.19
P07602	Prosaposin	7.24E-03	4.2
P02774	Vitamin D-binding protein	1.77E-04	4.25
Q8N2S1	Latent-transforming growth factor beta-binding protein 4	3.60E-03	4.32
P02675	Fibrinogen beta chain	3.50E-02	4.33
P04746	Pancreatic alpha-amylase	1.35E-03	4.45
P39060	Collagen alpha-1(XVIII) chain	2.53E-02	4.66
P43652	Afamin	4.13E-02	4.77
P00734	Prothrombin	1.75E-03	4.77
P51884	Lumican	2.78E-03	4.9

P26927	Hepatocyte growth factor-like protein	1.75E-03	4.91
P05067	Amyloid-beta precursor protein	5.31E-03	4.95
P02458	Collagen alpha-1(II) chain	5.54E-03	4.96
P03951	Coagulation factor XI	5.59E-04	5.01
P01023	Alpha-2-macroglobulin	5.70E-04	5.08
Q13822	Ectonucleotide pyrophosphatase/phosphodiesterase family member 2	6.94E-04	5.22
P02771	Alpha-fetoprotein	3.23E-04	5.24
P02750	Leucine-rich alpha-2-glycoprotein	3.59E-02	5.34
Q9Y264	Angiopoietin-4	1.16E-03	5.42
P08697	Alpha-2-antiplasmin	1.62E-04	5.5
P49747	Cartilage oligomeric matrix protein	2.91E-04	5.54
P12111	Collagen alpha-3(VI) chain	2.01E-03	5.6
P02768	Albumin	3.01E-02	5.86
P02753	Retinol-binding protein 4	4.47E-04	7.51
P29400	Collagen alpha-5(IV) chain	2.79E-03	8.64
P05543	Thyroxine-binding globulin	1.61E-02	18.3

Supplementary Table 4-A: Differentially regulated secreted identified with SC at NI 96h/24h.
Total: 44 proteins- Red; Downregulated proteins : 0 - Green; Upregulated proteins: 44 proteins

Uniprot	Protein	Ratio NI 96H/24H
P14543	Nidogen-1	1.57
Q14118	Dystroglycan 1	1.67
O43278	Kunitz-type protease inhibitor 1	1.79
Q6EMK4	Vasorin	1.81
Q16651	Prostasin	1.83
P49763	Placenta growth factor	1.96
P50897	Palmitoyl-protein thioesterase 1	2.00
Q96NY8	Nectin-4	2.00
Q03167	Transforming growth factor beta receptor type 3	2.03
P19021	Peptidyl-glycine alpha-amidating monooxygenase	2.03
P02751	Fibronectin	2.14
P10915	Hyaluronan and proteoglycan link protein 1	2.14
P30740	Leukocyte elastase inhibitor	2.16
Q13361	Microfibrillar-associated protein 5	2.25
O00391	Sulfhydryl oxidase 1	2.26
P62937	Peptidyl-prolyl cis-trans isomerase A	2.31
Q8NCC3	Phospholipase A2 group XV	2.42
P07602	Prosaposin	2.44
P07858	Cathepsin B	2.60
O75487	Glypican-4	2.67
Q9H4A4	Aminopeptidase B	2.70
Q86Y38	Xylosyltransferase 1	2.75
P07237	Protein disulfide-isomerase	2.80
Q9Y653	Adhesion G-protein coupled receptor G1	2.85
P27797	Calreticulin	2.87
P0DMV8	Heat shock 70 kDa protein 1A	2.94
O43852	Calumenin	2.94
P07355	Annexin A2	3.06
P06744	Glucose-6-phosphate isomerase	3.40
P31947	14-3-3 protein sigma	3.40
Q14050	Collagen alpha-3(IX) chain	3.60
Q8WUM4	Programmed cell death 6-interacting protein	3.84
Q96P44	Collagen alpha-1(XXI) chain	4.00
Q9H1B5	Xylosyltransferase 2	4.29
P17693	HLA class I histocompatibility antigen, alpha chain G	4.67
Q92824	Proprotein convertase subtilisin/kexin type 5	5.00
Q10471	Polypeptide N-acetylgalactosaminyltransferase 2	5.33
Q02818	Nucleobindin-1	7.00
P08253	72 kDa type IV collagenase	10.00
Q99988	Growth/differentiation factor 15	13.00
P53621	Coatomer subunit alpha	15.00
P67809	Y-box-binding protein 1	Inf
Q15109	Advanced glycosylation end product-specific receptor	Inf
Q9Y264	Angiopoietin-4	Inf

Supplementary Table 4-B: Differentially regulated secreted identified with SC and XIC at NI 96h/24h.
Total: 32 proteins - Red; Downregulated proteins: 13 proteins - Green; Upregulated proteins: 20 proteins

Uniprot	Protein	Ratio NI 96H/24H
Q92876	Kallikrein-6	0.15
P55268	Laminin subunit beta-2	0.25
Q12884	Prolyl endopeptidase FAP	0.29
P36955	Pigment epithelium-derived factor	0.5
Q86UX2	Inter-alpha-trypsin inhibitor heavy chain H5	0.52
P09958	Furin	0.55
Q6H9L7	Isthmin-2	0.56
Q08380	Galectin-3-binding protein	0.58
P07711	Procathepsin L	0.59
O00560	Syntenin-1	0.6
P00746	Complement factor D	0.62
P08174	Complement decay-accelerating factor	0.64
P55058	Phospholipid transfer protein	0.67
P08572	Collagen alpha-2(IV) chain	1.52
Q9GZN4	Brain-specific serine protease 4	1.53
Q96HE7	ERO1-like protein alpha	1.63
P05067	Amyloid-beta precursor protein	1.67
P10599	Thioredoxin	1.67
P55145	Mesencephalic astrocyte-derived neurotrophic factor	1.7
M5A8F1	Suppressyn	1.74
O76061	Stanniocalcin-2	1.78
Q99542	Matrix metalloproteinase-19	1.79
Q15046	Lysine--tRNA ligase	1.97
Q66K79	Carboxypeptidase Z	2
P21810	Biglycan	2.01
P04083	Annexin A1	2.49
P43490	Nicotinamide phosphoribosyltransferase	2.52
P41250	Glycine--tRNA ligase	2.62
A6NKQ9	Choriogonadotropin subunit beta variant 1	2.94
P22626	Heterogeneous nuclear ribonucleoproteins A2/B1	3.23
P05121	Plasminogen activator inhibitor 1	3.32
P51858	Hepatoma-derived growth factor	4.21

Supplementary Table 4-C: Differentially regulated secreted identified with XIC at NI 96h/24h.
Total: 110 proteins - Red; Downregulated proteins: 107 proteins - Green; Upregulated proteins: 3 proteins

Uniprot	Protein	Ratio NI 96H/24H
Q96PD5	N-acetylmuramoyl-L-alanine amidase	0.08
P00751	Complement factor B	0.11
P02768	Albumin	0.24
P07358	Complement component C8 beta chain	0.24
P51884	Lumican	0.24
P12111	Collagen alpha-3(VI) chain	0.24
P49747	Cartilage oligomeric matrix protein	0.25
P01008	Antithrombin-III	0.26
P0C0L4	Complement C4-A	0.27
O60568	Multifunctional procollagen lysine hydroxylase and glycosyltransferase LH3	0.27
P16112	Aggrecan core protein	0.27
P43652	Afamin	0.27
P12109	Collagen alpha-1(VI) chain	0.27
P02452	Collagen alpha-1(I) chain	0.27
P03973	Antileukoproteinase	0.27
P00740	Coagulation factor IX	0.28
P12107	Collagen alpha-1(XI) chain	0.28
P04114	Apolipoprotein B-100	0.28
Q6PCB0	von Willebrand factor A domain-containing protein 1	0.28
P06727	Apolipoprotein A-IV	0.29
P02461	Collagen alpha-1(III) chain	0.29
O15230	Laminin subunit alpha-5	0.3
O60462	Neuropilin-2	0.3
P00734	Prothrombin	0.3
P01024	Complement C3 stimulating protein	0.3
P19823	Inter-alpha-trypsin inhibitor heavy chain H2	0.3
Q06828	Fibromodulin	0.3
P26927	Hepatocyte growth factor-like protein	0.3
Q06033	Inter-alpha-trypsin inhibitor heavy chain H3	0.3
P35443	Thrombospondin-4	0.31
P04746	Pancreatic alpha-amylase	0.31
Q14624	Inter-alpha-trypsin inhibitor heavy chain H4	0.31
Q04756	Hepatocyte growth factor activator	0.31
Q15582	Transforming growth factor-beta-induced protein ig-h3	0.31
P04004	Vitronectin	0.32
P20849	Collagen alpha-1(IX) chain	0.32
P02774	Vitamin D-binding protein	0.32
P08123	Collagen alpha-2(I) chain	0.32

P01031	Complement C5	0.32
P02749	Beta-2-glycoprotein 1	0.32
P03951	Coagulation factor XI (FXI)	0.33
Q9BXJ4	Complement C1q tumor necrosis factor-related protein 3	0.33
P13591	Neural cell adhesion molecule 1	0.33
P03952	Plasma kallikrein	0.33
P08697	Alpha-2-antiplasmin	0.35
P61916	NPC intracellular cholesterol transporter 2	0.35
Q9Y2E5	Epididymis-specific alpha-mannosidase	0.35
P22303	Acetylcholinesterase	0.35
Q13822	Ectonucleotide pyrophosphatase/phosphodiesterase family member 2	0.35
P06396	Gelsolin	0.35
Q8IUL8	Cartilage intermediate layer protein 2	0.35
P19827	Inter-alpha-trypsin inhibitor heavy chain H1	0.35
P05543	Thyroxine-binding globulin	0.35
P02787	Serotransferrin	0.36
P01023	Alpha-2-macroglobulin	0.36
P02771	Alpha-fetoprotein	0.36
P12259	Coagulation factor V	0.37
P02748	Complement component C9	0.37
P01706	Immunoglobulin lambda variable 2-11	0.37
O14786	Neuropilin-1	0.37
P02765	Alpha-2-HS-glycoprotein	0.38
P10643	Complement component C7	0.38
P10909	Clusterin	0.38
P20742	Pregnancy zone protein	0.38
Q16610	Extracellular matrix protein 1	0.38
P02675	Fibrinogen beta chain	0.38
P07996	Thrombospondin-1	0.39
P02788	Lactotransferrin	0.39
P16035	Metalloproteinase inhibitor 2	0.4
P23142	Fibulin-1	0.43
P02458	Collagen alpha-1(II) chain	0.43
Q9NPH3	Interleukin-1 receptor accessory protein	0.43
P00747	Plasminogen	0.44
P20908	Collagen alpha-1(V) chain	0.44
Q9BTY2	Plasma alpha-L-fucosidase	0.44
P07942	Laminin subunit beta-1	0.44
Q14520	Hyaluronan-binding protein 2	0.44
P01033	Metalloproteinase inhibitor 1	0.44
P25391	Laminin subunit alpha-1	0.44

Q15063	Periostin	0.45
P05452	Tetranectin	0.46
P15328	Folate receptor alpha	0.47
Q99715	Collagen alpha-1(XII) chain	0.47
P40189	Interleukin-6 receptor subunit beta	0.48
O00468	Agrin	0.48
P61769	Beta-2-microglobulin	0.49
P02753	Retinol-binding protein 4	0.49
P01034	Cystatin-C	0.5
P09486	SPARC	0.51
Q92520	Protein FAM3C	0.51
P11047	Laminin subunit gamma-1	0.51
P34096	Ribonuclease 4	0.51
Q92820	Gamma-glutamyl hydrolase	0.51
O75882	Attractin	0.52
Q9HAT2	Sialate O-acetylesterase	0.52
P02786	Transferrin receptor protein 1	0.53
O00584	Ribonuclease T2	0.53
Q8WVQ1	Soluble calcium-activated nucleotidase 1	0.53
P02679	Fibrinogen gamma chain	0.54
P15509	Granulocyte-macrophage colony-stimulating factor receptor subunit alpha	0.55
Q9UBX5	Fibulin-5	0.55
Q9UBQ6	Exostosin-like 2	0.55
P35052	Glypican-1	0.58
P20827	Ephrin-A1	0.59
Q6ZRP7	Sulfhydryl oxidase 2	0.63
P21926	CD9 antigen	0.64
P00533	Epidermal growth factor receptor	0.65
P08238	Heat shock protein HSP 90-beta	1.7
Q92626	Peroxidasin homolog	1.71
P09429	High mobility group protein B1	2.1

Supplementary Table 5: Tables showing the data obtained from TOPCONS and SignalP v.5 online bioinformatic tools. TMs; Transmembrane domains, SP; Signal Peptide (TRUE/FALSE- corresponds to the indication of TOPCONS of whether there is a SP or not), Prediction; whether there is a SP identified with SignalP (values closer to 1 are a strong indicator of SP), CS Position; Cleavage site. Colour scale: **orange**- presence of Signal peptide in agreement with both softwares, **blue**- Low prediction of SP with SignalP, **white**- absence of SP in agreement with both tools. **(A)** Downregulated I/NI 24h, **(B)** Upregulated I/NI 24h, **(C)** Upregulated I/NI 96h and **(D)** Downregulated I/NI 96H.

A) Downregulated I/NI 24h						
TOPCONS				SignalP v.5		
TMs	SP	Uniprot	Protein name	Prediction	SP(Sec/SPI)	CS Position
7	TRUE	Q9Y653	Adhesion G-protein coupled receptor G1	SP(Sec/SPI)	0.992237	CS pos: 25-26. AHG-RG. Pr: 0.9011
3	TRUE	O00391	Sulfhydryl oxidase 1	SP(Sec/SPI)	0.998622	CS pos: 29-30. ANA-AP. Pr: 0.9676
2	TRUE	P0C0L4	Complement C4-A	SP(Sec/SPI)	0.689987	CS pos: 17-18. TLS-LQ. Pr: 0.2427
2	FALSE	Q6ZRP7	Sulfhydryl oxidase 2	OTHER	0.438486	
2	FALSE	O75882	Attractin	OTHER	0.089563	
2	FALSE	P27487	Dipeptidyl peptidase 4	OTHER	0.421859	
1	TRUE	P01023	Alpha-2-macroglobulin	SP(Sec/SPI)	0.997613	CS pos: 23-24. TDA-SV. Pr: 0.7113
1	TRUE	Q9BTY2	Plasma alpha-L-fucosidase	SP(Sec/SPI)	0.99687	CS pos: 30-31. AHS-AT. Pr: 0.6652
1	TRUE	Q9NPH3	Interleukin-1 receptor accessory protein	SP(Sec/SPI)	0.962803	CS pos: 20-21. SDA-SE. Pr: 0.8583
1	TRUE	Q8NCC3	Phospholipase A2 group XV	SP(Sec/SPI)	0.983371	CS pos: 33-34. ALP-AG. Pr: 0.7029
1	TRUE	P35052	Glypican-1	SP(Sec/SPI)	0.996416	CS pos: 23-24. ARG-DP. Pr: 0.7453
1	TRUE	P19021	Peptidyl-glycine alpha-amidating monooxygenase	SP(Sec/SPI)	0.957733	CS pos: 20-21. CLA-FR. Pr: 0.8994
1	FALSE	Q8WVQ1	Soluble calcium-activated nucleotidase 1	OTHER	0.000785	
1	TRUE	P20827	Ephrin-A1	SP(Sec/SPI)	0.994691	CS pos: 18-19. AAA-DR. Pr: 0.8767
1	TRUE	P13591	Neural cell adhesion molecule 1	SP(Sec/SPI)	0.928245	CS pos: 19-20. AVS-LQ. Pr: 0.5837
1	FALSE	Q13822	Ectonucleotide pyrophosphatase/phosphodiesterase family member 2	SP(Sec/SPI)	0.57647	CS pos: 27-28. CLG-FT. Pr: 0.3431
1	TRUE	Q14520	Hyaluronan-binding protein 2	SP(Sec/SPI)	0.935753	CS pos: 23-24. ACG-FS. Pr: 0.5507
1	TRUE	P31431	Syndecan-4	SP(Sec/SPI)	0.981084	CS pos: 20-21. AES-IR. Pr: 0.5193
1	TRUE	P20742	Pregnancy zone protein	SP(Sec/SPI)	0.993736	CS pos: 23-24. SDS-NS. Pr: 0.3529
1	TRUE	Q6EMK4	Vasorin	SP(Sec/SPI)	0.999759	CS pos: 23-24. VQG-CP. Pr: 0.9901
1	TRUE	O60462	Neuropilin-2	SP(Sec/SPI)	0.997716	CS pos: 22-23. VRG-QP. Pr: 0.9871

1	FALSE	P15291	Beta-1,4-galactosyltransferase 1	OTHER	0.00995	
1	TRUE	O43278	Kunitz-type protease inhibitor 1	SP(Sec/SPI)	0.987716	CS pos: 35-36. TQA-GP. Pr: 0.9038
1	TRUE	P05156	Complement factor I	SP(Sec/SPI)	0.998179	CS pos: 23-24. TYT-SQ. Pr: 0.3759
1	TRUE	O75487	Glypican-4	SP(Sec/SPI)	0.997763	CS pos: 22-23. LLA-AE. Pr: 0.6786
1	TRUE	P08174	Complement decay-accelerating factor	SP(Sec/SPI)	0.991923	CS pos: 34-35. VWG-DC. Pr: 0.9414
1	TRUE	Q08345	Epithelial discoidin domain-containing receptor 1	SP(Sec/SPI)	0.985353	CS pos: 20-21. GDA-DM. Pr: 0.7897
1	FALSE	P02786	Transferrin receptor protein 1	OTHER	0.002869	
1	TRUE	Q03167	Transforming growth factor beta receptor type 3	SP(Sec/SPI)	0.986518	CS pos: 20-21. ATA-GP. Pr: 0.6717
1	TRUE	Q16651	Prostasin	SP(Sec/SPI)	0.941106	CS pos: 30-31. TGA-EG. Pr: 0.4271
1	TRUE	P00533	Epidermal growth factor receptor	SP(Sec/SPI)	0.996929	CS pos: 24-25. SRA-LE. Pr: 0.8895
1	TRUE	P15509	Granulocyte-macrophage colony-stimulating factor receptor subunit alpha	SP(Sec/SPI)	0.7958	CS pos: 19-20. AFL-LI. Pr: 0.4553
1	TRUE	Q96NY8	Nectin-4	SP(Sec/SPI)	0.960709	CS pos: 31-32. CPA-GE. Pr: 0.5313
1	TRUE	P15328	Folate receptor alpha	SP(Sec/SPI)	0.997812	CS pos: 22-23. GEA-QT. Pr: 0.7552
1	TRUE	P05067	Amyloid-beta precursor protein	SP(Sec/SPI)	0.998792	CS pos: 17-18. ARA-LE. Pr: 0.9796
1	TRUE	Q92673	Sortilin-related receptor	SP(Sec/SPI)	0.966016	CS pos: 28-29. ALC-EV. Pr: 0.9059
1	TRUE	P40189	Interleukin-6 receptor subunit beta	SP(Sec/SPI)	0.996474	CS pos: 22-23. STG-EL. Pr: 0.6789
1	TRUE	Q14118	Dystroglycan 1	SP(Sec/SPI)	0.889937	CS pos: 27-28. VMA-QS. Pr: 0.4630

B) Upregulated I/NI 24h

TOPCONS				SignalP v.5		
TMs	SP	Uniprot	Protein name	Prediction	SP(Sec/SPI)	CS Position
1	TRUE	Q9NZV1	Cysteine-rich motor neuron 1 protein	SP(Sec/SPI)	0.99674	CS pos: 34-35. TRA-LV. Pr: 0.9499
1	TRUE	P17693	HLA class I histocompatibility antigen, alpha chain G	SP(Sec/SPI)	0.95945	CS pos: 24-25. TWA-GS. Pr: 0.8409
1	FALSE	M5A8F1	Suppressyn	SP(Sec/SPI)	0.611839	CS pos: 39-40. STA-AP. Pr: 0.4750

C) Upregulated I/NI 96h						
TOPCONS				SignalP v.5		
TMs	SP	Uniprot	Protein name	Prediction	SP(Sec/SPI)	CS Position
1	FALSE	M5A8F1	Suppressyn	SP(Sec/SPI)	0.611839	CS pos: 39-40. STA-AP. Pr: 0.4750
1	TRUE	Q9NZV1	Cysteine-rich motor neuron 1 protein	SP(Sec/SPI)	0.99674	CS pos: 34-35. TRA-LV. Pr: 0.9499

D) Downregulated I/NI 96h						
TOPCONS				SignalP v.5		
TMs	SP	Uniprot	Protein name	Prediction	SP(Sec/SPI)	CS Position
7	TRUE	Q9Y653	Adhesion G-protein coupled receptor G1	SP(Sec/SPI)	0.992237	CS pos: 25-26. AHG-RG. Pr: 0.9011
4	FALSE	P21926	CD9 antigen	OTHER	0.005398	
3	TRUE	O00391	Sulfhydryl oxidase 1	SP(Sec/SPI)	0.998622	CS pos: 29-30. ANA-AP. Pr: 0.9676
2	FALSE	Q6ZRP7	Sulfhydryl oxidase 2	OTHER	0.438486	
2	FALSE	O75882	Attractin	OTHER	0.089563	
1	TRUE	Q92673	Sortilin-related receptor	SP(Sec/SPI)	0.966016	CS pos: 28-29. ALC-EV. Pr: 0.9059
1	TRUE	Q15109	Advanced glycosylation end product-specific receptor	SP(Sec/SPI)	0.994816	CS pos: 23-24. VGA-QN. Pr: 0.8421
1	TRUE	Q9BTY2	Plasma alpha-L-fucosidase	SP(Sec/SPI)	0.99687	CS pos: 30-31. AHS-AT. Pr: 0.6652
1	TRUE	Q16651	Prostasin	SP(Sec/SPI)	0.941106	CS pos: 30-31. TGA-EG. Pr: 0.4271
1	TRUE	O75487	Glypican-4	SP(Sec/SPI)	0.997763	CS pos: 22-23. LLA-AE. Pr: 0.6786
1	TRUE	P35052	Glypican-1	SP(Sec/SPI)	0.996416	CS pos: 23-24. ARG-DP. Pr: 0.7453
1	TRUE	P09958	Furin	SP(Sec/SPI)	0.987121	CS pos: 26-27. AQG-QK. Pr: 0.3910
1	FALSE	Q8WVQ1	Soluble calcium-activated nucleotidase 1	OTHER	0.000785	
1	TRUE	P19021	Peptidyl-glycine alpha-amidating monooxygenase	SP(Sec/SPI)	0.957733	CS pos: 20-21. CLA-FR. Pr: 0.8994
1	TRUE	Q6EMK4	Vasorin	SP(Sec/SPI)	0.999759	CS pos: 23-24. VQG-CP. Pr: 0.9901
1	FALSE	P02786	Transferrin receptor protein 1	OTHER	0.002869	
1	FALSE	P15291	Beta-1,4-galactosyltransferase 1	OTHER	0.00995	
1	TRUE	Q03167	Transforming growth factor beta receptor type 3	SP(Sec/SPI)	0.986518	CS pos: 20-21. ATA-GP. Pr: 0.6717
1	TRUE	P31431	Syndecan-4	SP(Sec/SPI)	0.981084	CS pos: 20-21. AES-IR. Pr: 0.5193
1	TRUE	P05067	Amyloid-beta precursor protein	SP(Sec/SPI)	0.998792	CS pos: 17-18. ARA-LE. Pr: 0.9796
1	TRUE	Q8NCC3	Phospholipase A2 group XV	SP(Sec/SPI)	0.983371	CS pos: 33-34. ALP-AG. Pr: 0.7029
1	TRUE	O43278	Kunitz-type protease inhibitor 1	SP(Sec/SPI)	0.987716	CS pos: 35-36. TQA-GP.

						Pr: 0.9038
1	TRUE	Q14118	Dystroglycan 1	SP(Sec/SPI)	0.889937	CS pos: 27-28. VMA-QS. Pr: 0.4630
1	TRUE	P40189	Interleukin-6 receptor subunit beta	SP(Sec/SPI)	0.996474	CS pos: 22-23. STG-EL. Pr: 0.6789
1	TRUE	P08174	Complement decay-accelerating factor	SP(Sec/SPI)	0.991923	CS pos: 34-35. VWG-DC. Pr: 0.9414
1	TRUE	P21860	Receptor tyrosine-protein kinase erbB-3	SP(Sec/SPI)	0.948293	CS pos: 19-20. ARG-SE. Pr: 0.7467
1	TRUE	Q08345	Epithelial discoidin domain-containing receptor 1	SP(Sec/SPI)	0.985353	CS pos: 20-21. GDA-DM. Pr: 0.7897
1	FALSE	Q9UHI8	A disintegrin and metalloproteinase with thrombospondin motifs 1	SP(Sec/SPI)	0.687348	CS pos: 51-52. ALG-RP. Pr: 0.3618
1	TRUE	O14786	Neuropilin-1	SP(Sec/SPI)	0.99912	CS pos: 21-22. AGA-FR. Pr: 0.9317
1	FALSE	O75503	Ceroid-lipofuscinosis neuronal protein 5	OTHER	0.326765	
1	TRUE	P20827	Ephrin-A1	SP(Sec/SPI)	0.994691	CS pos: 18-19. AAA-DR. Pr: 0.8767
1	TRUE	P00533	Epidermal growth factor receptor	SP(Sec/SPI)	0.996929	CS pos: 24-25. SRA-LE. Pr: 0.8895
1	TRUE	Q14520	Hyaluronan-binding protein 2	SP(Sec/SPI)	0.935753	CS pos: 23-24. ACG-FS. Pr: 0.5507
1	TRUE	O60462	Neuropilin-2	SP(Sec/SPI)	0.997716	CS pos: 22-23. VRG-QP. Pr: 0.9871
1	TRUE	Q96NY8	Nectin-4	SP(Sec/SPI)	0.960709	CS pos: 31-32. CPA-GE. Pr: 0.5313
1	TRUE	P01023	Alpha-2-macroglobulin	SP(Sec/SPI)	0.997613	CS pos: 23-24. TDA-SV. Pr: 0.7113
1	TRUE	Q9NPH3	Interleukin-1 receptor accessory protein	SP(Sec/SPI)	0.962803	CS pos: 20-21. SDA-SE. Pr: 0.8583
1	TRUE	P22455	Fibroblast growth factor receptor 4	SP(Sec/SPI)	0.999483	CS pos: 21-22. VLS-LE. Pr: 0.8501

Supplementary Table 6: Down-regulated biological processes identified using the DAVID database (p-value < 0.05), based on SC and XIC quantification methods. Black boxes denote the absence of a function at specific time points. The protein count indicates the number of proteins associated with each biological process. Table is sorted based on p-value of I/NI 96h.

DOWNREGULATED	I/NI 24h			I/NI 96h		
Biological Process	Protein count	p-value	Fold Enrichment	Protein count	**p-value**	Fold Enrichment
Angiogenesis	9	1.17E-05	8.25	12	**1.21E-10**	16.13
Host-virus interaction	14	1.87E-03	2.66	14	**3.44E-05**	3.91
Cell adhesion	26	1.63E-14	6.81	11	**1.98E-04**	4.23
Complement pathway	10	3.53E-12	36.92	4	**7.72E-04**	21.66
Complement alternate pathway	4	1.17E-04	39.76	3	**1.99E-03**	43.73
Innate immunity	15	3.26E-06	4.61	8	**5.80E-03**	3.61
Inflammatory response	9	1.07E-04	6.06	5	**1.74E-02**	4.94
Immunity	20	6.62E-05	2.76	11	**2.11E-02**	2.23
Blood coagulation	6	3.77E-05	15.51			
Hemostasis	6	3.77E-05	15.51			
Acute phase	4	5.21E-04	24.61			
Mineral balance	2	3.03E-02	64.61			
Tissue remodeling	2	3.03E-02	64.61			

Supplementary Table 7: Up-regulated biological processes identified using the DAVID database (p-value < 0.05), based on SC and XIC quantification methods. Black boxes denote the absence of a function at specific time points. The protein count indicates the number of proteins associated with each biological process. Table is sorted based on p-value of I/NI 96h.

UPREGULATED	I/NI 24h			I/NI 96h		
Biological Process	Protein count	p-value	Fold Enrichment	Protein count	**p-value**	Fold Enrichment
Host-virus interaction	7	9.05E-03	3.66	8	**4.89E-04**	5.15
Inflammatory response	5	1.73E-03	9.25	4	**8.29E-03**	9.11
Innate immunity	6	5.16E-03	5.08	5	**1.25E-02**	5.21
Stress response				3	**2.53E-02**	11.61
Apoptosis	6	1.57E-02	3.87	5	**3.07E-02**	3.97
Immunity	7	3.81E-02	2.66			

Supplementary Table 8: Downregulated KEGG pathways identified using the DAVID database (p-value < 0.05), based on SC and XIC quantification methods. Black boxes denote the absence of a function at specific time points. The protein count indicates the number of proteins associated with each biological process. Table is sorted based on p-value of I/NI 96h.

DOWNREGULATED	I/NI 24h			I/NI96h		
KEGG Pathways	Protein count	p-value	Fold Enrichment	Protein count	**p-value**	Fold Enrichment
ECM-receptor interaction	24	3.50E-27	26.49	12	**4.95E-11**	17.4
PI3K-Akt signalling pathway	23	4.08E-12	6.29	16	**5.48E-08**	5.75
Focal adhesion	22	3.96E-16	10.65	12	**3.17E-07**	7.63
Lysosome	8	3.50E-04	5.95	8	**6.08E-05**	7.82
Proteoglycans in cancer	11	3.69E-05	5.27	9	**1.54E-04**	5.66
Complement and coagulation cascades	17	1.40E-16	19.42	6	**4.81E-04**	9
Human papillomavirus infection	21	5.96E-11	6.23	10	**8.56E-04**	3.9
AGE-RAGE signalling pathway in diabetic complications	6	3.27E-03	5.89	6	**9.58E-04**	7.74
Amoebiasis	13	3.21E-10	12.52	6	**1.05E-03**	7.59
Protein digestion and absorption	15	1.24E-12	14.3	6	**1.09E-03**	7.52
HIF-1 signalling pathway				6	**1.41E-03**	7.1
MAPK signalling pathway				9	**1.95E-03**	3.86
Pathways in cancer	14	2.36E-03	2.59	12	**2.08E-03**	2.92
EGFR tyrosine kinase inhibitor resistance				5	**3.03E-03**	8.17
Fluid shear stress and atherosclerosis				6	**4.07E-03**	5.57
Rap1 signalling pathway				7	**5.17E-03**	4.3
Small cell lung cancer	9	3.56E-06	9.61	5	**5.24E-03**	7.01
Ras signalling pathway				7	**9.01E-03**	3.83
Relaxin signalling pathway	6	9.54E-03	4.57	5	**1.67E-02**	5
Coronavirus disease - COVID-19	10	5.14E-04	4.23	6	**3.17E-02**	3.34
Bladder cancer				3	**3.89E-02**	9.44
Staphylococcus aureus infection	7	3.92E-04	7.16			
Toxoplasmosis	6	5.11E-03	5.31			
Pertussis	5	7.08E-03	6.46			
Phagosome	6	1.83E-02	3.88			
Viral myocarditis	4	2.97E-02	5.86			
Platelet activation	5	3.61E-02	3.96			
Systemic lupus erythematosus	5	4.90E-02	3.58			

Supplementary Table 9: Upregulated KEGG pathways identified using the DAVID database (p-value < 0.05), based on SC and XIC quantification methods. Black boxes denote the absence of a function at specific time points. The protein count indicates the number of proteins associated with each biological process. Table is sorted based on p-value of I/NI 96h.

UPREGULATED	I/NI 24h			I/NI 96h		
KEGG Pathways	Protein count	p-value	Fold Enrichment	Protein count	**p-value**	Fold Enrichment
Protein processing in endoplasmic reticulum	4	1.12E-02	8.14	4	**5.74E-03**	10.17
Antigen processing and presentation	3	1.95E-02	13.3	3	**1.24E-02**	16.62
Necroptosis				3	**4.69E-02**	8.15

Résumé étendu en français

Chapitre 1 - Conclusions sur la phase chronique de *L. monocytogenes* - Infection des cellules trophoblastiques

Cette étude vise à permettre de mieux comprendre les mécanismes par lesquels *L. monocytogenes* peut établir et maintenir une infection chronique dans les cellules du trophoblaste. Grâce à l'analyse protéomique, les stratégies employées par *L. monocytogenes* pour manipuler les environnements cellulaires de l'hôte ont été suggérées, ce qui permet de comprendre comment ce pathogène peut persister dans la dormance.

Régulation à la baisse et à la hausse de processus biologiques clés

L'un des résultats les plus remarquables est la diminution significative de l'angiogenèse et de la voie de signalisation HIF-1α au cours de l'infection chronique. L'angiogenèse est étroitement régulée par le HIF-1α et la suppression observée des deux voies pourrait probablement perturber l'homéostasie cellulaire normale, entraver la surveillance immunitaire et permettre à *L. monocytogenes* d'échapper à la détection (Osherov et Ben-Ami, 2016 ; Knight et Stanley, 2019). En inhibant l'angiogenèse, le *L. monocytogenes* peut limiter la formation de vaisseaux sanguins et l'infiltration de cellules immunitaires dans les tissus infectés, réduisant ainsi la clairance à médiation immunitaire (Osherov et Ben-Ami, 2016).

En outre, les voies impliquées dans la signalisation cellulaire et la régulation immunitaire, telles que la cascade de signalisation MAPK, ont également été modifiées. La voie de signalisation MAPK, essentielle pour l'inflammation et les réponses immunitaires, était spécifiquement régulée à la baisse pendant la phase chronique de l'infection, ce qui pourrait favoriser la survie des cellules dans les trophoblastes infectés en inhibant les réponses pro-inflammatoires (Zhong et Kyriakis, 2017 ; Nandi et Aroeti, 2023). Dans l'ensemble, il a été démontré que les bactéries pouvaient se comporter différemment dans la phase aiguë ou chronique des infections et de nombreux pathogènes, tels que les entéropathogènes ou les pathogènes comme *Mtb* et *Helicobacter pylori*, se sont révélés manipuler les MAPK et les voies de signalisation pour établir un environnement favorable à une infection à long terme (Koul et al., 2004 ; Brodsky et Medzhitov, 2009 ; Muller et al., 2011 ; Hashino et al., 2015).

Modulation des réponses immunitaires de l'hôte

L'étude met en évidence la capacité de *L. monocytogenes* à moduler les réponses immunitaires dans les cellules du trophoblaste au cours d'une infection chronique. Des similitudes ont été observées entre ce modèle d'infection et l'infection chronique des hépatocytes, telle que décrite par Descoeudres et al. en 2021, notamment en ce qui concerne la manipulation des voies immunitaires telles que les cascades du complément et de la coagulation. Cependant, dans les cellules du trophoblaste, ces voies ont été fortement régulées à la baisse pendant la phase aiguë, suivie d'une phase continue mais une diminution de l'expression moins intense vers la phase chronique. Cela pourrait suggérer que la dynamique de la modulation de la réponse immunitaire pourrait différer en fonction du tissu infecté. La régulation la baisse des voies immunitaires, du complément et de la coagulation au cours de l'infection aiguë peut aider *L. monocytogenes* à éviter une détection immunitaire précoce, tandis qu'une réactivation plus légère au cours de l'infection chronique pourrait potentiellement permettre au pathogène de persister sans induire une réponse inflammatoire robuste.

En outre, les données suggèrent que *L. monocytogenes* peut moduler son interaction avec le système immunitaire de l'hôte pour maintenir un équilibre qui évite une évasion immunitaire complète mais limite les défenses de l'hôte. En particulier, la suppression potentielle de l'angiogenèse et des voies de signalisation immunitaire pourrait témoigner d'une stratégie visant à minimiser le recrutement de cellules immunitaires dans le tissu infecté, facilitant l'établissement d'un environnement favorable à une infection persistante qui pourrait servir réservoir pour des infections récurrentes dans les tissus maternels (Bakardjiev et al., 2005). Les analyses transcriptomiques des placentas prématurés infectés par *L. monocytogenes* mettent également en évidence des altérations des signatures inflammatoires, soulignant l'impact du pathogène sur l'équilibre immunitaire materno-fœtal (Johnson et al., 2020). Il pourrait être essentiel de comprendre cette dynamique immunitaire pour mettre au point des interventions thérapeutiques visant à réduire la capacité de l'agent pathogène à persister, afin d'éviter à la mère et au fœtus des complications pendant la grossesse.

Résumé de l'infection chronique à *L. monocytogenes*

L'infection chronique par *L. monocytogenes* dans les cellules du trophoblaste révèle une manipulation potentielle des processus de l'hôte, y compris la diminution de l'expression de

l'angiogenèse, de la signalisation immunitaire et des voies de communication cellulaire, qui sont cruciales pour la surveillance immunitaire et l'homéostasie tissulaire. La capacité de l'agent pathogène à supprimer ces processus clés contribue probablement à sa capacité à établir une infection dormante et persistante au sein de l'hôte. Ces résultats posent des défis importants pour le traitement et l'éradication de *L. monocytogenes*, en particulier dans les tissus vulnérables. La compréhension des mécanismes moléculaires à l'origine de la persistance de *L. monocytogenes*, y compris sa modulation de l'angiogenèse et des voies de signalisation immunitaire, pourrait être essentielle pour le développement de stratégies de lutte contre les infections chroniques.

Chapitre 2 - Conclusions sur l'état de la VBNC de *L. monocytogenes*

Notre étude permet de mieux comprendre l'entrée potentielle de *L. monocytogenes* dans un état VBNC, en particulier dans des conditions de privation de nutriments. Ce phénomène a des implications cruciales pour comprendre persistance et la pathogénicité de *L. monocytogenes*, en particulier dans les environnements où les bactéries sont exposées à des conditions de stress qui pourraient autrement être mortelles, comme dans les FPE.

Preuve protéomique de la transition d'état de la VBNC

L'analyse protéomique réalisée sur une période de 28 jours dans des conditions de privation de nutriments a révélé des schémas distincts qui suggèrent que *L. monocytogenes* peut entrer dans un état VBNC comme stratégie de survie (Claessen et Errington, 2019 ; Carvalho et al., 2024). L'observation d'une importante augmentation de l'expression et à la baisse de diverses protéines, en particulier après la J14, indique une réponse dynamique à un stress environnemental prolongé. La diminution de l'expression des protéines impliquées dans le métabolisme de la paroi cellulaire est particulièrement remarquable. Cette diminution de l'expression s'aligne sur des découvertes antérieures selon lesquelles la modification de la paroi cellulaire est une caractéristique des bactéries entrant dans un état VBNC, comme cela a été observé chez d'autres espèces telles que *Bacillus*, *Vibrio*, les espèces *Enterococci* et *E. coli* (Baker et al., 1983 ; Signoretto et al., 2000 ; Signoretto et al., 2002 ; Dominguez-Cuevas et al., 2012 ; Kawai et Errington, 2023). Les données de l'étude suggèrent que *L. monocytogenes* pourrait également employer une stratégie d'altération de la paroi cellulaire, conduisant potentiellement à la formation de bactéries déficientes en paroi cellulaire (CWD), qui sont plus résistantes aux stress environnementaux (Claessen et Errington, 2019 ; Carvalho et al., 2024). Cet état d'activité métabolique réduite et de structure cellulaire altérée peut aider *L. monocytogenes* à conserver de l'énergie et des ressources, soutenant ainsi sa viabilité sur des périodes prolongées dans des environnements défavorables (Claessen et Errington, 2019 ; Carvalho et al., 2024).

Rôle des autolysines dans l'entrée dans la VBNC

L'étude met en évidence la diminution de l'expression des autolysines, dont NamA, qui sont des enzymes responsables de la dégradation du peptidoglycane (Holtje et al., 1998 ; Bierne et Cossart, 2017). L'activité réduite, c'est-à-dire la diminution de l'expression, de ces protéines pourrait faciliter

la transition vers un état VBNC en permettant des transitions morphologiques de forme, par exemple de la forme de bâtonnet à celle de cocci, agissant comme un mécanisme d'adaptation bactérienne (Claessen et Errington, 2019 ; Carvalho et al., 2024). Par exemple, le lien entre NamA et la transition plus lente vers un état VBNC suggère un rôle régulateur de cette protéine dans le maintien de l'intégrité de *L. monocytogenes* pendant le stress (Carvalho et al., 2024). L'implication potentielle d'autres régulateurs autolytiques et facteurs de transcription, comme discuté dans thèse, soutient encore l'idée que *L. monocytogenes* peut moduler son métabolisme de la paroi cellulaire en réponse à un stress prolongé, entrant potentiellement dans un état dormant (Carvalho et al., 2024). Les données protéomiques montrent une diminution de l'expression cohérente des protéines associées au métabolisme de la paroi cellulaire tout au long de l'étude, ce qui renforce l'hypothèse selon laquelle ces changements font partie intégrante de la stratégie de survie de la bactérie en cas de privation de nutriments.

Implications de l'état VBNC pour la pathogénicité et la survie

Le passage à l'état de VBNC a de profondes implications pour la pathogénicité de *L. monocytogenes*. Sous cette forme dormante, la bactérie est moins détectable par les techniques de culture standard, ce qui représente un défi majeur pour la sécurité alimentaire (Wideman et al., 2021 ; Aryapetyan et al., 2018 ; Lotoux et al., 2022). Cette persistance est particulièrement préoccupante dans les EPF, où *L. monocytogenes* peut survivre dans un état dormant jusqu'à ce que les conditions deviennent favorables à la réactivation et à la croissance, entraînant potentiellement une contamination et des épidémies de listériose. Notre étude a également observé l'augmentation globale du système PTS, qui est associé à la conservation de l'énergie et à l'adaptation au stress. Cette implication du PTS dans la transition vers un état VBNC met en évidence les mécanismes de régulation sophistiqués que *L. monocytogenes* emploie pour survivre dans des conditions de privation de nutriments (Gray et al., 2021). Cependant, le mutant de délétion de notre étude n'a pas montré d'effet significatif concernant l'entrée de *L. monocytogenes* dans l'état VBNC.

Résumé de l'état de la VBNC de *L. monocytogenes*

En conclusion, notre analyse protéomique a étudié le comportement de *L. monocytogenes* lors de sa transition vers l'état VBNC dans des conditions de privation de nutriments. Plus précisément, la bactérie régule à la baisse les protéines de virulence et de synthèse de la paroi cellulaire tout en régulant à la hausse les protéines impliquées dans les voies de piégeage des nutriments et de

réponse au stress. Cette modulation stratégique permet à *L. monocytogenes* d'optimiser sa survie dans des environnements pauvres en nutriments, ce qui suggère que l'état VBNC fonctionne comme un mécanisme clé de persistance. Les recherches futures devraient viser à identifier d'autres marqueurs protéomiques essentiels à cette transition et à examiner les interventions susceptibles d'inhiber l'entrée ou le maintien de l'état VBNC, avec des implications significatives pour la santé publique et la sécurité alimentaire.

Conclusions sur l'état de dormance de *L. monocytogenes* dans les contextes de l'hôte et de l'environnement - Chapitres 1 et 2

Tout d'abord, les résultats combinés des chapitres 1 et 2 offrent une vue d'ensemble des stratégies de survie de *L. monocytogenes* dans des conditions d'infection et de privation de nutriments, en mettant l'accent sur la capacité de l'agent pathogène à persister dans les cellules de l'hôte et dans l'environnement. Dans l', ces deux chapitres fournissent des informations protéomiques sur la possibilité pour *L. monocytogenes* a) d'échapper aux réponses immunitaires et b) d'entrer dans un état VBNC en cas de stress.

Dans le chapitre 1, nous avons exploré le sécrétome des cellules trophoblastes infectées. Les données ont révélé que la sécrétion de l'hôte est régulée à la baisse pendant les phases aiguës (24h p.i.) et chroniques (96h p.i.). En particulier, de nombreux systèmes de transduction des signaux intermédiaires, tels que les voies de signalisation MAPK, Ras, Rap1, EGFR et Shear stress sont régulés à la baisse spécifiquement à 96h p.i., ce qui permet probablement à *L. monocytogenes* d'échapper à la détection et d'établir une infection persistante dans la niche du trophoblaste (Nandi et Aroeti, 2023). De même, on pense que des pathogènes tels que *Mtb* et *H. pylori* manipulent les réponses immunitaires de l'hôte pour établir un état d'infection persistant (Koul et al., 2004 ; Muller et al., 2011). Le chapitre 2 se concentre sur l'état VBNC de *L. monocytogenes*, une forme non cultivable mais viable qui permet à l'agent pathogène de survivre dans des environnements dépourvus de nutriments tels que l'eau minérale filtrée et autoclavée. L'analyse protéomique de *L. monocytogenes* dans ces conditions met en évidence la capacité de l'agent pathogène à conserver de l'énergie et à renforcer les mécanismes de réponse au stress afin de maintenir sa viabilité sur une période prolongée. La faible activité métabolique de *L. monocytogenes*, associée à la augmentation de l'expression des protéines de stress, reflète une stratégie de survie de type dormance qui représente un défi majeur pour la détection et le contrôle des bactéries (Claessen et Errington, 2019 ; Carvalho et al., 2024).

Les deux chapitres soulignent la capacité d'adaptation de *L. monocytogenes*, que ce soit dans le contexte d'une infection de l'hôte ou en réponse à des stress environnementaux. Le chapitre 1 émet l'hypothèse que l'agent pathogène échappe non seulement à la détection immunitaire, mais qu'il manipule également les processus cellulaires de l'hôte pour proliférer au fil du temps. De même,

dans le chapitre 2, l'état VBNC de *L. monocytogenes* représente non seulement une approche protéomique de la stratégie de survie de l'état VBNC, mais il offre également une validation des études précédentes où il est confirmé que les réponses au stress et les modifications de la paroi cellulaire, en particulier la perte de la paroi cellulaire, contribuent à la transition de *L. monocytogenes* vers l'état VBNC (Claessen et Errington, 2019 ; Carvalho et al., 2024).

L'intégration des résultats de ces deux chapitres pourrait souligner plusieurs aspects de la persistance de *L. monocytogenes*.

Tout d'abord, la capacité du pathogène à moduler ses stratégies d'évasion métabolique et immunitaire est essentielle à sa survie à long terme. Dans le chapitre 1, *L. monocytogenes* pourrait conduire à une suppression immunitaire et à une modulation sécrétoire pour maintenir une infection chronique, tandis que dans le chapitre 2, il conserve de l'énergie, renforce les réponses au stress et parvient à s'adapter aux nouveaux défis environnementaux par le biais de changements phénotypiques. Ces stratégies parallèles suggèrent que *L. monocytogenes* est très adaptable, capable de s'adapter aux conditions intracellulaires et extracellulaires pour assurer sa survie. En outre, l'identification de biomarqueurs potentiels dans les états d'infection et de VBNC offre de nouvelles possibilités de détection et de lutte contre *L. monocytogenes*. Dans les cellules trophoblastes infectées, les protéines spécifiques à la phase d'infection chronique peuvent servir de marqueurs diagnostiques pour les infections persistantes, contribuant ainsi au développement de thérapies ciblées. Par ailleurs, les protéines de stress identifiées dans l'état VBNC pourraient constituer des candidats appropriés pour le développement de méthodes de détection plus sensibles pour le contrôle de la sécurité des aliments et de l'eau.

Enfin, les idées combinées de ces chapitres soulignent l'importance de développer des stratégies globales pour lutter contre la persistance de *L. monocytogenes* dans les environnements cliniques et environnementaux. Dans les infections cliniques, le ciblage des mécanismes d'évasion immunitaire de l'agent pathogène peut offrir de nouvelles approches thérapeutiques pour éliminer les infections chroniques. Dans les systèmes environnementaux, l'amélioration des méthodes de détection des populations de Listeria VBNC pourrait renforcer les protocoles de sécurité alimentaire et réduire le risque d'épidémies.

En conclusion, les travaux présentés dans les chapitres 1 et 2 permettent de comprendre en détail les mécanismes de persistance de *L. monocytogenes* dans différentes niches. Ces recherches démontrent notamment que l'organisme peut ajuster avec précision sa réponse moléculaire à différentes conditions environnementales, afin d'obtenir un phénotype persistant. Cela facilite la persistance dans divers environnements, de l'hôte intracellulaire où l'immunosuppression est essentielle à une persistance prolongée, aux environnements extracellulaires dépourvus de nutriments, où le piégeage des nutriments et la résistance au stress sont prioritaires. En examinant à la fois l'interaction hôte-pathogène dans les cellules de trophoblaste infectées et les réponses adaptatives dans l'état de VBNC, cette recherche met en évidence la remarquable capacité du pathogène à survivre et à se développer dans diverses conditions. Ces résultats ont des implications importantes pour la santé publique et la gestion clinique des infections à *L. monocytogenes*, car ils offrent de nouvelles perspectives en matière de détection, de diagnostic et de stratégies de traitement des états bactériens persistants.

Perspectives d'avenir

Les résultats de cette étude devraient être approfondis afin de comprendre à la fois la complexité de l'interphase hôte- *L. monocytogenes* et les mécanismes supplémentaires qui aident à l'entrée et à la sortie de *L. monocytogenes* de l'état VBNC. Les recherches futures pourraient approfondir la compréhension de la dynamique moléculaire et cellulaire observée à la fois dans le sécrétome et les phénotypes VBNC en utilisant les données protéomiques de cette étude comme étape fondamentale.

Premièrement, pour valider les changements protéomiques observés dans l'étude du sécrétome, d'autres approches telles que le western blotting et l'ELISA peuvent être employées. Ces techniques permettent non seulement de vérifier les résultats, mais aussi d'effectuer une évaluation quantitative des principales protéines d'intérêt. Deuxièmement, l'analyse du lysat de cellules entières est cruciale pour obtenir une compréhension plus complète de l'activité sécrétomique de l'organisme profil protéomique intracellulaire. Troisièmement, des études fonctionnelles, y compris des expériences de surexpression et l'analyse de l'ARN, pourraient permettre d'élucider davantage le rôle de protéines spécifiques dans la modulation des résultats de l'infection. En outre, le profilage des niveaux variables de cytokines à l'aide de profileurs de cytokines permettrait d'identifier les cytokines qui auraient pu être négligées lors de la récupération du sécrétome et de mieux comprendre les réponses immunitaires de l'hôte et les voies de signalisation potentiellement influencées par l'infection. Enfin, l'étude de l'implication de facteurs de virulence spécifiques dans la modulation de la sécrétion de l'hôte, notamment par l'utilisation de mutants de délétion, pourrait fournir des informations précieuses sur leur contribution au processus d'infection.

Les recherches futures sur le phénotype VBNC pourraient se concentrer, tout d'abord, sur l'identification de mutants de délétion supplémentaires afin d'explorer leurs rôles dans l'entrée dans l'état VBNC. L'accent pourrait d'abord être mis sur les mutants associés au métabolisme de la paroi cellulaire, en particulier les enzymes synthétisant le peptidoglycane, afin de déterminer si l'inhibition de la paroi cellulaire joue un rôle dans ce processus. Deuxièmement, le rôle de ces mutants dans la sortie de l'état VBNC pourrait être étudié en introduisant des mutants de délétion dans des œufs embryonnés afin d'évaluer leur impact sur la transition et la viabilité ultérieure de *L. monocytogenes* (Carvalho et al., 2024). Troisièmement, l'élargissement de ces études à de multiples mutants de délétion permettrait de mieux comprendre les interactions potentielles entre les voies impliquées

dans le processus d'entrée ou de sortie de l'état VBNC. En outre, l'analyse phosphoprotéomique pourrait être utilisée pour étudier les changements de phosphorylation au cours des transitions vers et hors de la VBNC, offrant ainsi une compréhension plus approfondie des modifications post-traductionnelles.

If you can make one heap of all your winnings
And risk it on one turn of pitch-and-toss,
And lose, and start again at your beginnings
And never breathe a word about your loss;
If you can force your heart and nerve and sinew
To serve your turn long after they are gone,
And so hold on when there is nothing in you
Except the Will which says to them: "**Hold on**";

If, Rudyard Kipling